The Carbon Catalyzed Hydrazine Reduction Of Nitroaromatic Compounds And Molten Salts As A Catalytic Reforming Medium.

Order Number 9406032

The carbon catalyzed hydrazine reduction of nitroaromatic compounds and molten salts as a catalytic reforming medium

Stuart, John Lawrence, Ph.D.

Lehigh University, 1993

U·M·I
300 N. Zeeb Rd.
Ann Arbor, MI 48106

The Carbon Catalyzed Hydrazine Reduction of Nitroaromatic Compounds and Molten Salts as a Catalytic Reforming Medium

by

John Lawrence Stuart

Presented to the Graduate and Research Committee
of Lehigh University
in Candidacy for the Degree of
Doctor of Philosophy
in Chemistry

Lehigh University

September 17, 1993

Approved and recommended for acceptance as a dissertation on partial fulfillment of the requirements for the degree of Doctor of Philosophy.

17 Sept. 1993
Date

Committee Members:

Dr. J. W. Larsen, Chairman

Dr. N. Heindel

Dr. K. Klier

Dr. R. Steiner

The Carbon Catalyzed Hydrazine Reduction of Nitroaromatic Compounds

List of Tables

List of Figures

Abstract

The carbon catalyzed hydrazine hydrate reduction of nitroaromatic compounds has been studied. Reaction conditions were optimized for reaction temperature, nitro concentration, and type and amount of catalyst. Possible reaction intermediates and reaction pathways were also studied. Hydrazine decomposition on the carbon catalysts used for the reaction will also be discussed.

Molten salts as a reaction medium for reforming reactions was also studied. Cyclohexene reactivity was investigated on a Pt catalyst in a K-Li-Na|| Cl eutectic. The valence state and selectivity of this uniquely supported reforming catalyst is also discussed.

Carbon Catalyzed Hydrazine Reduction of Nitroaromatic Compounds

Introduction

The transformation of a nitroaromatic compound to the corresponding aromatic amine is an important synthetic and industrial process.[1] This transformation can be accomplished using a variety of reducing agents, which have been reviewed extensively and discussed.[2,3,4,5,6,7,8,9,10] There is no need to repeat such a summary here. The goal of this project was to develop an efficient, selective, and inexpensive procedure for the conversion of nitro aromatic compounds, particularly several dye intermediates, into their corresponding aromatic amines. Hydrazine based reducing systems were studied because they are selective and efficient.[11] Carbon catalyzed hydrazine hydrate reactions were especially examined because of the ease of use and low cost. A general synthetic method that cleanly and easily converts nitroaromatic compounds to their aromatic amines was developed.

Hydrazine Reduction of Nitro Aromatic Compounds

Hydrazine as a reducing agent for the conversion of nitro aromatics to aromatic amines has been investigated.[12] The first reported reduction of nitrobenzene with hydrazine hydrate (Eq. 1) was carried out by Rothenburg in the absence of a catalyst in 1893.[13]

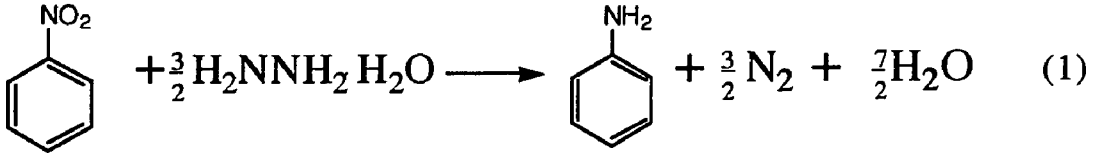

(1)

The only experimental details given in this early publication are that the reaction was conducted in alcohol with stirring and heat. Others have

attempted similar reductions in the absence of a catalyst with poor, irreproducible results.[11] At temperatures above 200°C in diethylene glycol, 4-nitrotoluene and its derivatives are reduced to p-toluidine by hydrazine.[14] Nitro groups are reduced with great specificity using hydrazine and a catalyst, such as platinum on carbon or graphite.[11] The ancillary products from the reaction, nitrogen and water, are easily separated from the aromatic amine. In most cases, the presence of a small amount of water will not affect the reaction, allowing the use of a hydrated form of hydrazine such as hydrazine monohydrate (85% wt hydrazine) or hydrazine hydrate (55% wt hydrazine) with the catalyst.

The hydrazine monohydrate reduction of nitrobenzene is a thermodynamically favored process. The enthalpy for the reaction is calculated to be -148.6 kcal/mol at 25°C.[15]

$$C_6H_5NO_2(l) + 1.5H_4N_2 \cdot H_2O(l) \rightarrow C_6H_5NH_2(l) + 3.5H_2O(l) + 1.5\ N_2(g) \quad (2)$$

ΔH_f^o (kcal/mol):

3.8	-57.9	7.4	-68.3	0.0

Metal catalysts used for the hydrazine hydrate reduction of nitro aromatic compounds include platinum, palladium, ruthenium, and Raney nickel.[16] Unlike reductions using hydrogen and a noble metal catalyst, pressurized reaction vessels are not required. High yields of aromatic amines are produced from Raney nickel catalyzed hydrazine reductions and are selective for nitro groups in the presence of all halogens.[17] Table 1 compares the reduction of p-nitrotoluene using Raney nickel with several other hydrazine reducing systems. A comparison of the selectivity is shown in Table 2.

Table 1. Reduction of p-Nitrotoluene With Hydrazine and a Catalyst

Catalyst (Amount)	mole of Nitro	Equivalents of hydrazine	Time(h)	°C	Yield[a,b]
Raney Ni (0.3 g)[18]	0.1	3	6	78	95
Zn-Cu (2 g)[19]					
prepared	0.01	4	2	25	92 (86)
commercial	0.01	4	2	25	(7)
Montmorillonite(3g)[21]					
H_2NNH_2	0.01	6.25	6	78	90 (85)
H_2NNH_2 (85%)	0.01	6.25	6	78	(50)
Graphite(3g)[24]	0.01	2	2[c]	78	95
FeCl3 / Carbon[25] (20.6mg/ 2 g)	0.1	1.54	5	78	98.9
β-Iron(III) oxide hydroxide (1g)[26]	0.1	1.7	5	60	100

a-isolated yield
b-yields in parentheses are for nitrobenzene
c-not optimized

Table 2. Selectivity of Various Catalysts Using Hydrazine as a Reducing Agent

Catalyst	Reactive Functional Groups	Unreactive Functional groups
Raney Ni[16]	$ArNO_2$	F,Cl,Br,I
Montmorillonite[21]	$ArNO_2$	RNO_2,Cl,Br
Zn-Cu[19]	$ArNO_2$	RNO_2,Cl
graphite[24]	$ArNO_2$,RNO_2	Cl
Carbon/$FeCl_3$[25]	$ArNO_2$	Cl

Ar-aromatic
R-aliphatic

The use of a Zn-Cu couple has also been investigated as a catalyst for the hydrazine hydrate reduction of nitroaromatics.[19] The conversion using Zn-Cu couples is dependent on the method of catalyst preparation. Commercially available 'couple' gave less than 10% of the aromatic amine, while the freshly prepared material gave 92% aromatic amine.[19] Improvements have been made by applying ultrasonic irradiation to hydrazine reductions catalyzed with Zn-$NiCl_2$ couples.[20] Decreased reaction times under ultrasonic irradiation have been attributed to removal of the oxide shell of the catalyst.

Montmorillonite clay has been investigated as a catalyst for the hydrazine reduction of nitroaromatics.[21] High yields of aromatic amine are obtained when a large excess of anhydrous hydrazine is used in dry refluxing ethanol. Conversion to the aniline is significantly reduced if 1% water is added to the solvent. The use of a large excess of hydrazine under anhydrous conditions is a significant drawback of the montmorillonite system.

The use of sodium nitrate in combination with carbon was recently examined as a catalyst for the hydrazine reduction of aromatic nitro compounds.[22] This procedure has been successfully applied to 1-nitronaphtalene, but anhydrous hydrazine must be used to obtain high yields.

Oxidized carbons have also been used as catalysts for the reduction of aromatic nitro compounds with hydrazine hydrate.[23] Yields of 70-80% aromatic amine were obtained from nitrobenzene or 2-nitrotoluene by refluxing with hydrazine hydrate in the presence of several oxidized carbons. Conversions obtained from the hydrazine reduction with these oxidized carbons are lower than those observed with other carbonaceous materials such as graphite.

Han, Shin, and Cho[24] reported the use of graphite as a catalyst for the reduction of nitroaromatics to aromatic amines. They report (see Table 1) excellent conversion of several aromatic nitro compounds in refluxing ethanol within two hours using a 30% (mole) excess of hydrazine hydrate. Their procedure, although not optimized, uses twice as much graphite (by weight) as nitro compound for complete reduction within two hours. This procedure produces very high yields of the desired aliphatic or aromatic

amine, quickly and selectively. Unfortunately a large amount of graphite was used, which can cause stirring problems.

Hirashima and Manabe[25] first reported the iron trichloride-activated carbon catalyzed hydrazine hydrate reduction of substituted nitrobenzenes. Carbon (~20% weight) is used in combination with a catalytic amount of $FeCl_3$ (1% weight). This procedure requires only a slight excess (0.04 mol eq) of hydrazine hydrate, unlike the other methods described. The iron recovered after the reaction has been identified as β-Iron (III) oxide hydroxide.[26] Experiments using catalytic amounts of β-Iron (III) oxide hydroxide, without carbon, gave quantitative conversion of the aromatic nitro compound to the aromatic amine. Other iron oxides gave excellent conversion of p-nitrotoluene to p-toluidine when used in large amounts (i.e. 1 g iron oxide for 1.3 g nitro compound). Substantial amounts of starting material remained when catalytic amounts of iron oxide other than β-Iron (III) oxide hydroxide were used (Table 3). β-Iron (III) oxide hydroxide is effective, but must be freshly prepared via a tedious procedure, making the carbon-$FeCl_3$ combination more attractive.[21]

Reduction Pathways of Nitro Aromatic Compounds to Aromatic Amines and Coupling Reactions of Possible Intermediates

Nearly a century ago Haber proposed a pathway for the electrochemical reduction of nitrobenzene in an alcoholic solution, which is still accepted.[27] This is a stepwise reduction to nitrosobenzene, β-phenylhydroxylamine, and then aniline. Coupled products (azobenzene and azoxybenzene) are

Table 3. Reduction of p-Nitrotoluene with Hydrazine Hydrate and Various Iron Oxides.[26]

	Yield (%) of p-methylaniline after 5hrs. with different amounts of oxide	
Iron oxide	1g	0.1g
none	0.2	0.2
β-Iron(III) oxide hydroxide	100	93.2
Goethite	99.8	55.2
Magnetite	100	18.7
α-Iron(III) oxide	100	12.8
γ-Iron(III) oxide	100	18.3
Hematite	98.9	13.2

1.37g p-nitrotoluene (0.1 mol), 60°C, 100 ml methanol, hydrazine hydrate (0.17 mol)

frequently observed, which are attributed to the reaction of nitrosobenzene and/or phenylhydroxylamine intermediates.

The intermediates observed during the electrochemical reduction of nitrobenzene depend on the pH of the solution.[28] The electrochemical reduction of nitrobenzene in neutral or basic solutions proceeds with one 6 electron wave (Eq. 3).[28] At lower pH, the reaction proceeds with a four electron wave, followed by a two electron wave. The first wave results in

β-phenylhydroxylamine formation, which has a reduction potential of -0.118 V vs. NHE (Normal Hydrogen Electrode, 25°C, pH=6) and the second wave converts the β-phenylhydroxylamine to aniline.[29] Nitrosobenzene has been detected in controlled potential reductions of nitrobenzene conducted at low temperatures and low pH (0-2).[30]

Oxidation of hydrazine to nitrogen is a 4 electron process whose potential increases with pH. In acidic solutions the reduction potential is 0.22 V vs. NHE @ 25°C, which increases to 0.34 V vs. NHE @ 25°C in neutral aqueous solutions (Eq. 4).[31] In basic solutions the reduction potential increases to 1.16 V vs. NHE @ 25°C.[31]

The reaction of hydrazine and nitrobenzene to aniline (Eq. 5) is a favorable reaction in neutral solutions, indicated by the positive E^o_{rxn} of +0.045 V vs. NHE @ 25°C. In base the reaction is thermodynamically favorable (E^o_{rxn}= 0.865 V) and is unfavorable in acid (E^o_{rxn}= -0.075 V).

$$C_6H_5\text{-}NO_2 + 4\,H_2O + 6\,e^- \rightleftharpoons C_6H_5NH_2 + 6\,OH^- \quad E^o = -0.295V \quad (3)$$

$$H_2NNH_2 \rightleftharpoons N_2 + 4\,H^+ + 4\,e^- \quad E^o = +0.34V \quad (4)$$

$$C_6H_5\text{-}NO_2 + 1.5H_2NNH_2 \rightleftharpoons C_6H_5NH_2 + 2\,H_2O \quad E^o_{rxn} = 0.045V \quad (5)$$

The mechanism of dissolving metal reductions is also thought to proceed through nitrosobenzene and phenylhydroxylamine intermediates. Under dissolving metal conditions, partial reduction to phenylhydroxylamine, azobenzene, or azoxybenzene are observed.[2] It has also been postulated that nitrosobenzene is formed in the first step of the catalytic hydrogenation of a nitroaromatic.[11] Although formation of a

nitrosobenzene intermediate has been suggested, one has never been isolated. A phenylhydroxylamine, which has been isolated, can be further reduced to the aromatic amine.

There is a series of reactions in which coupled products are formed from the combination of a nitrosobenzene, β-phenylhydroxylamine, and/or aniline. In systems where these intermediates are formed, coupling reactions may compete with reduction to the aromatic amine. In the Mills[32] reaction, an azo compound is formed (Eq. 6) from the combination of an aromatic nitroso compound with an aromatic amine in acetic acid. This method can be used to prepare unsymmetrical azo compounds in high yields at room temperature.

$$\varphi\text{-}NH_2 \quad + \quad \varphi\text{-}N{=}O \quad \longrightarrow \quad \varphi\text{-}N{=}N\text{-}\varphi \quad + \quad H_2O \qquad (6)$$

Azobenzenes are readily formed from the coupling (Eq. 7) of a nitrosoaromatic compound with a phenylhydroxylamine.[33] This reaction is limited to symmetrical products because of a redox reaction that equilibrates the nitrosobenzene and the phenylhydroxylamine.[34] If the nitrosobenene and the phenylhydroxylamine have different substituents, some of the nitrosobenzene will be reduced to the phenylhydroxylamine and some of the phenylhydroxylamine will be oxidized to the nitrosobenzene. Coupling preferentially occurs between a nitrosobenzene and phenylhydroxylamine with the same substituents, leading to the formation of two different symmetrical azoxy compounds.

$$\varphi\text{-}NH(OH) \quad + \quad \varphi\text{-}N{=}O \quad \longrightarrow \quad \varphi\text{-}N{=}N(O)\text{-}\varphi \quad + \quad H_2O \qquad (7)$$

Azobenzenes can be formed by coupling of the phenylhydroxylamine disproportionation products (Eq. 8) at approximately 100°C.[35] Azoxybenzenes

are formed when some of the phenylhydroxylamine is oxidized (by air) to the nitrosobenzene, which couples with the phenylhydroxylamine.[36] Azobenzenes and azoxybenzene can also be obtained in the absence of air because some of the phenylhydroxylamine is converted to both the aromatic amine and nitrosobenzene through a disproportionation reaction (Eq. 8 and 9).[36]

$$2\ \varphi\text{-NH(OH)} \longrightarrow \varphi\text{-N=N-}\varphi + 2\ H_2O \quad (8)$$

$$3\ \varphi\text{-NH(OH)} \longrightarrow \varphi\text{-NH}_2 + \varphi\text{-N=N(O)-}\varphi + 2\ H_2O \quad (9)$$

A lot of chemistry can occur between nitrosobenzenes, phenylhydroxylamines, and/or anilines intermediates formed during the reduction of an aromatic nitro compound. The concentration of nitrosobenzene developed in a reaction is small because nitrosobenzene is more easily reduced than the nitrobenzene.[36] The particular coupling reaction, if any, that takes place is a function of the acidity of the solution.[37] In the presence of a strong reducing agent coupled intermediates are reduced to the aniline.

In basic solutions, azoxycompounds are formed from the coupling of a nitrosobenzene with an hydroxylamine (eq. 7).[36] Azoxy compounds can also be formed by the disproportionation of a phenylhydroxylamines in basic solutions (eq. 9). In neutral media, nitrobenzene can be reduced to β-phenylhydroxylamine with zinc dust. In acidic solutions the aromatic amine is usually formed by the reduction of a nitroaromatic compound. In acidic solutions rearrangement of an aromatic hydroxylamine intermediate to an amino phenol has been observed.[36] Formation of coupled products from the reduction of a nitro aromatic compound suggests the presence of some of

the mentioned intermediates, which are formed by competing pathways under the reaction conditions.[38]

Decomposition of Hydrazine

The decomposition of hydrazine may occur during the hydrazine reduction of a nitroaromatic compound. Thermal decomposition of hydrazine takes place at temperatures above 250°C.[31] A variety of catalysts can be used to significantly lower this temperature.[39] Hydrazine is known to undergo two thermodynamically favored decomposition reactions (Eq. 10,11). If hydrazine decomposes via reaction 11, the hydrogen produced can

$$H_2NNH_2 \rightarrow 4/3\ NH_3 + 1/3\ N_2 \qquad \Delta H_f^o = -26.4\ (kcal/mol) \qquad (10)$$

$$H_2NNH_2 \rightarrow N_2 + 2\ H_2 \qquad \Delta H_f^o = -12.1\ (kcal/mol) \qquad (11)$$

react with hydrazine to produce ammonia (Eq 12). The catalytic

$$H_2NNH_2 + H_2 \rightarrow 2\ NH_3 \qquad (12)$$

decomposition of hydrazine usually follows the stoichiometry of equation 10, which is also observed from the combination of equations 11 and 12.[31] Many catalysts that are used for the hydrazine reduction of a nitro compound are also effective for the decomposition of hydrazine.

Hydrazine decomposition has been observed on many catalysts.[40] The more common are noble metals.[36] Other catalysts that have been developed include molybdenum supported on aluminum, sodium silicates, or activated

carbon. Using one of the most effective catalysts, molybdenum supported on a mixture of aluminum and sodium silicates, decomposes one gram of anhydrous hydrazine decomposes in 45 seconds to nitrogen, ammonia, and hydrogen.[41] Catalysts of this effectiveness have been developed for use in the aerospace industry.

The mechanism of hydrazine decomposition on alumina supported metals (Ru, Co, Rh, Ir, Pd, Pt, Cu) or MgO-supported iron has been investigated using labeled hydrazine between 60-300°C.[42] Mixtures of labeled and unlabeled hydrazine ($H_2{}^{15}N{}^{15}NH_2$ and $H_2{}^{14}N{}^{14}NH_2$) have been used to determine whether the nitrogen produced is from one or two hydrazine molecules. The nitrogen produced consists only of ^{15}N-^{15}N or ^{14}N-^{14}N, indicating that the N-N bond of the hydrazine remains intact during decomposition on these metals.

A proposed reaction mechanism for the decomposition of hydrazine on palladium is shown below (Eqs.13-19).[43] This mechanism requires adsorption of hydrazine on the metal surface. The nitrogen produced would be formed from one hydrazine, which is consistent with the results from the decomposition of hydrazine on alumina and MgO supported iron.

$$N_2H_4 \rightleftharpoons N_2H_4(ad) \quad (13)$$

$$N_2H_4(ad) \rightarrow N_2H_3(ad) + H(ad) \quad (14)$$

$$N_2H_4(ad) + H(ad) \rightleftharpoons N_2H_5(ad) \quad (15)$$

$$N_2H_5(ad) + H(ad) \rightarrow 2NH_3 \quad (16)$$

$$N_2H_3(ad) \rightarrow N_2H_2(ad) + H(ad) \quad (17)$$

$$N_2H_2(ad) \rightarrow N_2H(ad) + H(ad) \quad (18)$$

$$N_2H(ad) \rightarrow N_2 + H(ad) \quad (19)$$

Carbonaceous Catalysts

Carbonaceous materials were used as catalysts for the reduction of nitroaromatic compounds in this work. Carbons as catalysts in isomerization and redox reactions have been recently reviewed.[44] The rate of racemization of substituted 1,1'-binaphthyls is increased in the presence of carbon, which is thought to donate electrons to the substrate.[45] Carbon can mediate the transfer of electrons between adsorbed reactants in some redox reactions carried out in solution.[46] If this occurs, reaction on the carbon can be viewed as a redox couple where one species is reduced simultaneously with oxidation of the other.

Austin[47] has developed three criteria for the carbon catalysis of an electrochemical reaction. First, the reactants must adsorb on the carbon for the reaction to take place. Secondly, the carbon must be a good electrical conductor. Thirdly, the rates of the oxidation and reduction reactions must be reasonably fast. The first two criteria are necessary for the transfer of electrons through the carbon. The need for fast half reactions is to produce a large current density, which can also be obtained by a large difference in Nernst potentials.

Dye Intermediates Examined

Several of the nitro compounds examined in this project are important dye intermediates. They include: (2-hydroxyethyl)-3-nitrophenylsulfone (Nitro Meta Base), 3-nitrobenzenesulfon(1-azacycloheptane)amide (Nitro HMI), 4-hydroxy-3-nitro-N-(3-propylisopropoxy)benzenesulfonamide (HPS),

3-hydroxy-4-nitrobenzenesulfonamide (HNBS), 4-(2'-hydroxypropoxy)-3-nitrotoluene (POP(1)), 4,4'-dinitrobenzanilide (DNBA).

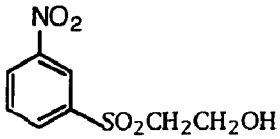

Nitro Meta Base

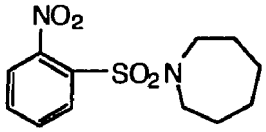

Nitro HMI

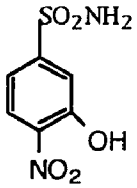

HNBS

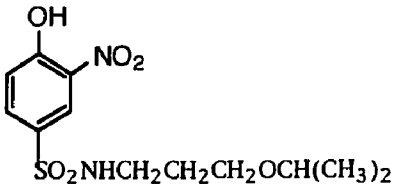

HPS

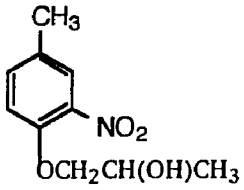

POP(1)

Experimental

Materials

The reduction of a variety of nitro aromatic compounds was examined using hydrazine, hydrazine monohydrate ($H_4N_4 \cdot H_2O$), and hydrazine hydrate ($H_4N_4 \cdot xH_2O$), and a catalyst. The dye intermediates were obtained from Crompton & Knowles Corporation and were used as received, unless otherwise indicated. The purity of these materials is unknown. They include: (2-hydroxyethyl)-3-nitrophenylsulfone (NMB, mp:76-84°C), 3-nitrobenzenesulfon(1azacycloheptane)amide (Nitro HMI, mp: 62°-72°C), 4-hydroxy-3-nitro-N-(3-propylisopropoxy)benzenesulfonamide (Nitro HPS, mp: 82-90°C), 3-hydroxy-4-nitrobenzenesulfonamide (Nitro HNBS, mp: 270-275°C), 4-(2'-hydroxypropoxy)-3-nitrotoluene (POP(1)), m-nitrobenzanilide, and 4,4'-dinitrobenzanilide (DNBA). Other nitro compounds that were used as received include; 1-bromo-4-nitrobenzene (Aldrich), 1-chloro-4-nitrobenzene (Eastman), 1-iodo-3-nitrobenzene (Aldrich), 1-iodo-4-nitrobenzene (Aldrich), 2,2'-dinitrobiphenyl (Lancaster), 4-nitroaniline (Aldrich), 2-nitroanisole (Aldrich), 4-nitroanisole (Aldrich), nitrobenzene (Fisher), 2-nitrobiphenyl (Aldrich), nitrocyclohexane (Aldrich), 2-nitrophenol (Eastman), 4-nitrophenol (Aldrich), 4-nitrotoluene (Aldrich), 5-nitro-m-xylene (Aldrich), and 3-nitro-α,α,α-trifluorotoluene (Aldrich).

Other compounds purchased include: azobenzene (Fisher), azoxybenzene (Fisher), and nitrosobenzene (Aldrich), which were used as received.

2-Amino-2'nitrobipheyl was prepared by the Pd/C catalyzed formic acid reduction of 2,2'-dinitroiphenyl.[47] The crude product was purified by silica

gel (225 g, 60-200 mesh, Aldrich) flash column chromatography using 750 mL of a hexane (Fisher) ethyl acetate (Fisher) mixture (1:4). NMR indicated that a small amount (~1%) of starting material was still present after this purification. The product was dissolved in diethyl ether and extracted three times with 30 mL of 0.5M HCl. The aqueous layer, which contained the 2-amino-2'nitrobiphenyl, was neutralized with sodium carbonate (Fisher) and further purified using a silica gel (200 g) flash column with 700 mL of a hexane : ethyl acetate (1:4) eluent. The product was obtained in a 22% yield and had a corrected melting point of 64.0°-65.0°C (lit 64.0°-64.5°C). The product did not show the presence of any impurities by TLC (CH_2Cl_2) or ^1H NMR. The NMR of the purified product is shown in Figure 1. The chemical shifts and splitting patterns observed are what is expected for 2-amino-2'-nitrobiphenyl. The aromatic protons on the ring containing the nitro group [7.97 ppm (d, J 8.9 Hz,1H), 7.68 ppm(t, 8.9 Hz,1H), 7.52 ppm(t, 8.9 Hz,1H), 7.48 ppm(d, 8.9 Hz,1H)] are upfield from those on the ring with the amino substituent [7.20 ppm(t, 8.9 Hz,1H), 6.99 ppm(d, 8.9 Hz,1H), 6.82 ppm(t, 8.9 Hz,1H), 6.78 ppm(d, 8.9 Hz,1H)].

Benzonitrile oxide ($PhC{\equiv}N^+O^-$) was generated in situ from the benzohydroxamoyl chloride precursor (PhC(Cl)=NOH), which was prepared by the chlorination (Matheson) of syn-benzaldehyde oxime (20.058 g [0.16 mol] Aldrich) in chloroform (150 mL, Fisher) at -5°C.[48] The product was hygroscopic and melted 44.0°-46.0°C (lit. 51°-52°C). The NMR spectrum of the presursor shows the hydroxylamine proton [8.30 ppm(bs, 1H)], and the aromatic protons [ortho: 7.85 ppm(dt, 7.1 Hz, 2.6 Hz, 2H), meta, para: 7.4 ppm (m, 1H)]. The nitrile oxide is rapidly generated in the presence of a base.[44]

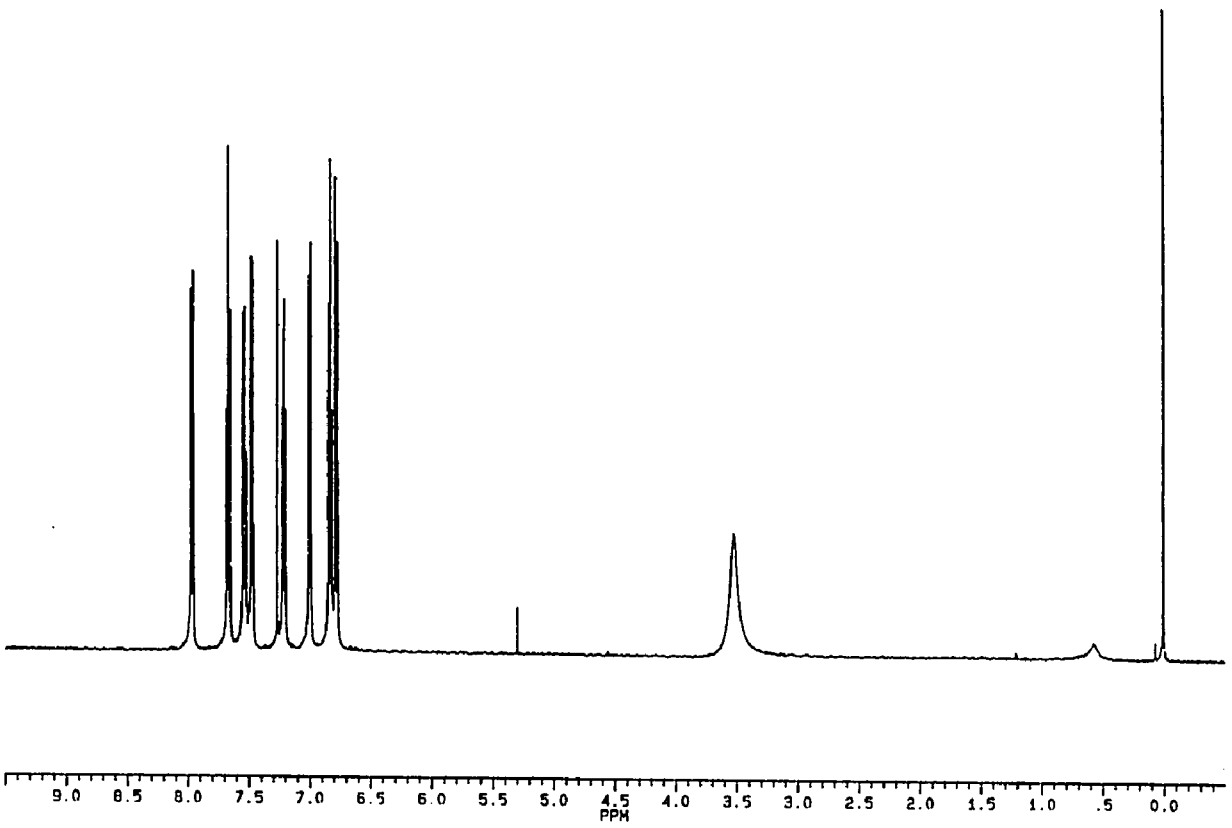

Figure 1. NMR Spectrum of 2-Amino-2′-nitrobiphenyl

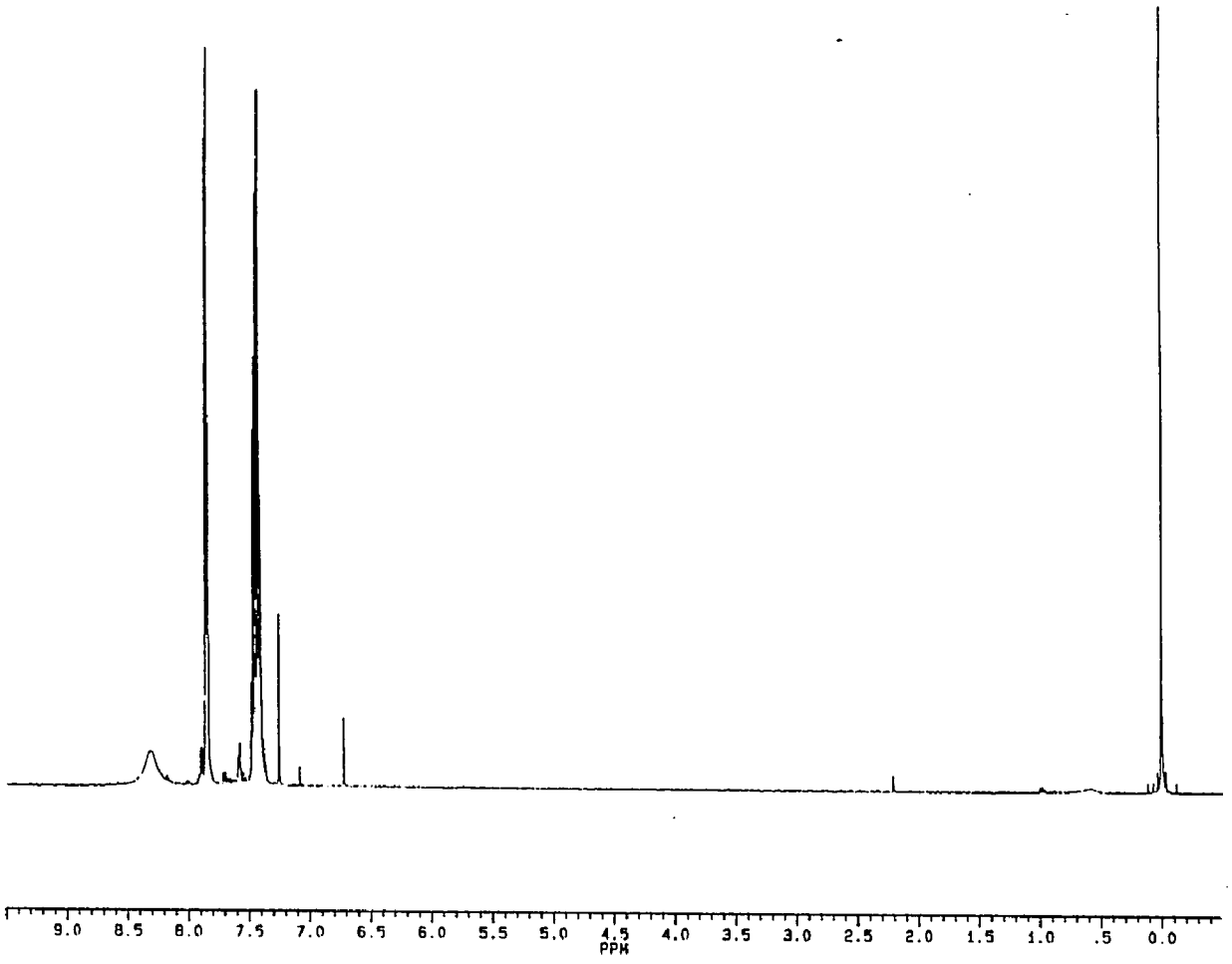

Figure 2. NMR Spectrum of Benzohydroxamoyl Chloride

Phenyl azide was prepared from phenylhydrazine hydrochloride (8.944 g, Aldrich) by treatment with hydrochloric acid (6 mL, Fisher) and sodium nitrite (5.0 g, Aldrich) in an aqueous solution (78 mL).[49] Sodium nitrite was added over 20 minutes, while a temperature between 0°-3°C was maintained. After the solution warmed to room temperature, diethyl ether (20 mL) was added. The material was steam distilled until a volume of 160 mL had been collected. The distillate was separated and the aqueous layer was washed with two 10 mL portions of ether. The crude product in ether was rinsed with two 15 mL portions of 0.3M NaOH (Fisher) to remove any phenol. The product distilled at room temperature (22.5°C) under vacuum (< 1 mm Hg, lit. value 49-50°C at 5 mmHg[48]) to yield phenylazide in 56% yield. The refractive index of the product was measured as 1.5583 (25°C) [literature value is 1.5588 (24.9°C)].[50] The chemical shifts and splitting pattern (Figure 3) correspond to a monosubstituted aromatic compound: [meta (7.29 ppm{ t,8.5 Hz, 2H}, para (7.08 ppm{t,8.5 Hz, 1H}, and ortho positions (6.98 ppm{d,8.5 Hz, 2H})]. The ortho protons are shifted upfield because of the added electron density from the azide substituent.

β-Phenylhydroxylamine was prepared by the zinc (39 g, Fisher) reduction of nitrobenzene (20 mL) in an aqueous (350 mL) ammonium chloride (12 g) solution.[51] The hydroxylamine was salted (124 g NaCl, Fisher) out of the aqueous solution. Kamm's[51] procedure was modified by dissolving the crude product in diethyl ether (100 mL, Fisher), to separate the β-phenylhydroxylamine from the sodium chloride. After filtration, to remove the sodium chloride, the ether was removed by rotary evaporation to give β-phenylhydroxylamine in a 46% yield. The product had an uncorrected

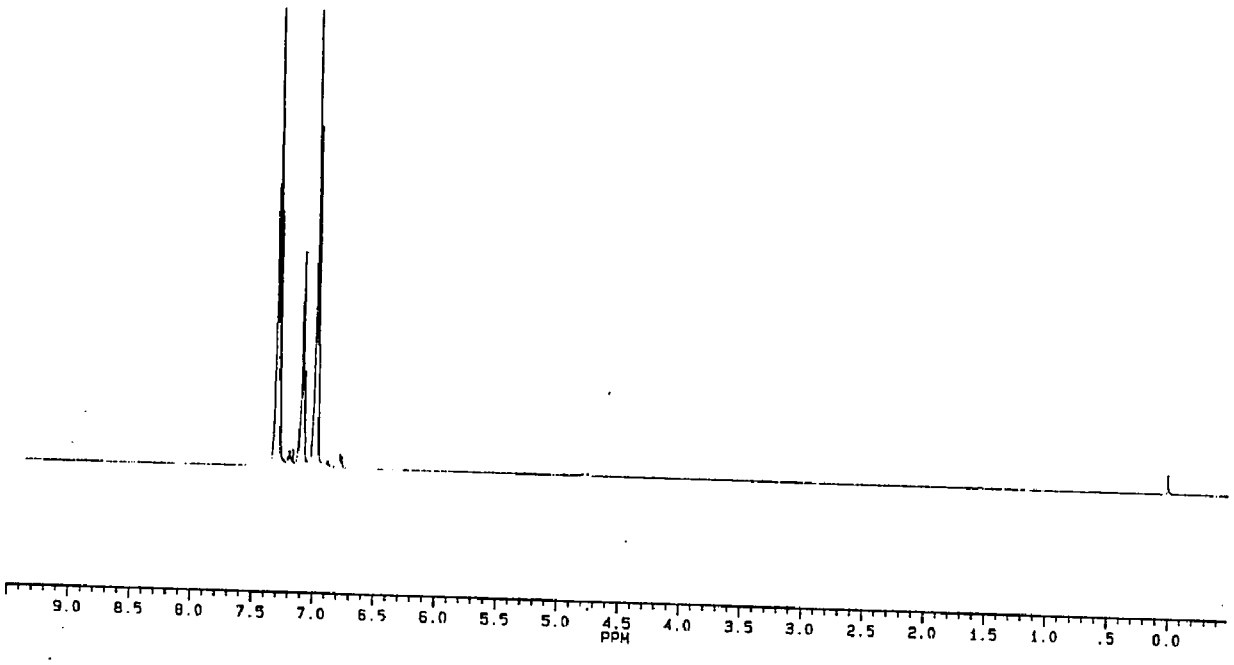

Figure 3. NMR Spectrum of Phenyl Azide

melting point 79.5°-80.5°C (lit[52] 82°C). The β-phenylhydroxylamine was used immediately after preparation to minimize the amount of impurities that would be generated during storage.

N-Phenylphenyl nitrone [PhC(H)=N^+Ph(O^-)] was prepared by the condensation of β-phenylhydroxylamine (1.827 g, preparation previously described) and benzaldehyde (1.839 g, Aldrich) in ethanol (10 mL, Midwest Grain Products).[53] After stirring at room temperature for 20 minutes, the product precipitated from solution. The product was isolated in a 58% yield following suction filtration and melted at 112.0°-112.5°C (uncorrected, lit[53] value 116°C). The compound was also characterized by NMR (Figure 4). The olefinic proton is downfield [7.95 ppm (s,1H)], the ortho protons on each ring are unique [8.40 ppm (dd, 8.5 Hz, 1.5 Hz,2H) for the phenyl ring on the nitrogen and 7.78 ppm (dd, 8.5 Hz, 1.5 Hz,2H) for the phenyl ring on the carbon] and the remaining protons are contained in the multiplet [7.50 ppm (m,6H)]. This sample also contained a small amount of IPA (3.7, 1.2 ppm).

The hydrazines were used as received. In all reactions, except one conducted under anhydrous conditions, hydrazine was used as either the monohydrate (85% mole hydrazine, Aldrich) or the hydrate (55% mole hydrazine, Aldrich). Hydrazine-d_4 hydrate-d_2 (MSD Isotopes) was used as received. Other hydrazines used include 1,1-dimethylhydrazine (Lancaster) and 1,2-dimethylhydrazine dihydrochloride (TCI). 1,2-Dimethylhydrazine dihydrochloride was neutralized with sodium carbonate (Fisher) *in situ* to generate the free hydrazine.

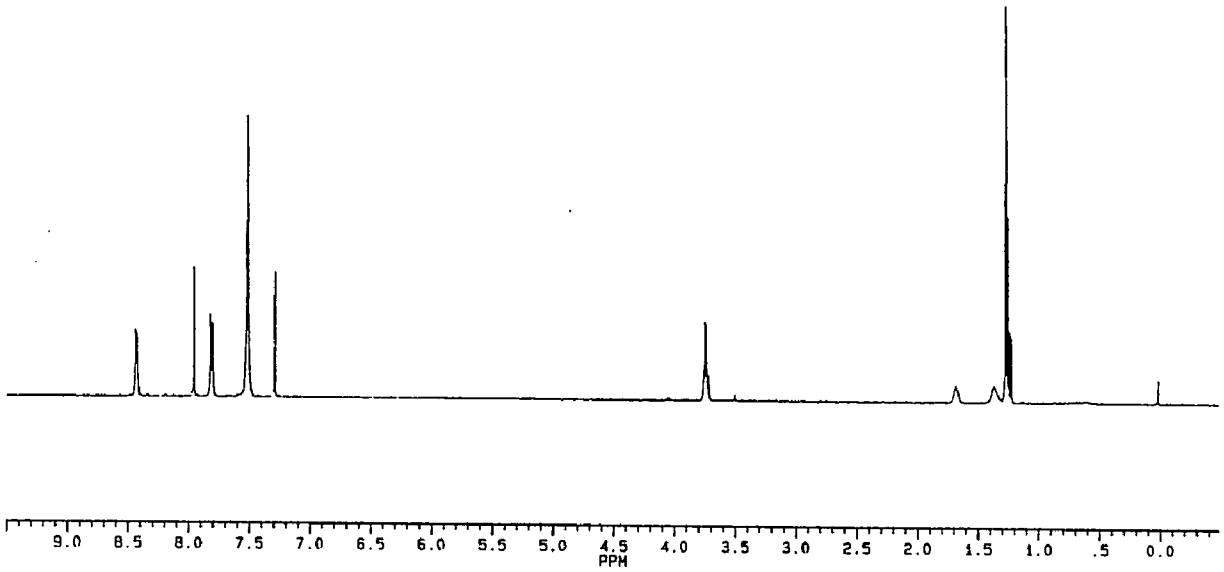

Figure 4. NMR Spectrum of N-Phenyl-phenylnitrone

A variety of carbonaceous materials was examined as catalysts. All were used as received unless otherwise indicated. Graphite (Fisher) was examined as well as a variety of wood based carbons that are primarily used for wastewater treatment. They include: Aqua A (Westvaco), SA (Westvaco), SA-20 (Westvaco), SN-20 (Westvaco). It should be noted that the sample of Aqua A has been in the laboratory for at least ten years and is no longer commercially available. Other carbons that were examined include: Darco (Kodak), Coconut Charcoal (Fisher), Norit (Fisher), Kingsford Charcoal Briquets (The Kingsford Products Company). The charcoal briquet was ground prior to use. Two coals, Beulah Zap and Illinois #6 (Argonne Coal Bank), were examined. Carbon blacks obtained from Cabot include: Mogul L, Monarch 1000, Monarch 1300, Regal 400R, Vulcan XC-72 R, Black Pearls 2000, and Black Pearls L. Non-carbonaceous materials examined as possible catalysts include alumina (F-20, Alcola), Cabosil (Cabot), and montmorillonite (Aldrich).

The effect of adding a metal ion as a co-catalyst with carbon was also examined. The following metal ions were used: $FeCl_3$ (Fisher), Fe_2O_3 (Aldrich), Fe_2SO_3 (Fisher), $ZnCl_2$ (Aldrich), $SnCl_4$ (Aldrich), $NiCl_2$ (Aldrich), $CuCl_2$ (Aldrich), $TiCl_4$ (Aldrich), $CoCl_2$ (Aldrich), $MnCl_2$(Aldrich), and TiO_2 (Aldrich) as received.

Most of the reactions were conducted in isopropyl alcohol (IPA, Fisher), which was used as received. Tetrahydrofuran (THF, Aldrich) was dried over calcium hydride (Aldrich) and distilled over sodium metal (Fisher) prior to use. Glyme (Aldrich) and glyme-d_{10} (MSD Isotopes) were used without purification.

Aqua A and Nuchar SA were oxidized by adding nitric acid to the carbon in an aqueous suspension. The mixture was stirred at room temperature for the desired amount of time (Details in Table 4). The solution was then filtered and rinsed with distilled water until the filtrate was neutral. The carbons were dried at 110°C prior to use.

Table 4. Oxidation of Carbons with Nitric Acid

Carbon (g)	H_2O(mL)	HNO_3(mL)	time	H_2O Wash(mL)
Nuchar SA-(5.029)	50	29	16 h	141
Nuchar SA-(5.026)	50	30	1 h	270
Nuchar SA-(5.002)	-	50	contact	175
Aqua A-(5.007)	50	30.5	24 h	250
Aqua A-(5.081)	50	29.5	1h	200

Equipment

The reductions were carried out using standard glassware. A two neck 100ml round bottom flask with 24/40 joints was used with a reflux condenser and a 30 mL pressure balancing addition funnel. Positive pressure of nitrogen was maintained over the reaction from the inlet at the top of the reflux condenser. The reaction was initiated by the addition of hydrazine to the refluxing mixture of the compound and carbon in IPA.

Many experiments were monitored by measuring the amount of gas produced as a function of time. In these experiments the nitrogen inlet was replaced with the inlet to a gas measuring apparatus. The gas measuring apparatus was composed of a 1 L volume calibrated addition funnel and a 1 L separatory funnel, which will be referred to as the buret and the reservoir, respectively. The top of the buret was connected to the top of the reflux condenser of the reaction apparatus using Tygon® tubing and a vacuum adaptor with a hose connector. The bottom of the reservoir was connected to the bottom of the buret with Tygon® tubing. Wherever tubing was attached to glass, copper wire was wrapped around the connection to insure a tight seal.

All NMR spectra were run on a Bruker AM-500 spectrometer. GC-MS results were obtained using either a Finnigan 4023 operating in the electron ionization mode or a HP 5970 mass detector. IR spectra were obtained using a Mattson Polaris. UV spectra were obtained using a Perkin Elmer Lambda 5 spectrometer. GC analysis of the gaseous samples was performed using a HP-5880 with a 6' Porapak QS column. The detection limit for hydrogen was determined to be 5% H_2 in N_2, which was determined by analysis of known mixtures.

Procedures

The standard procedure developed for the hydrazine hydrate reduction follows. All reactions were carried out in a hood and care was taken to ensure safety when working with the hydrazines. The carbon catalyst (approximately 0.7 g) was added to 0.017 mol nitro compound in the round bottom flask. If

used for a reaction, the metal ion (approximately 1%(wt) based on nitro compound) was also added. The solvent, about 10 mL isopropanol (IPA) depending on the particular substrate (see Table 5), was added to the mixture. A magnetic stir bar and a magnetic stir plate were used to mix the reactants. Hydrazine hydrate (0.034 mol) or hydrazine monohydrate (0.034 mol), two moles relative to the nitro compound, was placed in the addition funnel. Nitrogen (Linde) was passed through the system from the top of the reflux condenser for five minutes before the ground glass stopper was placed on the addition funnel. All of the ground glass joints were thoroughly greased to insure a tight seal. After the system had been purged with nitrogen, the flask was heated using an electric heating mantle controlled with a variable power controller. The system was brought to reflux and the reaction was started by addition of hydrazine hydrate.

Table 5. Solvent Amounts and TLC Eluants for the Substrates Examined

Substrate	TLC Solvent	Rf NO_2	Rf NH_2	IPA (mL)
Nitro Meta Base	EtOH/Toluene (1/5)	0.35	0.18	10
Nitro HMI	CH_2Cl_2	0.47	0.32	11
POP(1)	EtOH/Toluene (1/5)	0.59	0.47	10
HPS	EtOH/Toluene (1/10)	0.28	0.46	15
HNBS	$CHCl_3$/MeOH/Et_3N (3/2/1)	0.48	0.22	10
DNBA	EtOH/Toluene (1/5)	0.55	0.11	10[a]
Others (ie. $PhNO_2$)	CH_2Cl_2	~0.88	~0.34	10

a-Solvent was Methanol

In experiments measuring the amount of gas produced, the gas buret was attached after the solvent began to reflux. When the system was stable, determined by no change in gas volume for at least 15 minutes, the reaction began with addition of all of the hydrazine hydrate from the addition funnel. The reaction was followed by measuring the volume of water displaced from the buret into the reservoir at atmospheric pressure.

The progress of many of the reactions was followed by Thin Layer Chromatography (TLC). Whatman TLC plates with 250mm of silica gel were used. Table 5 shows the eluents used for substrates examined and the Rf's of the starting materials and the products. The appearance of products and intermediates was followed as well as the disappearance of starting material.

When the reaction was complete the product mixture was filtered by suction filtration to remove the carbon catalyst. The solvent was removed by rotary evaporation. Products analyzed by NMR were dissolved in $CDCl_3$ (CIL). Measurement of the amount of gas produced from the reduction of a nitro aromatic compound as a function of time was used to determine a rate constant for the consumption of hydrazine. The rate of gas production is approximately equal to the rate of nitro reduction if the rate of hydrazine decomposition is slow compared to the reduction rate. The fraction of hydrazine consumed is related to the volume of gases produced (V_t) at some time t over the calculated amount of nitrogen produced (V_c), if all of the hydrazine were to reduce the nitro compound. A first order rate constant for the consumption of hydrazine in the reduction of nitrobenzene is the initial slope of the plot of the (Figure 5) natural log of the fraction of hydrazine remaining, $\ln [(1-V_t / V_c)]$, vs. time. A second order rate constant was

determined from the slope of $(1-V_t/V_c)^{-1}$ vs. time, as shown in Figure 6. As shown in Figures 5 and 6, a slightly better fit is observed for the gas production from the reduction of 4-nitrotoluene from first order kinetics than second order.

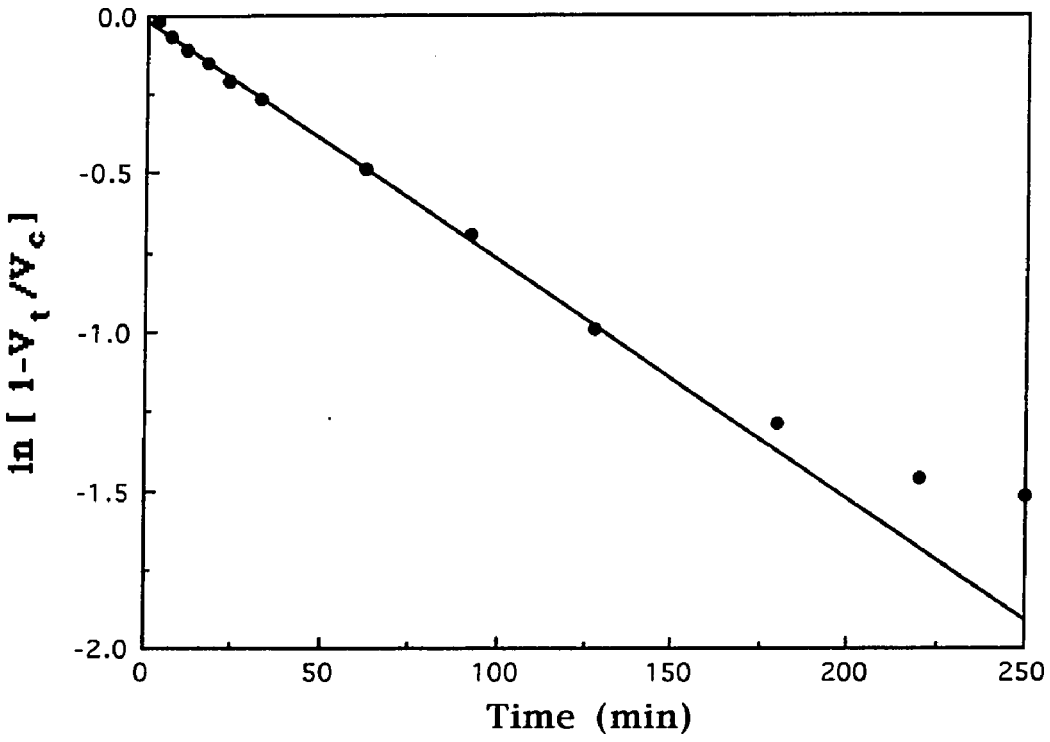

Figure 5. Data from the Hydrazine Hydrate Reduction of 4-Nitrotoluene Following 1st Order Kinetics.

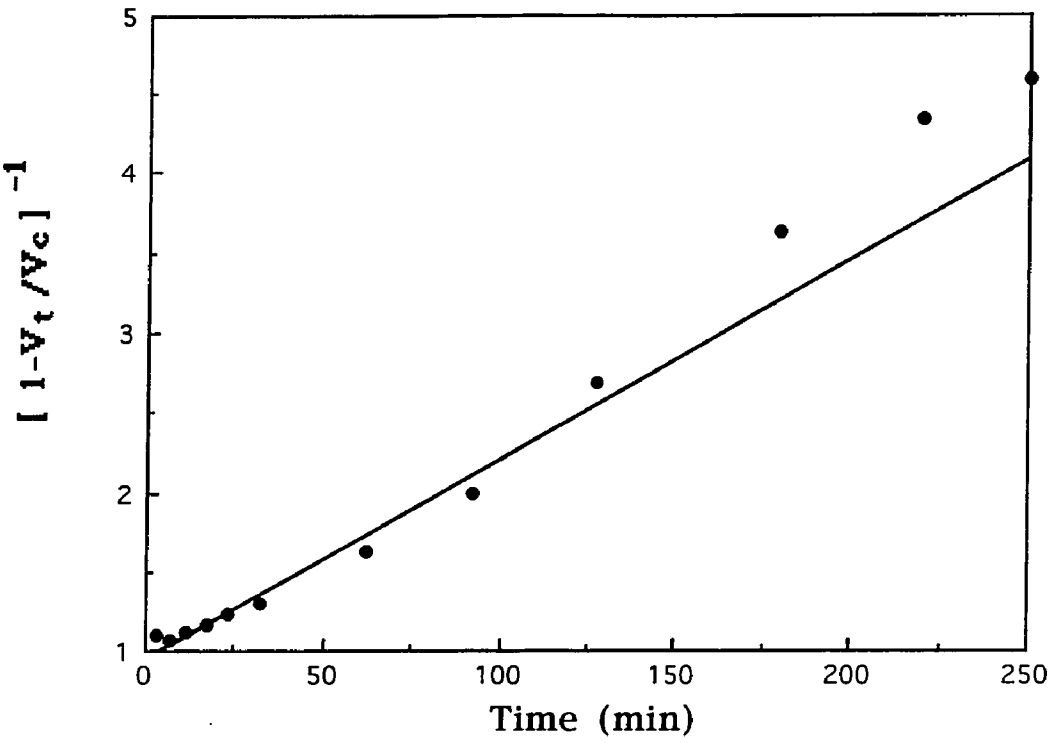

Figure 6. Data from the Hydrazine Hydrate Reduction of 4-Nitrotoluene Following 2nd Order Kinetics

In many cases, the rate of gas production was used to determine apparent reaction order for one component. The apparent reaction order was determined from the slope of a plot of the ln [k] as a function of ln [component].

The decomposition of hydrazine on several carbonaceous catalysts was also examined. The procedure and apparatus were the same as for the reduction of a nitro compound, except the nitro compound was not included. The data for the rate of gaseous product formation is not described by first,

second, or third order kinetics (see results section). A first order rate constant will be used for comparison of different carbons.

Several experiments were conducted to elucidate the reaction mechanism and the role of carbon in the reduction. In one, the reaction was followed by ^1H NMR in a 5mm NMR tube using glyme-d_{10} as the solvent with $D_4N_2 \cdot D_2O$ as the reducing agent in the presence of carbon (Black Pearls L). The NMR tube was placed in a water bath maintained at 80°C. After 60 minutes, the tube was transferred from the hot water bath to an ice bath to rapidly cool the contents. The tube was then centrifuged for two minutes to bring most of the carbon to the bottom of the tube (out of the receiver coil of the NMR) to minimize line broadening. An NMR spectrum was obtained at room temperature and the tube was returned to the hot water bath. This process was repeated every 60 minutes until there was no noticeable change in the spectra. It took approximately 15 minutes from the time the sample was removed from the hot water bath until it was returned.

The adsorption of hydrazine hydrate and separately, POP(1) (structure on p. 15) on Black Pearls L from an isopropanol solution was examined. The amount of hydrazine adsorbed from solution was determined by titration with standardized iodate solution after removal of the carbon.[54] A measured amount of hydrazine hydrate was added to a weighed amount of carbon in a 10 mL volumetric flask. The volume was brought to 10.0 mL with IPA. After 10 minutes of stirring at room temperature the solution was filtered through a 2mm syringe filter (Waters) to remove the carbon. The mixture was allowed to equillibrate for ten minutes because oxidation of the hydrazine by atmospheric oxygen would occur at longer times.[50] An alliquot of the filtered

solution was titrated with an iodate solution (0.002218M). This procedure was repeated for several concentrations of hydrazine and various amounts of carbon.

The amount of POP(1) adsorption on the carbon was measured by the change in ultraviolet adsorption of the solution. The molar absorptivity of POP(1) was determined to be 2,400 l/cm mol at 260.0 cm^{-1}. Examination of standard solutions indicated that the response was linear between .0315 mM and 0.841 mM. A known amount of nitro compound in an isopropanol solution was added to a weighed amount of carbon in a 10 mL volumetric flask. A small stir bar was added to the flask after the volume was brought to 10.0 mL with IPA and stirred for 24 hours. To remove the carbon, the solution was filtered using a 2mm syringe filter. It was determined that there was no change in nitro concentration as a result of the filtration method employed. An alliquot of the solution was diluted so that it remained within the concentration region standardized. The amount of nitro adsorbed on the carbon was determined by the difference of the amount of nitro added to the carbon and the amount of nitro remaining in solution, determined from the UV measurement. Equilibrium had been reached in 24 h because there was no change in the nitro concentration of solutions that were stirred for five additional days.

Residual hydrazine, found in the solution after the nitro compound had been reduced, is significant because its presence can affect subsequent reactions in dye syntheses. There is a TLC procedure for the determination of residual hydrazine, but it was not useful because of interference of aromatic amines. In that TLC method, the hydrazine is derivatized with

4-(dimethylamino)-benzaldehyde to form the hydrazone.[55] After TLC separation the plate is sprayed with Dragendorff's reagent. A red color is positive for the presence of hydrazine. This method has been calibrated to yield a quantitative measure of the amount of hydrazine present.[55] The problem with this method is that amines have similar Rf's to the hydrazone and interfere with the color producing false positive results.

The procedure was modified to overcome aromatic amine interference by performing 2-dimensional TLC. The first direction was used to separate the amine, which moves with the eluant (see Table 5 for eluant) from hydrazine, which remains at the origin. After separation of the components, the origin was spotted with a solution of 4-(dimethylamino)-benzaldehyde. Derivatization was allowed to take place for ten minutes and then the plate was dried with warm air. The second TLC dimension ($CHCl_3$: MeOH: NH_4OH = 85:15:1, v:v:v) was used to move the hydrazine derivative from the origin. The derivatized material appears as a yellow-to-orange spot near the solvent front. After the plate was sprayed with Dragendorff's reagent,[55] the color changed to an intense orange or red color, depending on the amount of hydrazine present. The more hydrazine present, the deeper the red color of the spot. Semi-quantitative results were obtained by using 10 μl of the sample (approximately 1.5 M in nitro). The test was red if more than 310 μmol of hydrazine were present and orange if less than 106 μmol of hydrazine were present.

The gaseous products from the 1,1-dimethyl hydrazine and the 1,2-dimethylhydrazine reduction of HMI were examined to determine the fate of the hydrazine. The standard apparatus, previously described, was used

with a minor modification. A trap was attached to the top of the condenser that was maintained at -78°C and used to collect the gaseous products swept through the condenser with a stream of nitrogen from an inlet on the addition funnel. An IR spectrum was taken using a portion of the sample collected from the 1,1-dimethylhydrazine reduction that was transferred to a 100cm path length IR cell under vacuum. The product of the 1,2-dimethylhydrazine reduction was examined by NMR and GC/MS after 0.7 g D_2O (CIL) was added to the sample at -78°C.

Results

The carbon catalyzed hydrazine hydrate reduction of nitroaromatic compounds was optimized to provide complete conversion to the amine without the formation of side or intermediate products. The conversion and yield of the reaction were more important that the reaction time, as long as complete reduction was observed in less than 24 hours. Variables that were altered to provide an optimized system for nitro aromatic dye intermediates include: reaction temperature, nitro concentration, amount and type of carbonaceous catalyst, addition of a metal ion as a co-catalyst, amount of water present, and catalyst age. Hydrazine hydrate was found to decompose on the carbonaceous catalysts used for the reduction of the nitro aromatic compounds. Experiments were conducted with compounds having functional groups other than an aromatic nitro group to determine the scope and mechanistic features of the reaction.

Adsorption of Reactants on Carbon

The adsorption of hydrazine and POP(1) was examined on Black Pearls L, one of the carbonaceous catalysts used for the reduction of nitroaromatic compounds. The adsorption of the hydrazine on the carbon follows a high affinity isotherm (Figure 7, Table 6).[56] The nitro compound, POP(1) (Table 7), also adsorbs to the carbon. The adsorption of POP(1) follows a constant partition isotherm shown in Figure 8.[56]

Table 6. Adsorption of Hydrazine on Black Pearls L.

BPL(g)	Inital[a] $[H_4N_2]$ mM	Solution[b] $[H_4N_2]$ mM	mmole adsorbed	mmole H_4N_2 per g BPL
0.08939	8.81	0.0	0.088	0.99
0.01613	8.81	7.8	0.010	0.61
0.03725	8.81	4.4	0.045	1.20
0.01892	10.62	8.9	0.017	0.91
0.03905	10.62	7.4	0.032	0.82
0.04635	10.62	6.2	0.044	0.95
0.06480	10.62	2.5	0.081	1.25

a-total volume was 10.0 mL
b-measured after 10 min at room temperature with stirring

Table 7. Adsorption of POP(1) on Black Pearls L

BPL(g)	Inital[a] [POP(1)] mM	Adsorbance (Dilution, mL)	Solution[b] [POP(1)] mM	m mole adsorbed	mmole POP(1) per g BPL
0.09611	5.25	0.125 (100)	4.65	5.97	6.27
0.10345	0.52	0.127 (10)	0.47	0.47	0.51
0.11792	0.52	0.131 (10)	0.49	0.31	0.30
0.16752	5.25	0.119 (100)	4.41	8.30	5.04
0.30910	5.25	0.106 (100)	3.88	13.66	4.43

a-total volume was 10.0 mL
b-measured after 24 hr at room temperature with stirring

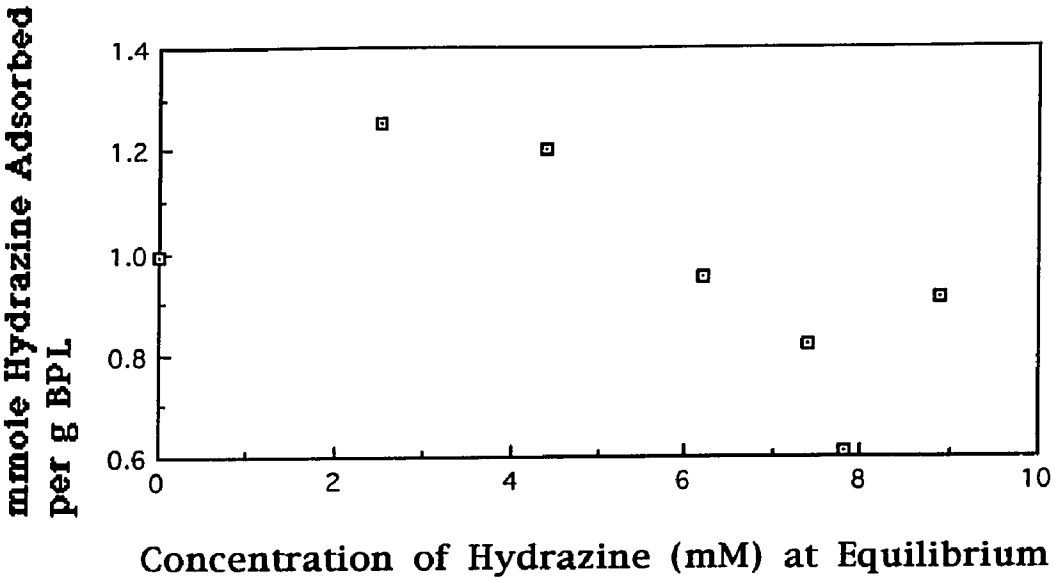

Figure 7. Isotherm for the Adsorption of Hydrazine on BPL

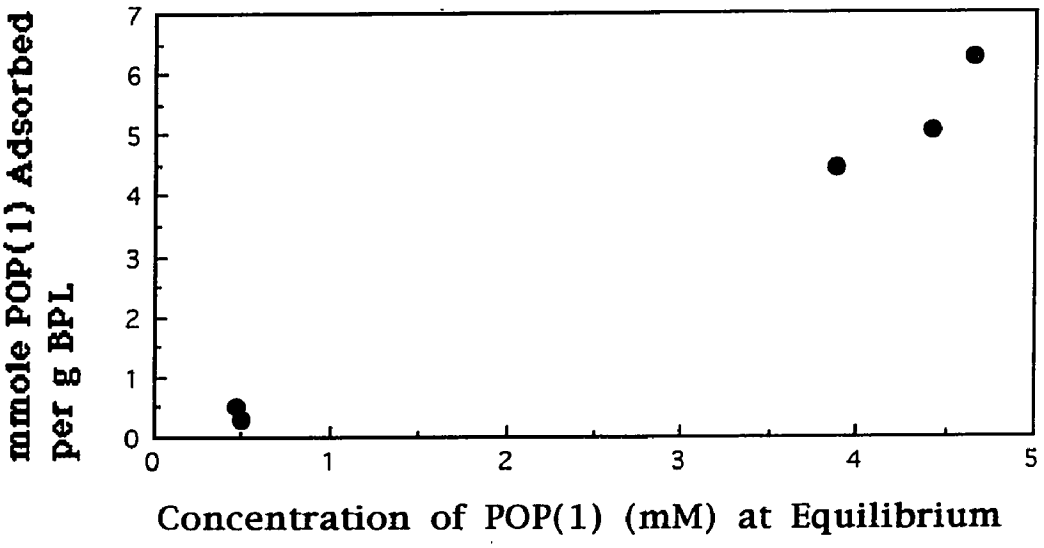

Figure 8. Adsorption Isotherm for POP(1) on BPL

Hydrazine Decomposition

The decomposition of hydrazine hydrate or hydrazine monohydrate was studied on graphite, Aqua A, Mogul L, and Black Pearls L (Table 8) in refluxing IPA. Decomposition was monitored by measuring the amount of gaseous products collected as a function of time using the gas collection apparatus described in the experimental section. Determination of the rate of hydrazine decomposition is discussed below.

Table 8. Hydrazine Decomposition on Several Carbons in Refluxing IPA.

Carbon	Amount (g)	$FeCl_3$ (g)	$[H_4N_2]$ M	IPA (mL)	k_c X 100 $(min^{-1})^a$	Langmuir Order[b]
Graphite[c]	3.037		3.45	10.0	0.3	1.1
Aqua A[c]	0.803	0.402	3.14	11.0	3.2	0.9
Mogul L[d]	0.707		3.14	11.0	0.9	0.9
Mogul L[d]	0.734	0.043	3.14	11.0	1.1	0.8
BLP[d,e]	0.697		3.14	11.0	0.4	1.0
BPL[d,e]	0.098	0.049	3.14	11.0	1.2	0.8

a-complete plots are shown in Appendix 1
b-isotherms are shown in Appendix 2
c-hydrazine monohydrate (1.68 mL)
d-hydrazine hydrate (1.95 mL)
e-BPL-Black Pearls L

Decomposition of hydrazine can lead to either the formation of ammonia and nitrogen (Eq. 20) or to nitrogen and hydrogen (Eq. 21).

$$3\,H_2NNH_2{\bullet}H_2O \rightarrow 4\,NH_3(g) + N_2(g) + 3\,H_2O \quad (20)$$

$$H_2NNH_2{\bullet}H_2O \rightarrow 2\,H_2(g) + N_2(g) + H_2O \quad (21)$$

The gaseous products from the decomposition of hydrazine on Black Pearls L were examined for the presence of hydrogen by gas chromatography (GC). A sample of gas was obtained using a gas syringe through a septum in a Swagelok® Tee in the Tygon® tubing connecting the condenser to the gas collection apparatus. A detection limit of 5%(mol) H_2 in N_2 was determined by examination of known mixtures of hydrogen in nitrogen. The gaseous products from the decomposition of hydrazine on Black Pearls L or Black Pearls L-$FeCl_3$ in refluxing IPA after 75% of the the reaction did not show the presence of hydrogen indicating that the main decomposition pathway is to nitrogen and ammonia (Eq. 20).

Rate constants for the decomposition of hydrazine were determined from the volume of gasses produced. The fraction of hydrazine decomposed was calculated from the ratio of the amount of gas produced (V_t) at time t to the calculated amount of gaseous product. The calculated volume (V_c) was determined from the amount of nitrogen and ammonia produced via Equation 20. Ammonia was included because the amount of gaseous product exceeded the theoretical amount of nitrogen (Eq. 20). The water in the gas collection apparatus was not changed and became saturated with ammonia after a few runs. The data were treated using first, second, and third order rate laws. The rate constant (k_c), following first order kinetics, was determined

from the slope of the $[\ln(1-V_t/V_c)]$ vs. time. A second order rate constant for hydrazine decomposition was obtained from the equation: $(1-V_t/V_c)^{-1} = kt + 1$. A third order rate constant was obtained from $[(1-V_t/V_c)^{-2} = 2kt + 1]$. None of the simple treatments adequately describes the reaction kinetics. First order rates are given for comparison of different carbon catalysts.

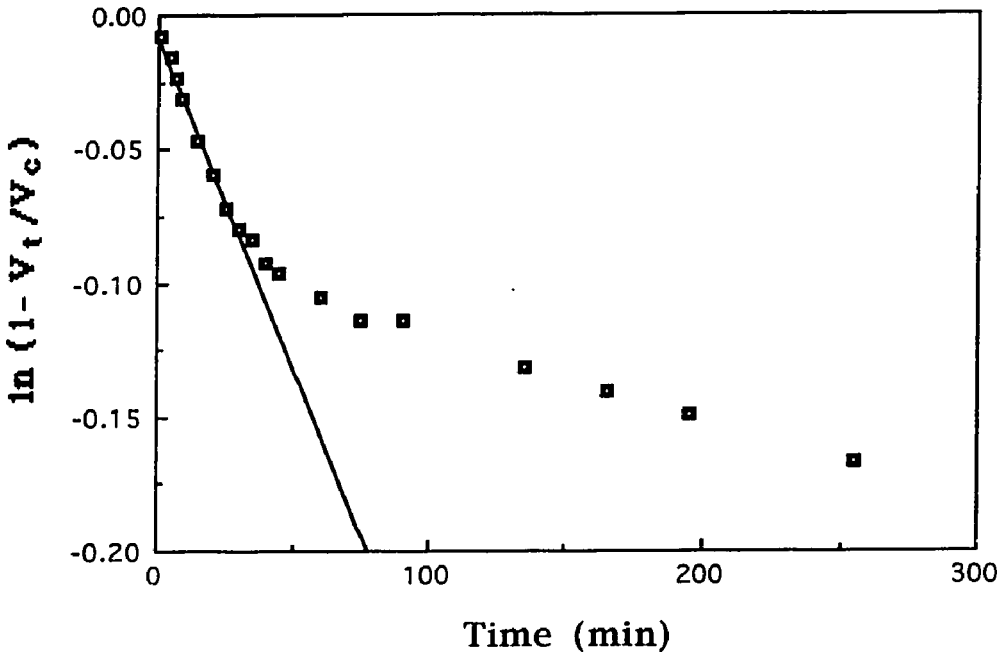

Figure 9. First Order Plot for the Decomposition of Hydrazine on Graphite

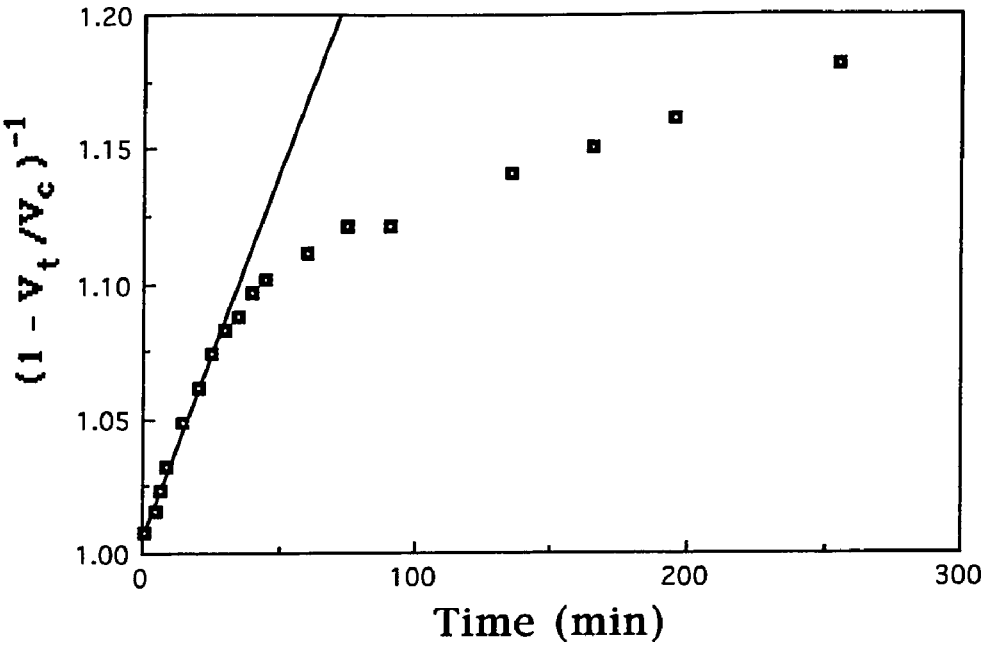

Figure 10. Second Order Treatment of Data from the Decomposition of Hydrazine on Graphite

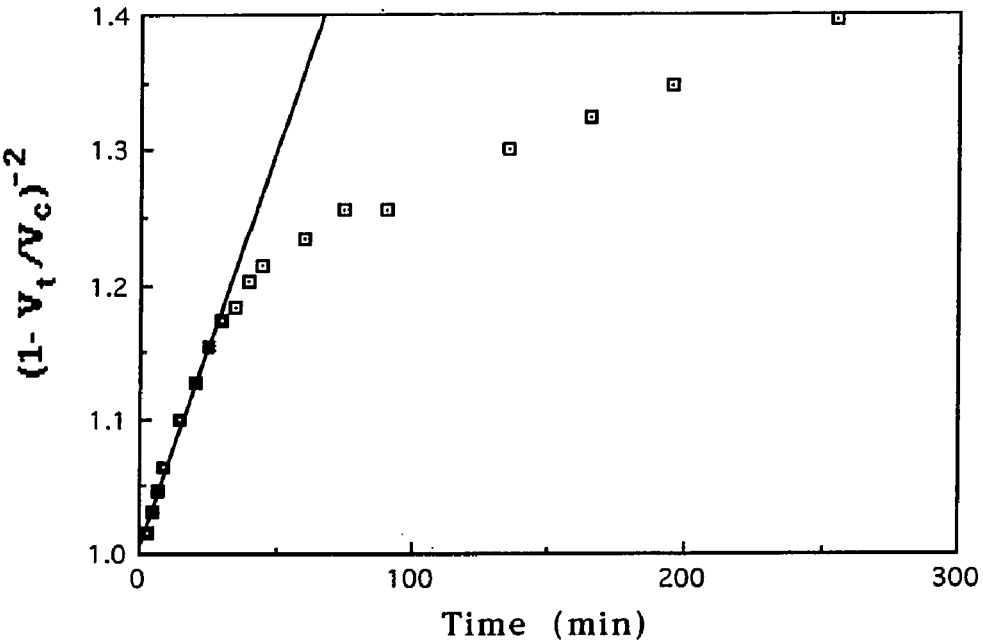

Figure 11. Third Order Kinetics for the Decomposition of Hydrazine on Graphite

First order rates of hydrazine decomposition on several carbonaceous materials are shown in Table 8. Complete plots for the production of gaseous products for these systems are shown in Appendix 1. It should be noted that at long time periods the amount of gaseous products slowly decreases. This may have been caused by the adsorption of ammonia in the water of the gas collection apparatus. The water in the gas collection apparatus became saturated with use, decreasing the amount of ammonia dissolving in the water.

The effect of adding a catalytic amount of $FeCl_3$ on the decomposition of hydrazine was examined because $FeCl_3$ has been shown to enhance the carbon catalyzed hydrazine reduction of nitroaromatic compounds.[25] Hydrazine decomposed at a faster rate when $FeCl_3$ was added to the carbonaceous catalyst (Table 8). In the reduction of a nitro compound, decomposition of hydrazine is important because it competes with the reduction of the nitro compound.

The data from the decomposition of hydrazine on various carbons were also treated using Langmuir adsorption.[57] A Langmuir order for hydrazine adsorption was obtained from the slope of a plot of ln (t) vs. ln (V_t/V_∞). An order of 1 indicates that one reactant is weakly adsorbed on the surface. If a reactant is more strongly adsorbed on the surface the order approaches zero, which is indicative of strong adsorption. The observed orders are shown in Table 8.

Nitro Reduction

The carbon catalyzed hydrazine monohydrate and hydrazine hydrate reductions of nitro aromatic compounds were examined. The conversion of a pure nitroaromatic compound to the corresponding aromatic amine and/or phenylhydroxylamine requires both hydrazine and carbon (Table 9) and could be followed by thin layer chromatography (Table 5, pg 26). Most substrates were completely reduced in 24 h without the formation of any other products. Some reactions, such as the hydrazine hydrate reduction of Nitro HMI with graphite, showed the presence of an intermediate during the reaction. The intermediate was identified as an hydroxylamine, which is discussed below.

Table 9. Control Experiments Using Nitrobenzene in Refluxing IPA

Nitrobenzene (g)	BPL(g)	$H_2NNH_2 \cdot H_2O$(mL)	IPA	results[a]
2.147	0.805		10.0	no reaction
2.135		1.95	10.0	no reaction
2.154	0.706	1.95	10.0	80% aniline

a-after 24 hours in refluxing IPA

Rate constants for the nitroaromatic reductions were determined by following the formation of gaseous products in reactions using 2.0 mole equivalents of hydrazine, a 0.5 mole equivalent more than the stiochiometric amount necessary for complete nitro reduction (Eq. 22). Hydrazine can also decompose under the reaction conditions to nitrogen and ammonia (Eq. 23) as previously described.

$$C_6H_5\text{-}NO_2 + 1.5\ H_2NNH_2\bullet H_2O \rightarrow C_6H_5\text{-}NH_2 + 1.5\ N_2(g) + 2H_2O \quad (22)$$

$$0.5\ H_2NNH_2\bullet H_2O \rightarrow 0.65\ NH_3 + 0.15N_2(g) + 0.5\ H_2O \quad (23)$$

A first order rate constant was determined from the equation: $\ln [1-V_t/V_c] = -kt$; where V_t is the volume of gas produced at time t and V_c is the calculated amount of gas produced when reaction 22 is complete. Measured gas volumes (V_∞) can be used in place of the calculated amount of gas produced (V_c). Rates calculated using V_∞ are similar to those using V_c, and will be discussed for the reduction of Nitro HMI with various carbons. Rate constants using the actual volume (V_∞) of gas produced are a better measure of the rate of gas production because the theoretical amount of gaseous products was never observed in the reduction of nitro aromatic compounds. Discrepancies ranged from 10% to 40%, with most being about 15%. The rate constant determined using the calculated volume of gaseous products is smaller than the rate of nitro reduction derived from the observed amount of gaseous product formation because V_∞ was be smaller than the calculated amount V_c.

Many of the compounds used were unpurified commercial samples used in manufacturing processes. Volumetric measurement of gas production from this heterogeneous reaction was not affected by adsorption of components on the carbon or the opaque nature of the reaction mixture, which would make optical measurements impossible. The data treatment is phenomenological and ignores the fact that the reaction is taking place on a surface. In all of the reactions examined, an excess amount of hydrazine was used. The amount of gas produced indicated that some hydrazine remains after the reduction of the nitro compound has been completed. This was confirmed by a positive spot test for hydrazine.

Stirring. The rate of stirring was examined to insure that adequate mixing had been achieved. Different stirring rates were set by adjusting the setting on a Corning Model PC-351 Stirrer Plate. Differences in stirring rates were visually observed. The rates of gas production observed at all stirring speeds are comparable (Table 10) indicating that the reaction is not mass transport limited. Complete plots are shown in Appendix 3.

Temperature. The hydrazine hydrate reduction of Nitro HMI with graphite was examined in a series of six refluxing alcohols to determine the effect of reaction temperature on the time necessary for complete reduction, determined by TLC.[52] Solvent effects are assumed to be negligible in this rough study. The synthetic utility of the reaction is enhanced if reaction times at various temperatures are known. Alcohols were chosen because

Table 10. Effect of Stirring Speed on the rate of NMB Reduction.

Stir Speed	NMB (g)	graphite (g)	volume (mL)	Rate X 100(min^{-1})[a]
1	0.841	0.102	20	0.9
2	0.84	0.099	20	0.9
4	0.84	0.100	20	1.0
5	0.839	0.098	20	0.9

a-complete plots are shown in Appendix 3

they are inexpensive and environmentally sound. Figure 12 shows that the reaction temperature affects the time necessary for complete nitro reduction, checked by TLC every 30 minutes. A useful index of the effect of solvent and temperature on the reaction rate are provide from these approximate results. Although ethanol seems to be the the best solvent, production considerations favored isopropanol (IPA), which was chosen for development of this reaction. The aromatic amines were readily isolated from isopropanol, unlike ethylene glycol, which required a CH_2Cl_2 extraction for product isolation. IPA was preferred over isobutyl alcohol and isoamyl alcohol because isolation of the aromatic amine was easier due to the lower boiling point of IPA.

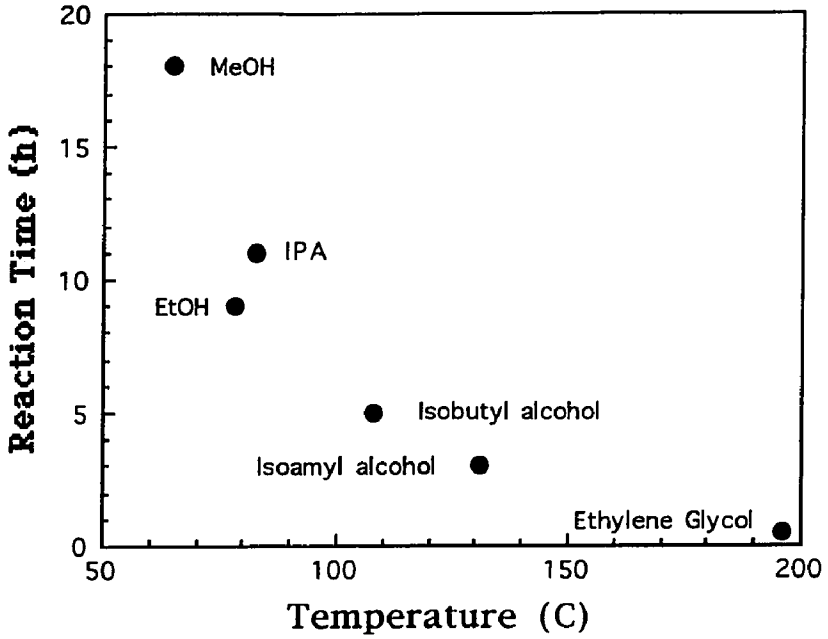

- Reactions carried out using 10 mmol Nitro HMI, 3 g graphite, 20 mmol Hydrazine Monohydrate, and 20 mL Solvent

Figure 12. Time for Complete Reduction of Nitro HMI in Various Alcohols

Nitro Concentration. The effect of varying the concentration of NMB (structure p.15) from 0.121M to 1.48M (hydrazine monohydrate reduction with a ratio of 1g graphite per 1g NMB, Table 11) was examined. Complete reduction (TLC) was observed for all of the reactions. The rate of gas production was greater at higher nitro concentrations without compromising the conversion or the yield. The solubility of NMB in IPA is 1.4g/10ml at room temperature, which limited the maximum concentration. Subsequent reactions were carried out at ~1.5M because complete nitro reduction was

observed in shorter times than at lower concentrations. The concentration of NMB, graphite, and hydrazine were changed in these reactions, although the ratio of NMB to graphite and hydrazine remained constant.

Table 11. Effect of Nitro Concentration on the Rate of Hydrazine Monohydrate Reduction of Nitro Meta Base in Refluxing IPA

M NMB	g NMB[a]	g graphite	IPA (mL)	k_∞ X 100 (min^{-1})[b]
0.121	0.839	0.840	30.0	1.6
0.182	0.842	0.838	20.0	2.4
0.364	0.840	0.838	4.7	4.3
0.762	1.676	1.678	9.3	7.2
1.08	2.00	2.00	7.2	13.
1.48	4.00	4.00	10.0	15.

a-reactions were carried out with two mole equivalents of hydrazine per mole of nitro compound in refluxing IPA
b-complete plots are shown in Appendix 4

Amount of Catalyst. The effect of varying the amount of carbonaceous catalyst for the hydrazine reduction of Nitro Meta Base was examined in refluxing IPA. Data from the reduction of NMB with hydrazine monohydrate in refluxing IPA with various amounts of graphite (Table 12) show that the rate of gas production is affected by the amount of graphite present. The rate decreases with decreasing amounts of graphite. During this study we learned that this substrate used as received from the manufacturer is reduced by hydrazine hydrate in the absence of a catalyst. It is the only

Table 12. Effect of Ratio of Graphite to Nitro Compound on the Hydrazine Hydrate reduction of Nitro Meta Base in Refluxing IPA

Ratio[a]	g NMB[b]	g graphite	IPA (mL)	k_∞ X 100 $(min^{-1})^c$
1.26	0.839	1.06	20.0	3.4
1.02	0.838	0.852	20.0	2.1
0.57	0.830	0.470	20.0	1.6
0.53	0.832	0.439	20.0	2.0
0.12(a)	0.840	0.098	20.0	1.3
0.12(b)	0.839	0.098	20.0	.9
0.06	0.839	0.050	20.0	.7
0.056	0.843	0.047	20.0	.9
0.031(a)	0.840	0.026	20.0	1.0
0.031(b)	0.840	0.026	20.0	1.0
0.0	0.847	0.000	20.0	1.1

a-ratio of graphite to Nitro Meta Base
b-two moles equivalents of hydrazine monohydrate used per mole of nitro compound
c-complete plots are shown in Appendix 5

compound studied showing this behavior. When purified NMB (4.00 g, ethanol recrystallized) was subject to hydrazine monohydrate (1.68 mL) without graphite in refluxing IPA (10.0 mL) no reduction occurred.

The amount of graphite present also affected the rate of gas production for the hydrazine monohydrate reduction of Nitro HPS and POP(1). The rate of gas production decreased for the reduction of Nitro HPS (Table 13) when the amount of graphite was reduced, but complete nitro reduction was observed by TLC. The effect on the rate of gas production for the reduction of POP(1) shows a similar effect for the two reactions examined (Table 13). The

apparent reaction order calculated from the rate data of the reduction of Nitro HPS show that the reaction is first order in graphite.

The amount of catalyst can be reduced without decreasing the conversion, but the rate of gas production decreases. The utility of the hydrazine-carbon reducing system is increased by reducing the amount of catalyst, which decreases stirring problems and cost. We chose to maintain the amount of carbon catalyst at ~15% (wt) of the nitro compound.

Table 13. Effect of Graphite Concentration for Nitro HPS and POP(1)

Substrate	Ratio[a]	Nitro (g)	g graphite	k_∞ X 100(min^{-1})[b]
Nitro HPS[c]	1.0	5.499	5.514	4.0
Nitro HPS[c]	0.30	5.583	1.659	3.7
Nitro HPS[c]	0.10	5.568	0.550	1.2
Nitro HPS[c]	0.05	5.553	0.284	.6
POP(1)[d]	1.0	3.670	3.670	2.0
POP(1)[d]	0.289	3.684	1.063	.9

a-ratio of graphite (g) to nitro compound (g)
b-complete plots are shown in Appendix 6
c-reaction carried out in refluxing IPA (15.0 mL) with hydrazine monohydrate (1.68 mL)
d-reactions carried out in refluxing IPA (10.0 mL) with hydrazine monohydrate (1.68 mL)

Type of Catalyst. We examined a series of 17 carbonaceous materials as catalysts for the hydrazine monohydrate reduction of Nitro HMI. Nitro HMI was chosen for reaction development after encountering the impurity catalyzed reduction of NMB. All of the carbonaceous materials examined catalyzed the reduction of this compound with various rates of gas production (Table 14). First order rates of gas production are shown using both V_∞ and V_c. The rate calculated using V_∞ is always greater than V_c because V_c is never reached. With many of the carbons, a small amount (< 5%) of starting material and/or hydroxylamine were observed by TLC after 24 h (Table 15). To examine the possibility that the reaction could be catalyzed by any surface three non-carbonaceous materials were also investigated (Table 14). Alumina, Cabosil, and Montmorillonite did not catalyze the reduction because no amine, hydroxylamine, or gaseous products formed.

The sample of Aqua A had been in the lab for several years and is no longer commercially available. The effectiveness of this material may be due to oxidation that occurred over time. Nitric acid was used to treat samples of Nuchar SA and Aqua A for several different time periods. Nuchar SA was chosen because it is the replacement product for Aqua A. The rate of gas production is enhanced by oxidizing the carbon with nitric acid (Table 16).

Table 14. Reduction of Nitro HMI with Various Carbons

Carbon	Nitro HMI (g)[a]	Carbon (g)	k_∞ X 100 (min^{-1})	k_c X 100 (min^{-1})[b]
Aqua A	4.915	0.739	6.5	6.2
Beulah Zap Lignite	4.922	0.712	.3	.1
Black Pearls 2000	4.915	0.694	1.2	.6
Coconut Charcoal	4.910	0.702	2.2	1.6
Darco	4.916	0.721	2.2	2.1
Graphite	4.918	0.712	1.6	1.1
Illinois #6 Coal	4.918	0.730	.2	.1
Kingsford Charcoal	4.916	0.713	1.5	.6
Monarch 1300	4.924	0.699	3.6	2.9
Monarch 1000	4.922	0.698	4.0	3.6
Mogul L	4.920	0.760	4.1	3.9
Norit	4.918	0.716	1.3	1.2
Nuchar SA	4.919	0.700	3.7	2.9
Nuchar SA-20	4.915	0.696	2.1	1.9
Nuchar SN-20	4.917	0.718	3.3	2.3
Regal 400R	4.924	0.692	1.4	1.3
Vulcan XC-72R	4.917	0.695	1.6	.2
Alumina	4.916	0.747	no reduction	
Cabosil	4.912	0.160	no reduction	
Montmorillonite	4.914	0.708	no reduction	

a-reaction carried out in refluxing IPA (11.0 mL) with hydrazine monohydrate (1.68 mL)
b-complete plots are shown in Appendix 7

Table 15. TLC Observations for the Reduction of Nitro HMI with Various Carbons

Carbon	Starting Material[a]	Intermediate (hydroxylamine)	k_{∞} X 100 (min^{-1})
Aqua A	-	-	6.5
Beulah Zap Lignite	+	+	.3
Black Pearls 2000	+	+	1.2
Coconut Charcoal	-	+	2.2
Darco	-	-	2.2
Graphite	+	-	1.6
Illinois #6 Coal	+	+	0.2
Kingsford Charcoal	-	+	1.5
Monarch 1300	-	+	3.6
Monarch 1000	-	+	4.0
Mogul L	-	+	4.1
Norit	-	+	1.3
Nuchar SA	+	+	3.7
Nuchar SA-20	+	+	2.1
Nuchar SN-20	+	+	3.3
Regal 400R	-	+	1.4
Vulcan XC-72R	+	+	1.6

a-reactions carried out in refluxing IPA (11.0 mL) with hydrazine monohydrate (1.68 mL) for 24 hr

Table 16. Effect of Nitric Acid Oxidation on the Reduction of Nitro HMI

Carbon	HNO_3 Treatment	Nitro HMI (g)[a]	Carbon (g)	k_∞ X 100 (min^{-1})[b]
Nuchar SA		0.721	2.0	3.7
Nuchar SA	contact	4.918	0.696	7.5
Nuchar SA	1 h	4.914	0.716	6.1
Nuchar SA	16 h	4.923	0.706	5.9
Aqua A		4.915	0.739	6.5
Aqua A	1h	4.915	0.726	6.0
Aqua A	24 h	4.914	0.724	6.2

a-reductions carried out in refluxing IPA (11.0 mL) with hydrazine monohydrate (1.68 mL)
b-complete plots are shown in Appendix 8

The hydrazine hydrate reduction of POP(1) was examined using some of the same types of carbon used for the reduction of Nitro HMI. The six carbons examined catalyzed the reduction of POP(1) (Table 17). Thin layer chromatography showed complete conversion of the nitro to the aromatic amine for all of the carbons except Kingsford Charcoal. The rate of gas production is affected by the catalyst.

Table 17. Reduction of POP(1) using Various Carbons

Carbon	POP(1) (g)[a]	Carbon (g)	k_{∞} X 100 (min^{-1})[b]
Aqua A	3.691	0.737	5.0
Graphite	3.684	1.063	.9
Darco	3.703	0.709	1.9
Coconut	3.694	0.713	1.3
Kingsford	3.730	0.700	1.4
Norit	3.682	0.726	1.7

a-reductions carried out in refluxing IPA (10.0 mL) with hydrazine monohydrate (1.68 mL)
b-complete plots are shown in Appendix 9

Effect of Metal Ions. Several metal ions (9) were examined as co-catalysts with a carbon. Based on the rate enhancement of iron trichloride on the carbon catalyzed reduction of nitroaromatic compounds reported by Han,[24] we examined a variety of other transition metals as co-catalysts, most of which can act as a Lewis Acid. A moderately effective carbon, Darco, was chosen for these experiments so that both rate enhancements and decreases could be observed. Nitro HMI (~4.92 g) was reduced in the presence of a catalytic amount of the metal ion and Darco (~0.7 g) with hydrazine monohydrate (1.68 mL) in refluxing IPA (11.0 mL). The fastest rate of gas production with complete nitro reduction (TLC) was observed (Table 18) with $FeCl_3$ as a co-catalyst. Some of the other transition metals examined accelerated the rate of gas production.

The effect of varying the amount of $FeCl_3$ with a constant amount of carbon was examined for the hydrazine monohydrate reduction of Nitro HMI. The data (Table 19) show that the rate of gas production is more dependent on the amount of carbon than on the amount of $FeCl_3$. An apparent reaction order in $FeCl_3$ is calculated to be much less than one using the two data points available.

Table 18. Effect of Several Metal Ions on the Reduction of Nitro HMI

Metal	Nitro HMI (g)[a]	Darco (g)	Metal (g)	k_∞ X 100 (min^{-1})[b]	Acidity[58]
none	4.916	0.721		2.2	
$FeCl_3$	4.923	0.698	0.044	4.5	Hard Acid
$CrCl_3 \cdot 6H_2O$	4.915	0.712	0.046	2.8	Hard Acid
$MnCl_2$	4.919	0.704	0.046	2.7	Hard Acid
$SnCl_4$	4.922	0.700	0.051	2.2	Hard Acid
$TiCl_4$	4.925	0.687	0.115	1.9	Hard Acid
$CoCl_2 \cdot 6H_2O$	4.919	0.706	0.201	2.9	Borderline
$CuCl_2$	4.921	0.725	0.030	2.2	Borderline
$ZnCl_2$	4.923	0.698	0.027	2.0	Borderline
$NiCl_2 \cdot 6H_2O$	4.920	0.710	0.044	1.9	Borderline

a-reactions carried out in refluxing IPA (11.0 mL) with hydrazine monohydrate (1.68 mL).
b-complete plots are shown in Appendix 10

Table 19. Effect of Aqua A and $FeCl_3$ Concentrations on the Rate of Nitro HMI Reduction

g Nitro HMI[a]	g Aqua A	g $FeCl_3$	k_{∞} X 100 (min^{-1})[b]
4.915	0.739		6.5
4.915	0.351	0.019	7.0
4.918	0.380	0.109	6.4
4.918	0.721	0.018	12.
4.915	0.690	0.053	11.

a-reactions carried out using hydrazine monohydrate (1.68 mL) in refluxing IPA (11.0 mL)

b-complete plots are shown in Appendix 11

Hydrazine hydrate reductions carried out with a carbon (Mogul L or Black Pearls L (BPL)) catalyst did not always convert the nitro compound to the amine quantitatively, particularly in the case of Nitro HMI and Nitro HNBS. Both NMR and TLC indicated the presence of a small amount (< 4%, NMR) of starting material and/or the hydroxylamine after 24 h. The addition of $FeCl_3$ (0.042 g) to the hydrazine hydrate (1.95 mL) reduction of Nitro HNBS (3.79 g) in the presence of BPL (0.70 g) increased the rate of gas production (k=0.015 min^{-1}, k=0.16 min^{-1} w/$FeCl_3$) and completely converted the nitro to the amine (the product only contained the aniline by NMR). Complete conversion of Nitro HMI (4.915 g) using hydrazine hydrate (1.95 mL) with Mogul L (0.716 g)-$FeCl_3$(0.043 g) in refluxing IPA (11.0 mL) was observed,

whereas without iron (4.918 g HMI, 0.694 g Mogul L, 1.95 mL hydrazine hydrate, 11.0 mL IPA) the presence of an intermediate was observed by TLC. The addition of a catalytic amount of $FeCl_3$ increased the conversion to 100% for the substrates examined.

To check for catalysis by metals adsorbed or present in the carbon catalyst ethylenediaminetetraacetic acid (EDTA) was used to complex any metals present. EDTA (0.101 g) was added to the hydrazine monohydrate (1.68 mL) reduction of Nitro HMI (4.917 g) in refluxing IPA (11.0 mL) in the presence of Darco (0.774 g). EDTA was stirred with the carbon and nitro compound for 45 minutes in refluxing IPA (11.0 mL) prior to the addition of the hydrazine monohydrate. The reduction still occurred, but compared with Darco alone ($k=0.022\ min^{-1}$) the rate of gas production was reduced ($k=0.017\ min^{-1}$) slightly by the EDTA treatment.

Catalyst Age. Catalyst reusability was examined with the aim of reducing cost and the amount of waste. The catalyst was recovered from the reduction by filtration then dried and reused. The rate of gas production (Table 20) for the reduction of Nitro HMI (~4.91 g) using hydrazine hydrate (1.95 mL) with Mogul L(0.716 g)-$FeCl_3$(0.043 g) in refluxing IPA (11 mL) decreased with repeated use of catalyst. After the rate dropped significantly, more $FeCl_3$ (0.050 g) was added, but the rate did not change. A similar decrease in rate with usage (Table 21) was observed for Black Pearls L(0.702 g)-$FeCl_3$ (0.091 g). Black Pearls L(0.700 g)-$FeCl_3$ (0.130 g) was used to catalyze the hydrazine hydrate (1.95 mL) reduction of Nitro HPS (~5.5 g) in refluxing IPA (15.0 mL). The rate increased with usage for several runs (Table 22).

Complete conversion (no nitro or hydroxylamine by TLC) was observed for successive runs, but there was a reduction in the amount of catalyst recovered. The rates were normalized for the amount of carbon used in successive runs (Tables 20,21).

Table 20. Reusability of Mogul L-$FeCl_3$ for the Reduction of Nitro HMI

Run #	Nitro HMI (g)[a]	Catalyst Used(g)	Catalyst Recovered (g)	k_∞ X 100 (min^{-1})[b]	Normalized k X 100 (min^{-1})
1	4.915	0.759[c]	0.699	9.9	9.9
2	4.920	0.699	0.744	8.5	9.2
3	4.920	0.744	0.796	9.5	9.7
4	4.920	0.796	0.581	4.4	4.6
5	4.922	0.631[d]	0.448	3.0	3.6
6	4.919	0.448	0.448	3.0	5.1
7	4.925	0.448	0.335	2.9	4.9
8	4.914	0.335	0.311	2.5	5.7

a-reaction carried out in refluxing IPA (11.0 mL) with hydrazine hydrate (1.95 mL)
b-complete plots are shown in Appendix 12
c-0.716 g Mogul L and 0.043 g $FeCl_3$
d-0.050 g $FeCl_3$ added

Table 21. Reusability of Black Pearls L-$FeCl_3$ for the reduction of Nitro HMI

Run	Nitro HMI (g)[a]	Catalyst Used(g)	Catalyst Recovered (g)	k_∞ X 100 (min^{-1})[b]	Normalized k X 100 (min^{-1})
1	4.920	0.793[c]	0.800	7.0	7.0
2	4.928	0.800	0.696	6.3	6.2
3	4.923	0.696	0.635	5.7	6.5
4	4.915	0.635	0.531	4.7	5.9
5	4.930	0.531	0.559	3.3	4.9

a-reduction carried out in refluxing IPA (11.0 mL) with hydrazine hydrate (1.95 mL)

b-complete plots are shown in Appendix 13

c-0.072g Black Pearls L and 0.091 g $FeCl_3$

Table 22. Reusability of Black Pearls L for the Reduction of HPS

Run #	Nitro HPS (g)[a]	Catalyst Used(g)	Catalyst Recovered (g)	k_∞ X 100 (min^{-1})[b]
1	5.561	0.713[c]	0.940	3.9
2	5.564	0.940	0.740	7.7
3	5.552	0.740	0.590	7.5
4	5.559	0.590	0.360	7.0
5	5.563	0.360	0.175	4.7

a-reaction carried out in refluxing IPA (15.0 mL) with hydrazine hydrate (1.95 mL)

b-complete plots are shown in Appendix 14

c-0.700 g Black Pearls L and 0.130 g $FeCl_3$

Effect of Water Content. The effect of using hydrazine hydrate (55% hydrazine, 1.95 mL) rather than hydrazine monohydrate (85% hydrazine, 1.68 mL) was examined for the reduction of Nitro HMI (~4.9 g) in refluxing IPA (11.0 mL) in the presence of carbon (~0.7 g Nuchar SA). Hydrazine hydrate is preferred over hydrazine monohydrate because the hydrate is less expensive and has a higher flash point.[38] The data (Table 23) show that the rate of gas production for the reduction of Nitro HMI decreased when additional water was present. The effect of using hydrazine hydrate was also examined for the Aqua A (~0.7 g) catalyzed reduction of Nitro HPS (~5.53 g) in refluxing IPA (15.0 mL). Complete reduction (TLC) was obtained with both reagents and a slightly faster rate of gas production (Table 23) was observed for the monohydrate.

The effect of water on the reduction of nitrobenzene was further examined by conducting an experiment under anhydrous conditions. Nitrobenzene (2.158 g) was reduced with anhydrous hydrazine (1.192 g) in refluxing THF (10.0 mL) with Black Pearls L (0.693 g). An alliquot removed after 3h showed 50% starting material by NMR, 43% β-phenylhydroxylamine, and 6% aniline. After 24h: 47% nitrobenzene, 5% β-phenylhydroxylamine, and 47% aniline. The reduction of nitrobenzene (2.147 g) with hydrazine hydrate (1.95 mL) in refluxing THF (10.0 mL) in the presence of Black Pearls L (0.689 g) also showed the presence of β-phenylhydroxylamine (21%) and aniline (7%) after 3h. After 24 h the product mixture was composed of 33% aniline and 66% nitrobenzene.

pH of the Reaction. The initial pH of the nitrobenzene reaction mixture was 11.96, measured by a glass electrode. pH paper indicated a pH of approximately 12.

Table 23. The Reduction of Several Substrates Using Hydrazine Hydrate and Hydrazine Monohydrate

Substrate	Carbon	Nitro (g)	g Carbon	hydrazine	k_∞ X 100 $(min^{-1})^a$
Nitro HMI[b]	Nuchar SA	4.919	0.700	monohydrate	3.7
Nitro HMI[b]	Nuchar SA	4.919	0.711	hydrate	2.3
Nitro HPS[c]	Aqua A	5.530	0.700	monohydrate	5.6
Nitro HPS[c]	Aqua A	5.535	0.704	hydrate	4.2

a-complete plots are shown in Appendix 15
b-reaction carried out in refluxing IPA (11.0 mL) with 2.0 mol eq of the hydrazine
c-reaction carried out in refluxing IPA (15.0 mL) with 2.0 mol eq of the hydrazine

Other Nitro Compounds. The reduction of a series of substituted nitrobenzenes was examined to investigate substituent effects. The results are summarized in Table 24. In all cases NMR indicated that the substituent group was not modified by the reaction conditions.

Table 24. Reduction of Substituted Nitrobenzenes

Substitution	σ^{+}[59]	g Compound[a]	BPL (g)	NMR[b] Yield	k_{∞} X 100 (min^{-1})[c]
3-CF_3		3.249	0.692	66	1.8
3-I	0.36	4.329	0.704	86	1.4
4-Br	0.15	3.508	0.711	83	1.7
4-Cl	0.11	2.750	0.697	56	1.5
H	0.0	2.154	0.706	80	1.5
4-CH_3	-0.30	2.379	0.692	23	1.9
4-OCH_3	-0.78	2.653	0.694	30	2.2
4-OH	-0.92	2.431	0.730	38	1.9
4-NH_2	-1.30	2.421	0.706	50	2.0

a-reactions carried out in refluxing IPA (10.0 mL) with hydrazine hydrate (1.95 mL)
b-after 24 h
c-initial rates, complete plots are shown in Appendix 16

Attempts to Trap Reaction Intermediates

The reduction of 2-amino-2'-nitrobiphenyl was examined to try to trap a nitroso intermediate. Since the amine is in close proximity to the nitro, coupling could ocurr if the reduction proceeded through a nitroso intermediate. The hydrazine hydrate (0.48 mL) reduction of 2-amino-2'nitrobiphenyl (0.928 g) was carried out in refluxing IPA (5.0 mL) with Black Pearls L (0.165 g). The only product (NMR, Figure 13) from the reaction after 24 h was 2,2'-diaminobiphenyl (37.5% conversion).

2-Nitrobiphenyl (1.825 g) was treated with anhydrous hydrazine (0.75 mL) in refluxing THF (15 mL) in the presence of Black Pearls L (0.322 g). The formation of carbazole from the reduction could be rationalized by a nitrene intermediate,[60] however the only product of this reaction after 24 h was 2-aminobiphenyl (41%).

2,2'-Dinitrobiphenyl (2.131 g) was also reduced with hydrazine hydrate (1.95 mL) and Black Pearls L (0.778 g) in refluxing IPA (10.0 mL). After 24 h the isolated material consisted of (NMR): starting material (55%), benzo[c]cinnoline (3.5%) and benzo[c]cinnoline n-oxide (41%).

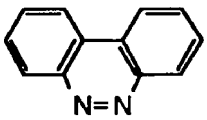

Benzo[c]cinnoline

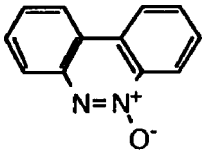

Benzo[c]cinnoline n-oxide

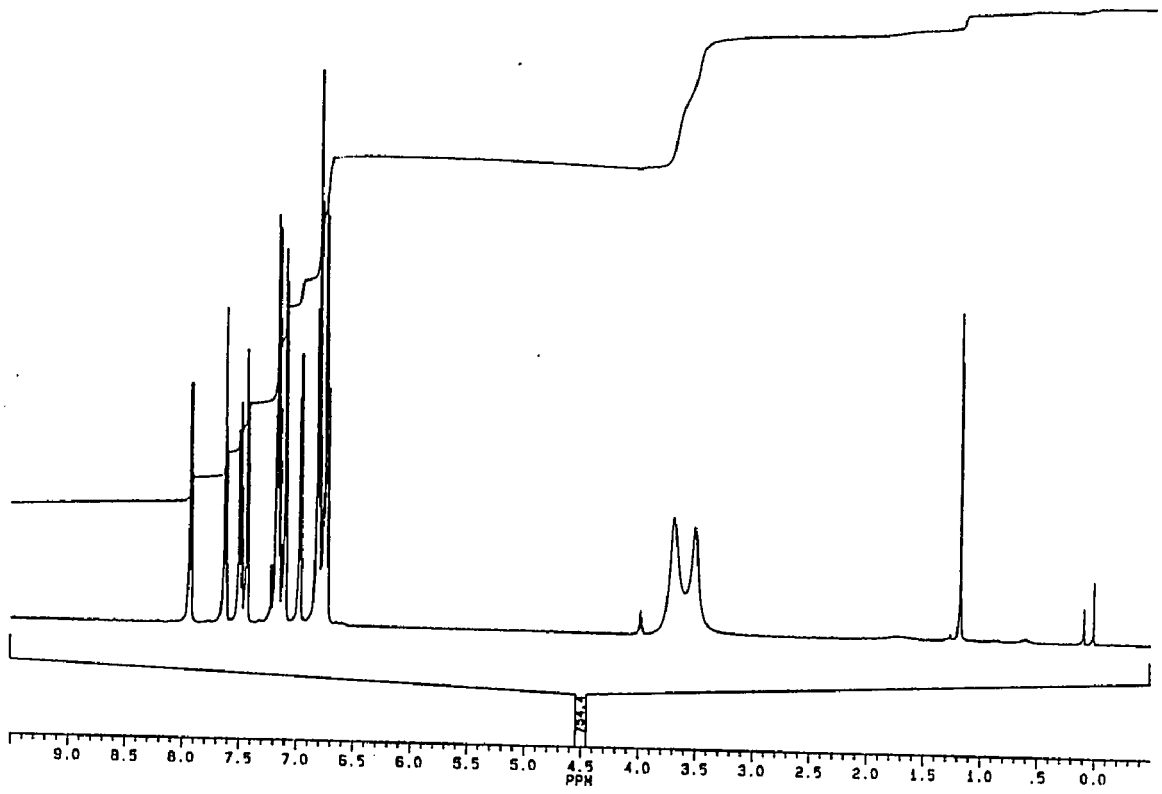

Figure 13. NMR Spectrum of the Product from the Reduction of 2-Amino-2'-nitrobiphenyl With Hydrazine Hydrate and Black Pearls L in Refluxing IPA

The reduction of 4,4'-dinitrobenzanilide was examined to determine whether there is preferential reduction of either of the nitro groups. Aliquots (1 mL) of solution were removed from the reaction mixture of 4,4'-dinitrobenzanilide (4.50 g) with hydrazine monohydrate (5.0 mL) in refluxing IPA (15 mL) with Black Pearls L (0.35 g). The samples were analyzed using NMR and compared with authentic samples of possible intermediates. The spectra indicate that the nitro group on the ring attached to the carbonyl is reduced first, resulting in formation of 4-amino-4'-nitrobenzanilide, as shown below.

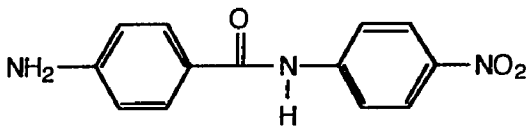

Reduction of an Aliphatic Nitro Compound

Nitrocyclohexane (2.182 g) was treated with hydrazine hydrate (1.95 mL) in refluxing IPA (10.0 mL) in the presence of Black Pearls L (0.670 g). Only starting material (2.01g) was recovered after 24 h. Ferric chloride (0.059 g) in combination with Black Pearls L (0.714 g) for the hydrazine hydrate (1.95 mL) reduction of nitrocyclohexane (2.218 g) did not catalyze the reaction.

Substrates Other than Nitro Compounds

Nitro groups can be classified as 1,3-dipoles ($X^+=Y-Z^-$). The possibility of the nitroaromatic group acting as a 1,3-dipole in the carbon catalyzed hydrazine reduction to an aromatic amine was studied by examining the reactivity of phenyl azide, N-phenyl-phenylnitrone, benzonitrile oxide, and azoxybenzene. The reduction of phenyl azide (0.520 g) with hydrazine

hydrate (0.50 mL) in the presence of Black Pearls L (0.176 g) in refluxing IPA (11.0 mL) showed (NMR) aniline (8%) and phenyl azide (92%) after 24 h.

The hydrazine hydrate (0.50 mL) reduction of N-phenyl-phenylnitrone [PhC(H)=N^+Ph(O^-)] was examined. In refluxing IPA (10.0 mL) with Black Pearls L, the nitrone (0.716 g) was converted to aniline (46%), benzaldehyde hydrazone [$C_6H_5CHN=NH_2$ (29%, NMR): benzylic proton at 7.55 ppm(s 1H), aromatic protons: 7.42 ppm(d, 8.9 Hz, 2H), 7.22 ppm (t, 8.9 Hz, 2H) and 7.18 ppm (d, 8.9 Hz, 1H)], GC/MS (m/z: 120, 103, 93, 77, 65, 51)], and dibenzal hydrazine [$C_6H_5CH=N-N=CHC_6H_5$ (25%), NMR: (benzylic proton at 8.58 ppm (s), aromatic protons: 7.85 ppm (d, 7.1 Hz, 2H) and 7.43ppm (m, 3H), GC/MS (mz: 182, 152, 105, 77, 64, 51)]. A comparable reaction monitored by TLC indicates that N-phenyl-phenylnitrone is rapidly hydrolyzed (within two minutes) to benzaldehyde and β-phenylhydroxylamine. In the absence of carbon, aniline (3%), β-phenylhydroxylamine (28%), and benzaldehyde hydrazone (69%) were recovered after 24 h.

Benzohydroxamoyl chloride was reduced *in situ* to generate benzonitrile oxide (Eq. 24). The benzonitrile oxide produced from benzohydroxamoyl chloride (0.586 g) reacted with hydrazine hydrate (2.0 mL) in refluxing IPA (10.0 mL) to produce benzaldehyde oxime (Eq. 25). The same result, by NMR analysis of the product, was obtained from the hydrazine

$$\varphi C(Cl)=N-O-H \rightarrow \varphi C\equiv N^+O^- + HCl \quad (24)$$

$$2\,\varphi C\equiv N^+O^- + H_4N_2 \rightarrow 2\,\varphi CH=N-O-H + N_2 \quad (25)$$

hydrate (5.0 mL) reduction of benzohydroxamoyl chloride (1.07 g) in refluxing IPA (20.0 mL) in the presence of Black Pearls L (0.430 g).

The hydrazine hydrate (1.95 mL) reduction of azoxybenzene (3.288 g) was examined in refluxing IPA (10.0 mL) with Black Pearls L (0.934 g). Azobenzene (39%, NMR), aniline (7%), and azoxybenzene (54%) were recovered. Only starting material (3.405 g azoxybenzene, NMR) was recovered in the absence of carbon in refluxing IPA (10.0 mL) after 24 h.

The reduction of benzophenone, 9-fluorenone and syn-benzaldehyde oxime were investigated. Benzophenone (0.364 g) and 9-fluorenone (0.374 g) were subject to hydrazine monohydrate (0.3 mL) with graphite (0.8 g) in refluxing IPA (10 mL). Only the hydrazones of these compounds were isolated after 24 h. syn-Benzaldehyde oxime (0.246 g) was unaffected after 24 h in the presence of hydrazine monohydrate (0.35 mL) with graphite (0.78 g) in refluxing IPA (10 mL).

Isolation of HMI Hydroxylamine from the Hydrazine Hydrate Reduction of Nitro HMI

As previously mentioned, the reduction of Nitro HMI with hydrazine hydrate sometimes produced an intermediate product. This intermediate could be formed in larger quantities by reducing purified Nitro HMI (8.52 g, 30 mmol) in refluxing THF (30.0 mL) with hydrazine hydrate (40 mmol) in the presence of Black Pearls L (5.2 g). The product (6.2 g) was isolated by removal of THF under vacuum and purified by flash column chromatography [silica gel (500 mL), 1.5 l eluent CH_2Cl_2:hexane 3:1]. This product was identified as the hydroxylamine of Nitro HMI by NMR (Figure 14).

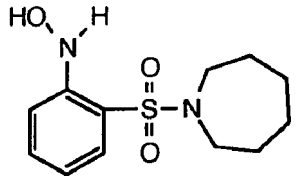

Hydroxylamine of Nitro HMI

The aliphatic protons on the seven membered ring have the same chemical shifts and splitting patterns as HMI (aniline) [1.50 ppm (s, 4H); 1.65 ppm (s, 4H); 3.25 ppm(t, 3.o Hz, 4H)]. The aromatic protons are located at 6.88 ppm (t, 8.Hz, 1H), 7.38 ppm (m, 2H), 7.59 ppm (d, 8.7 Hz, 1H). The amino proton is at 5.22 ppm (bs, 1H) and the hydroxyl proton is at 8.53 ppm (bs, 1H). The hydroxylamine of Nitro HMI (80% yield) was also produced from the zinc (3.01 g) reduction[51] of purified (ethanol recrystallization) Nitro HMI (5.065 g) with ammonium chloride (1.17 g) in water (30 mL), which had an NMR spectrum identical to the material isolated from the hydrazine reduction of Nitro HMI. This material was completely reduced to the aniline with hydrazine in the presence of Black Pearls L in refluxing IPA.

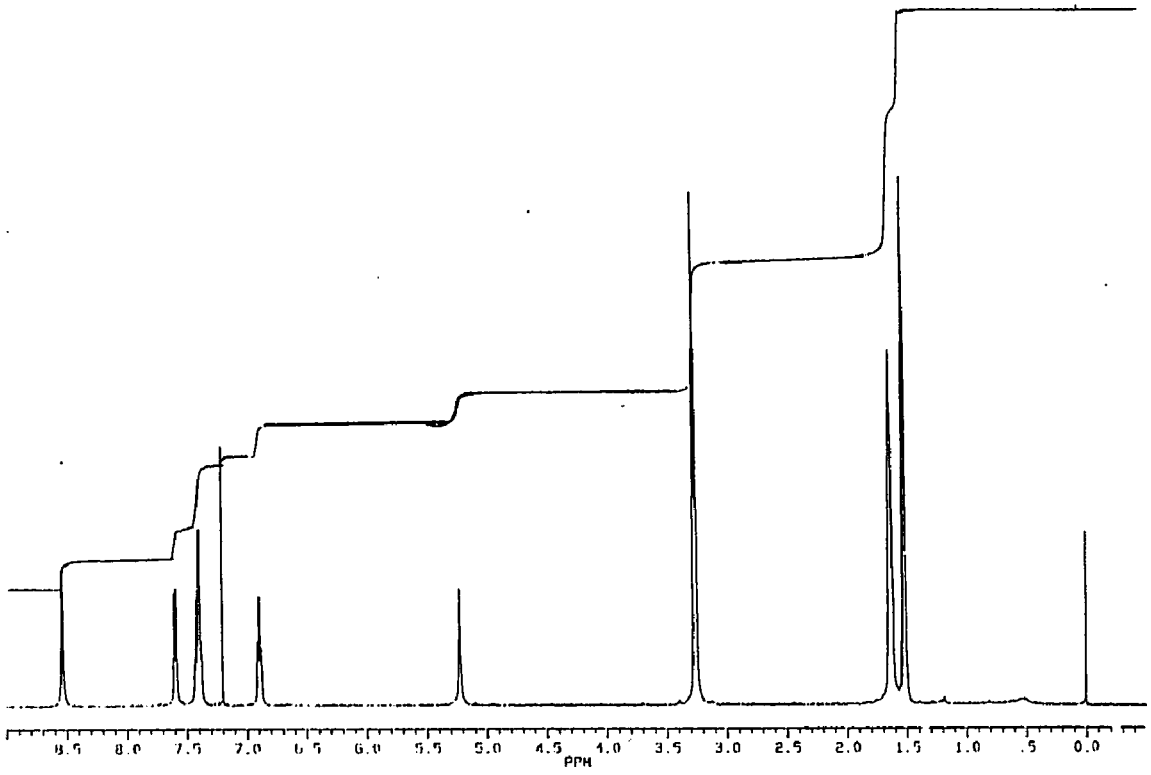

Figure 14. NMR Spectrum of the Hydroxylamine of Nitro HMI

The reduction of nitrobenzene followed by NMR also showed the formation of a hydroxylamine. Nitrobenzene (0.476), Black Pearls L (0.0337 g), $D_2NNH_2 \cdot D_2O$ (0.125 g), and glyme-d_{10} (0.512 g) were placed in a 5mm NMR tube. Glyme was used so the reaction could be carried out at 80°C without solvent loss. An NMR spectrum was obtained prior to heating the sample. The sample was heated in a water bath at 80°C for 60 minutes, cooled, and an NMR spectrum obtained. This procedure was repeated at one hour intervals for a total reaction time of 5 hours. The spectra are shown in Figure 15. β-Phenylhydroxylamine is formed prior to the formation of aniline. There were no other products or intermediates observed.

Behavior of Conventional Intermediates (Nitrosobenzene, Phenylhydroxylamine) Under the Reaction Conditions

The behavior of possible reaction intermediates under the reaction conditions used was investigated. Nitrosobenzene (1.871 g) was reduced with hydrazine hydrate (1,95 mL) in refluxing IPA (10.0 mL) in the presence of Black Pearls L (0.706 g). When hydrazine hydrate was added to the mixture of nitrosobenzene and carbon in refluxing IPA, extreme foaming occurred. After 2 minutes the formation of azoxybenzene was observed (TLC, CH_2Cl_2); after 30 minutes azobenzene, azoxybenzene, hydrazobenzene, and aniline were observed (TLC). Azobenzene (3%), azoxybenzene (47%), and aniline (50%) were formed after 24 h (NMR). β-Phenylhydroxylamine (1.887 g) in refluxing IPA (10.0 mL) with Black Pearls L (0.698 g) and hydrazine hydrate (1.95 mL) gave no reaction after 2 minutes (TLC). Starting material, aniline, azobenzene, azoxybenzene, and hydrazobenzene were formed (TLC) after

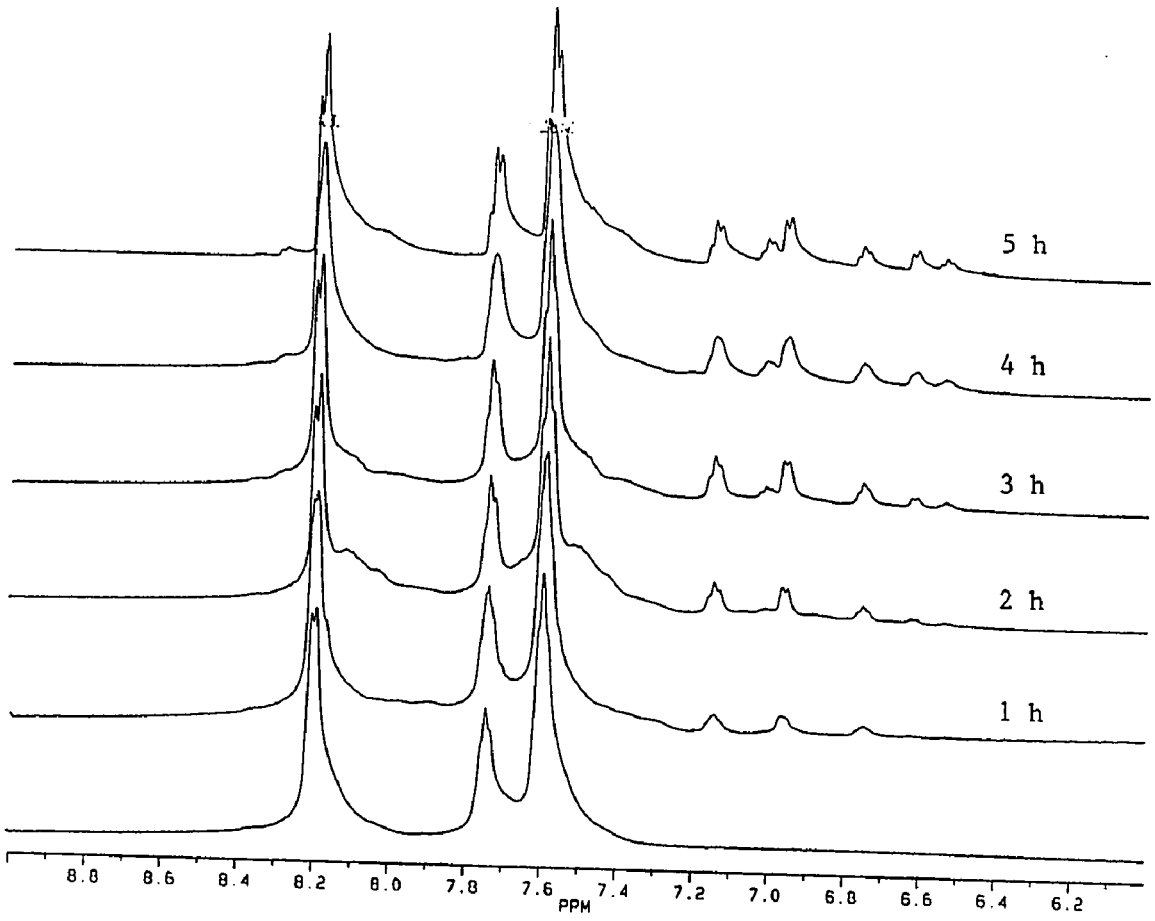

Figure 15. Reduction of Nitrobenzene in Glyme-d_{10} with $D_2NND_2 \bullet D_2O$ in an NMR Tube at 80°C with Black Pearls L

60 min. With increased reaction time more starting material was consumed, the amount of aniline increased and the amount of azoxybenzene and hydrazobenzene decreased. After 24 h the mixture contained (NMR): aniline (50%), azoxybenzene (3%), and azobenzene (47%).

The reactivity of nitrosobenzene and β-phenylhydroxylamine was also examined in the absence of hydrazine and/or carbon. Coupled products (Table 25, Table 26) were formed from nitrosobenzene in the absence of hydrazine and/or Black Pearls L within 30 minutes (TLC). Coupled products are also formed from β-phenylhydroxylamine with and without carbon and/or hydrazine after the reaction had been refluxing for 1 h.

The reduction of the coupled products was also investigated. The reduction of azobenzene (3.200 g) with hydrazine hydrate (1.95 mL) in refluxing IPA (10.0 mL) in the presence of Black Pearls L (0.555 g) produced 36% aniline after 24 h. The balance (64%) was starting material. The reduction of azoxybenzene has already been described. Hydrazobenzene (1.184 g) in refluxing IPA (10 mL) with Black Pearls L (0.490 g) (no hydrazine) is completely converted to azobenzene (92%) and aniline (8%) after 24 h.

Table 25. Products Obtained in 24 h From the Reduction of Nitrobenzene, Nitrosobenzene, and in the Presence of Carbon and/or Hydrazine

			Reaction Products				
	C[a]	H_4N_2	φ-NO_2	φ-NH(OH)	φ-NH_2	φ-N=N-φ	φ-N=N(O)-φ
φ-NO_2	(IPA)						
	X	X	20		80		
		X	100				
	(THF, anhydrous)						
	X	X	47	5	47		
φ-N=O	(IPA)						
	X	X			64	34	2
		X				10	90
	X				57	7	36
	-	-				15	85
φ-NH(OH)	(IPA)						
	X	X			50	47	3
		X		29	60	8	3
	X				42		58
	-	-		60	11	17	11

a-X-indicates that the component was present for a particular reaction, Black Pearls L used for all of the reactions

Table 26. Reaction Conditions for Nitrosobenzene and β-Phenylhydroxylamine Reduction.

	Starting Material (g)	C(g)	H_4N_2(mL)	IPA (mL)
φ-N=O				
	2.151	-	1.95	10.0
	2.127	0.649	-	10.0
	0.872	-	-	5.0
φ-NH(OH)				
	1.874	-	1.95	10.0
	0.755	0.547	-	5.0
	0.714	-	-	5.0

The experimental procedure was examined to see if small amounts of coupled products could be observed. Nitrosobenzene (0.022 g) was added to a refluxing mixture of aniline (1.895 g) and Black Pearls L (0.504 g) in IPA (10.0 mL). After 24 h the mixture was filtered and the solvent was removed. An NMR (Figure 16) of the isolated product shows that 1% azobenzene, formed by the coupling of aniline and nitrosobenzene, could be detected.

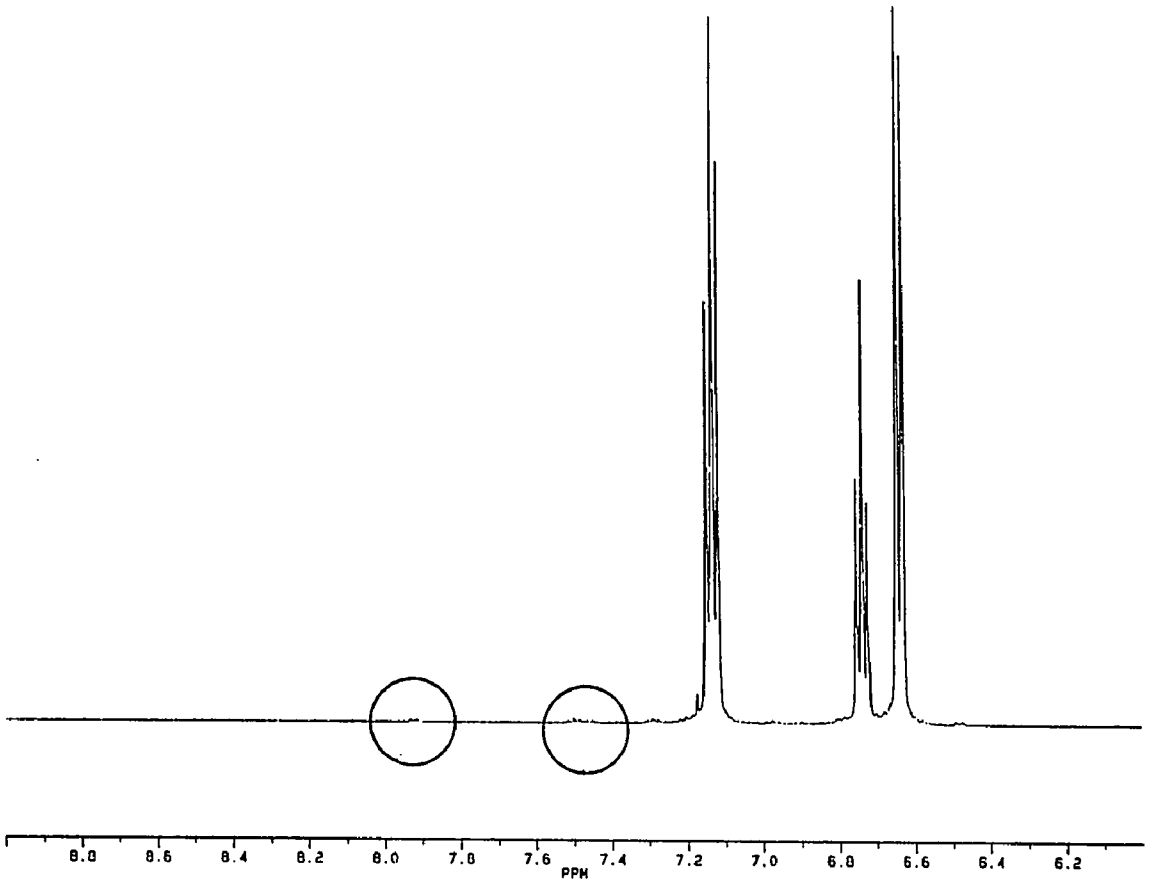

Figure 16. NMR of the Product of 1% Nitrosobenzene with Aniline in REfluxing IPA with Black Pearls L

Substituted Hydrazines

1,1-Dimethylhydrazine. The reduction of Nitro HMI was studied using dimethyl hydrazines. Nitro HMI (4.917 g) was reduced with 1,1-dimethylhydrazine (4.290 g) in refluxing IPA (11.0 mL) in the presence of Black Pearls L (0.704 g). Gaseous products were swept from the reaction with a stream of nitrogen and trapped at -78°C. The gaseous product was identified by IR (Figure 17) as N,N-dimethylamine. The recovered material (NMR) consisted of hydroxylamine (3%) and aniline (97%). Complete reduction of Nitro HMI (4.916 g) to the aniline was observed with 1,1-dimethylhydrazine (5.0 g) in the presence of Black Pearls L (0.698 g) and $FeCl_3$ (0.057 g) in refluxing IPA (11 mL). In the absence of carbon, complete reduction of Nitro HMI (2.457 g) was observed with 1,1-dimethylhydrazine (2.4 g) with $FeCl_3$ (0.040 g) in refluxing IPA (5.0 mL). There were no gaseous products formed from 1,1-dimethylhydrazine (2.0 g) alone in refluxing IPA (5.5 mL) with Black Pearls L (0.345 g). NMR and TLC indicated that no reduction of Nitro HMI (2.467 g) was not reduced in refluxing IPA (5.0 mL) with 1,1-dimethylhydrazine (2.393 g) after 24 h when carbon and $FeCl_3$ were omitted.

1,2-Dimethylhydrazine. Nitro HMI was also reduced with 1,2-dimethylhydrazine dihydrochloride. An aqueous (10.0 mL) solution of 1,2-dimethylhydrazine dihydrochloride (1.78 g) was added to a refluxing mixture of Nitro HMI (1.230 g), sodium carbonate hexahydrate (3.833 g) in IPA (10.0 mL). The gaseous products were swept from the reaction flask and collected at -78°C. Deuterium Oxide (0.7 g) was added to trapped, frozen products. The mixture of reaction products and D_2O were warmed to room

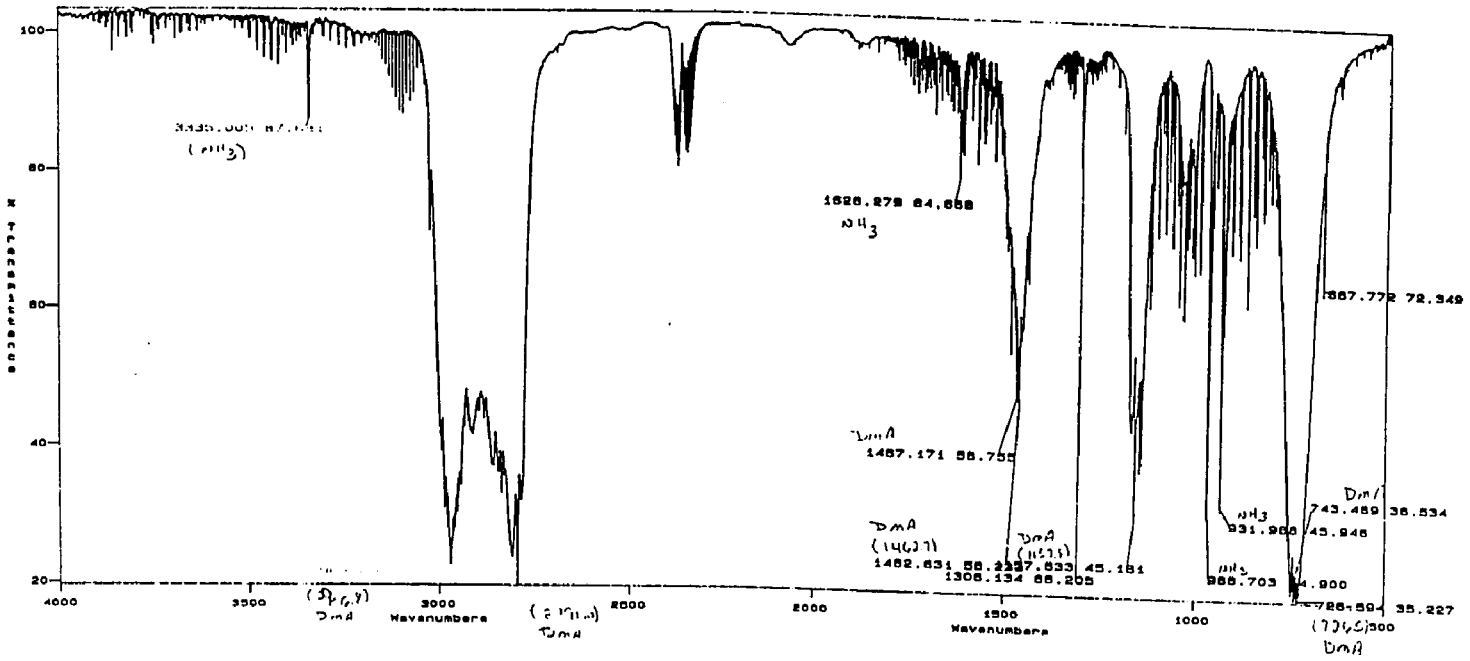

Figure 17. IR of the Gaseous Products from the 1,1-Dimethylhydrazine Reduction of Nitro HMI in Refluxing IPA with Black Pearls L

temperature. The sample of collected material contained azomethane ($CH_3N=NCH_3$ GC/MS (m/z: 58; 43;28), NMR 3.59 ppm (s)), water, and isopropanol. The chemical shift indicates that this cis-azomethane (3.57 ppm) is produced, rather than trans-azomethane (3.67 ppm).[61] The isolated product mixture contained starting material (28%), hydroxylamine (30%), and HMI Base (42%).

The reduction of Nitro HMI (1.219 g) with 1,2-dimethylhydrazine dihydrochloride (1.78 g) using sodium hydroxide (1.153 g), rather than sodium carbonate, to neutralize the hydrochloride in refluxing IPA (10.0 mL) without carbon, produced the hydroxylamine (46%) and the aniline (54%). The presence or absence of azomethane (CH_3-N=N-CH_3) was not examined in this experiment. Complete reduction of Nitro HMI (2.458 g) was observed with 1,2-dimethylhydrazine dihydrochloride (4.59 g dissolved in 3 mL H_2O, neutralized with 2.792 g NaOH) with Black Pearls L (0.357 g) and $FeCl_3$ (0.051 g) in refluxing IPA (9 mL). Complete reduction of Nitro HMI (2.450 g) was also observed with 1,2-dimethylhydrazine dihydrochloride (3.42 g, dissolved in 3 mL H_2O, neutralized with 2.68 g NaOH) with $FeCl_3$ (0.044 g) in refluxing IPA (5 mL). Gaseous products were not produced from the reaction using 1,2-dimethylhydrazine dihydrochloride (4.54 g, dissolved in 3 mL H_2O, neutralized with 2.758 g NaOH) with Black Pearls L (0.357 g) in refluxing IPA (5 mL). The results are summarized in Table 27.

Table 27. Results of the Reduction of Nitro HMI with Dimethylhydrazines

hydrazine	BPL	$FeCl_3$	Products[a] NO_2	NH(OH)	NH_2
1,1-dimethyl	X			3	97
1,1-dimethyl	X	X			100
1,1-dimethyl		X			100
1,1-dimethyl			100		
1,2-dimethyl[b]	X	X			100
1,2-dimethyl[b]		X			100
1,2-dimethyl[b]				46	54
1,2-dimethyl[c]			28	30	42

X-presence of BPL or $FeCl_3$
a-products (NMR) after 24 h in refluxing IPA
b-sodium hydroxide used to liberate the free hydrazine
c-sodium carbonate used to liberate the free hydrazine

Other Reducing Agents. Ammonia and hydrogen were studied as reducing agents for nitro aromatic compounds in the presence of carbon. m-Nitrobenzanilide (8.002 g) with graphite (7.555 g) in IPA (400 mL) was combined with hydrogen (50 p.s.i.) for 24 h in a Parr shaker at room temperature. The pressure did not decrease because no reaction took place. Liquid ammonia was bubbled (3 mL/min) into a refluxing IPA (100 mL) solution of Nitro Meta Base (10.013 g) with Aqua A (1.413 g) for 3 h. After an additional 5 h, TLC showed only starting material, indicating that no reduction took place.

Discussion

The work described here resulted in the development of a procedure for the efficient, selective, inexpensive, and convenient conversion of nitroaromatic compounds to the corresponding amines. This procedure utilizes hydrazine hydrate in combination with an inexpensive carbonaceous catalyst in a refluxing alcohol. A recommended procedure for the carbon catalyzed hydrazine hydrate reduction of nitroaromatic compounds is given in Appendix 17. One example of the effectiveness is the reduction of POP(1),

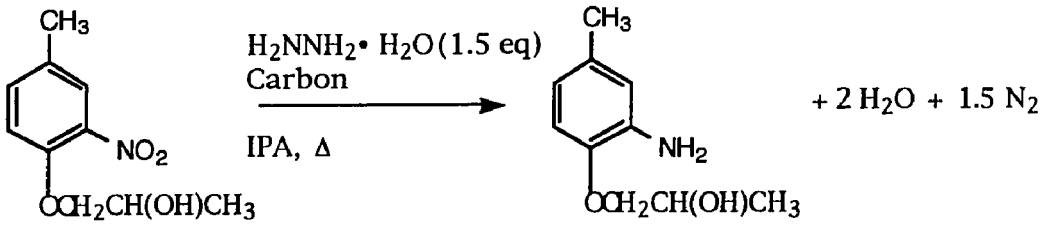

which was completely reduced to the corresponding aniline within three hours using Aqua A (an activated carbon) without affecting the other functional groups present (Table 17, p. 55). In cases where the carbon catalyzed reduction was slow or incomplete, such as in the reduction of Nitro HMI using Mogul L (a carbon black) as a catalyst, the addition of a catalytic amount of $FeCl_3$ increased the conversion and the reaction rate. Without $FeCl_3$ only the phenylhydroxylamine (43%) was formed (Table 19, p. 57).

The carbon catalyzed hydrazine hydrate reduction of nitroaromatic compounds was studied because the procedure is convenient and effective. Hydrazine was the reducing reagent of choice because reduction to an aromatic amine is clean and complete. The by-products from the catalyzed

hydrazine reduction, nitrogen and water, are easily separated from the aromatic amine and are not an environmental hazard. The inexpensive carbon catalyzed hydrazine reducing system is very selective for nitroaromatic compounds, unlike other systems that also reduce other functional groups, such as the replacement of halides during metal catalyzed hydrogenations.[17] The reaction conditions developed are for the reduction of compounds used in the dye industry, but the procedure is general and can be adapted for many other aromatic nitro compounds.

As with many processes, the hydrazine reduction of nitroaromatic compounds has several negative aspects. Because hydrazine will damage many grades of stainless steel, reactions must be carried out in a glass reactor or a vessel constructed of another material compatible with hydrazine.[40] Hydrazine hydrate, the reducing agent for the reaction developed, must be used cautiously.[40]

The Chemistry of Hydrazine on Carbon

Adsorption of Hydrazine on Carbon. Adsorption is obviously required for either the decomposition of hydrazine or the hydrazine reduction of a nitroaromatic compound (Table 9, p. 43) in refluxing IPA. As shown in Figure 7 (p. 37), hydrazine strongly adsorbs on Black Pearls L. The adsorption is rapid (Figure 18) and follows a high affinity isotherm.[56] Adsorption is initially very high and decreases as multiple layers are formed on the carbon (Figure 7).

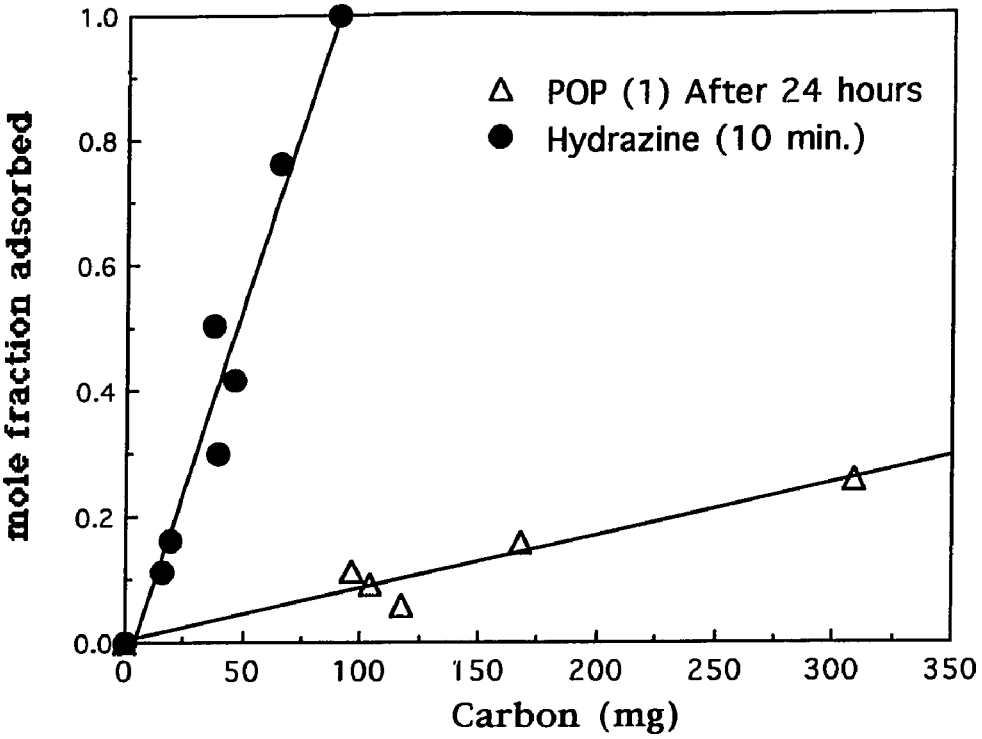

Figure 18. Adsorption of Hydrazine and POP(1) on Black Pearls L at 25°C

Carbon Catalyzed Hydrazine Decomposition. Carbons used to catalyze the hydrazine reduction of the nitroaromatic compounds in refluxing IPA also catalyzed the decomposition of hydrazine (Table 8, p. 38). There may be mechanistic features common to both of these reactions, which occur competitively. Under the reaction conditions used for the reduction of nitroaromatic compounds H_2 was not observed. This indicates that hydrazine decomposed to nitrogen and ammonia (Eq. 25). Excess hydrazine

$$3\ N_2H_4 \rightarrow 4\ NH_3 + N_2 \qquad (25)$$

can be removed from the reduction of a nitroaromatic compound by maintaining the reaction conditions until the hydrazine has decomposed,

which can be monitored using the 2-dimensional TLC method described in the experimental section. There is a published example hydrazine decomposition to ammonia and nitrogen (Eq. 25) on an active carbon under unspecified reaction conditions.[62] Another published example of hydrazine decomposition on a carbonaceous material involves $[C_2(NH_3)_{0.26}(H_2O)_{0.28}]$ synthesized by dehydrochlorination of polyvinylidene hydrochloride.[63] The major products (>90%) from the gas phase (1mm) decomposition of hydrazine on this material at temperatures between 23°C and 97°C are nitrogen and ammonia. The products observed from hydrazine decomposition in this work are the same as the only two literature examples found.

The reactions of 1,1-dimethylhydrazine and 1,2-dimethylhydrazine with carbon in refluxing IPA were also examined. Unlike hydrazine, the dimethyl hydrazines did not decompose (no gaseous products observed). Decomposition of methylhydrazine has been observed on metal catalysts, but at a much slower rate than hydrazine.[40]

Role of the Carbon in Hydrazine Decomposition. The decomposition of hydrazine in refluxing IPA requires carbon. As discussed in the introduction, carbons catalyze several types of reactions. We found that hydrazine adsorbed on carbon, which is one of the criteria established by Austin for a carbon catalyzed reaction.[46] As discussed in the introduction, hydrazine decomposition on a metal (ie. Pd) is thought to proceed through hydrazine dissociation followed by a series of hydrogen transfers between adsorbed species (Eq. 13-19, p.13).[43] Carbon may provide a surface for

hydrogen transfer between hydrazine molecules in the decomposition reaction.

Hydrazine decomposition is also catalyzed by combinations of carbon and iron trichloride. As shown in Table 8, iron (III) accelerates hydrazine decomposition. The Langmuir orders for hydrazine decomposition indicate that hydrazine adsorbs more strongly on the $FeCl_3$ containing catalyst (Table 8). The increase suggests that the catalyst accepts electrons from the hydrazine. The effect of iron on the carbon will be discussed in the section on the reduction of nitroaromatic compounds.

Electron transfer from hydrazine to carbon may result in a change in the hydrazine geometry. The most stable conformation of neutral hydrazine is tetrahedral at the nitrogens with the lone electron pairs at approximately 90° to each other (X-Ray and IR spectra).[64] The geometry of neutral hydrazine, calculated with Spartan (2.0.0) with a 6-31G basis set, indicates that the lone electron pairs are separated by 71°, which is consistent Pasto's results.[65] Complete electron transfer from hydrazine to carbon is predicted to lead to a planar radical cation ($N_2H_4^{\bullet+}$).[66] The geometries and bond lengths of the radical cation were calculated with Spartan software (Table 28). The radical cation has parallel p orbitals on the nitrogen and a decreased N-N bond length. The energy difference between the HOMO of hydrazine and the HOMO of the radical cation is the ionization potential. The calculated ionization potential is 6.07 eV, which is lower than the literature value of 8.93 eV.[67]

Nelsen has used the planar radical cation geometry to calculate a molecular orbital diagram for planar hydrazine.[68] Neutral hydrazine has five σ bonds and two lone pairs. Hydrazine has two planes of symmetry: one

through the nitrogens and the other bisecting the N-N bond. Four bonding molecular orbitals are formed from the NH bonds with SS, SA, AS, AA symmetry. The N-N bonding orbital mixes with the SS N-H bonding orbital, resulting in two bonding orbitals ($\sigma_{(SS1)}$ and $\sigma_{(SS2)}$).[68] Similar antibonding orbitals are observed.[68] As shown in the molecular orbital diagram of neutral hydrazine in Figure 19, the HOMO contains a lone electron pair in an antibonding orbital.

A dication ($N_2H_4^{2+}$) could be formed by complete transfer of a second electron. The calculated ionization potential (Spartan Software) for the dication is 16.09 eV, which is in agreement with the literature value (16.44 eV[66]). The length of the N-N bond is shortened to 1.196Å (Table 28) with removal of a second electron, which is comparable to a nitrogen-nitrogen double bond. The p orbitals remain parallel, which can overlap resulting in a π bond (Table 28).

Table 28. Bond Lengths, Angles, and Charges of Hydrazine and Radical Cations.

	N_2H_4	$N_2H_4^{\bullet+}$	$N_2H_4^{2+}$
∠ (°)HNN	104.83	119.60	120.86
∠ (°)HNNH	-71.12	-0.033	-0.0046
N-H (Å)	1.0038	1.0017	1.0378
N-N (Å)	1.4517	1.2908	1.1964
Charge (H)	0.3804	0.4211	0.4729
Charge (N)	-0.7610	-0.3423	0.0542

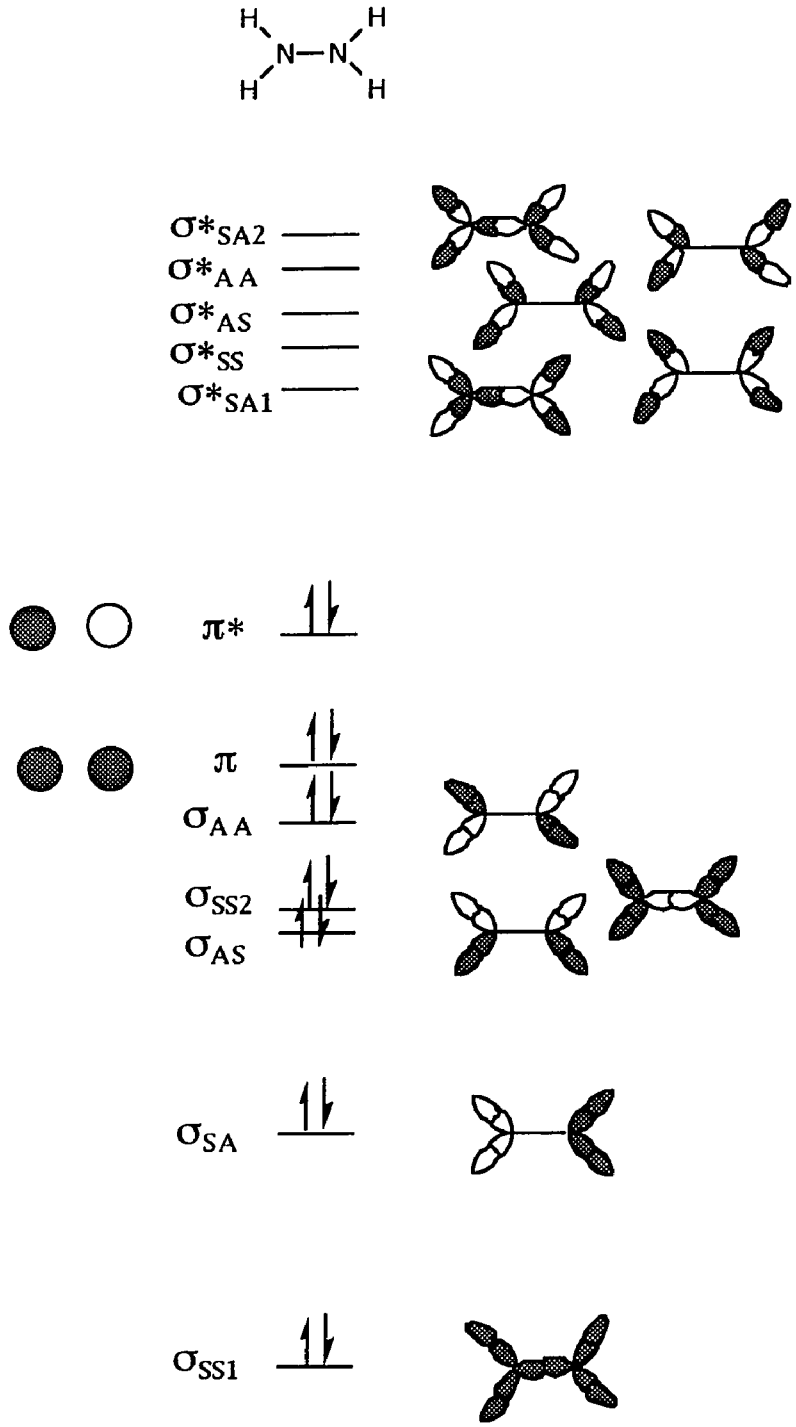

Figure 19. Molecular Orbital Diagram of Hydrazine, Viewed From Above.[66]

Radical cations of substituted hydrazines have been observed.[69] The radical cation of 1,1-dimethylhydrazine has been observed by oxidation of 1,1-dimethylhydrazine in a cold (0°C), aqueous, acidic solution.[70] Geometry changes accompining formation of a radical cation have been observed with tetraalkylhydrazines.[69] The nitrogens and substituents of the tetraalkylhydrazine become coplanar, forming a planar radical cation with the removal of an electron.[69] The radical cation is olefin-like because the p orbitals of the nitrogen become parallel, forming a π system.

A possible reaction mechanism for hydrazine decomposition on a carbon surface is shown below (Scheme 1). Partial electron transfer from hydrazine to carbon is involved. This is consistent with the observed reactivity increase caused by $FeCl_3$ and the removal of an electron from an antibonding orbital.

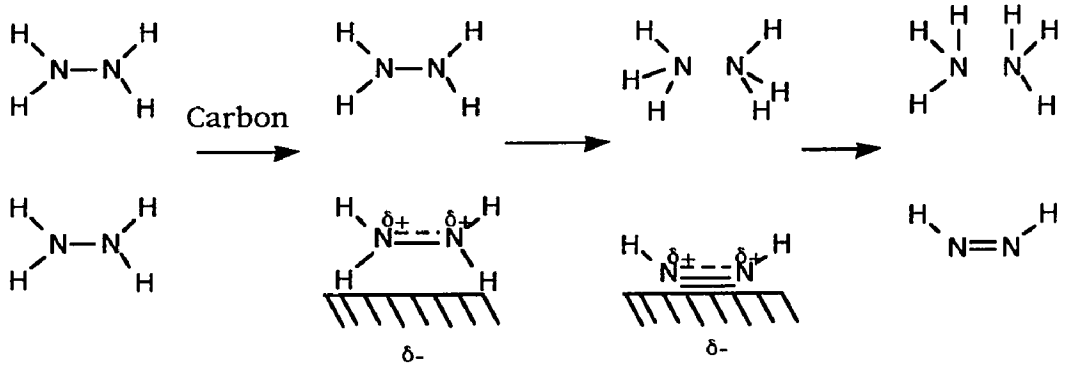

Scheme 1

The concerted reaction of two hydrazine molecules to form 2 molecules of ammonia and one diimide is not a symmetry allowed process, regardless of the hydrazine conformation. A correlation diagram using an

eclipsed hydrazine conformation is shown in Figure 20. The intermediates could be formed by the stepwise transfer of H·, which is not symmetry restricted.

The diimide formed (Scheme 1) could react in an analogous manner with another hydrazine, resulting in the formation of nitrogen and ammonia (Scheme 2). Nitrogen produced from this mechanism would result from one hydrazine molecule, which is observed on metals using labeled ($^{15}N^{15}N$) hydrazine.[39,42] Reaction of 1,1-dimethylhydrazine by this mechanism requires transfer of a methyl group, which may explain the inactivity. The inactivity of 1,2-dimethylhydrazine can not be explained by this mechanism, which would result in the formation of diimide and two methylamines.

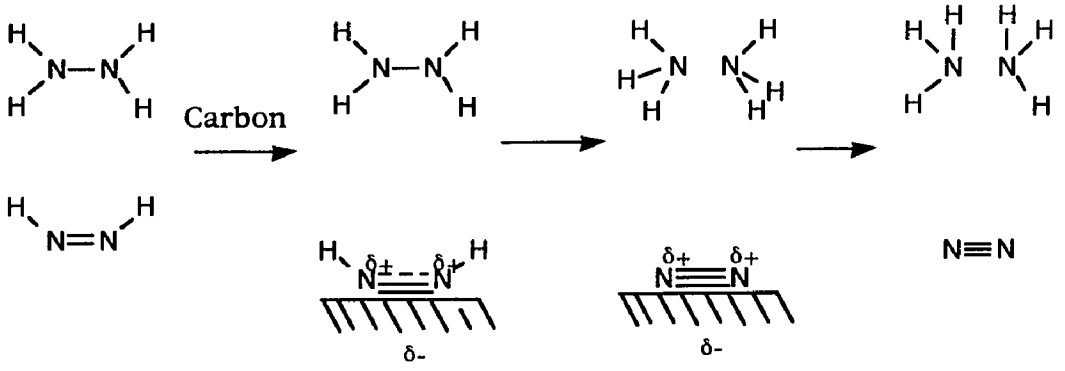

Scheme 2

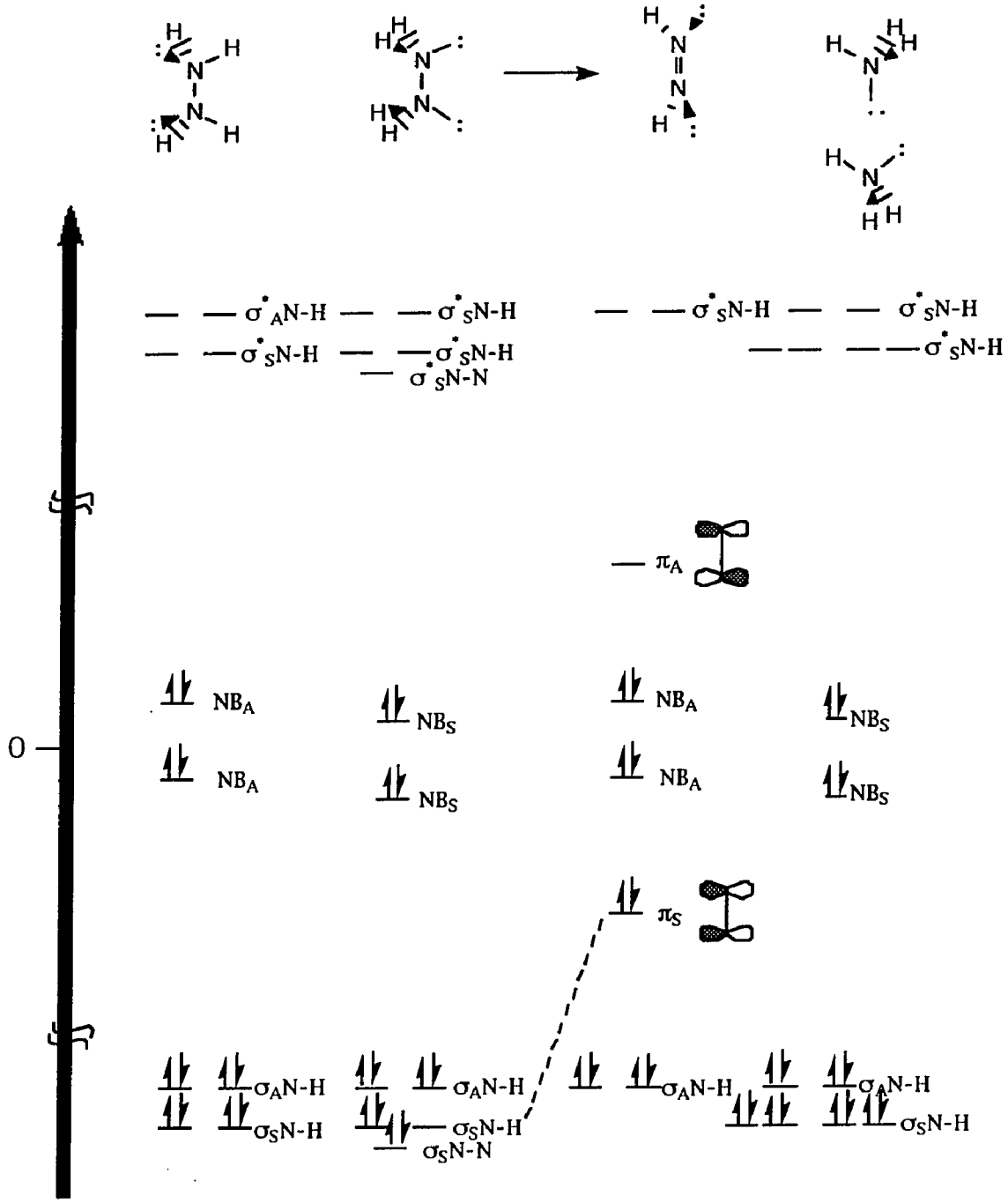

Figure 20. Correlation Diagram. Symmetry Element: plane of the paper.

A rate second order in hydrazine would be observed if hydrogen transfer from an adsorbed hydrazine to a 'free' hydrazine were rate determining (Scheme 1). The proposed mechanism is third order in hydrazine if the rate determining step is the association a 'free' hydrazine with a diimide adsorbed on the surface (Scheme 2). The rapid (Figure 18) and strong (Figure 7, p. 37) hydrazine adsorption is consistent with hydrogen transfer being rate determining. Gaseous product formation does not follow simple first, second, or third order kinetics, indicating more complicated kinetic expression.

Decomposition of hydrogen peroxide, which is isoelectronic with hydrazine has been observed on various carbons.[71] The products observed from hydrogen peroxide decomposition on carbon are consistant with a concerted reaction.[31] This concerted mechanism is different from the accepted mechanism, which is thought to proceed by exchange of an oxonium hydroxyl group with a hydrogen peroxide anion, shown in Scheme 3.[71] The intermediate produced is thought to decompose a 'free' hydrogen peroxide by an unspecified pathway.[71]

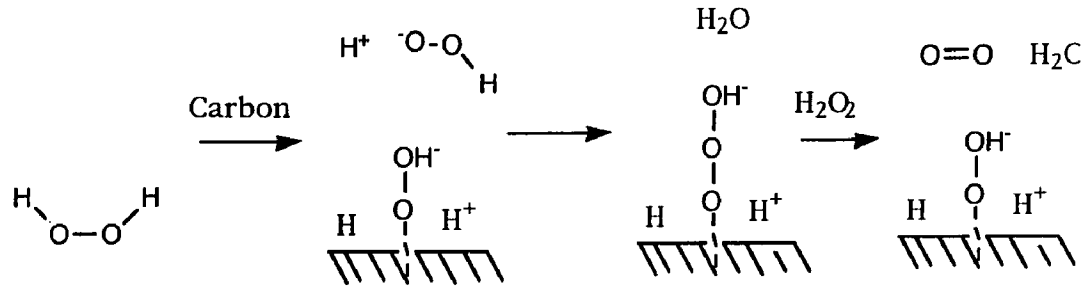

Scheme 3

Hydrazine could also decompose by a reaction simmilar to that proposed for the decomposition of hydrogen peroxide. As shown in Scheme 4, a diimide would be formed.

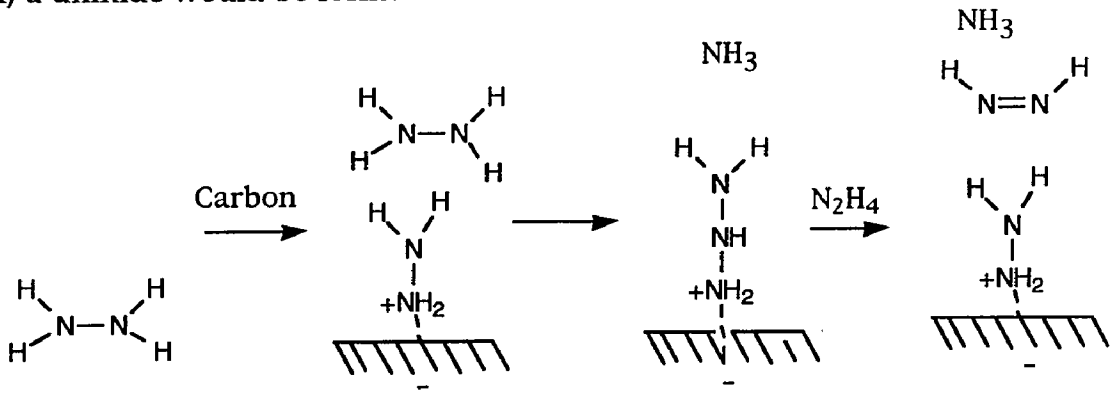

Scheme 4

Nitrogen, an experimentally observed product, could be produced by reaction of the diimide in an analogous reaction (Scheme 5). Nitrogen produced from this pathway would result from one hydrazine, which is observed on metals using labeled hydrazine.[39,42] Decomposition of 1,1-dimethylhydrazine by this reaction pathway would require migration of a methyl group, which may explain the inactivity of this compound. The inactivity of 1,2-dimethylhydrazine can not be explained by this reaction mechanism.

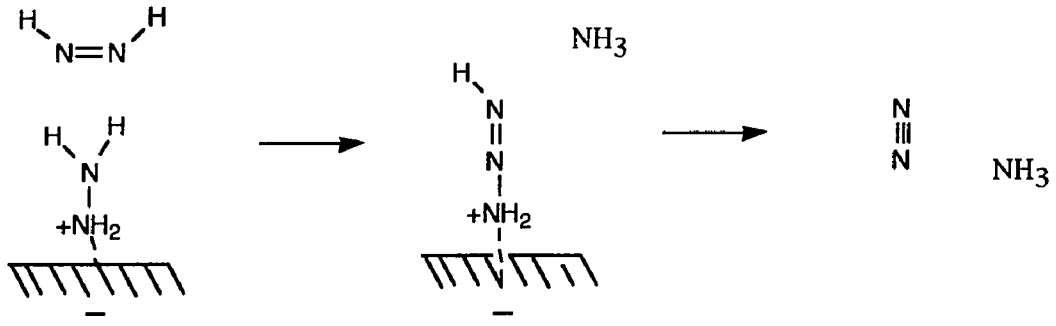

Scheme 5

Hydrazine decomposition could also take place by a redox reaction. The two half reactions are shown below (Eq 27 & 28):

$$N_2H_4 \rightarrow N_2 + 4\,H^+ + 4e^- \qquad E^o = 0.34 \text{ V vs NHE}^{40} \qquad (27)$$

$$4\,H^+ + 4e^- + 2\,N_2H_4 \rightarrow 4\,NH_3 \qquad E^o = 0.1 \text{ V vs NHE}^{40} \qquad (28)$$

The overall reaction is favorable (0.44 V vs NHE). The carbon would serve to mediate electron transfer from one hydrazine to another. Nitrogen would result from one hydrazine molecule, which is observed using labeled hydrazine.[39,42]

Decomposition of hydrogen peroxide could also take place by redox reactions. The half reactions (Eq. 29 and 30) indicate a favorable reaction (Eq. 31).[72]

$$H_2O_2 \rightarrow O_2 + 2\,H^+ + 2\,e^- \qquad E^o = -0.682 \text{ V vs NHE} \qquad (29)$$

$$2\,e^- + 2\,H^+ + H_2O_2 \rightarrow 2\,H_2O \qquad E^o = 1.776 \text{ V vs NHE} \qquad (30)$$

$$2\,H_2O_2 \rightarrow O_2 + 2\,H_2O \qquad E^o_{rxn} = 1.094 \text{ V vs NHE} \qquad (31)$$

Hydrogen peroxide decomposition can occur on $FeCl_3$, which enhanced the the carbon catalyzed hydrazine decomposition.[73] This is another similarity between the decomposition of hydrogen peroxide and hydrazine.

Hydrogen peroxide decomposes readily in the presence of carbon at room temperature, unlike hydrazine, which requires elevated temperatures for rapid decomposition. Decomposition of hydrogen peroxide has a greater thermodynammic driving force than hydrazine, indicated by the more favorable reduction potential. The central bond of hydrogen peroxide (O-O, 51 kcal/mol[74]) is weaker than hydrazine (N-N, 69 kcal/mol[74]), which may also explain the increased reactivity of hydrogen peroxide at lower temperatures.

The concerted pathway is discounted because the reaction is not a symmetry allowed process. A differentiation between the redox pathway and the mechanism analogous to hydrogen peroxide decomposition can not be made. Both dimethylhydrazines, which were unreactive, are predicted to react via the redox pathway. The difference in reactivity might be explained if the substituted hydrazines did not adsorb on the carbon, which has not been examined.

Hydrazine Reduction of Nitroaromatic Compounds

Adsorption of POP(1) on Carbon. As shown in Figure 8 (p.37), adsorption of POP(1) on Black Pearls L follows a constant adsorption isotherm.[56] It is not as strongly adsorbed on the carbon as the hydrazine (Figure 18, p. 83).

Optimization of Reaction Conditions

The reaction conditions were optimized to achieve complete conversion of the nitroaromatic dye intermediates to the corresponding amine without formation of any side or intermediate products. Minimization of the time necessary for quantitative conversion was not the primary concern, although conditions that yield the aniline in shorter time periods are desirable. Reaction temperature, nitro concentration, amount and type of catalyst, metal ions, age of catalyst, and water content all were examined and will be discussed. Comparable rates of gas production with different stirring rates (Table 10, p.46) indicate that the reaction is not mass transport limited.

Two dye intermediates (structures, p.15) were chosen for reaction condition optimization. Nitro Meta Base was the first substrate studied, but was discontinued when we found that an ethanol insoluble impurity present in the commercial sample catalyzed the reaction. The empirical formula of the impurity has been determined to be: $Na_5Fe_1O_{50}S_{4.5}$.[75] Nitro HMI was used to conclude optimization of the reaction conditions.

Temperature. The effect of the reaction temperature on the time necessary for complete reduction of Nitro HMI was studied in six refluxing alcohols. Alcohols are practical solvents for the hydrazine reduction because of the high solubility of the nitroaromatic compounds. The best compromise between the ease of work-up and reaction time for the solvents examined was sought. These reactions were followed by TLC, which provided an approximate time necessary for complete reduction. As shown in Figure 12 (p. 47), the time necessary for complete reduction generally decreases with increasing reaction temperature. Although complete reduction was observed in shorter reaction times in ethanol, IPA was the solvent of choice industrially because it is slightly less flammable. For small scale reactions both ethanol and isopropanol are quite satisfactory.

Nitro Concentration. The effect of increasing the concentration of the nitroaromatic compound was studied to determine the reaction order and as a way to reduce cost. The optimum nitro concentration is ~1.5M (Table 11, p.48). This was the highest concentration of Nitro Meta Base examined because at room temperature higher concentrations were not soluble in IPA. The apparent reaction order in nitro compound is one (Table 11), indicating

that one aromatic nitro is involved in the transition state. The other nitro compounds studied were reduced at approximately the same concentration (1.5M). It is assumed that the rate of reduction of other nitro compounds also increases with nitro concentration.

Amount of Carbon. In addition to reducing cost, stirring is improved by reducing the amount of catalyst in the reaction vessel. Nitro HPS and POP(1) were completely reduced with 5% carbon (Table 13, p. 50). This was the smallest amount of carbon examined. The procedure had to be modified to include a small amount of $FeCl_3$ (~1%) to attain complete conversion of Nitro HMI with ~5% of a carbon catalyst. If the amount of graphite is doubled, the half life of the reaction drops by approximately one third (Table 13).

Choice of Catalyst. All of the carbonaceous materials that we studied catalyzed the reduction of Nitro HMI. The system developed utilizes any carbonaceous material, not only graphite[24] or combinations of activated carbon and $FeCl_3$,[25] which have been studied previously. Iron trichloride was found to enhance the reaction rate, but is not required. A variety of carbonaceous materials were examined (Table 14, p. 52) because the specific role the carbon played in the reaction was not known. The carbons studied included charcoals, coals, and carbon blacks. All of the carbons studied, including Kingsford Charcoal, catalyzed the hydrazine reduction of Nitro HMI in refluxing IPA. The criteria used to determine the best catalyst include: availability, completeness of reduction, rate of gaseous product formation, ease of catalyst removal, and cost. Of the materials studied (Tables 14 and 15,

pp.52 and 53), the best carbonaceous catalyst is Mogul L, a carbon black. Mogul L ($1.22/ lb) is approximately one third the cost of the carbon that showed a comparable rate of gas production, Monarch 1000 ($2.95/lb). Complete reduction of Nitro HMI with the fastest rate of gas production was observed using Aqua A. However, Aqua A is no longer commercially available. Filtration to separate the carbon from the product was difficult for several of the carbonaceous catalysts studied, such as Regal 400R and Vulcan XC-72R. Black Pearls L, an unground form of Mogul L, is preferred because separation of the carbon from the aromatic amine is easier.

Several non-carbonaceous materials were studied to see if any surface would catalyze the hydrazine hydrate reduction of a nitroaromatic compound in refluxing IPA. The materials examined included Alumina, Cabosil and Montmorillonite. Alumina and Cabosil were chosen for the different types of oxygen present; oxygen in alumina is incorporated in the framework whereas Cabosil contains surface oxygen. Montmorillonite was selected because of its effectiveness as a catalyst for the hydrazine reduction of nitroaromatic compounds under anhydrous conditions.[21] None of the non-carbonaceous materials studied were catalysts for the hydrazine hydrate reduction of Nitro HMI, as indicated by the lack of nitro reduction (Table 14). These results indicate that a particular property of the carbonaceous materials, not any surface, results in the observed catalysis. The possible role of the carbon catalyst will be discussed below.

A correlation between the rate reduction of Nitro HMI and a property of the bulk carbon was sought. As shown in Figure 21 there is no correlation between the surface area and the rate of gas production. Carbon blacks having a higher volatile content, which is a measure of the amount of surface

oxygen,[76] show higher rates of gas production from the reduction of Nitro HMI than those with a lower volatile content (Figure 22). The amount of surface oxygen on the carbon may affect the rate and amount of hydrazine adsorbed. This was not examined.

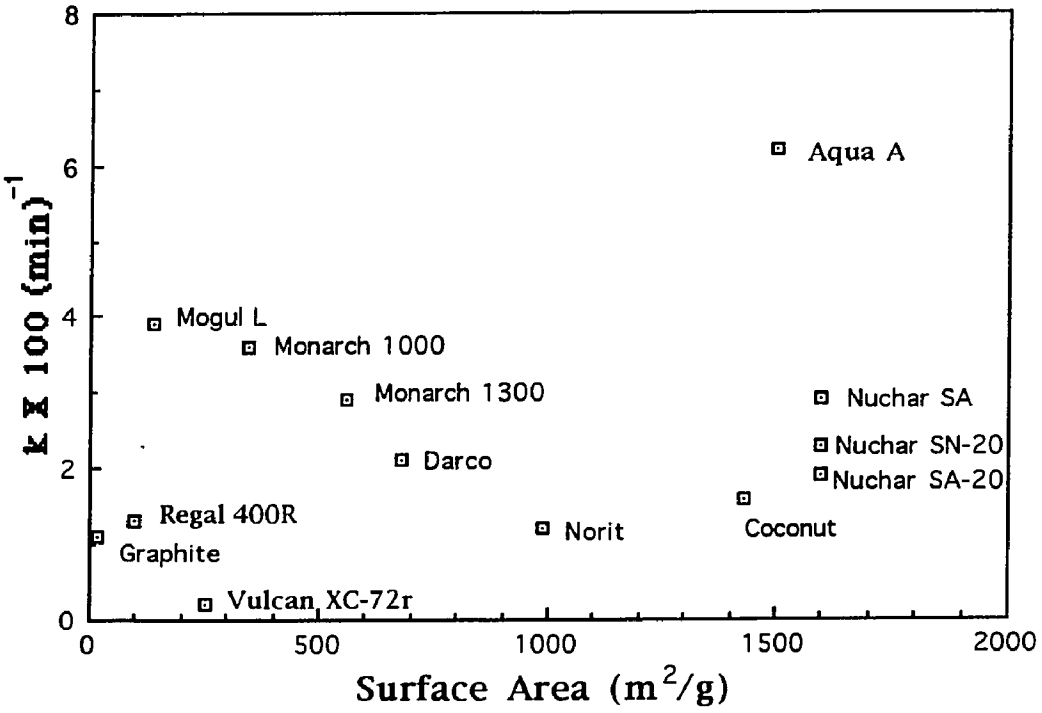

Figure 21. Rate of Gas Production from the Reduction of Nitro HMI With Hydrazine Monohydrate in Refluxing IPA vs. Nitrogen Surface Area of the Carbon

The role of surface oxygen was studied by oxidation of a carbon, Nuchar SA. This simulated oxidation that may have occurred with the sample of Aqua A that had been in the lab for several years. A faster rate of gas production was observed using oxidized Nuchar SA than for the untreated carbon (Table 16, p. 54). This shows that surface oxygen is an important

property of the catalyst for the hydrazine reduction of nitroaromatic compounds.

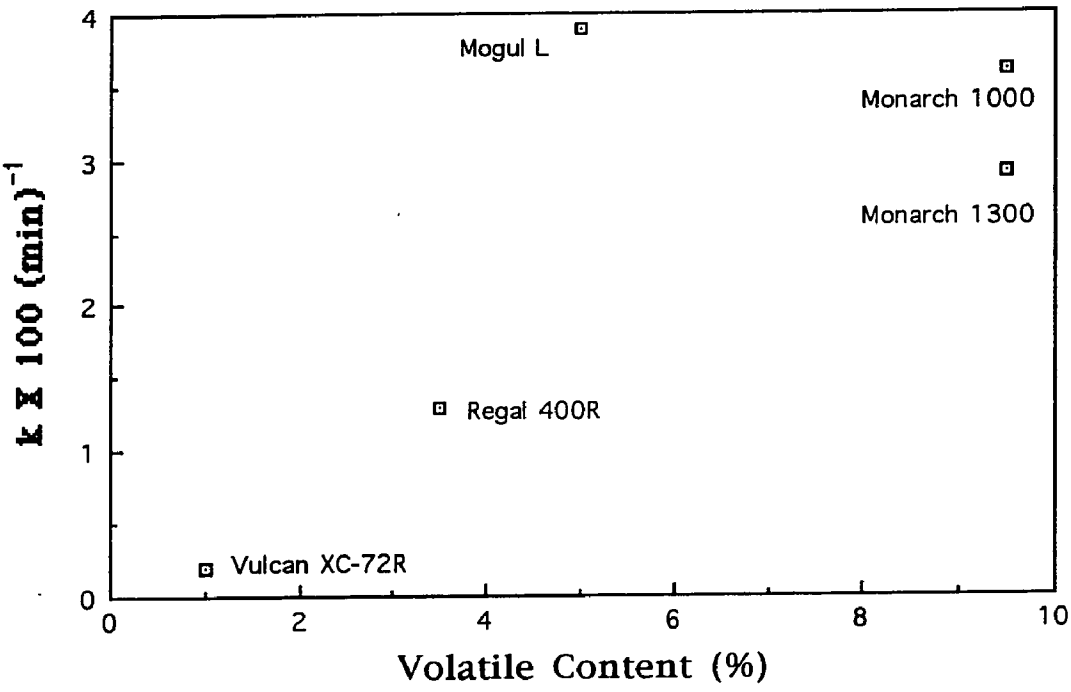

Figure 22. Rate of Gas Production from the Reduction of Nitro HMI With Hydrazine Monohydrate in Refluxing IPA vs. Volatile Content of the Carbon

The amount of surface oxygen affects the resistivity of a carbon.[77] In general, the higher the amount of surface oxygen the higher the restivity of the bulk carbon.[71] Graphite, a pure form of carbon, does not have a high volatile content, and has a low restivity (300 X 10^{-6} ohms/inch) compared to other carbons (1000-3000 ohms/inch). The role of the carbon is probably more than an electrical conductor because higher reaction rates are observed with carbons having more oxygen.

The effect of adding a catalytic amount of $FeCl_3$ to the carbon catalyst for reduction of Nitro HMI was studied. The use of activated carbon containing a small amount of $FeCl_3$ for the reduction of aromatic nitro compounds has previously been investigated and is discussed in the introduction.[25] The addition of a catalytic amount of $FeCl_3$ was successful in increasing the conversion of Nitro HMI to the corresponding aniline as well as increasing the rate of hydrazine decomposition. The data (Table 19, p. 57) show that the amount of carbon has a greater effect on the rate of gas production than the amount of $FeCl_3$, when present.

The role of the iron may be to alter the conductivity of the carbon. Increased electrical conductivity is observed in intercalation compounds of graphite with iron (III). Electron transfer from carbon to iron results in increased electrical conductivity.[78] If electron transfer from hydrazine to carbon is involved, a positively charged surface could increase the rate and amount of hydrazine adsorption. In this case iron acts as a Lewis Acid, accepting electrons from the carbon, generating a positively charged surface.

Having observed the effectiveness of one transition metal, we examined several others. The choice of the transition metal ions examined was based on their capability to act as a Lewis Acid. None of the other metal ions examined were as effective as $FeCl_3$ (Table 18, p.56) for the reduction of Nitro HMI with Darco in refluxing IPA. There is a correlation with the rate of gas production and the Lewis acidity, based on Hard-Soft Acid Base Principles.[58] The metal ions examined that are better co-catalysts with carbon are classified as hard acids (Table 18). All of the less effective metal ions examined are classified as borderline acids. This limited data suggests that the

increase in reactivity is due to the ability of the metal ion to accept electrons, which is consistent with electron donation from hydrazine to the catalyst.

A reaction with the addition of EDTA was carried out to see if trace metals on the carbon are responsible for the catalysis observed. The reaction using carbon with EDTA still took place, indicating that trace metals present in the carbon are not the cause of the observed catalysis. The rate of gas production is decreased, suggesting an inhibitory effect of EDTA or a small amount of metal catalysis. Complexation of hydrazine with EDTA may have caused the rate decrease observed. One possible complex is shown below.

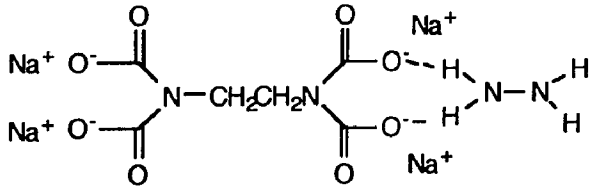

Catalyst Reusability. Catalyst reusability was studied as a way to reduce cost, but even more importantly to decrease the amount of waste generated from the reduction of nitroaromatic compounds. Even though the rate of gas production decreased with repeated use, complete conversion to the aromatic amine was observed. Generally, the mass of recovered catalyst and the rate of gas production decreased with use in the hydrazine reduction of Nitro HMI (Tables 20 and 21, pp. 59 and 60) using either Mogul L-$FeCl_3$ or Black Pearls L-$FeCl_3$. Similar results for catalyst reusability were observed for the reduction of Nitro HPS (Table 22) using the combination of Black Pearls L and $FeCl_3$. The decrease in mass with use suggests degradation of the carbon with use. The small increases in mass after some reactions may be due to adsorption of impurities, reactants, and/or products.

Effect of Water. The effect of water on the reaction was examined using hydrazine monohydrate (85% hydrazine), hydrazine hydrate (55% hydrazine), and anhydrous hydrazine. Water is not required for the reduction of nitrobenzene, which was reduced under anhydrous conditions in THF. The initial concentration of water was shown to affect the reaction rate (Table 23). The initial concentration of water in the reaction using hydrazine monohydrate is 1.2M, compared with hydrazine hydrate 4.0M. The large effect of water content on the rate of gas production is surprising because as the hydrazine reduction of a nitro compound progresses the amount of water in the reaction increases because water is a side product from the reaction.

Selectivity. The combination of hydrazine hydrate and carbon in refluxing IPA showed very high selectivity for the reduction of nitroaromatic functional groups. A list of functional groups stable under the reaction conditions is given in Table 29. Several other functional groups were studied to explore the selectivity of the reducing system. Two ketones, benzophenone and 9-fluorenone, were studied to see whether the addition of carbon would catalyze the reaction past the formation of a hydrazone, which is readily formed at room temperature with hydrazine hydrate.[2] Conditions typically used to reduce a ketone to the alkane with hydrazine are carried out with large amounts of base at high temperatures.[14] The reaction of both of these ketones stopped with formation of the hydrazone when subjected to hydrazine hydrate with carbon in refluxing IPA.

The reactivity of benzaldehyde oxime was studied because of its similarity to phenylhydroxylamine, a known intermediate from the

reduction of a nitroaromatic compound. This compound was unaffected under the reaction conditions.

Table 29. Functional Groups Unaffected by Hydrazine in the presence of carbon in Refluxing IPA (After 24 H)

aniline
ether
ester
sulfone
sulfonamide
alcohol
phenol
chloride (aromatic)
bromide (aromatic)
iodide (aromatic)
trifluromethyl (aromatic)
ketones (hydrazone formed)

1,3-Dipoles. The tendency of nitro compounds to act as a 1,3-dipole, albeit poorly in thermal reactions, led to the investigation of several other 1,3-dipoles.[79] The 1,3-dipoles examined are representative of the various categories of 1,3-dipoles containing nitrogen as the central atom, which are shown in Table 30.

A small amount of aniline (7%) was produced from the reaction of phenylazide with hydrazine and Black Pearls L. The low reactivity of this compound may be due to formation of phenyl pentazole, which is also formed from the reaction of lithium azide and phenyl diazonium. The breakdown of this intermediate favors formation of phenyl azide, which is the starting material in the reaction studied.[80]

Table 30. Groups of 1,3-Dipoles Studied

Nitrilium Betaines

$R\text{-}C^{+}\equiv N\text{-}C^{-}R_2$	↔	$R\text{-}C^{-}=N^{+}=C\text{-}R_2$	Nitrile Ylides
$R\text{-}C^{-}=N^{+}=N\text{-}R$	↔	$R\text{-}C\equiv N^{+}\text{-}N^{-}\text{-}R$	Nitrile Imines
$R\text{-}C^{-}=N^{+}=O$	↔	$R\text{-}C\equiv N^{+}\text{-}O^{-}$	Nitrile Oxides *

Diazonium Betaines

$N^{-}=N^{+}=C\text{-}R_2$	↔	$N\equiv N^{+}\text{-}C^{-}\text{-}R_2$	Diazoalkanes
$N^{-}=N^{+}=N\text{-}R$	↔	$N\equiv N^{+}\text{-}N^{-}\text{-}R$	Azides *
$N^{-}=N^{+}=O$	↔	$N\equiv N^{+}\text{-}O^{-}$	Nitrous oxide

Allyl Type - Nitrogen as Middle Center

$R_2\text{-}C^{-}\text{-}N^{+}(R)=C\text{-}R_2$	↔	$R_2\text{-}C=N^{+}(R)\text{-}C^{-}\text{-}R_2$	Azomethine Ylides
$R_2\text{-}C^{-}\text{-}N^{+}(R)\text{-}N\text{-}R$	↔	$R_2\text{-}C=N^{+}(R)\text{-}N^{-}\text{-}R$	Azomethine Imines
$R_2\text{-}C^{-}\text{-}N^{+}(R)=O$	↔	$R_2\text{-}C=N^{+}(R)\text{-}O^{-}$	Nitrones *
$R\text{-}N=N^{+}(R)\text{-}N^{-}\text{-}R$	↔	$R\text{-}N^{-}\text{-}N^{+}(R)=N\text{-}R$	Azimines
$R\text{-}N=N^{+}(R)\text{-}O^{-}$	↔	$R\text{-}N^{-}\text{-}N^{+}(R)=O$	Azoxy Compounds *
$O^{-}\text{-}N^{+}(R)=O$	↔	$O=N^{+}(R)\text{-}O^{-}$	Nitro Compounds *

*- a compound of this type was studied

The reactivity of a nitrile oxide and a nitrone was also studied. Benzonitrile-N-oxide, generated from benzohydroxamoyl chloride (Eq. 32), reacted with hydrazine to form benzaldehyde oxime in the presence and/or absence of Black Pearls L (Eq.33).

$$\varphi C(Cl)=N\text{-}O\text{-}H \rightarrow \varphi C\equiv N^{+}O^{-} + HCl \quad (32)$$

$$2\ \varphi C\equiv N^{+}O^{-} + H_4N_2 \rightarrow 2\ \varphi CH=N\text{-}O\text{-}H + N_2 \quad (33)$$

As previously described, benzaldehyde oxime was stable under the reaction conditions. N-Phenyl-phenylnitrone was hydrolyzed by hydrazine hydrate in the presence and/or absence of Black Pearls L (Eq. 34).

$$2\ \varphi C(H)=N^{+}(\varphi)\text{-}O^{-} + H_2O \rightarrow \varphi C(H)=O + \varphi N(H)\text{-}OH \quad (34)$$

The hydrolysis products, benzaldehyde and β-phenylhydroxylamine, reacted with hydrazine. Benzaldehyde coupled with hydrazine to form a hydrazone (Eq. 35). In the reaction containing carbon, some of the hydrazine decomposed, resulting in formation of the dihydrazone, dibenzal hydrazine (Eq. 36).

$$\varphi C(H)=O + N_2H_4 \rightarrow \varphi C(H)=N\text{-}NH_2 + H_2O \quad (35)$$

$$\varphi C(H)=N\text{-}NH_2 + \varphi C(H)=O \rightarrow \varphi C(H)=N\text{-}N\text{-}C(H)\varphi + H_2O \quad (36)$$

β-Phenylhydroxylamine formed was reduced to aniline in the presence of carbon. The nitrile oxide and the nitrone were reactive without carbon, indicating that hydrolysis also occurred.

The stability of products produced from coupling reactions of aniline, nitrosobenzene, and phenylhydroxylamine was also examined. Azoxybenzene, both a coupled product and a 1,3-dipole, was reduced to azobenzene and aniline (Eq. 37) in the presence of hydrazine and carbon.

$$2\ \varphi N=N^{+}(\varphi)\text{-}O^{-} + 2\ N_2H_4 \rightarrow \varphi N=N\varphi + 2\ \varphi NH_2 + 2H_2O + 2N_2 \quad (37)$$

Although azoxybenzene showed similar reactivity patterns to nitrobenzene, the extent of the reduction was not very large. Aniline (7%) and azobenzene (39%) were produced from the reduction of azoxybenzene after 24 h with hydrazine in refluxing IPA. Azoxybenzene was unreactive with hydrazine hydrate in the absence of carbon. Azobenzene was converted to aniline (36%) after 24 h at reflux in IPA in the presence of hydrazine and Black Pearls L (Eq. 38).

$$\varphi N{=}N\varphi \quad + \; N_2H_4 \quad \rightarrow \quad 2\,\varphi NH_2 \quad + \; N_2 \qquad (38)$$

Other Nitro Compounds. A series of substituted nitrobenzenes was examined to examine a substituent effect on the rate of nitro reduction. All of the compounds (4-CH_3, 4-OCH_3, 4-Cl, 4-Br, 3-I, 4-NH_2, 3-CF_3, 4-OH: Table 24, p.63) were partially reduced to their corresponding anilines. None of the substituents reacted. The similarity in observed rates of gas production indicate that there is not a large substituent effect on the rate of nitro reduction. The Hammett rho value (using σ) for the reaction is calculated to be -0.07, but with a poor correlation. A small rho value (-0.09), with a slightly better correlation is obtained using σ^+ (Figure 23). The absence of a substituent effect is surprising.

Nitrocyclohexane, a secondary aliphatic nitro compound, was examined to see aliphatic nitro compounds could be reduced. This compound was unreactive with hydrazine hydrate and Black Pearls L in refluxing IPA. The reduction of an aliphatic nitro compound has been reported. Nitroethane has been reduced to ethylamine by hydrazine with a graphite catalyst.[24] Nitrocyclohexane is not reduced by hydrazine in the presence of carbon, which may be explained by the half wave reduction

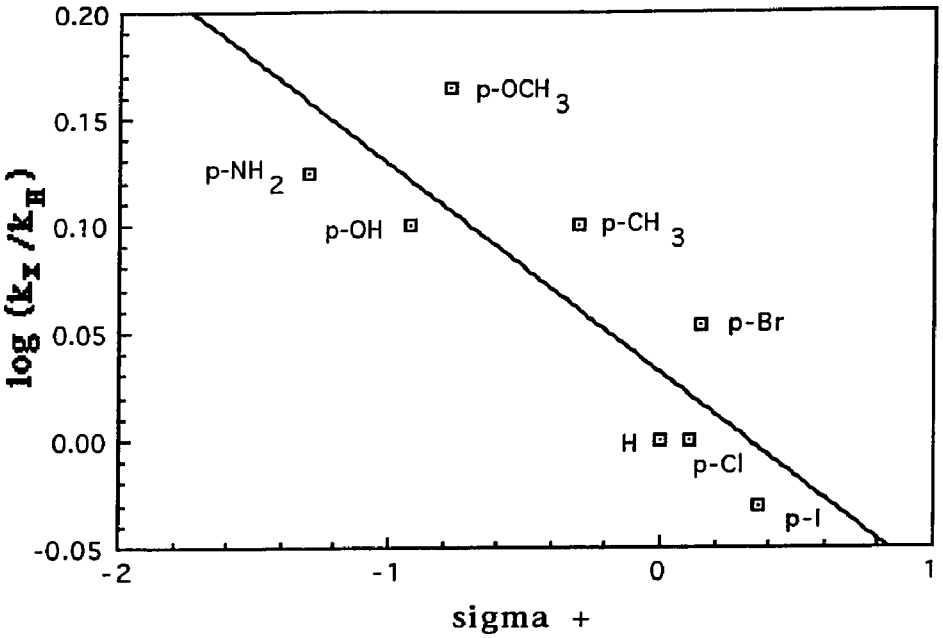

Figure 23. Hammett Plot for the Hydrazine Reduction of Substituted Nitrobenzene

potential. The only available half wave reduction potential for nitrocyclohexane was measured in dimethyl formamide (DMF) at 0°C, and is -1.41 V vs. NHE.[81] The half wave potential of nitrobenzene in DMF is -0.85 V vs. NHE.[82] An oxidation potential for hydrazine is not available under comparable conditions. The reduction of nitrocyclohexane is likely to be electrochemically unfavorable because the hydrazine reduction of nitrobenzene is only slightly favored in aqueous systems (0.045 V).

The selectivity for the reduction of nitroaromatic groups by hydrazine in refluxing IPA may correlate with the half wave reduction potentials. Table 31 shows the half wave potentials for several of the compounds studied, measured in DMF. Included in the table are values for chlorobenzene, bromobenzene, and other functional groups that are unaffected under the

reaction conditions. All of the compounds studied, except nitrosobenzene, have greater half wave reduction potentials than nitrobenzene. The reduction potential for nitrosobenzene is smaller than nitrobenzene and it undergoes reaction with hydrazine. This suggests that the reaction is thermodynamically controlled.

In summary, the only functional groups readily affected by the combination of hydrazine hydrate and carbon in refluxing IPA were the nitroaromatic, aromatic nitroso, and aromatic hydroxylamine. The reactivity of several of the compounds examined was not due to the combination of hydrazine hydrate and carbon, but to hydrolysis (N-phenyl-phenyl nitrone and benzohydroxamoyl chloride) or reaction with hydrazine (ketones).

Table 31. $E_{1/2}$ for Selected compounds in DMF at 25°C[82]

Substrate	Reference	$E_{1/2}$ V(vs. NHE)
azobenzene	S.C.E.	-1.12
acetophenone	S.C.E.	-1.75
benzaldehyde	S.C.E.	-1.56
benzophenone	S.C.E.	-1.48
bromobenzene	Ag/AgBr	-1.74
chlorobenzene	S.C.E.	-2.36
nitrobenzene	S.C.E.	-0.85
nitrosobenzene	S.C.E.	-0.57

The Reaction Mechanism

Possible Intermediates. The reduction of nitrobenzene is thought to proceed in a stepwise fashion through a nitrosobenzene and phenylhydroxylamine intermediate.[11]

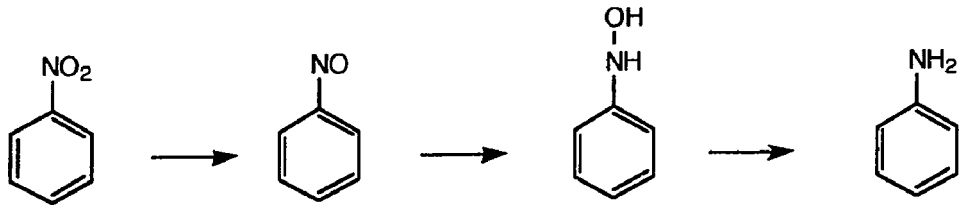

This pathway has been supported by isolation of a phenylhydroxylamine and formation of coupled products, which are attributed to the reaction of a nitrosobenzene intermediate.[2] Nitrosobenzene can be reduced to phenylhydroxylamine or rapidly couple with either phenylhydroxylamine or aniline to form an azoxybenzene or azobenzene, respectively.[32] The reaction may stop with formation of coupled products or the coupled products may be reduced, depending on the pH of the solution. Formation of phenyltriazine as an intermediate has been suggested for the Raney Nickel catalyzed hydrazine hydrate reduction of nitrobenzene, but there is no evidence to support triazine formation.[83] The easiest way to explore nitrosobenzene and phenylhydroxylamine as possible intermediates in the hydrazine reduction was to subject them to the reaction conditions.

Behavior of Conventional Intermediates Under the Reaction Conditions. The reactivity of nitrosobenzene was examined in refluxing isopropanol with hydrazine hydrate and Black Pearls L. Coupled products were observed from the reduction of nitrosobenzene under the standard

reaction conditions (Table 25, p. 74). These products are different from those formed by nitrobenzene reduction and suggest that nitrosobenzene is not a likely reaction intermediate.

Nitrosobenzene could be an intermediate if the concentration was so small that bimolecular coupling did not occur. An intramolecular trap for a nitrosobenzene intermediate was designed to eliminate concentration as a factor for coupling. 2-Amino-2'-nitrobiphenyl was chosen because benzo[c]cinnoline could be formed if the aniline is in close proximity to a nitroso intermediate (Scheme 6).

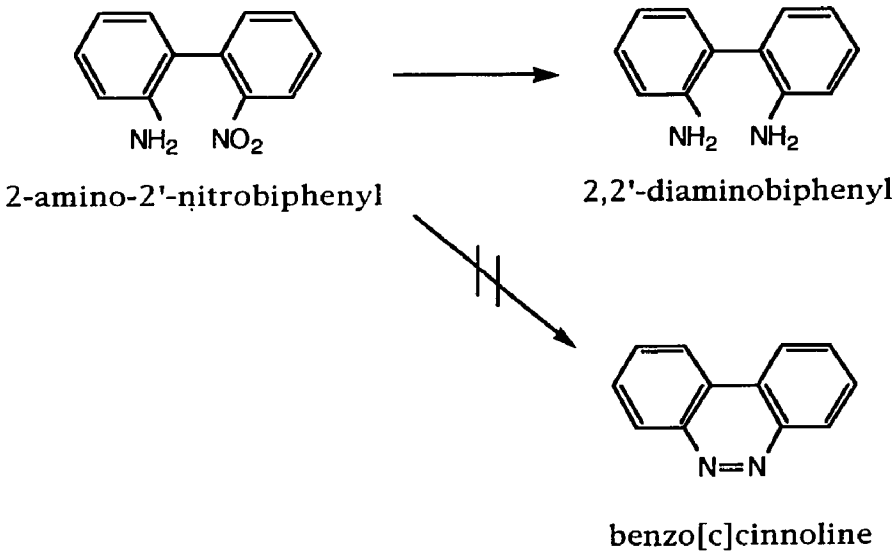

2-amino-2'-nitrobiphenyl

2,2'-diaminobiphenyl

benzo[c]cinnoline

Scheme 6

The only product from the reduction of 2-amino-2'-nitrobiphenyl was 2,2'-diaminobiphenyl (38% yield). The lack of coupled product formation indicates that a nitroso is not formed during the reaction.

The reactivity of the coupled products was also examined. Control experiments showed that the coupled products are not fully reduced under

the reaction conditions (azoxybenzene 54% unreacted, azobenzene 64% unreacted). This indicates that some of the coupled products would remain after 24 h, if they were formed during the reaction. In all of the reductions of mono nitroaromatic compounds examined, coupled products were not observed. The procedure described in the experimental section shows that >1% azobenzene (Figure 16, p. 76) would be observed.

The reactivity of β-phenylhydroxylamine was also studied under the reaction conditions developed for the reduction of nitro aromatic compounds. Coupled products were observed from the reduction of β-phenylhydroxylamine with hydrazine hydrate and carbon (Table 25, p. 74), but not the reduction of nitrobenzene. The difference in observed products suggests that β-phenylhydroxylamine is not a reaction intermediate in the reduction of nitrobenzene.

An experiment was carried out in an NMR tube to see if any intermediates could be observed. The reduction of nitrobenzene in glyme-d_{10} using $D_4N_2 \cdot D_2O$ with Black Pearls L showed the formation of β-phenylhydroxylamine prior to the formation of aniline (NMR, Figure 15, p. 72), without the observation of coupled products or any other intermediates. The same observations were made by TLC when hydrazine hydrate was used with Black Pearls L in refluxing IPA. Coupled products, which were shown to be stable under the reaction conditions, were not observed from the reduction of nitrobenzene.

The observation of β-phenylhydroxylamine as a reaction product, but the lack of coupled product formation is a contradiction. If phenylhydroxylamine was a reaction intermediate, the same reactivity of the intermediate would be observed during the reaction as a reaction using

β-phenylhydroxylamine as the starting material. The contradiction suggests that aniline is produced by a different reaction pathway than the formation of β-phenylhydroxylamine.

The reduction of 2,2′-dinitrobiphenyl was the only reaction in which a coupled product was observed. The product isolated from this reaction contained benzo[c]cinnoline n-oxide (37%) and benzo[c]cinnoline (3%).

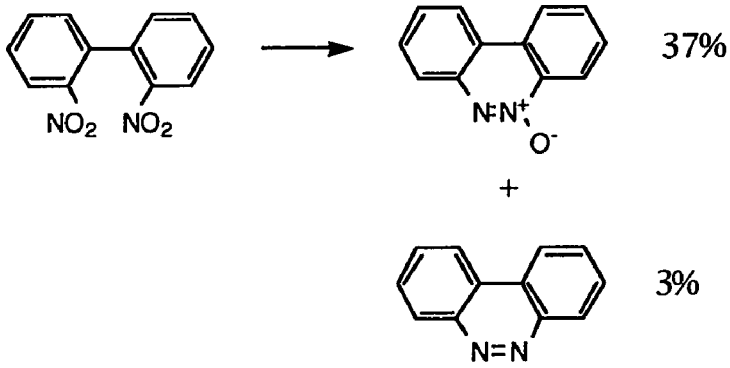

Scheme 7

The coupling of the aromatic amine and nitrosobenzene is eliminated because benzo[c]cinnoline-n-oxide would not be formed (Scheme 8).

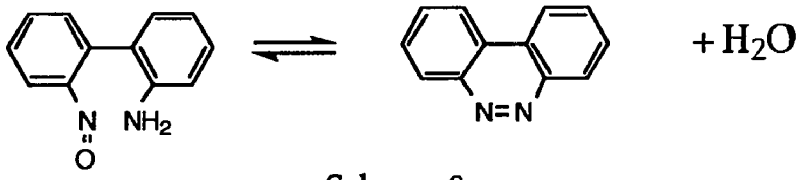

Scheme 8

Benzo[c]cinnoline n-oxide could also be fourmed by coupling of two phenylhydroxylamines, as shown in Scheme 9.[32] Reduction of 2,2′dinitrobiphenyl using conventional reduction methods has produced 2,2′-diaminobiphenyl and/ or benzo[c]cinnoline.[84]

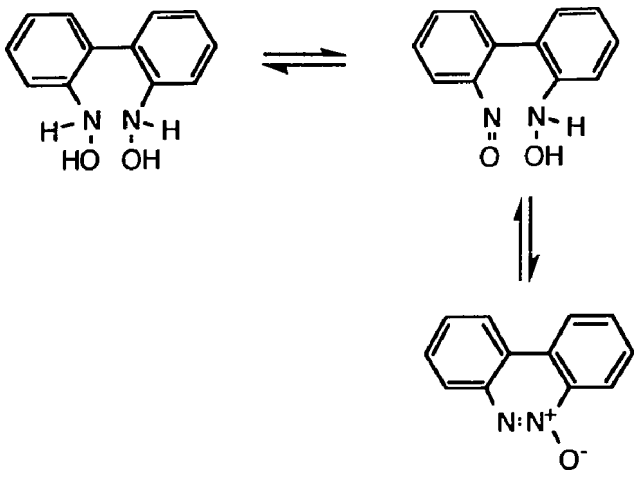

Scheme 9

Possible Reaction Mechanisms

There are many pathways for the reduction of a nitroaromatic compound to the corresponding amine. Hydrogen or ammonia (possible hydrazine decomposition products) were not considered as the reducing species because they were ineffective for the reduction of m-nitrobenzanilide and Nitro Meta Base in the presence of carbon, respectively. The role of β-phenylhydroxylamine is uncertian because the reduction of nitrobenzene did not show the same reactivity as a reaction starting with β-phenylhydroxylamine. Several reaction pathways will be discussed, some interesting pathways involving nitrosobenzene or β-phenylhydroxylamine intermediates have been included, although the data demonstrate that nitrosobenzene is not a reaction intermediate.

Electrocyclic Processes. The plausibility of an electrocyclic processes between a nitroaromatic compound and hydrazine was examined. The feasibility of this reaction pathway (Scheme 10) depends on the conformation

of the hydrazine. The only conformation that can provide orbital overlap leading to a N-N double bond and lead to an energetically favored process is when the angle between the lone electron pairs of hydrazine is 180°, which is not the most stable conformation.[65] A correlation diagram is shown in Figure 24 for this reaction, which is an allowed process based on orbital symmetry.

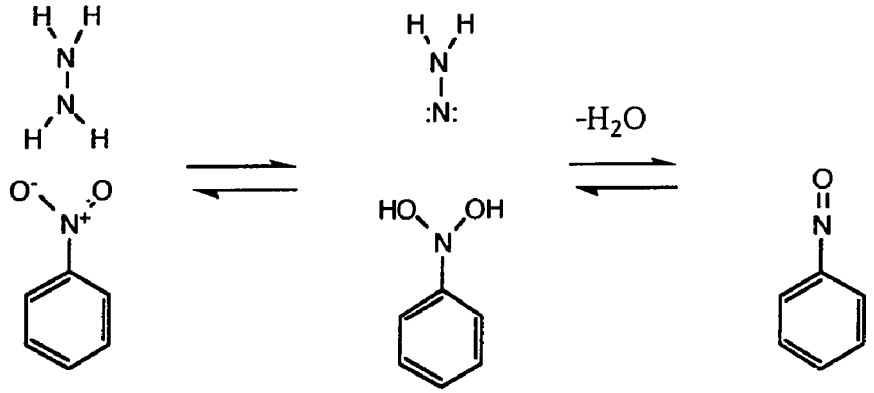

Scheme 10

The nitro group is treated as an 'allyl' analogue using a plane of symmetry perpendicular to the planer 0=N-O. Hydrazine is tetrahedral at the nitrogens with the lone electron pairs at 180° and has a plane of symmetry passing through both of the lone electron pairs. The reaction is not energetically favored using any other conformation of hydrazine other than that discussed. 1,1-Dimethylhydrazine could react with a nitro compound via this reaction pathway, but 1,2-dimethylhydrazine could not. Nitro HMI was reduced by both dimethylhydrazines in refluxing IPA in the presence of carbon. The reduction with 1,2-dimethylhydrazine goes through a mechanism not requiring carbon because carbon was not required for the 1,2-dimethylhydrazine reduction of Nitro HMI.

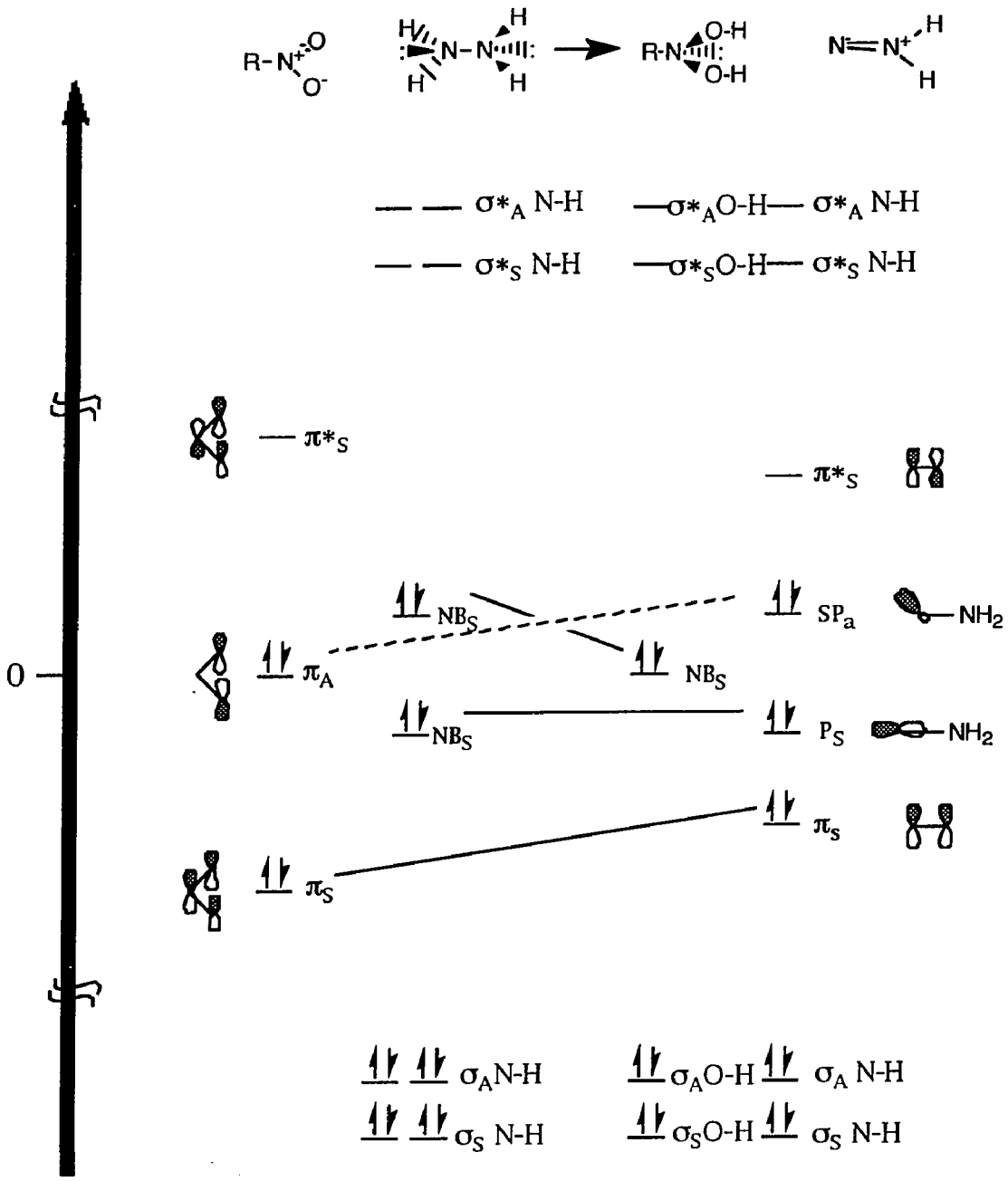

Figure 24. Correlation Diagram. Symmetry Element: plane through the R-N and N-N Bonds and the LEP's of Hydrazine.

An alternative reaction pathway is shown in Scheme 11, which is also restricted by orbital overlap and symmetry. Hydrazine must have the lone electron pairs at 0° to one another for this reaction to be energetically favorable. This reaction pathway is plausible if 1,2-dimethylhydrazine reduced a nitro compound and 1,1-dimethylhydrazine was ineffective. The reduction of Nitro HMI by 1,1-dimethylhydrazine in the presence of carbon indicates a reaction pathway other than that shown in Scheme 11.

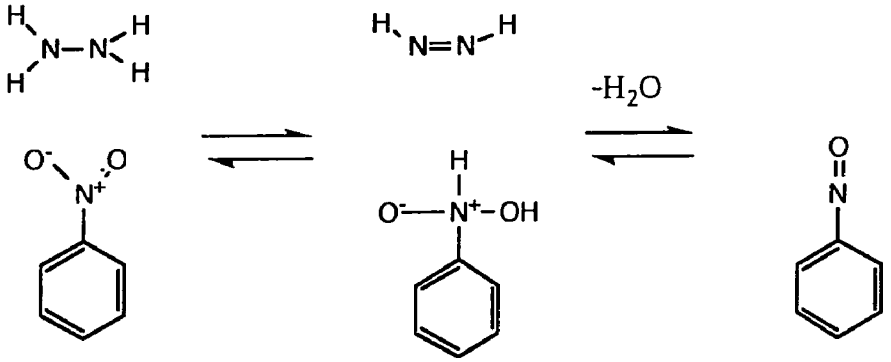

Scheme 11

Both of these electrocyclic processes are eliminated because there is no evidence, directly or indirectly, for the formation of a nitrosobenzene intermediate.

Hydrazine as a Nucleophile. The nucleophilic attack of hydrazine on the nitro does not result in the formation of a nitroso intermediate. This reaction pathway, shown in Scheme 12, is comparable to hydrazone formation in ketones. The only role for carbon in this mechanism is to adsorb the reactants, creating high localized concentrations of the reactants.

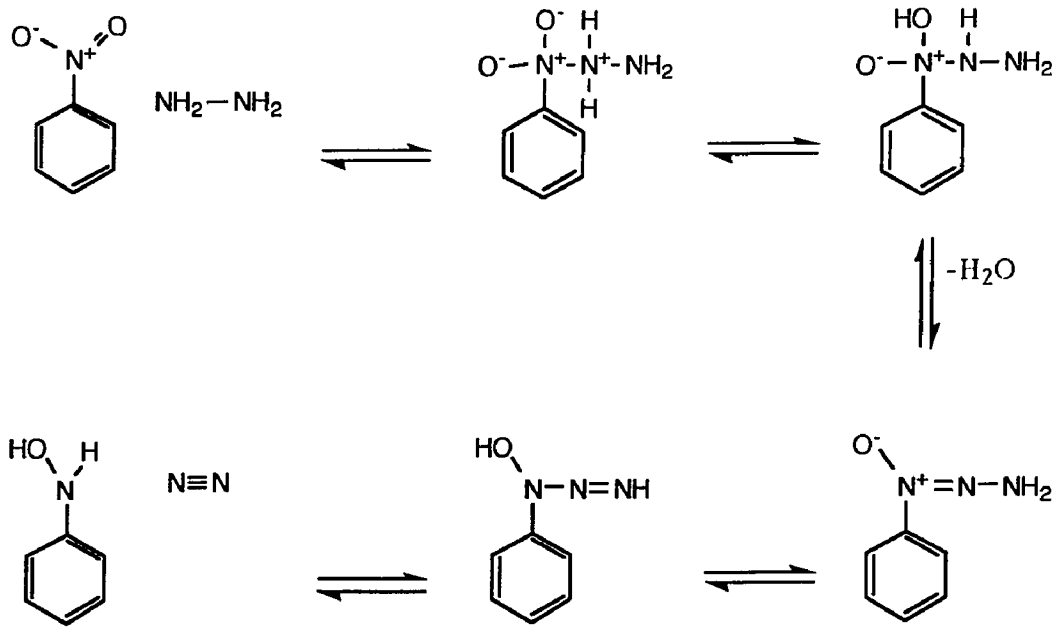

Scheme 12

This pathway results in the formation of β-phenylhydroxylamine, which could be reduced to aniline or undergo a coupling reaction. This reaction pathway also does not account for the 1,1-dimethylhydrazine reduction of Nitro HMI. Dehydrogenation of the terminal nitrogen would not be possible because of the methyl substitutents.

Nitro Group As a 1,3-Dipole. The nitro group could react with an adsorbed hydrazine as a 1,3-dipole. Reaction of nitrobenzene as a 1,3-dipole with an adsorbed hydrazine (Scheme 13) could proceed through a similar intermediate to the photochemical reaction of nitrobenzene with 2-methyl-2-butene.[85] Breakdown of this intermediate can lead to a nitrene, which would be rapidly quenched by the solvent to form aniline. The only other 1,3-dipole examined that showed any reactivity in the presence of hydrazine and carbon was azoxybenzene. The other 1,3-dipoles (N-phenylphenylnitrone,

benzonitrile oxide) were rapidly hydrolyzed by hydrazine hydrate. The inactivity of phenyl azide can be explained by formation of phenylpentazole intermediate, which is the same intermediate that is formed from the reaction of a phenyl diazonium salt with sodium azide, whose dissociation favors formation of phenyl azide, which is the starting material in this reaction.

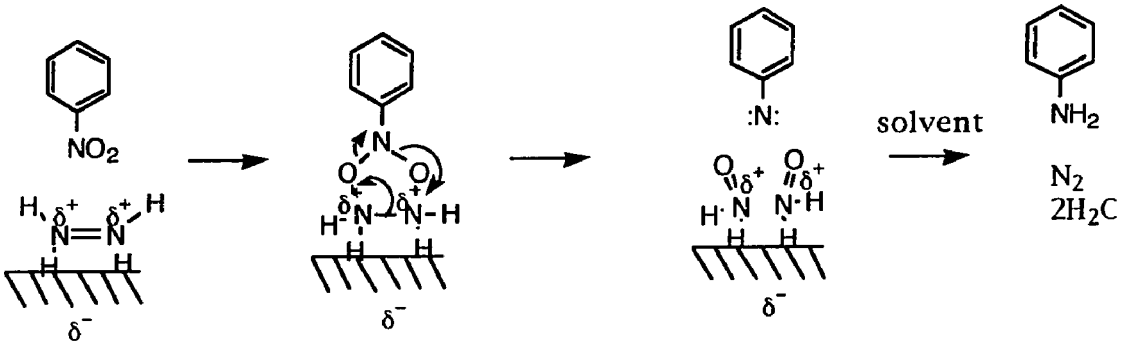

Scheme 13

Formation of a nitrene intermediate has also been proposed for the sodium trimethylsilanethiolate reduction of nitro aromatic compounds by 1,1 elimination of [$C_6H_5N(S^-)(OSiMe_3)$].[86] The formation of carbazole from 2-nitrobiphenyl has been used to confirm the formation of a nitrene intermediate.[87] 2-Aminobiphenyl was the only product from the reduction of 2-nitrobiphenyl in anhydrous THF. The lack of carbazole formation suggests that a nitrene intermediate is not formed. This mechanism accounts for the reaction of 1,1-dimethylhydrazine. The species adsorbed on the carbon from the 1,1-dimethylhydrazine reduction [$(CH_3)_2N^+=O$] could be reduced to dimethylamine by the hydrazine.

The cyclic intermediate can also decompose without the formation of a nitrene intermediate. Attack of water on this intermediate would lead to a phenylhydroxylamine and the same adsorbed intermediates as the nitrene mechanism, as shown in Scheme 14. This mechanism is discounted because water is not necessary for the reaction to take place, as shown by the reduction of nitrobenzene under anhydrous conditions (Table 23, p. 62).

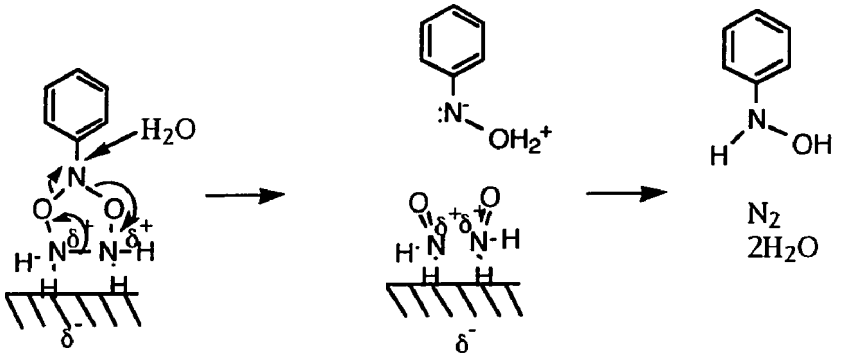

Scheme 14

Redox Reaction Pathway. The reaction may proceed by redox reactions, comparable to an electrochemical reaction. As previously described, the electrochemical reduction can proceed by a 2, 4, or 6 electron wave. The pH of the solution affects the number of electrons transferred. In acidic solutions at low temperatures nitrobenzene is reduced to nitrosobenzene.[37] The role of carbon would be to mediate the transfer of electrons between the hydrazine and the nitro being reduced. Nitrosobenzene could undergo a coupling reaction or further reduced to β-phenylhydroxylamine or aniline. The two electron reduction of nitrobenzene is not possible because the reaction is carried out in a basic solution (pH=12).

β-Phenylhydroxylamine can be produced by the four electron reduction of nitrobenzene. As shown in Scheme 15, the carbon would serve to mediate electron transfer between the adsorbed reactants. β-Phenylhydroxylamine could be reduced to aniline by two electrons, or undergo coupling reactions. As previously discussed, coupled products are observed from the hydrazine reduction of β-phenylhydroxylamine in the presence of carbon.

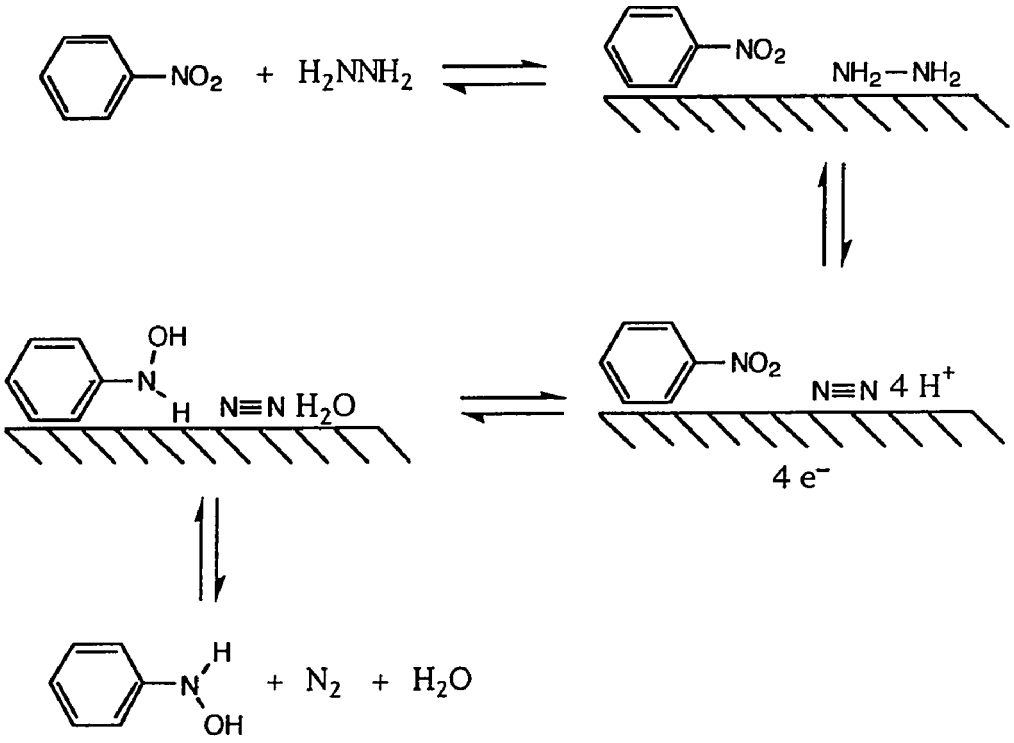

Scheme 15

Nitrobenzene can be reduced to aniline by reaction with six electrons. This conversion occurs in basic solutions without formation of intermediates that could undergo coupling reactions.[37] This possible because the initial pH of the reaction mixture is 12.

As discussed in the introduction, Austin[46] has described several criteria for the electron transfer through carbon, namely: that the reactants adsorb on the catalyst; that the catalyst be a good electronic conductor; and that the rates of the half reactions be reasonably fast. The reactants adsorb on the carbon (Figure 18, p. 83) and carbons are known conductors.[71] The ineffectiveness of the non-carbonaceous materials examined, Alumina and Cabosil, may be because they are not good conductors. As previously discussed, the effectiveness of using iron may result from the alteration of the insulating effect of the volatile content by modification of the surface.

The products observed from the reduction using 1,1-dimethylhydrazine are not consistent with an electrochemical reaction pathway. One possible product from the oxidation of 1,1-dimethylhydrazine is a diazene ($(CH_3)_2N^+=N^-$), which will dimerize to a tetrazene ($(CH_3)_2N-N=N-N(CH_3)_2$) under alkaline conditions.[88] Decomposition of tetramethyltetrazene produces formaldehyde, methylamine, nitrogen, and dimethylamine. Any formaldehyde produced would be trapped as a hydrazone. Nitrogen, methanol, formaldehyde, and dimethylamine have also been observed from the electrochemical reduction of 1,1-dimethylhydrazine.[89] There was no indication of methylamine or a hydrazone in the IR spectrum of the trapped material, indicating that 1,1-dimethylhydrazine reacts via another pathway.

As previously discussed, 1,2-dimethylhydrazine does not require carbon for the reduction of Nitro HMI. The electrochemical oxidation of 1,2-dimethylhydrazine goes through azomethane, which was observed from the 1,2-dimethylhydrazine reduction of Nitro HMI.[89] This reduction may involve direct electron transfer, not through the carbon. The electrochemical

reduction also accounts for the preferential reduction of the electron deficient nitro in 4,4'-dinitrobenzanilide (p. 66).

Conclusions. This work has developed a useful reaction for the reduction of nitro aromatic compounds, particularly dye intermediates. The hydrazine hydrate reduction can easily be carried out in a refluxing alcoholic solvent with any carbonaceous material as a catalyst. This work showed that any carbon can catalyze the hydrazine reduction of a nitroaromatic compound. As described, this reaction utilizes a carbon surface, which may mediate the transfer of electrons between the nitro being reduced and the hydrazine. Several mechanisms have been proposed and discussed. The most plausible pathway is an electrochemical reduction. This mechanism provides separate pathways (4 or 6 electron reactions) by which β-phenylhydroxylamine and aniline could be formed. The role of iron may be to disturb the insulating nature of the carbon black surface. The components must adsorb on the carbon, which is required for the reaction to take place in refluxing IPA, and a conductor must be present for the transfer of electrons from the hydrazine to the nitro compound being reduced.

A lot of chemistry is taking place in the hydrazine hydrate reduction of nitroaromatic compounds in refluxing IPA. This work only begins the examination of the decomposition of hydrazine on carbon and the utility of some of the coupling reactions observed in the presence and absence of carbon.

Molten Salts as a Catalytic Reforming Medium

Introduction

The goal of this project was to investigate reactions that occur on a platinum catalyst supported in a molten salt. Selectivity, due to diffusion through the molten salt, will be superimposed on the normal reaction selectivity of Pt^0 and the Pt catalyst may be modified by Pt-salt interactions.

The use of a molten salt as a solvent for organic reactions has not been extensively explored.[90] In a through review of organic reactions in molten salts, Pagni expressed the view that this is a result of organic chemists' not being versed in molten salt chemistry and the fact that molten salt scientists have focused on properties of melts rather than organic reactions in melts.[91] The majority of the literature of molten salts involves the physical, electrochemical, and chemical properties of the melts.

Catalytic Reforming

Catalytic reforming is an important process in the petroleum industry.[92] In this process, linear and branched hydrocarbons are transformed into cyclic compounds and dehydrogenated to aromatics. The resulting aromatic compounds have a higher octane number than the linear molecules from which they are derived.

This work investigated a reforming catalyst supported in a molten salt. The closest system that has been investigated is the hydrogenation of olefins, which is discussed below. A heterogeneous catalyst surrounded by a molten salt has not been intentionally investigated as a reaction medium. The components of known reforming systems will be discussed briefly, as well as the often studied reactions of cyclohexene under reforming conditions. The

mechanism of cyclohexene dehydrogenation on a Pt (111) crystal and the advantages and disadvantages of molten salts as solvents will also be addressed.

Effective reforming catalysts contain both an acidic component and a metallic component. The support, such as alumina, can provide the acidic component, which can cause the isomerization or cyclization of linear molecules.[93] This occurs through carbonium ion intermediates generated by acid catalyzed reactions. The role of the metallic component, usually a noble metal, is to dehydrogenate linear and cyclic species. Figure 25[94] shows how the two components act together to provide an effective route to the more important aromatic compounds. Reactions attributed to the acidic

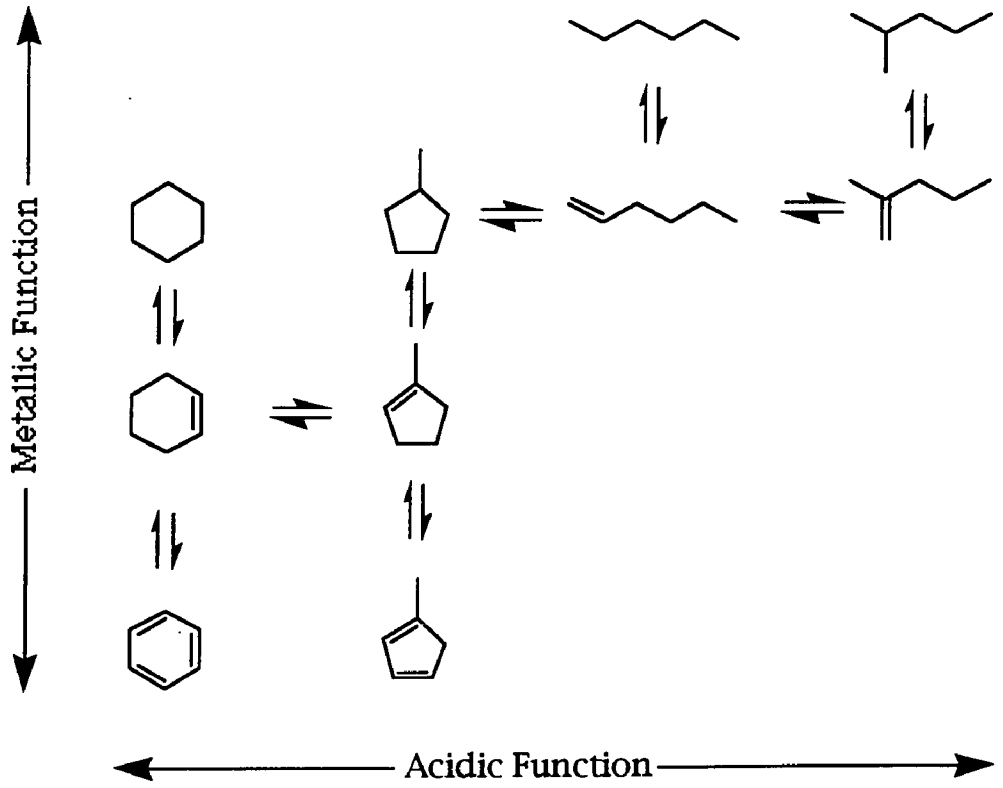

Figure 25. Bifunctional Nature of Reforming Catalysts[94]

component are shown in the horizontal direction: the vertical direction indicates transformations induced by the metallic component.

Typical reforming catalysts are supported group VII metals (Ni, Pd, Pt).[94] These catalysts are prepared by depositing an oxidized form of the metal on a solid support. The catalyst is then subject to a reducing atmosphere, usually hydrogen, to reduce the catalyst to the metallic state. Substantial hydrogen pressures are typically used to inhibit carbon deposition on the metal during the reaction. In many cases an additional metal, such as rhenium, is added to enhance the catalyst reactivity by increasing the dispersion of the catalyst on the support.[95]

The reactions of cyclohexene and cyclohexane have been examined as models for catalytic dehydrogenation that occurs in reforming reactions. Cyclohexane is dehydrogenated to benzene, or an intermediate product, under reforming conditions. Under reforming conditions, cyclohexene is either dehydrogenated to benzene and molecular hydrogen (Eq. 39) or disproportionates to benzene and cyclohexane (Eq. 40).

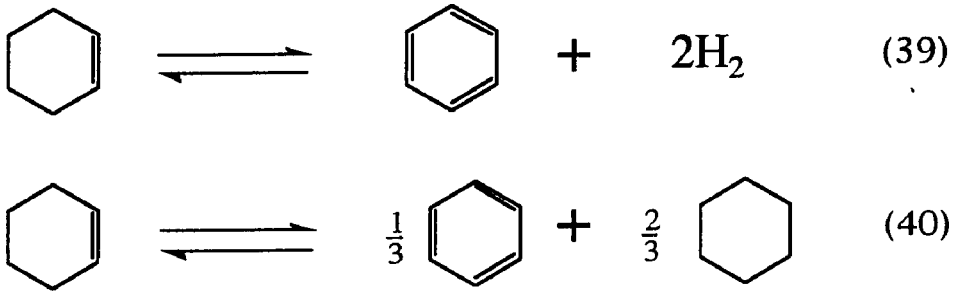

The selectivity between dehydrogenation and disproportionation is a function of the reaction temperature (Figure 26).[96] At temperatures above 275°C, dehydrogenation (Figure 26) is the thermodynamically favored

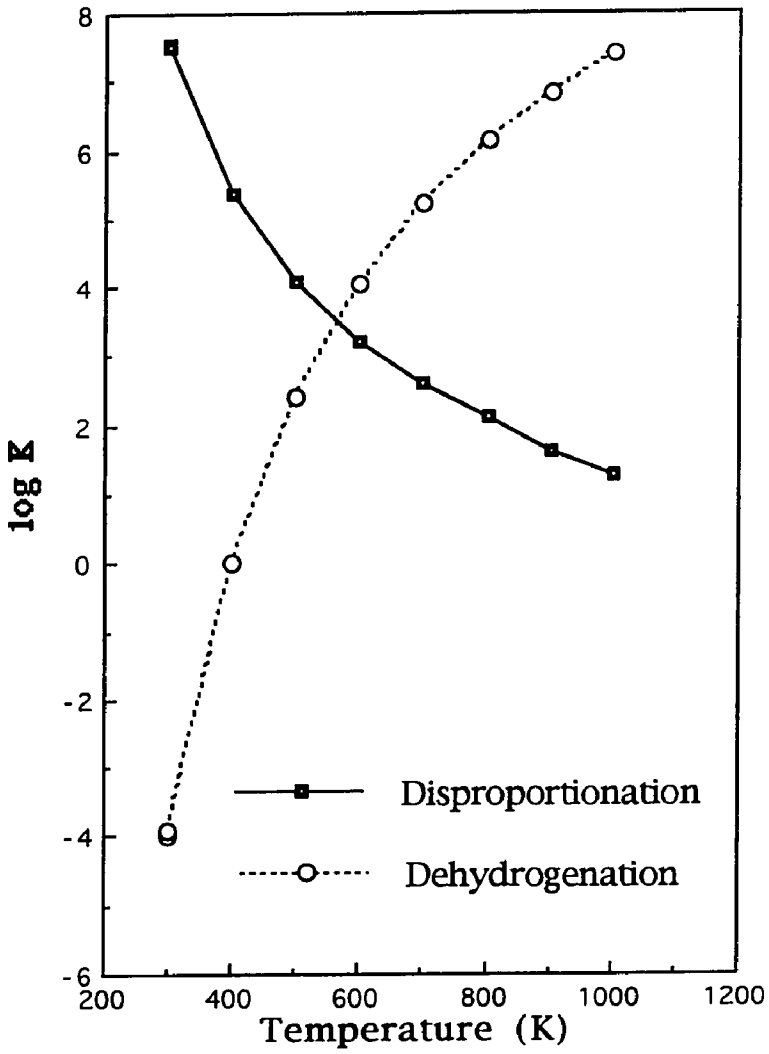

Figure 26. Equilibrium Constants for Cyclohexene Disproportionation and Dehydrogenation as a Function of Temperature[97]

reaction[97]. At lower temperatures disproportionation is the thermodynamically favored process.

Mechanism of Cyclohexane and Cyclohexene Dehydrogenation

The mechanism of cyclohexane dehydrogenation has been extensively studied because of its importance as a model reforming reaction. Cyclohexene has been observed as a an intermediate from the dehydrogenation of cyclohexane on Pt (111) by laser-induced thermal desorption and Fourier transform mass spectrometry (LITD/FTMS).[98] The experiment was carried out by depositing cyclohexane on the Pt (111) face of a crystal at a low temperature (180°K). A pulse from the laser desorbes molecules from the surface. The mass spectrum of the desorbed molecules is recorded and viewed to identify the adsorbed materials. This is repeated as the crystal is warmed in order to observe reaction products and intermediates. In this experiment cyclohexene was observed as an intermediate in the dehydrogenation of cyclohexane.

The dehydrogenation of cyclohexene on Pt(111) has also been examined using LITD/FTMS.[99] Pettiet-Hall, et al concluded that cyclohexene reacts on the surface of the platinum to form a surface species, which is further dehydrogenated to benzene. Benzene was produced from the adsorption of both 1,3-cyclohexadiene and 1,4-cyclohexadiene at temperatures below those required for catalytic dehydrogenation of cyclohexane. Because the cyclohexadiene isomers undergo reactions at a lower temperature than that of the adsorbed species, they are eliminated as possibible intermediates from the dehydrogenation of cyclohexene. Two possibilities for the surface intermediate are shown in Figure 27, which are postulated from mass

spectrometry data to be a C_6H_9 isomer. The removal of three axial hydrogens from a cyclohexane molecule leads to (A). The second species (B) is the result of the loss of an α-hydrogen from an adsorbed cyclohexene. These species are plausible intermediates for the dehydrogenation of cyclohexane and cyclohexene, respectively.

A B

Figure 27. Possible Modes of Cyclohexane(A) and Cyclohexene(B) Adsorption on Pt(111)[99]

Proposed mechanisms of cyclohexene disproporionation on supported group VII metals include a bimolecular surface mechanism and a mechanism requiring storage of hydrogen by the metal.[96,100] The bimolecular mechanism requires the direct transfer of hydrogen from one cyclohexene molecule to another, producing cyclohexane and 1,3-cyclohexadiene. Cyclohexadiene is then rapidly dehydrogenated to benzene. Alternatively, hydrogen can be removed from one cyclohexene molecule and stored on the metal surface. Another cyclohexene molecule then can be hydrogenated, producing cyclohexane.

Molten Salt Systems

The present study focused on the reactions of organic compounds, particularly cyclohexene, on a reforming catalyst supported in a molten salt.

A molten salt, as Pagni defines, is a compound or a mixture of components, such as a eutectic, that has a large ionic component in the liquid state.[91] Molten salts can either be used as a reactant source or as a solvent for a reaction.[101] Salts used as a reactant source have a limited lifetime because a component of the melt is consumed as the reaction progresses. Exchange reactions are an example of a reaction involving the melt.[101]

Molten salts have several advantages over traditional solvents. Molten salts are stable, nonvolatile solvents from which organic products can easily be separated.[102] A dry reaction medium can be obtained, which can eliminate undesirable side reactions due to trace amounts of water.[103] The nature of the solvent can be changed by varying the composition or components of the melt.

One disadvantage of some molten salt systems is their corrosive nature.[104] Carbonate melts are an example of a highly corrosive system, requiring an expensive gold or gold-palladium reaction vessel.[105,106] In many cases the melt can be changed to a system that is less or non-corrosive.

A metal catalyst, such as platinum, can be added to a molten salt supported on a solid. The Pt might be found in three different places. Platinum could be located on the solid support and not covered by the molten salt. This might occur if the Pt surface is not wet by the melt. The Pt could also be located on the outside surface of the melt. Similar reactivity and selectivity to a traditionally supported catalyst would be observed in these two cases. In the third situation, Pt could be dispersed throughout the melt. Catalyst selectivity would be altered because the substrate must diffuse through the melt to reach the catalyst. The effect of the Pt-melt interactions is

not known and may also alter the reaction selectivity. The reactivity may become mass transport limited.

Supporting a reforming catalyst within a molten salt has several advantages over traditional systems. The selectivity will be altered if the substrate must first diffuse through the salt to reach the catalyst. A particular valence state of the catalyst may be stabilized by the melt. If carbon deposition on the catalyst surface were minimized, high pressures of hydrogen would not be necessary to hydrogenate deposited materials, permitting the use of safer inert carrier gasses at low pressures.

If the catalyst is located within the molten liquid a solubility-diffusion based selectivity will be added to the catalytic chemical selectivity. The substrate must first diffuse through the molten salt to reach the catalyst. Only those starting materials soluble in the melt can react on the catalyst. This will superimpose solubility in the melt on the catalytic chemical selectivity of the metal. Reaction products will also be affected by the solubility in the melt because they will either diffuse out of the melt or remain on the catalyst's surface. If a product remains on the surface it may undergo further reaction. Diffusion rates for the organic substrates have not been investigated in the melts used in this work.

We studied Pt^o in halide melts. Not much is known about the behavior of Pt^o in such systems. High temperature stability of the catalyst is gained from the temperature of the melt, sometimes stabilizing a particular valence state of the catalyst. Pt(II) is stabilized in a tetraalkylammonium salts of $SnCl_3^-$, such that no platinum reduction takes place at 160°C and 100 atm. of hydrogen, which would occur in the absence of the salt.[101]

Parshall's[107] example of using a molten salt as a solvent for catalytic reactions involves several transition metal catalysts in molten trihalostannate(II) and trihalogermanate(II) salts for the hydrogenation of olefins or nitriles and the isomerization or carbonylation of olefins. The catalyst, $PtCl_2$, becomes dispersed in the salt and is stabilized as Pt(II).[108] Under these conditions $PtCl_2$ is stable at temperatures up to 200°C at high hydrogen pressures. This stability allows for the hydrogenation of difficultly hydrogenated olefins.[109,110] The temperature and hydrogen pressure necessary are dependant on the particular olefin examined.

By suspending a traditional metal reforming catalyst in a molten salt solvent, selectivity could be enhanced by diffusion, through the melt, to reach metal. A series of compounds was investigated to determine the types of reactions that could occur on this uniquely supported catalyst. The salts examined include group I and II halides, namely K-Li-Na | | Cl or K-Li-Na | | Br, Mg-K | | Br and Ni-Li-K | | Cl. During catalyst preparation, $PtCl_2$ was added to all of the eutectics except the one containing nickel. The melts chosen for this work are stable, have eutectics below 400°C, and contain Group I or II halides.

Results

K-Li-Na | | Cl System

The catalytic reforming of cyclohexene using the Pt-molten salt (K-Li-Na | | Cl) system was explored in detail. A series of other substrates was also examined and will be discussed below. Figure 28 shows the reactivity of cyclohexene, using the single injection apparatus (described in the experimental section) with 100μl injections, on a catalyst containing 10 wt% K-Li-Na | | Cl with 0.73 wt% Pt on Chromosorb P-AW (16.03g total) in a 6' long reactor at 425°C. The ratio of cyclohexene dehydrogenation to disproportionation is shown as a function of the moles cyclohexene introduced per mole of platinum in the reactor. This is a turnover number, normalizing the data to the amount of platinum used.

Two simultaneous reactions are occurring. Cyclohexene dehydrogenation to benzene and hydrogen (Eq. 39) and disproportionation to benzene and cyclohexane (Eq. 40). The ratio of the two reactions can be determined from the product analysis. The product stream from the single injection apparatus was not analyzed for hydrogen. Hydrogen analysis was not performed on experiments using the continuous flow apparatus because chromatography conditions providing separation of the organic materials

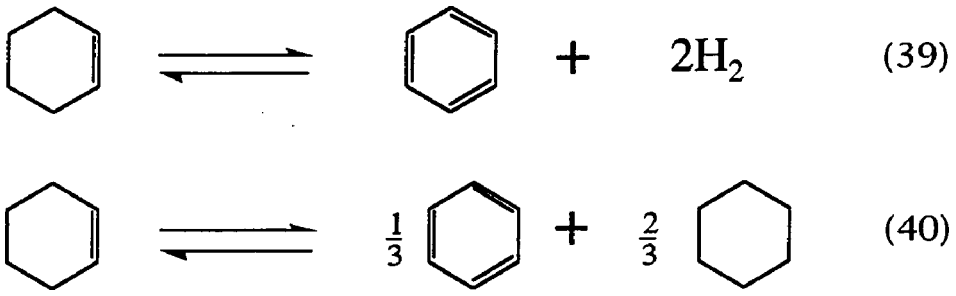

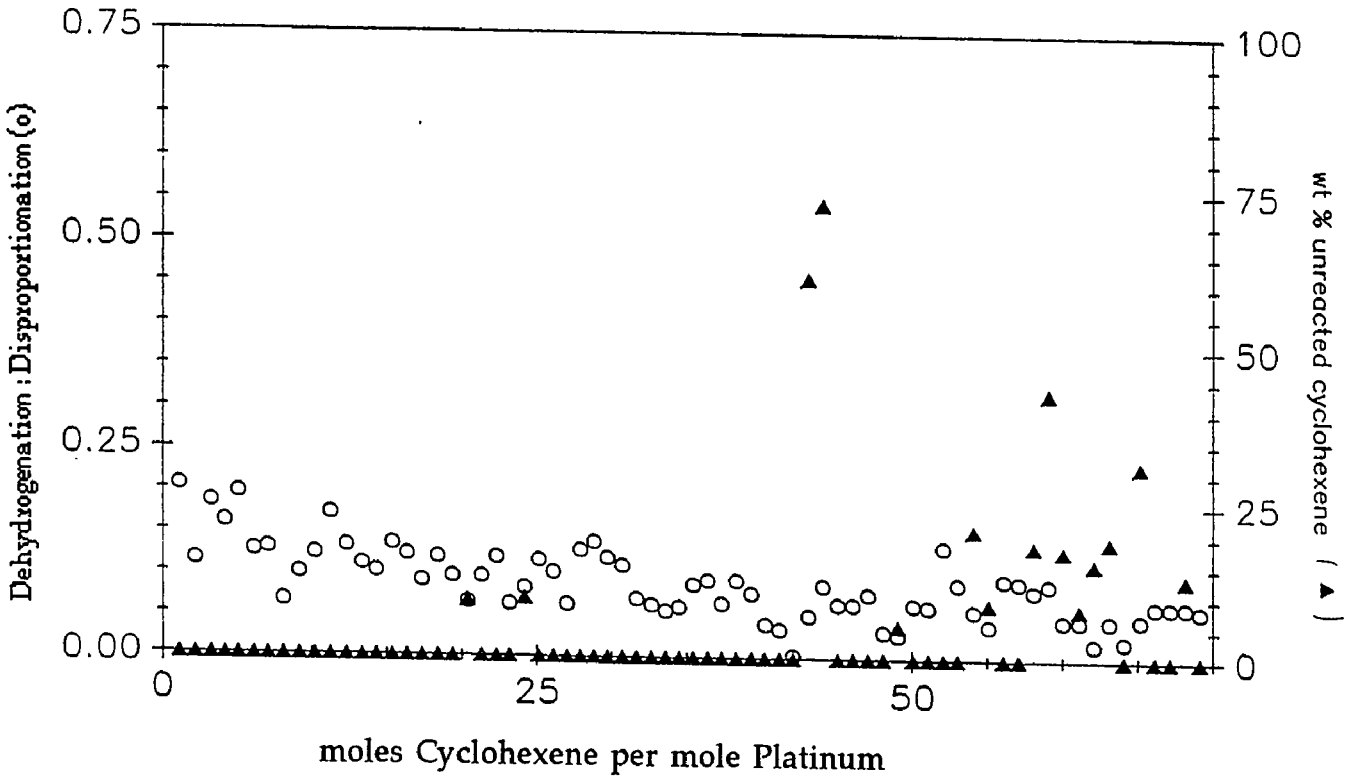

Figure 28. Reactivity of Cyclohexene on a Catalyst Containing 10% K-Li-Na||Cl with 0.73% Pt at 425°C with 1.7 ml/min N_2 Carrier Gas (25°C) Using the Single Injection Apparatus

did not separate hydrogen from the reactor carrier gas. Using the balanced equations (39) and (40), the the ratio of cyclohexene dehydrogenation to disproportionation can be determined. The ratio of dehydrogenation to disproportionation is equall to the amount of benzene formed from dehydrogenation over 3/2 the amount of cyclohexane produced, as shown below. The 3/2 enters because one mole of cyclohexane is produced by the disproportionation of 3/2 moles of cyclohexene. The amount of benzene formed by dehydrogenation is the difference between the total amount of benzene produced and that produced from the disproportionation reaction. The latter is availabe; it is equall to 1/2 of the cyclohexane produced (eq. 39).

$$\frac{\bigcirc_{\text{Dehydrogenation}}}{\bigcirc_{\text{Disproportionation}}} = \frac{\bigcirc_{\text{Dehydrogenation}}}{\frac{3}{2}\bigcirc} =$$

$$\frac{\bigcirc_{\text{Total}} - \bigcirc_{\text{Disproportionation}}}{\frac{3}{2}\bigcirc} = \frac{\bigcirc_{\text{Total}} - \frac{1}{2}\bigcirc}{\frac{3}{2}\bigcirc}$$

Cyclohexene disproportionation is the dominate reaction observed (Left Axis, Figure 28) under the reaction conditions used. The thermodynamically favored pathway, from the calculated equilibrium constants, is dehydrogenation.[97] The wt% of unreacted cyclohexene is also shown in the Figures (Right Axis).

The reactivity of cyclohexene was further explored, and will be discussed in detail below. After establishing that cyclohexene was reactive on a Pt catalyst in a K-Li-Na | | Cl eutectic melt, other substrates were screened

using the single injection apparatus with 100μl injections to determine the scope of reactivity in this system. Prior to and after screening a substrate, the reactivity of cyclohexene was examined. This showed that the catalyst was active before substrate introduction and any catalyst deactivation caused by the substrate could be observed. The substrates screened are important model compounds for reforming reactions or are related to the reforming process.

To insure that the reactivity observed was due to the combination of $PtCl_2$ and the molten salt, several control experiments were performed. Cyclohexene (97%) was recovered unchaned in a reactor containing only the solid support (Chromosorb P-AW, 14.32 g) at 425°C. It was also determined that there was no cyclohexene reactivity on the supported salts. A reactor containing 10.9% K-Li-Na||Cl supported on Chromosorb P-AW (15.21g total) did not show any cyclohexene reactivity at 425°C with a flow of nitrogen. Simmilarly, no reactivity was observed for tetralin under these conditions.

Cyclohexene showed some reactivity on supported $PtCl_2$ (no molten salt) at 425°C. The cyclohexene reactivity (1.09 ml/hr) under a nitrogen flow decreased very rapidly (Figure 29) in a reactor containing catalyst with 0.51% Pt supported on Chromosorb P-AW (15.23g total) using the continuous flow apparatus. The ratio of dehydrogenation to disproportionation is very different from that observed using Pt in the melt. The ratio of dehydrogenation to disproportionation is negative. This is not possible if these are the only two reactions occuring. Coke formation would produce hydrogen, which might result in the hydrogenation of cyclohexene, which would lead to a negative ratio of the two reactions.

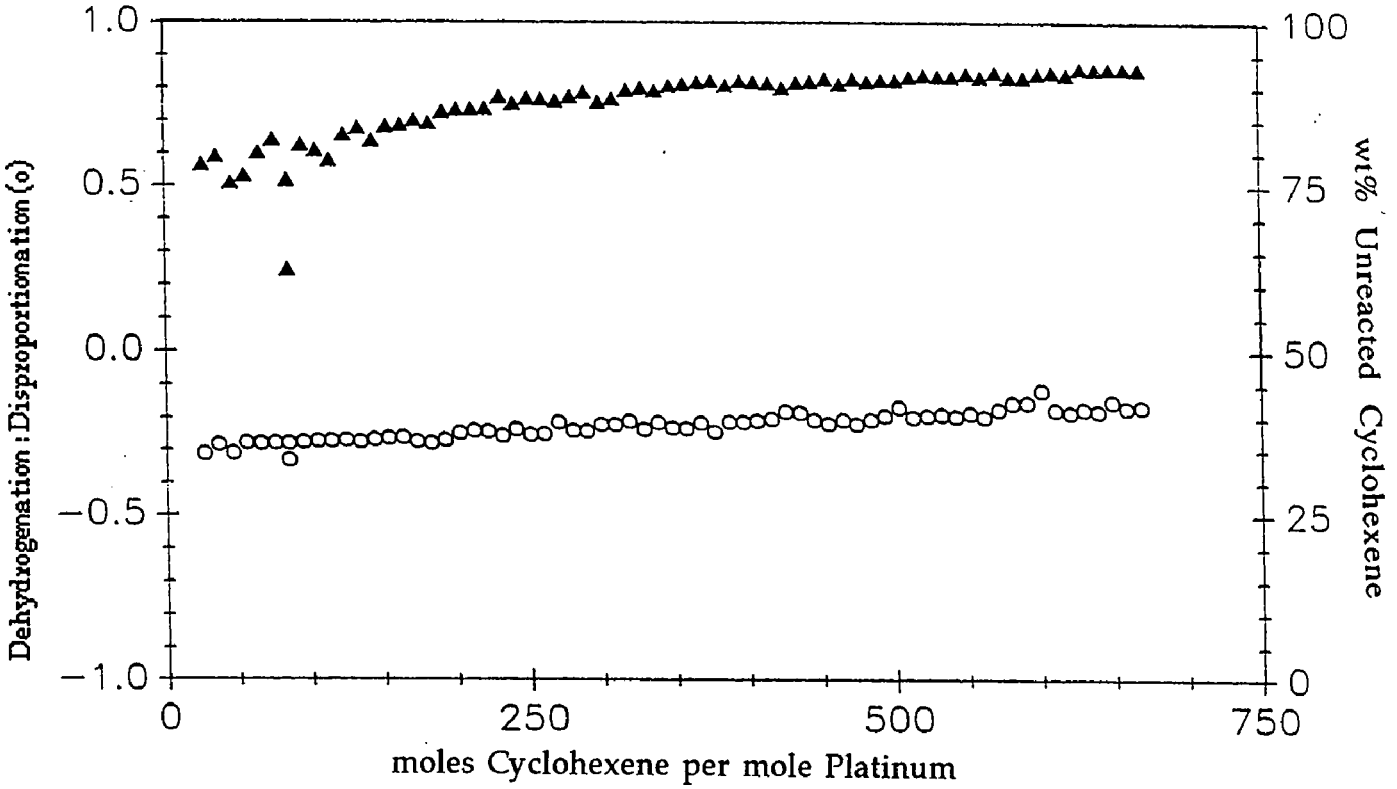

Figure 29. Reactivity of Cyclohexene on a Catalyst Containing 0.507% Pt at 425°C with 1.7 ml/min N_2 Carrier Gas (25°C).

A similar experiment using a catalyst containing 0.51% Pt without any salts supported on Chromosorb P-AW (14.63g total), but changing the carrier gas to a mixture of helium with 5% hydrogen, showed slightly enhanced cyclohexene reactivity (Figure 30). The carrier gas was changed include hydrogen to determine whether the catalyst's life would be prolonged by the presence of hydrogen. The negative ratio remained unchanged, demonstrating that low pressure hydrogen has little effect on what we presume to be coking.

The reactivity of both cyclohexadiene isomers was studied because they are possible reaction intermediates for the dehydrogenation and/or disproportionation of cyclohexene. The reactions were carried out using a reactor containing 10 wt% K-Li-Na||Cl with 0.73% Pt supported on Chromosorb P-AW (16.03g total) at 425°C under a flow of N_2. All of the reactors were 6' long, unless otherwise indicated. 1,3-Cyclohexadiene reacted in this system producing cyclohexane (17 wt%), cyclohexene (24%) and benzene (59%). The reactivity of cyclohexene immediately following this reaction was only 33%, compared with 100% prior to the reaction of 1,3-cyclohexadiene. Complete cyclohexene reactivity was restored (see Table 32) if the system was kept at 425°C for 10 hours (overnight) with a flow of an inert carrier gas. 1,4-Cyclohexadiene produced cyclohexane (15 wt%) and benzene (85%) without any catalyst deactivation.

The reactivity of 1,4-cyclohexadiene was also studied on supported salts without platinum. The reactor was shorter (2' long) than those previously described and it contained 2.55g of a catalyst containing 9.9% K-Li-Na||Cl. Cyclohexane (14 wt%), cyclohexene (16%), and benzene (70%) were produced, indicating that 1,4-cyclohexadiene undergoes a thermal reaction at 425°C.

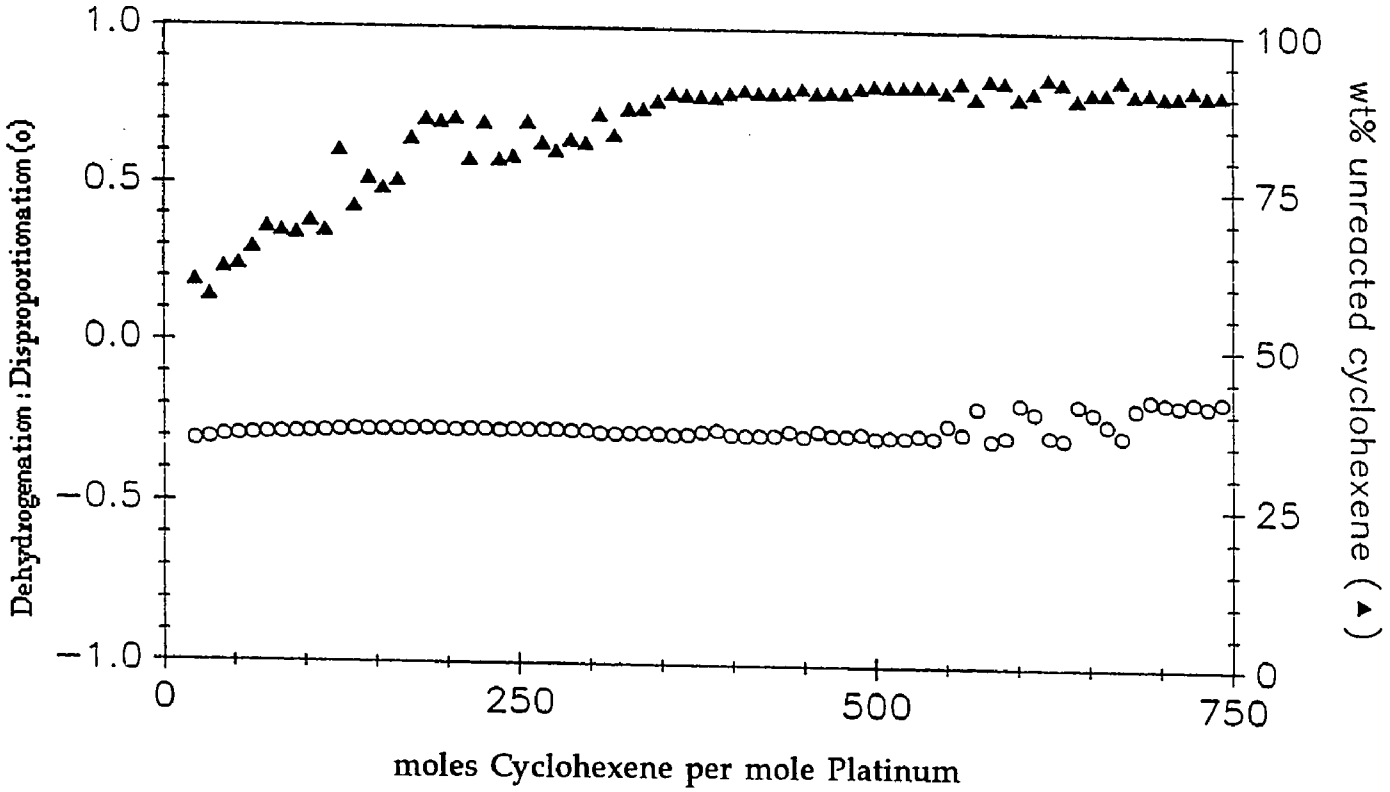

Figure 30. Reactivity of Cyclohexene on a Catalyst Containing 0.507% Pt at425°C with 1.7 ml/min He-H_2(5%) Carrier Gas (25°C).

Table 32. Reactivity of Several Substrates on 10% K-Li-Na | |Cl with 0.66% Pt at 425°C Using the Single Injection Apparatus with 100µl Injections.

		Products (wt %)		
Substrate	Time	C_6H_{12}	C_6H_{10}	C_6H_6
Cyclohexene	9:00 pm	66.5	-	33.5
1,3 Cyclohexadiene	9:50 pm	17.0	23.6	59.3
Cyclohexene	10:30pm	21.2	66.5	12.2
Cyclohexene	11:10pm	16.1	73.8	10.2
Cyclohexene	9:00 am	62.3	-	37.4
Cyclohexene	4:00 pm	58.8	-	41.2
1,4-Cyclohexadiene	5:00 pm	15.3	-	84.7
Cyclohexene	5:45 pm	61.1	-	38.9

Cyclohexane and benzene, the products observed from the cyclohexene reaction, were studied to see if they would undergo further reaction. The reactor contained 10% K-Li-Na | |Cl with 0.66% Pt supported on Chromosorb P-AW (14.67g total) at 425°C with a flow of nitrogen. Only starting material (97%) was recovered from the reaction of either cyclohexane(100µl) or benzene(100µl). Cyclohexane would be unreactive if it did not reach the Pt surface, which would occur if cyclohexane did not dissolve in the melt.

Tetralin reacted on a catalyst containing 10% K-Li-Na | |Cl with 0.33% Pt supported on Chromosorb P-AW (14.11g total) at 425°C under a flow of N_2. The catalyst was not deactivated from the reaction of tetralin (100µl), which was partially converted to napthalene (5%, 95 wt% starting material). The reactivity of n-butyl benzene, a tetralin precursor was examined using a reactor filled with catalyst containing 10% K-Li-Na | |Cl with 0.66% Pt

supported on Chromosorb P-AW (14.67g total). The substituted benzene was recovered unchanged (96%) under these reaction conditions.

Several linear molecules were examined to see if cyclization could occur in this system. A linear hydrocarbon, n-heptane did not produce any cyclic or olefinic products in a reactor containing a catalyst composed of 10% k-Li-Na| |Cl with 0.33% Pt supported on Chromosorb P-AW (14.11g) at 425°C under a flow of nitrogen. Toluene, the product from heptane reforming also was not reactive. A linear olefin, 1-hexene, also did not react under these conditions. The results are are summarized in Table 33.

Table 33. Summary of Reactivity on a Pt Catalyst Supported in a K-Li-Na| |Cl Eutectic at 425°C.

Reactant (100μl)	Products	[Recovery]	(Conversion)
Benzene	no reaction	[97%]	
n-Butyl Benzene	no reaction	[96%]	
Cyclohexane	no reaction	[97%]	
Cyclohexene	Cyclohexane, Benzene, H_2	[99%]	(100%)
Heptane	no reaction	[98%]	
1-Hexene	no reaction	[98%]	
Tetralin	naphthalene	[98%]	(5%)
Toluene	no reaction	[98%]	

As previously described, cyclohexene was highly reactive in a K-Li-Na| |Cl melt containing Pt. The results shown in Figure 28 (p. 133) are for an experiment using the single injection apparatus. Results for a similar catalyst (16.54g containing 10% K-Li-Na| |Cl, 0.73% Pt) using the continuous flow apparatus are shown in Figure 31. Cyclohexene introduced at 1.09 ml/hr

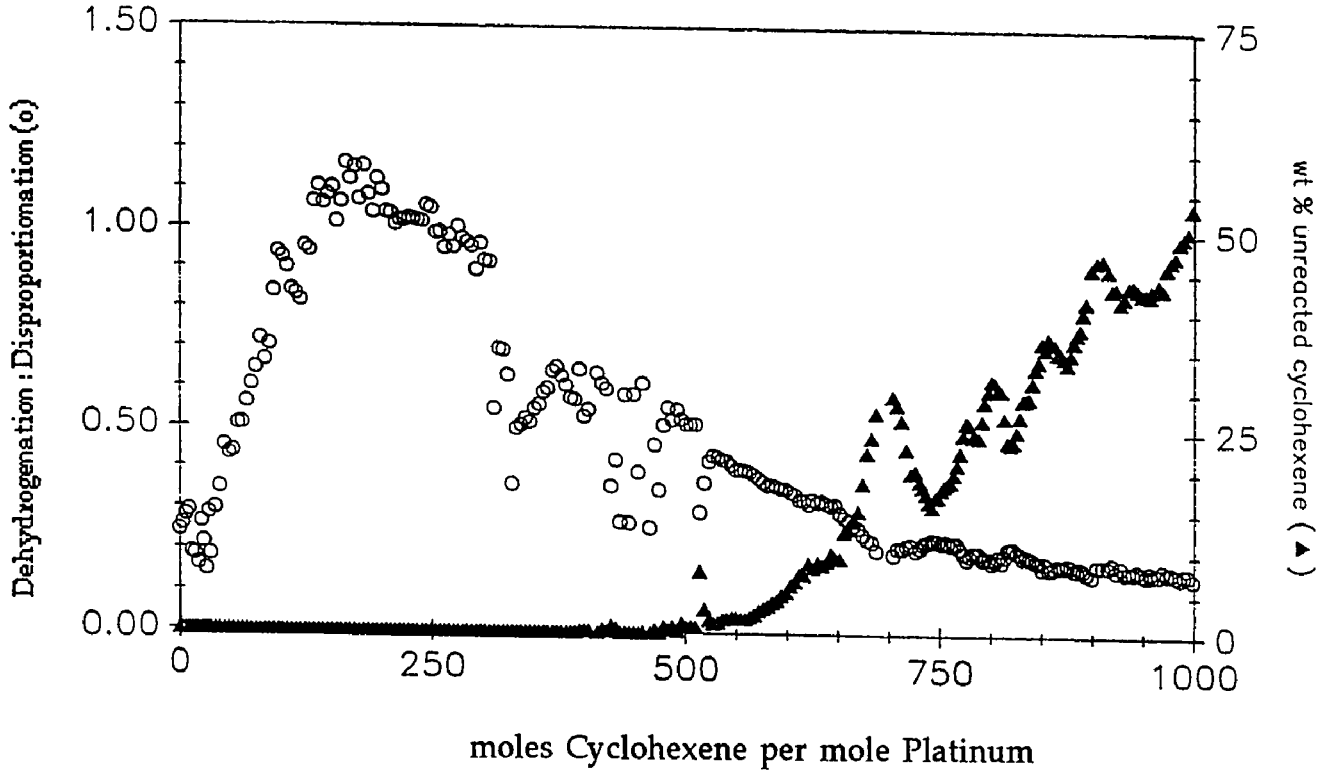

Figure 31. Reactivity of Cyclohexene on a Catalyst Containing 10% K-Li-Na I I Cl with 0.73% Pt at 425°C with 1.7 ml/min N_2 Carrier Gas (25°C) Using the Continuous Flow Apparatus.

reacts completely until a turnover of approximately 500 is reached. Disproportionation is the process initially favored, but dehydrogenation becomes the favored process for a period of time, and then disproportionation once again dominates as catalytic activity begins to fall off.

The fluctuation observed for the amount of unreacted cyclohexene in Figure 31 is a result of the experimental procedure. The apparatus used a syringe pump to introduce the cyclohexene. When the syringe was refilled, a deviation in the rate of starting material introduction occurred. A slight pulse of starting material resulted from reconnecting the syringe. Because an additional amount of starting material had been introduced temporarily overloading the catalyst, a decrease in reactivity was observed.

Several factors affecting the reaction of cyclohexene in a K-Li-Na||Cl melt containing Pt were explored. The effect of varying the carrier gas, catalyst regeneration, and the amount of salt were investigated.

Effect of Carrier Gas on Cyclohexene Reactivity

The effect of varying the carrier gas on cyclohexene reactivity was investigated using the continuous flow apparatus at 425°C. The reactivity of cyclohexene using nitrogen, helium, or helium with 5% hydrogen carrier gas was examined. The reactor for the nitrogen carrier gas experiment contained catalyst composed of 10% salts with 0.73% Pt supported on Chromosorb P-AW (16.64g total, Figure 31). The results for the reaction of cyclohexane (1.09 ml/hr) in a reactor with catalyst composed of 9.9% salts with 0.73% Pt supported on Chromosorb P-AW (14.24g total) using a helium carrier gas are shown in Figure 32. The reactor for the mixed carrier gas run contained 9.9% salts with 0.73% Pt supported on Chromosorb P-AW (14.24g total) and

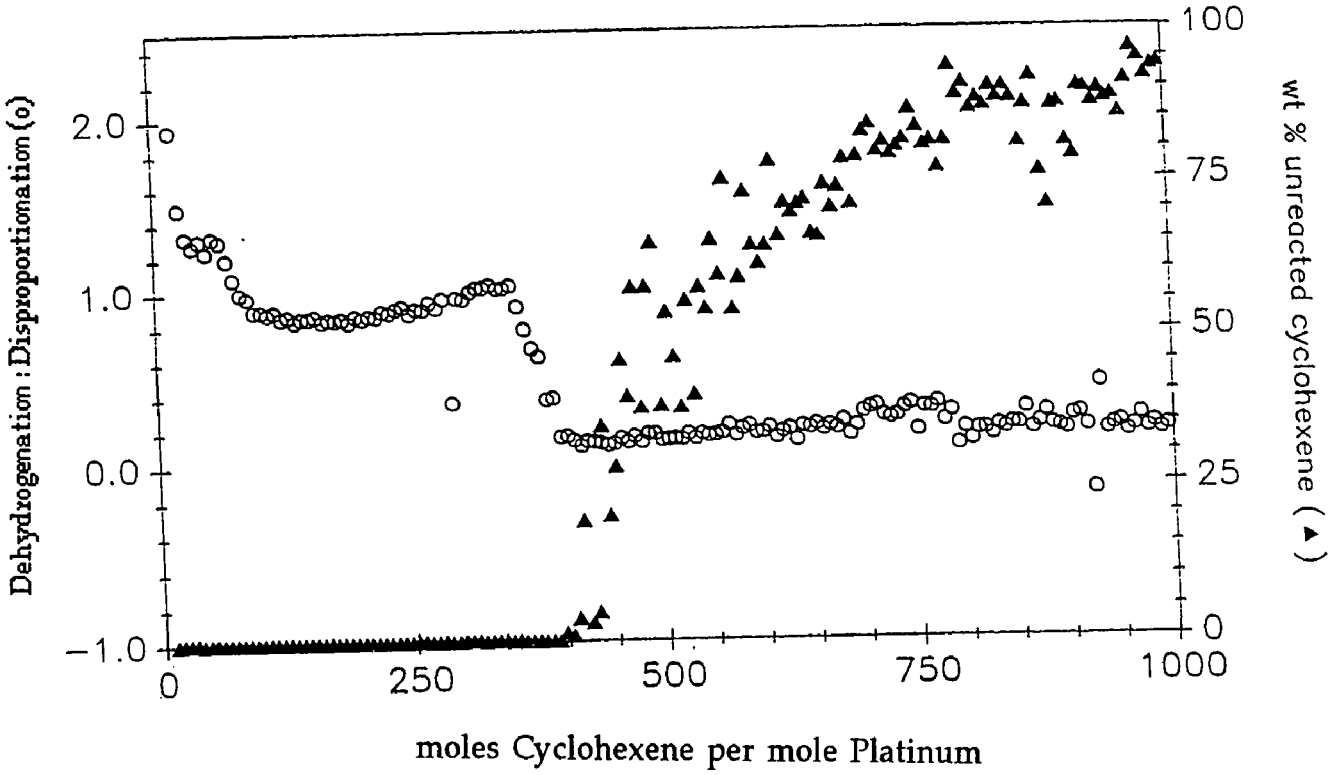

Figure 32. Reactivity of Cyclohexene on a Catalyst Containing 9.9% K-Li-Na||Cl with 0.73% Pt at 425°C with 1.7 ml/min He Carrier Gas (25°C).

cyclohexene was introduced at 1.09 ml/hr. The results for the He-H_2(5%) carrier gas mixture for the reaction of cyclohexene (1.09 ml/hr) are shown in Figure 33. All three systems show 100% cyclohexene reactivity to a turnover of at least 400. Figure 34 shows that the initially preferred reaction is dependant on the carrier gas used, suggesting an important role for mass transport. Although there is an initial preference, disproportionation is the favored reaction as the catalyst deactivates.

Catalyst Regeneration

A catalyst deactivated from the reaction of cyclohexene could be regenerated with oxygen. If deactivation is due to coke formation, it may be possible to burn off the coke. The original catalyst (12.77g total, containing 4.25% salts with 0.85% Pt) showed the same cyclohexene reactivity pattern as the other catalysts examined at 425°C using the continuous flow apparatus (Figure 35). When the catalyst showed less than 25% reactivity, cyclohexene introduction (1.55 ml/hr) was ceased and the carrier was switched from nitrogen to oxygen. A flow of oxygen at 1.7 ml/min (25°C) was passed over the catalyst at the 425°C for 5.5 hours. The carrier gas was changed to helium and cyclohexene introduction (1.55 ml/hr) was resumed. Catalyst reactivity was restored, but the catalyst had been altered. The catalyst was deactivated more rapidly than in the original run (Figure 36). Although disproportionation was still the predominate pathway, it was not as favored as before. When the catalyst again became inactive to cyclohexene, it was exposed to an oxygen flow of 1.7 ml/min for a period of seven days at 425°C. Catalyst activity comprable to the original material was observed, except that dehydrogenation was the favored reaction using the regenerated catalyst

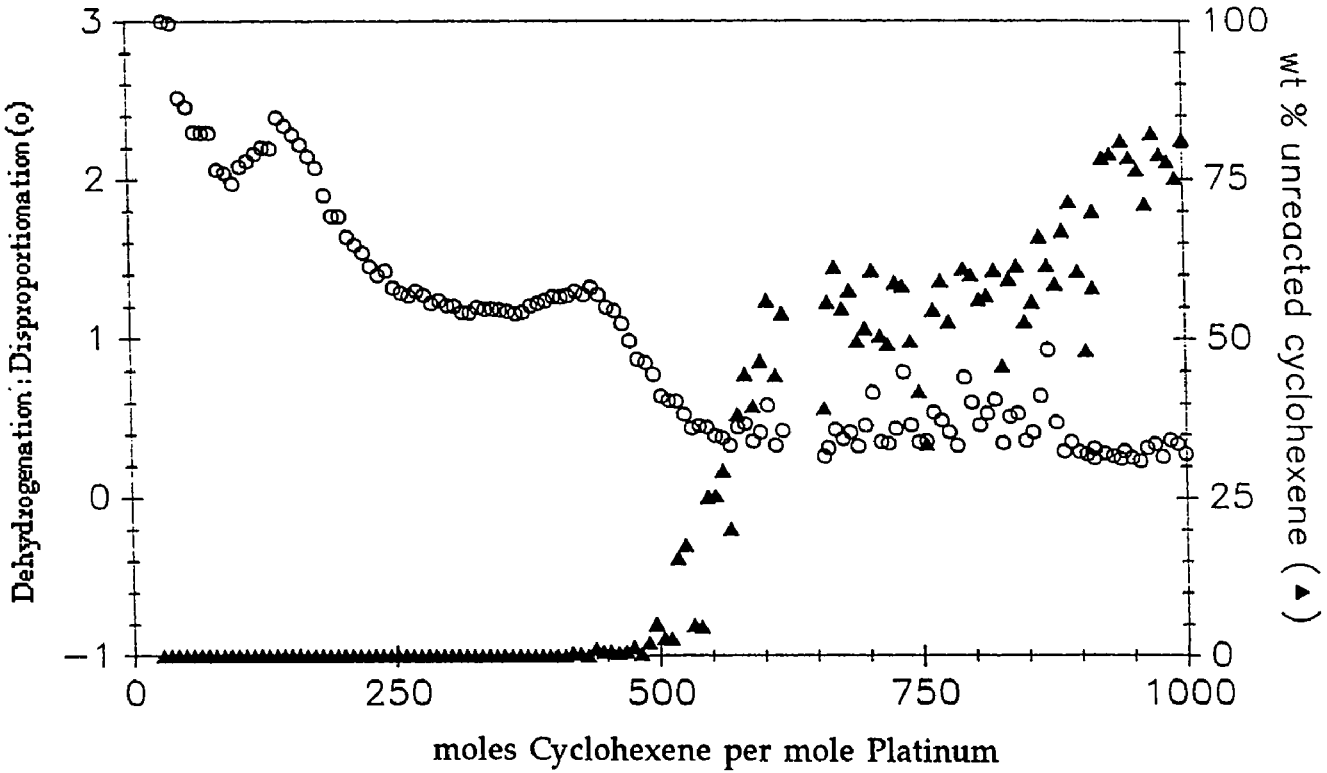

Figure 33. Reactivity of Cyclohexene on a Catalyst Containing 9.9% K-Li-Na | | Cl with 0.73% Pt at 425°C with 1.7 ml/ min He-H_2(5%) Carrier Gas (25°C).

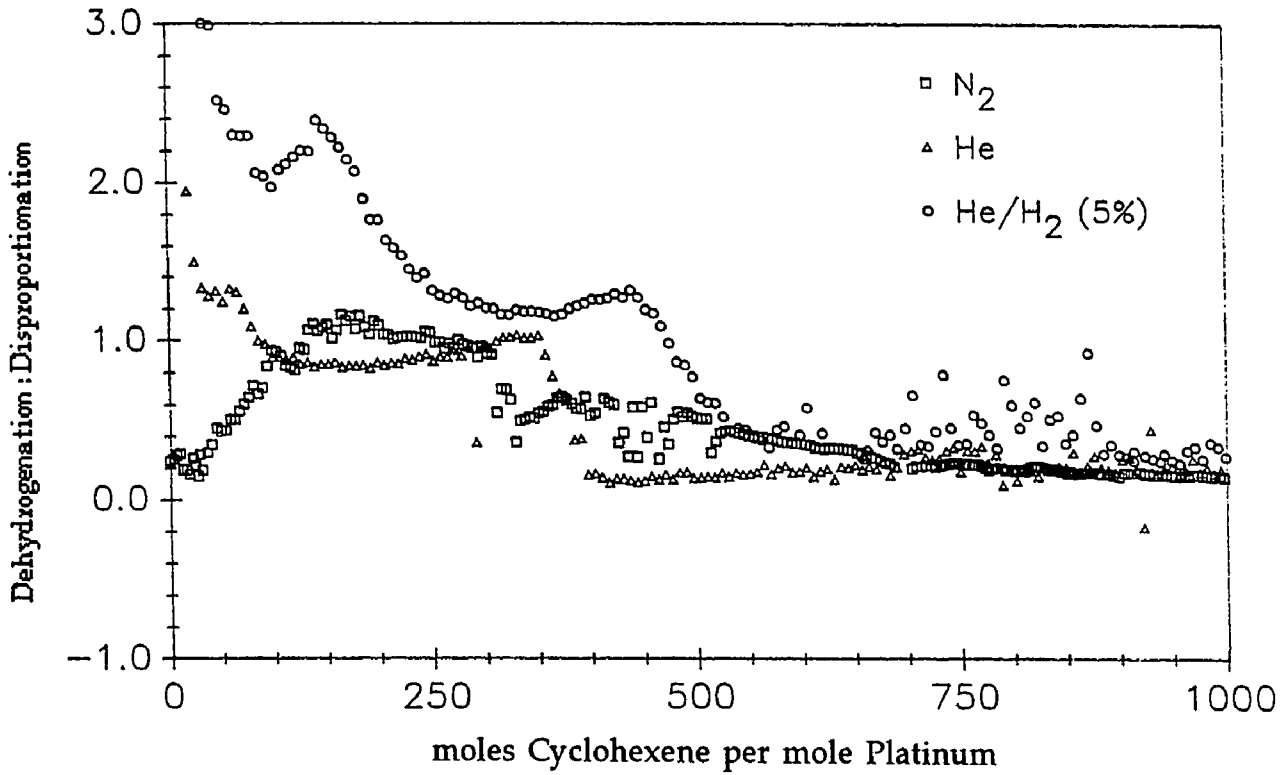

Figure 34. Effect of Carrier Gas on Product Distribution, 9.9% K-Li-Na | |Cl with 0.73% Pt at 425°C with 1.7 ml/min Carrier Gas (25°C).

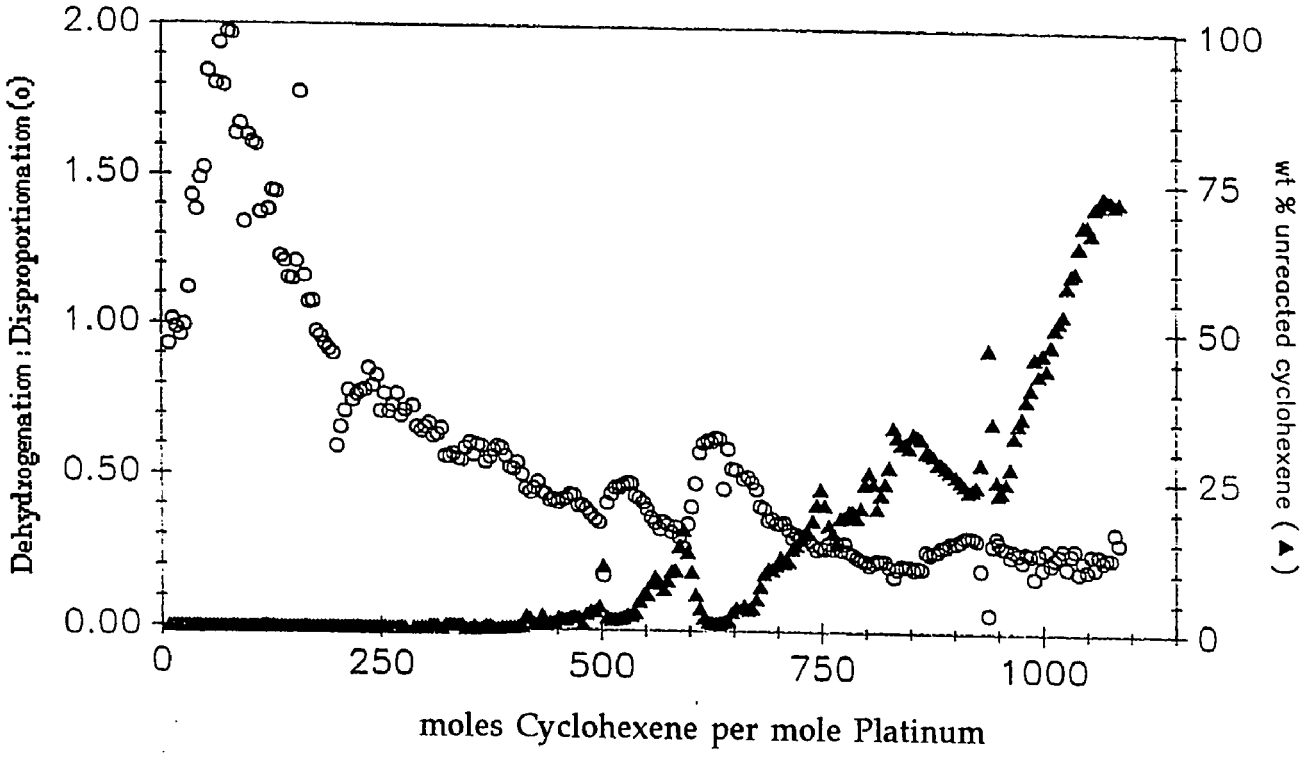

Figure 35. Reactivity of Cyclohexene on a Catalyst Containing 4.3% K-Li-Na | |Cl with 0.85% Pt at 425°C with 1.7 ml/min N_2 Carrier Gas (25°C).

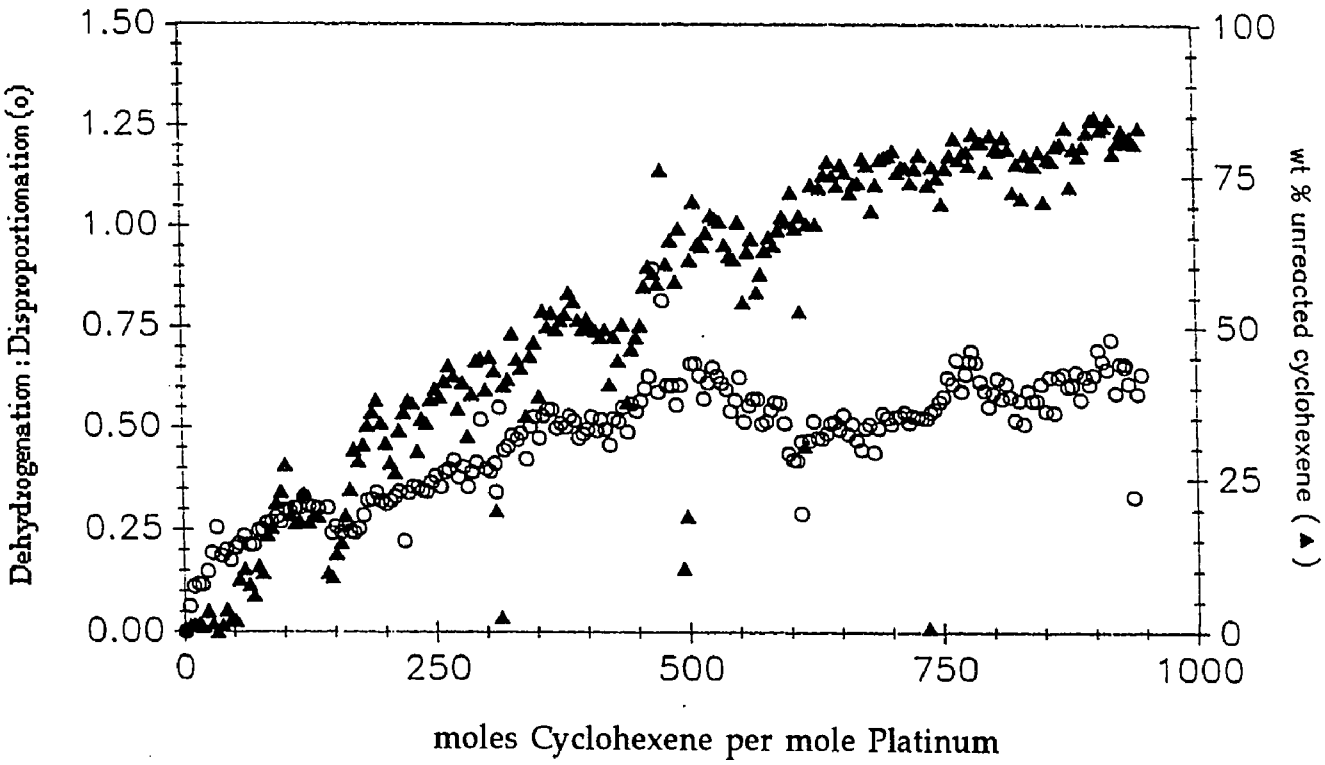

Figure 36. Reactivity of Cyclohexene on a Catalyst Containing 4.3% K-Li-Na | | Cl with 0.85% Pt at 425°C with 1.7 ml/min He Carrier Gas (25°C) After O_2 For 5.5 hr.

(Figure 37). The catalyst was regenerated once again for a period of 2.7 days with an oxygen flow (1.7 ml/min). Complete catalyst activity was regained but reactivity decreased more rapidly than the original catalyst (Figure 38). These results indicate that the catalyst is regenerable and the preferred reaction changes after regeneration.

Effect of Salt Loading on Cyclohexene Reactivity

The effect of varying the loading of the salt on the reactivity and reaction selectivity of cyclohexene was investigated using the continuous flow apparatus at 425°C with a nitrogen carrier gas. Three catalysts were examined that had different salt loading, but contained the same amount of platinum per gram of salt (constant Pt concentration). The cyclohexene (1.09 ml/hr) reactivity of a catalyst having 2.5 wt% salts with 0.19% Pt (0.0735g Pt/g salt) supported on Chromosorb P-AW (15.71g total) is shown in Figure 39. The reactivity decreases very rapidly and the preferred reaction changes with the amount of cyclohexene introduced into the system.

Increasing the amount of salt present to 7.4% shows a decrease in the rate of deactivation for the reaction of cyclohexene (1.09 ml/hr) from the sample containing 2.5% salts (Figure 40). Disproportionation is the preferred reaction for a catalyst (15.98g) containing 7.4% salts with 0.53% Pt (0.072g Pt/ g salt). A further increase to 10% salts (Figure 31) shows that the catalyst (0.73% Pt; 0.073g Pt/ 1g salt) does not deactivate readily.

The amount of unreacted cyclohexene for all three salt loadings is shown in Figure 41. Although the catalysts contain various amounts of platinum, the data have been normalized by plotting the amount of

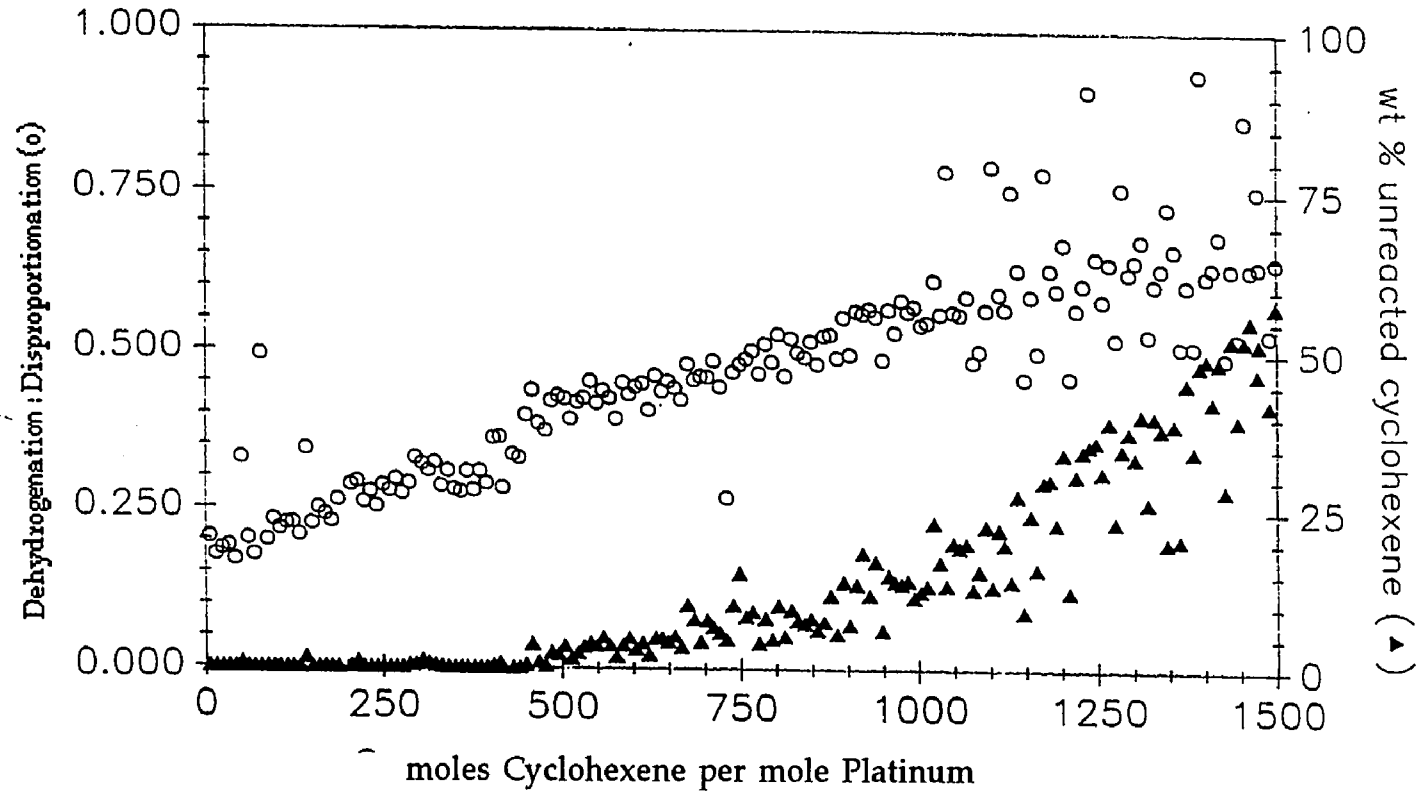

Figure 37. Reactivity of Cyclohexene on a Catalyst Containing 4.3% K-Li-Na | | Cl with 0.85% Pt at 425°C with 1.7 ml/min He Carrier Gas (25°C) After O_2 For 5.5 hr and 7 days.

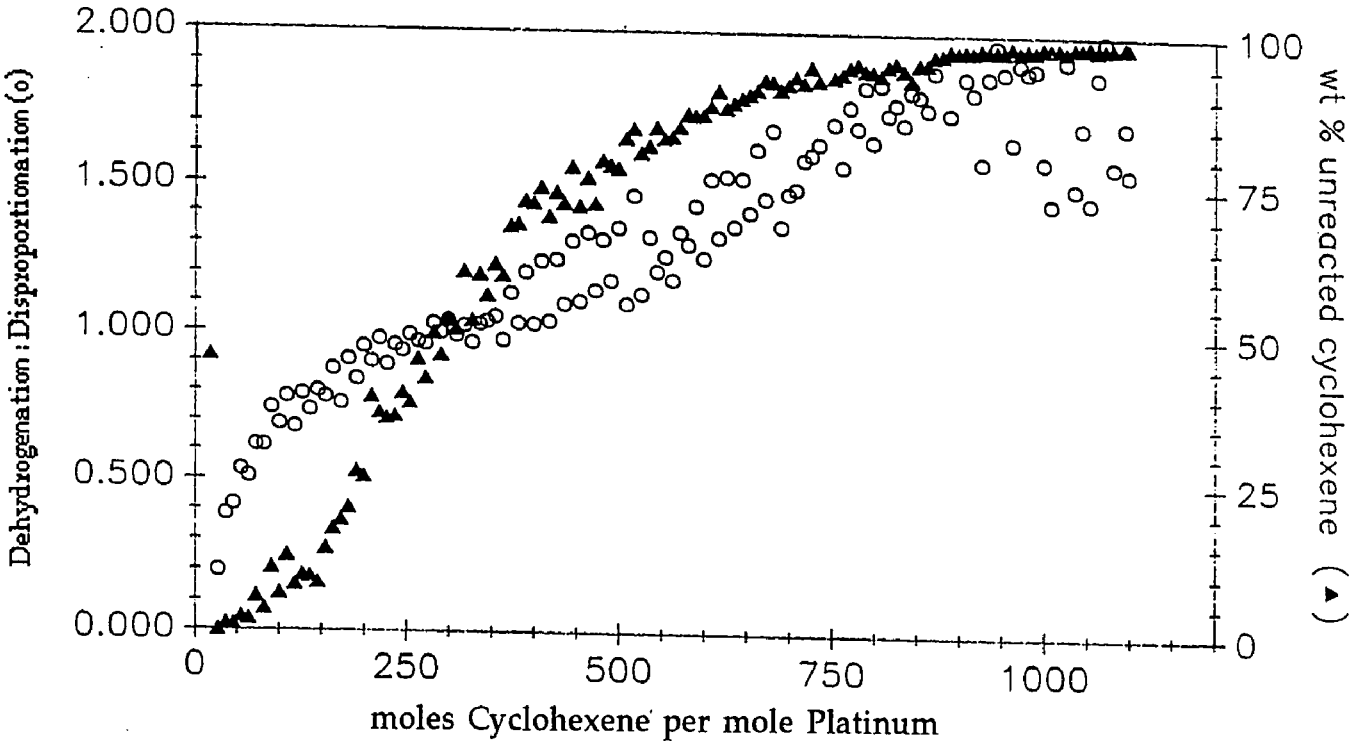

Figure 38. Reactivity of Cyclohexene on a Catalyst Containing 4.3% K-Li-Na||Cl with 0.85% Pt at 425°C with 1.7 ml/min He Carrier Gas (25°C) After O_2 For 5.5 hr and 7 days and 2.7 days.

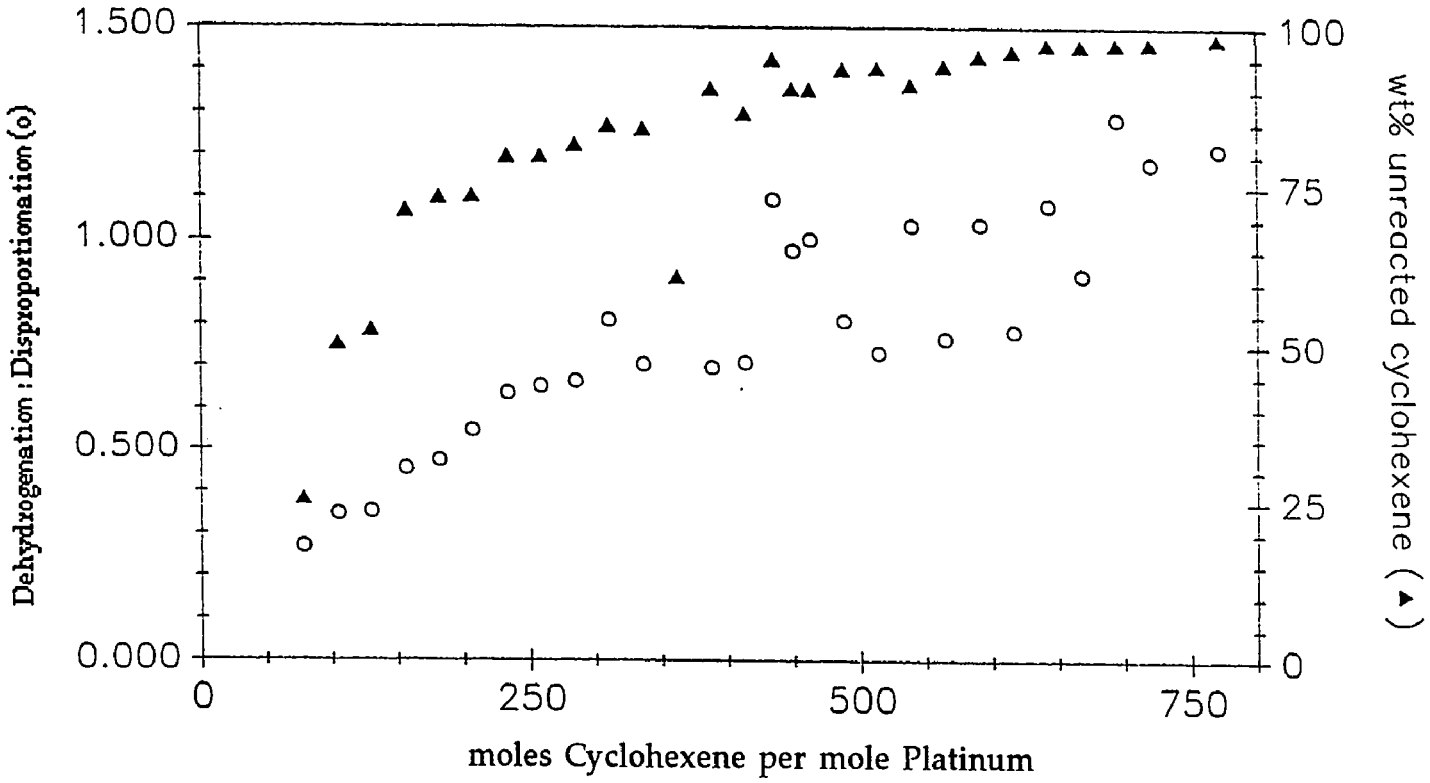

Figure 39. Reactivity of Cyclohexene on a Catalyst Containing 2.5% K-Li-Na | | Cl with 0.19% Pt (0.073g Pt/ g Salts) at 425°C with 1.7 ml/ min N_2 Carrier Gas (25°C).

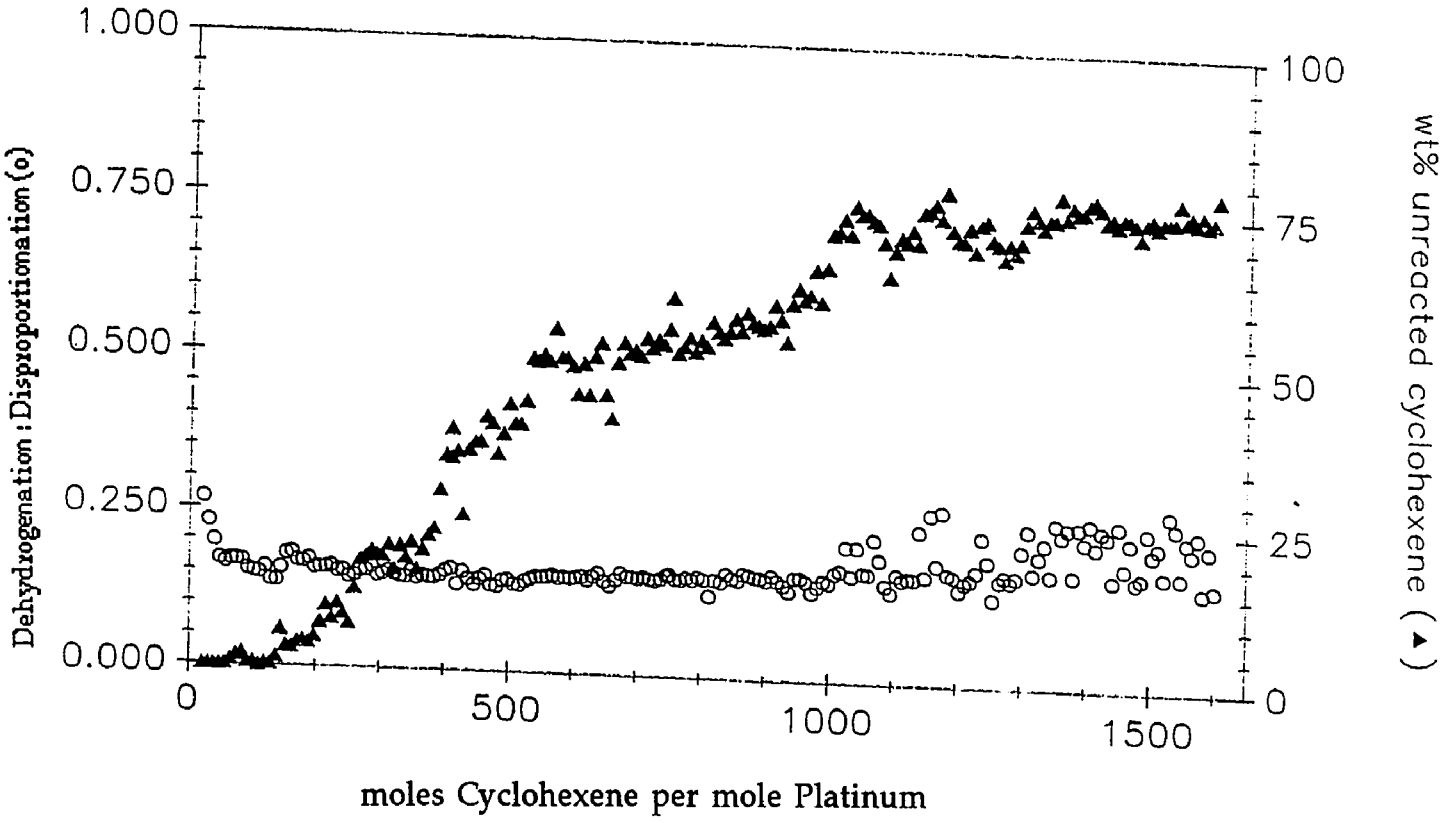

Figure 40. Reactivity of Cyclohexene on a Catalyst Containing 7.4% K-Li-Na | | Cl with 0.53% Pt (0.072g Pt/g Salts) at 425°C with 1.7 ml/min N_2 Carrier Gas (25°C).

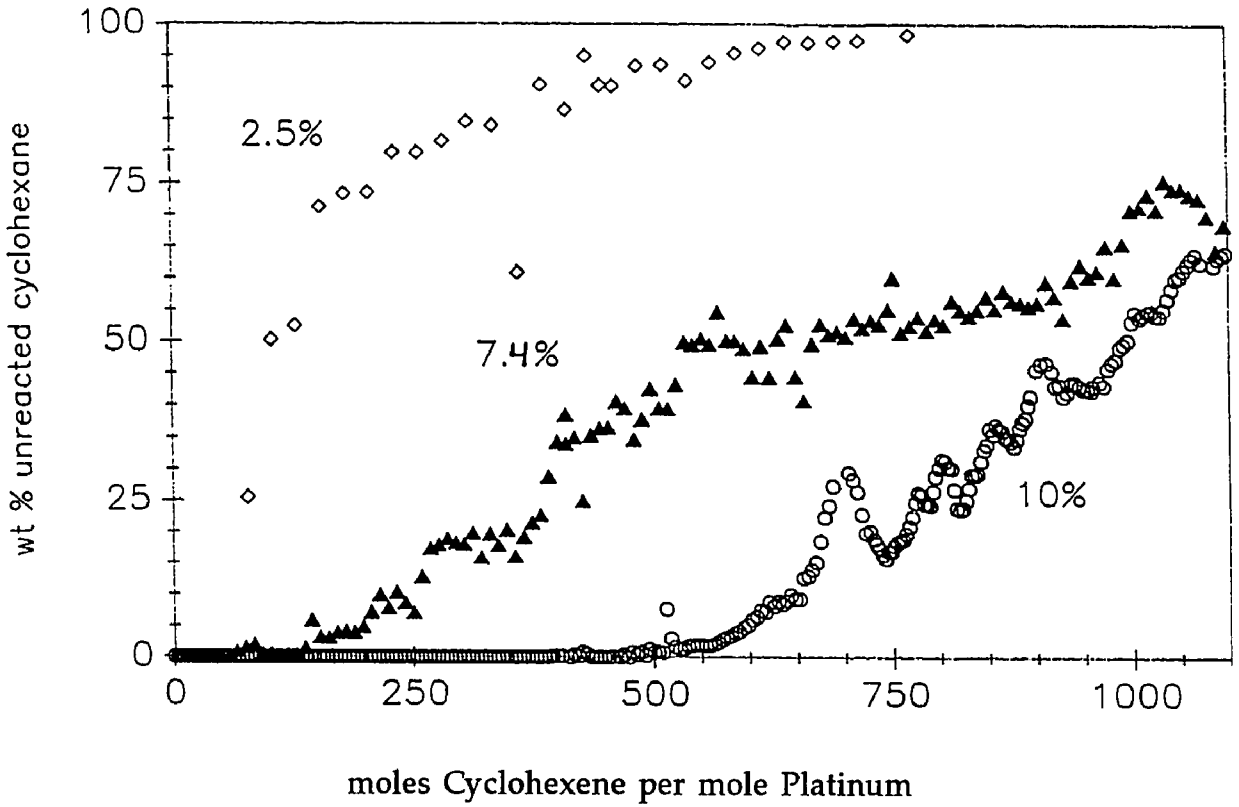

Figure 41. Effect of Salt Loading on Cyclohexene Reactivity of a K-Li-Na||Cl Eutectic with 0.072g Pt/g Salts at 425°C with 1.7 ml/min N_2 Carrier Gas (25°C).

cyclohexene injected per mole of platinum into the reactor. More unreacted cyclohexene is recovered using catalysts with lower salt loadings.

The reaction selectivity also changes with the salt loading. The catalyst that contained the smallest amount of salt (2.5%) behaved differently from the catalysts having a higher salt content. As this catalyst deactivated, dehydrogenation became the favored reaction. At the higher salt loadings examined (10, 7.4%) disproportionation becomes the favored reaction as the catalyst deactivates. A comparison of the selectivity of these three systems is shown in Figure 42.

Examination of the Catalyst

The catalyst was examined in an attempt to understand the observed reactivity pattern. The valence state of the platinum in the catalyst was determined and optical microscopic examination of the catalyst system was done. The valence state was examined using Electron Spectroscopy for Chemical Analysis (ESCA) to determine the platinum valence state. Due to charging that occurs because the support is an insulator peak tailing occurs. The binding energies of the platinum $4f_{7/2}$ and $4f_{5/2}$ electrons, which are dependant on the valence state and the coordination of the metal, were measured. The separation of the $4f_{7/2}$ and $4f_{5/2}$ binding energy of platinum, regardless of the valence state, is 3.35 eV, with the $4f_{5/2}$ peak at the higher energy.[111] The spectra were referenced to the aluminum oxide 2p peak (73.7 ev) of the support.[111] Depending on the valence state of the platinum, one of the platinum peaks may be masked by the aluminum oxide peak. The

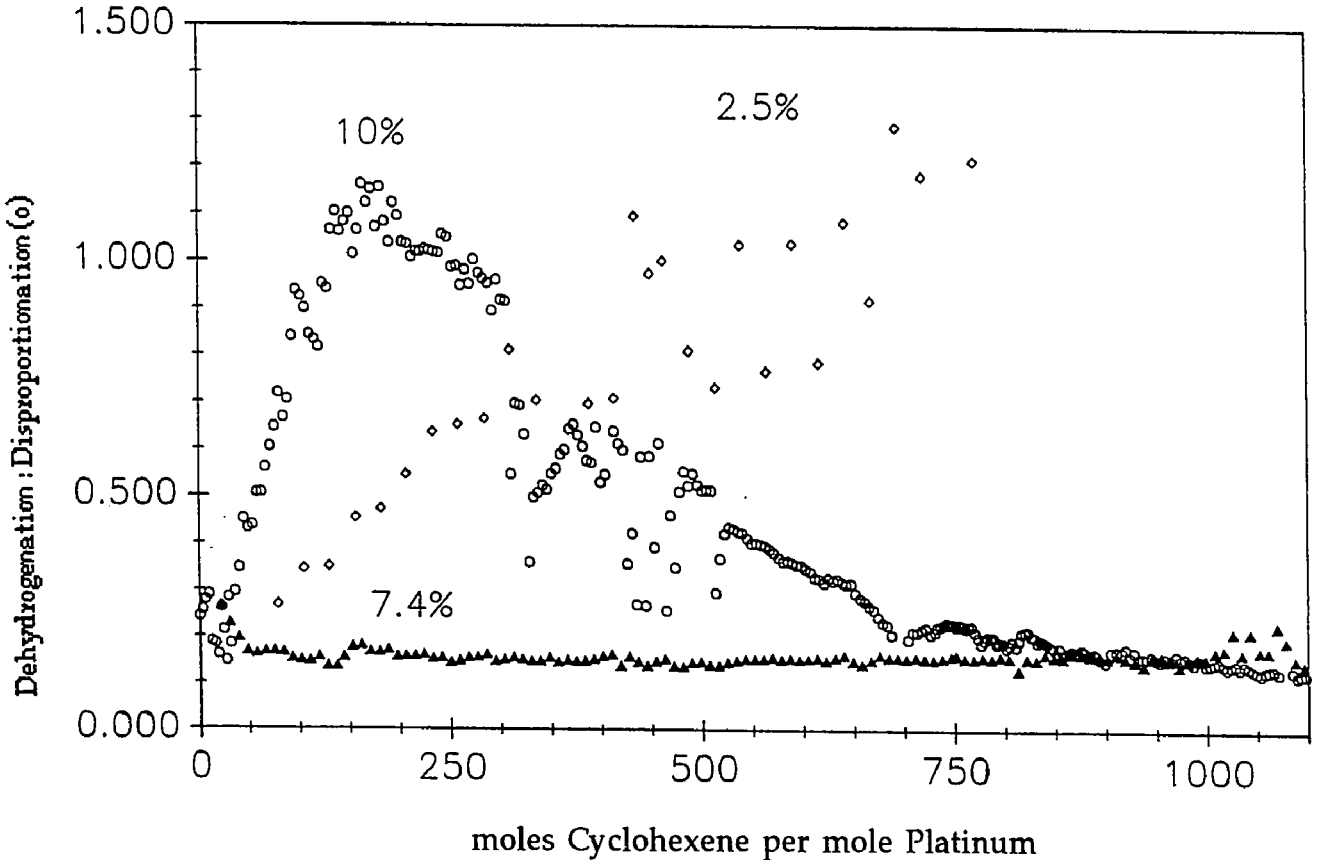

Figure 42. Effect of Salt Loading on Cyclohexene Selectivity of a K-Li-Na | |Cl Eutectic with 0.072g Pt/g Salts at 425°C with 1.7 ml/min N_2 Carrier Gas (25°C).

binding energies of unused, used once, and exhaustively used catalyst are shown in Table 34. The full scans are shown in Figure 43.

Table 34. Binding Energies of Platinum in the Catalyst

	$4f_{5/2}$	$4f_{7/2}$
Catalyst Used Once	74.3	71.0
Exhausted Catalyst	74.3	71.0
Unused Catalyst	78.4	75.0

Several samples of used catalyst were examined using an optical microscope at room temperature, exposed to air. A photograph of unused, untreated Chromosorb P-AW is shown in Figure 44. In Figure 45, a photograph of a supported catalyst containing 9.9% K-Li-Na | |Cl with 0.73% Pt is shown. The only difference between the two cases are the gloubles, which we believe is salt. The salt does not completely cover the solid support and salt does not appear on every support particle. Figure 46 is a photograph of a catalyst containing 9.9% K-Mg | |Br with 0.73% Pt added. It appears that the salts are hydrated and completely cover a few of the particles. Like the chloride eutectic, the potassium bromide and magnesium bromide eutectic does not cover every particle.

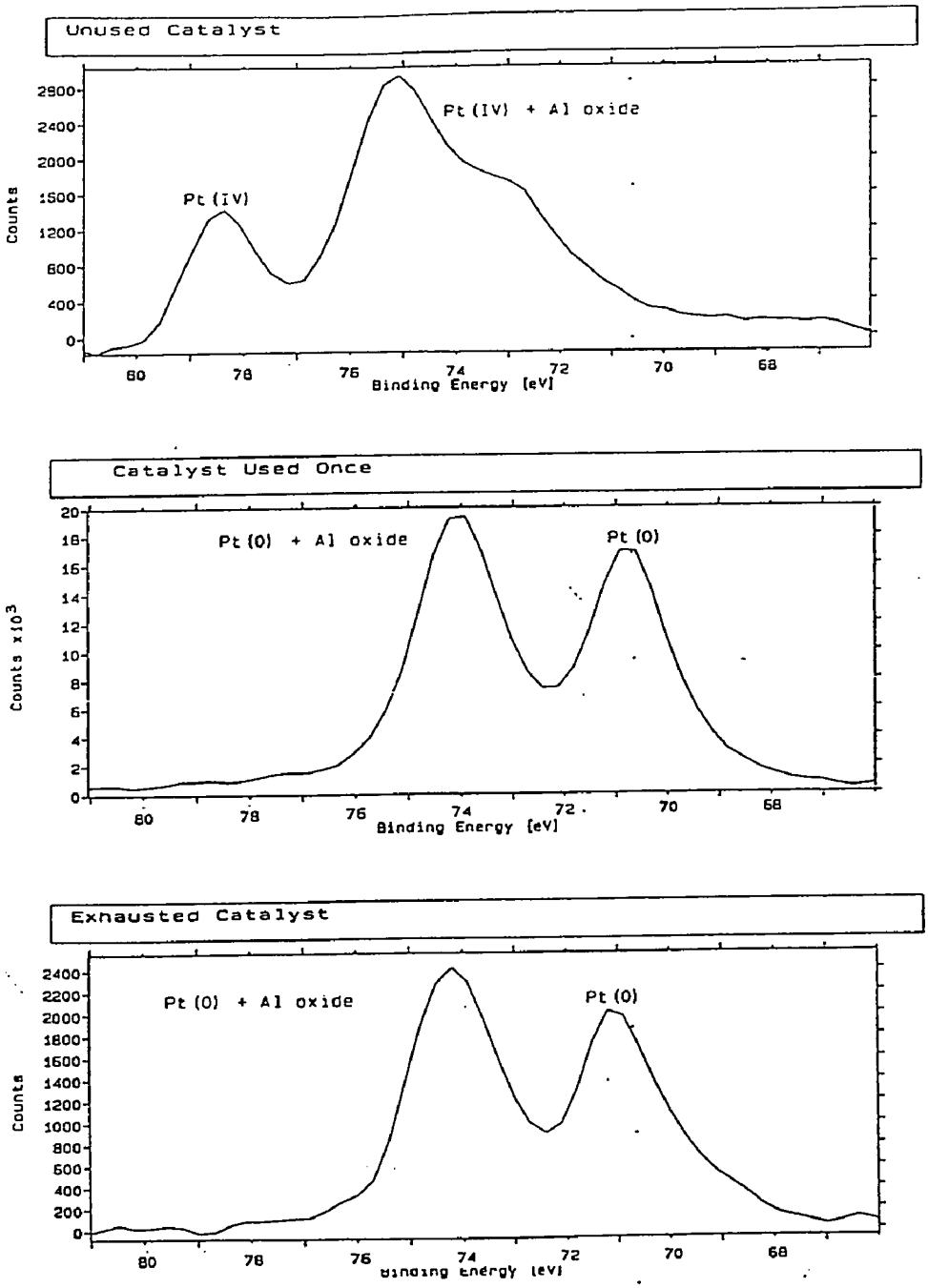

Figure 43. ESCA Spectra.

Figure 44. Photograph of Chromosorb P-AW at 60X Magnification

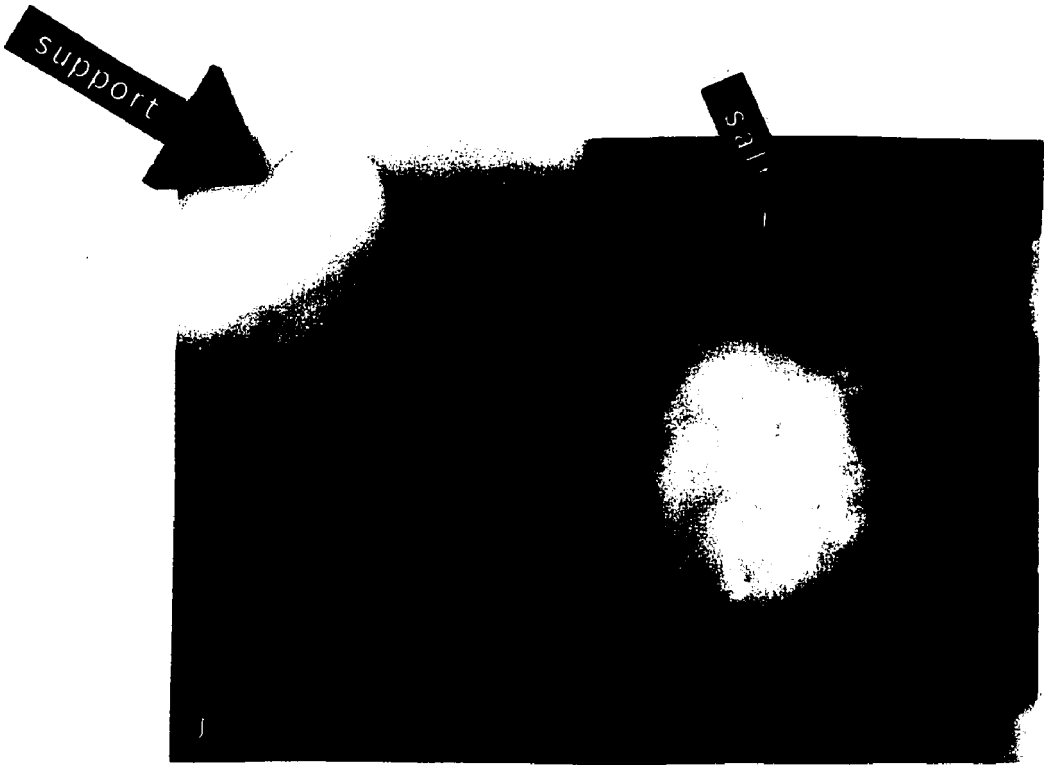

Figure 45. Photograph of 9.9% K-Li-Na | |Cl With 0.73% Pt at 60X Magnification

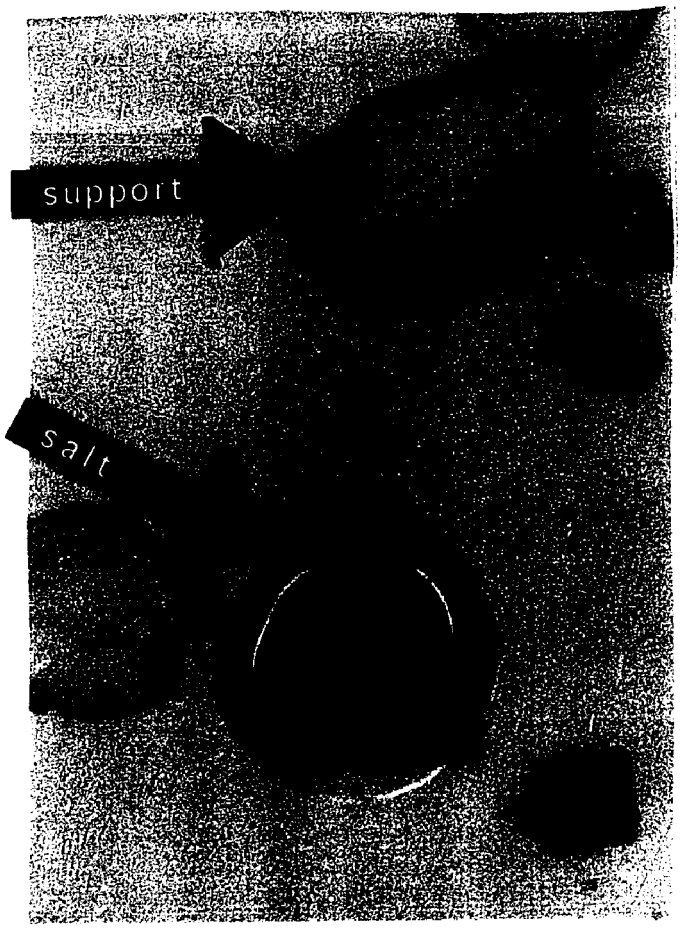

Figure 46. Photograph of 9.9% K-Mg | |Cl With 0.73% Pt at 64X Magnification

Other Melts Examined

Several other melts were screened to see if changing the melt would alter the cyclohexene reactivity. The use of nickel, rather than platinum, was also examined.

The reactivity of cyclohexene was measured in a K-Li-Na||Br melt containing Pt to see if there is any effect of changing the anion in the melt. The reaction was carried out using the continuous flow system with a reactor containing catalyst composed of 9.9 wt% salts with 0.69% Pt supported on Chromosorb P-AW (15.68g total) at 425°C with a helium carrier gas. Cyclohexene (1.09 ml/hr) reactivity was examined for six hours. During the period examined, cyclohexene reacted completely. The ratio of dehydrogenation to disproportionation is shown in Figure 47. As in the chloride melt, disproportionation is the favored reaction. Heptane was also examined but did not react in this system.

Cyclohexene reactivity was also examined in a Mg-K||Br melt containing Pt. This melt was examined because it contains a divalent cation. The reactor was filled with catalyst containing 10% salts with 0.36% Pt supported on Chromosorb P-AW (16.97g total) at 425°C with a flow of helium. The products of the reaction included cyclohexane, benzene, and a small amount of methylcyclopentane. The identity of the components was determined by gc retention times. The amount of methylcyclopentane produced was less than 1% wt, but was the first time that any product other than benzene and cyclohexane was observed from the reaction of cyclohexene.

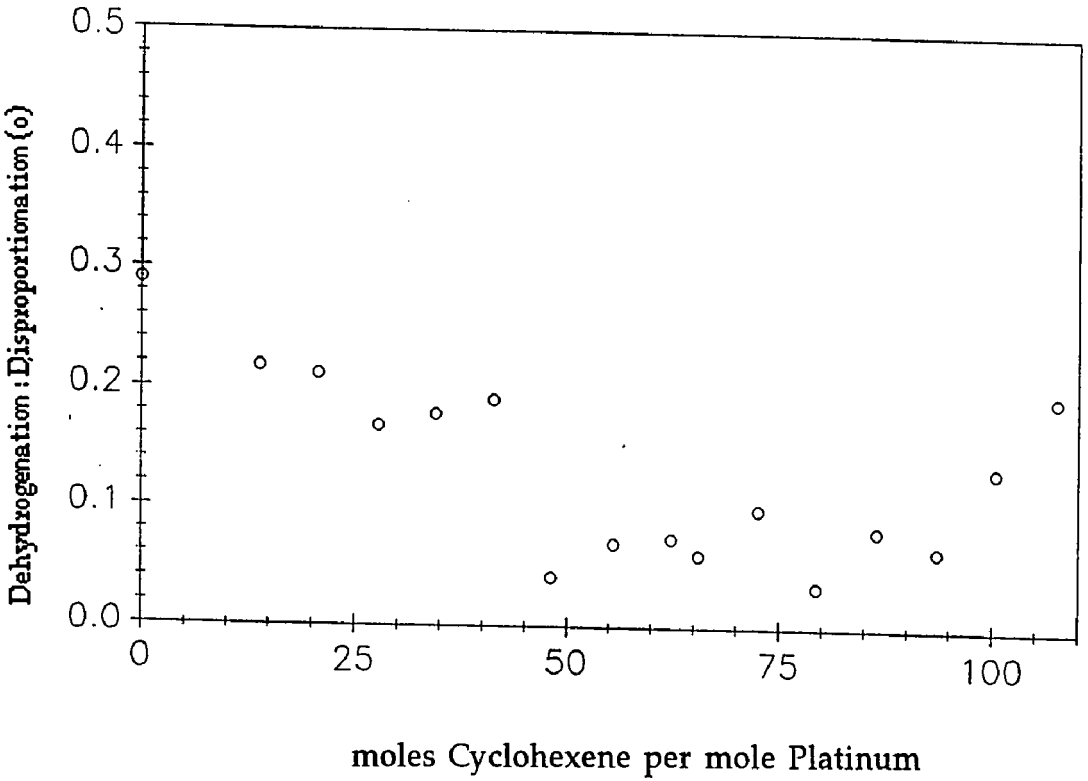

Figure 47. Reactivity of Cyclohexene on a Catalyst Containing 9.9% K-Li-Na | |Br with 0.69% Pt at 425°C with 1.7 ml/min He Carrier Gas (25°C).

The catalyst lost cyclohexene (1.55 ml/hr) reactivity more rapidly than the other systems investigated (Figure 48). The ratio of the two reactions did not stabilize before most of the reactivity had been lost. A similar catalyst was also studied at a lower temperature. This catalyst contained 10% salts with 0.39% Pt supported on Chromosorb P-AW (14.19g total). Figure 49 shows that at 380°C the cyclohexene (1.55 ml/hr) reactivity dropped off at approximately the same rate as at 425°C. At the lower temperature methylcyclopentane was also observed in amounts less than 1%. Again the mixture of reaction products changes before the catalyst looses most of its reactivity.

A catalyst containing nickel, rather than platinum, was also studied. This system, a Ni-Li-K||Cl eutectic containing nickel as part of the eutectic, compared with adding platinum to a eutectic composition of the salts. The only product observed from the reaction of cyclohexene (1.55 ml/hr) on a catalyst containing 10.9% Ni-Li-K||Cl eutectic supported on Chromosorb P-AW (18.22g total) was cyclohexene.

System Reactivity

The reactivity of all the systems previously described was inexplainably lost after one year. A fresh sample (15.92g) of catalyst containing 9.9 wt% K-Li-Na||Br with 0.69% Pt at 425°C, using helium as the carrier gas with cyclohexene introduced at 1.09 ml/hr, showed different results (Figure 50) from the same catalyst (Figure 47) several months earlier. The reactivity of the catalyst dropped off very rapidly, similar to supported $PtCl_2$ (Figure 29, p. 136).

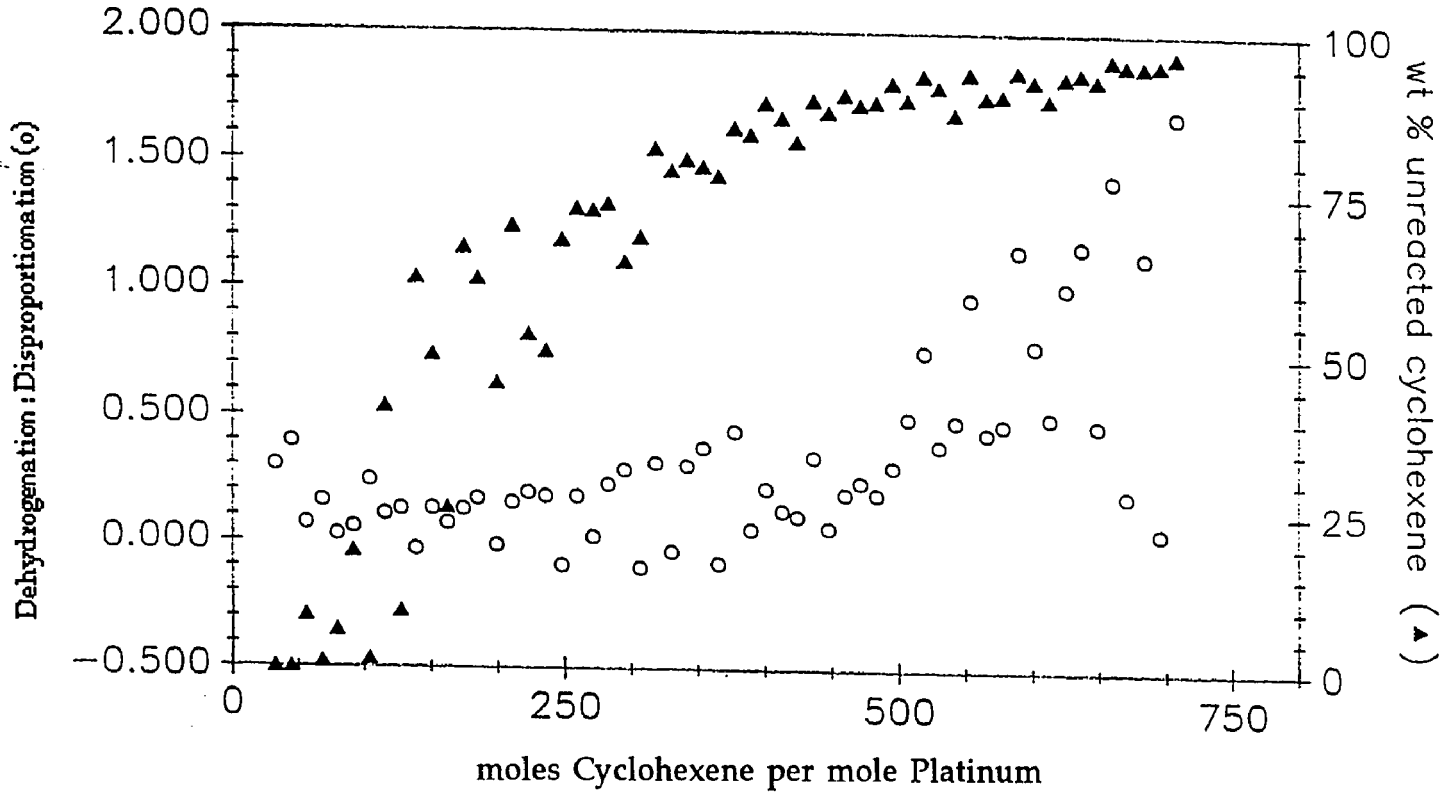

Figure 48. Reactivity of Cyclohexene on a Catalyst Containing 10% K-Mg | |Br with 0.36% Pt at 425°C with 1.7 ml/min He Carrier Gas (25°C).

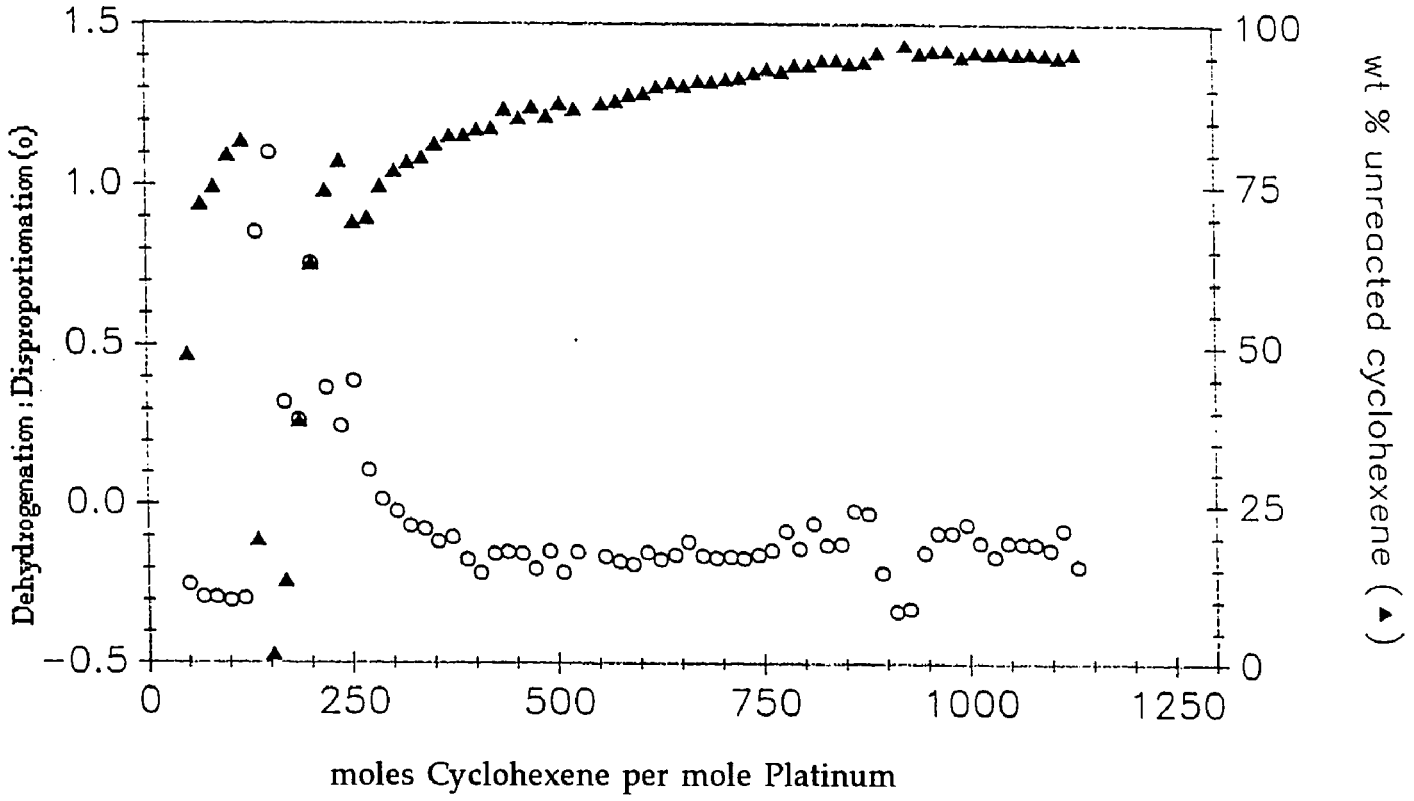

Figure 49. Reactivity of Cyclohexene on a Catalyst Containing 10% K-Mg | | Br with 0.39% Pt at 380°C with 1.7 ml/min He Carrier Gas (25°C).

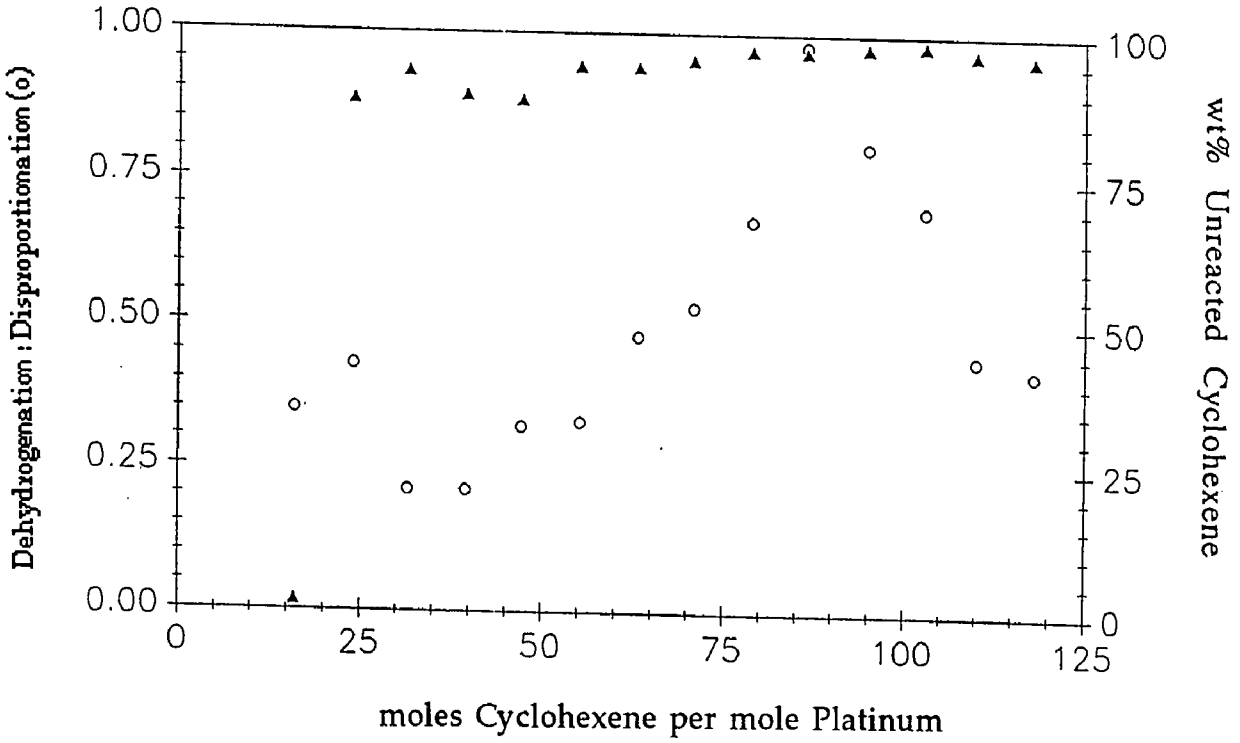

Figure 50. Reactivity of Cyclohexene on a Catalyst Containing 9.9% K-Li-Na | |Br with 0.69% Pt at 425°C with 1.7 ml/min He Carrier Gas (25°C).

Reactors that had been stored under nitrogen were no longer active. Approximatey 35% cyclohexene reactivty was observed in a reactor containing 10% K-Li-Na | |Cl with 0.73% Pt supported on Chromosorb P-AW (16.54g total, Figure 31, p. 142) prior to decomission. Only starting material was recovered from the reaction of cyclohexene in this reactor, under comparable conditions, after 14 months of storage. It was thought that a small amount of DMSO may have contaminated the system. The system was rebuilt with new materials in an attempt to resolve this inconsistency. To minimize the possibility of contamination this material was prepared under nitrogen in a dry box. No cyclohexene (1.09 ml/min) reactivity was observed on catalyst containing 10.1% K-Li-Na | |Cl with 0.78% Pt supported on Chromosorb P-AW (16.93g total, 1.7 ml/min flow of N_2). The possibility of contamination from the stainless steel reactor was investigated by using a quartz tube for the reactor. Again, the there was no cyclohexene (1.09 ml/hr) reactivity of the same catalyst (4.8 g total) in a quartz reactor (1' long) at 425°C under a flow of nitrogen (1.7 ml/min). The problem has not been solved.

Discussion

K-Li-Na | | Cl System

The data in Table 33 (p.140) demonstrate that a platinum reforming catalyst is active when supported in a K-Na-Li | | Cl melt. Cyclohexene is rapidly aromatized and disproportionated on a platinum catalyst supported in a K-Li-Na | | Cl eutectic at 425°C. High cyclohexene reactivity is observed using both the single injection apparatus (Figure 28, p. 133) and the continuous flow apparatus (Figure 30, p. 138). Control experiments (Table 35) show that the observed catalysis is a result of the molten salt-platinum system and is not due to the support or the melt. The reactivity observed for the molten salt-platinum system is different from a conventional supported Pt^o catalyst that completely dehydrogenates cyclohexene to to benzene at 425°C.[96]

Nature of the Catalyst

The valence state of the platinum in the molten salt was investigated because of the difference in reactivity compared with a traditionally supported platinum reforming catalyst.[96] The valence state was examined using Electron Spectroscopy for Chemical Analysis (ESCA). The binding energies of the platinum $4f_{7/2}$ and $4f_{5/2}$ electrons, which are dependant on the valence

Table 35. Control Experiments for the Reaction of Cyclohexene at 425°C.

Conditions	Result
K-Li-Na | | Cl on PAW	no reaction
PAW	no reaction

state and the coordination of the metal, were measured. As previously discussed the $4f_{7/2}$ and $4f_{5/2}$ binding energies of platinum, regardless of valence state, are separated by 3.35 eV.[111] The $4f_{7/2}$ binding energy of platinum in a sample of catalyst that was brought to temperature and tested for cyclohexene (100μl) reactivity was 71.0 eV (Used Once, Figure 43, p. 158). This corresponds to Pt^0, which has a $4f_{7/2}$ binding energy of 70.8-71.0 eV.[111] A sample of catalyst that was exhausted by reaction with cyclohexene also had a $4f_{7/2}$ binding energy of 71.0 eV (Exhausted catalyst, Figure 43). Either the Pt(II) was reduced by the cyclohexene or it decomposed to give Pt^0 and Cl_2. Unused catalyst shows a $4f_{5/2}$ binding energy of 78.4 eV (Figure 43). The $4f_{7/2}$ peak is expected to have a binding energy of 75.0, which is masked by the aluminum oxide. Possible species with a $4f_{7/2}$ binding energy of this magnitude are: $PtCl_4$ (75.2-75.4 eV) and $PtCl_4^{2-}$ (75.2-75.6 eV). The $PtCl_4^{2-}$ species is likely the result of complexation of chloride, from the hydrochloric acid solution in which the catalyst was prepared.[111] This is more plausible than $PtCl_4$, which would require the oxidation of platinum during catalyst preparation. The change in platinum valence state indicates that the melt does not stabilize the platinum as Pt(II), which is observed in molten salt systems used for the hydrogenation of olefins.[107-110]

Photographs of the catalyst were taken, using an optical microscope, to examine the distribution of the salts on the solid support. The salts (when exposed to air and viewed at room temperature) formed globules (Figure 45, p. 159) on the solid support, but did not provide a uniform coating on the solid support. The thickness of evenly distributed salt on the solid support with a 10% loading is calculated to be approximately 160Å (Appendix 18). The absence of salt on every particle indicates that there is not an even

distribution of the salts on the support. The photograph suggests that a limited number of particles are covered with salt. The volume of salt from one glouble on the catalyst shown in Figure 45 is estimated to be 0.008 cm^3, which corresponds to a salt thickness of 0.0003 cm. This is approximately twice the calculated 160Å thickness for an even distribution of salt on every particle. This suggests a greater amount of salt on a limited number of particles. Either the support was not wet by the molten salts and the globules persist at high temperatures, or the salt coagulated to form the observed globules upon cooling. We are not able to discern which occurred.

Location of the Platinum

The platinum could be located on the surface of the salt, within the bulk salt, or on neighboring solid support not covered by salt. Uncovered Pt^o on the solid support would be expected to show the normal reactivity and selectivity of supported Pt^o. We observed the preferential disproportionation of cyclohexene (Figure 42, p. 156) rather than dehydrogenation, which is observed on traditionally supported Pt catalysts. Because we did not observe the normal reaction selectivity we conclude that the amount of Pt^o unassociated with the molten salt is insignificant. If the Pt^o were on the surface of the salt (Case 1, Figure 51), the reaction rate would scale with the surface area. If the Pt^o were in the bulk salt (Case 2, Figure 51), the reaction rate should scale as the volume of the salt. Since significant changes in the amount of salt result in small changes of the surface area, the location of the platinum could be determined by reaction kinetics.

The system was modeled for two possible locations of platinum in the molten salt. The relative reaction rate was determined as a function of the

salt thickness, which varies with salt loading. The complete calculation of the relative rates is given in Appendix 19. The relative rates as a function of the salt thickness are shown in Figure 52, assuming a rate constant of $10^7 sec^{-1}$ and uniform coverage on the support. Although uniform coverage is assumed the relative rate would show the same difference as if globules are present.

Figure 51. Two Cases for the Location of Platinum in the Salt.

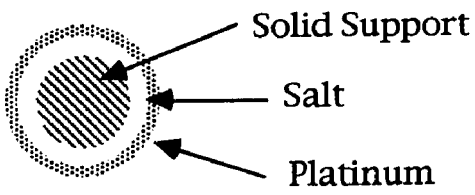

Case 1.
Platinum on the
Outer Surface of the
Salt.

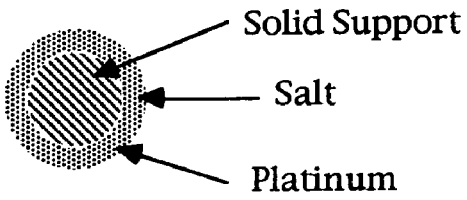

Case 2.
Platinum throught
the Salt.

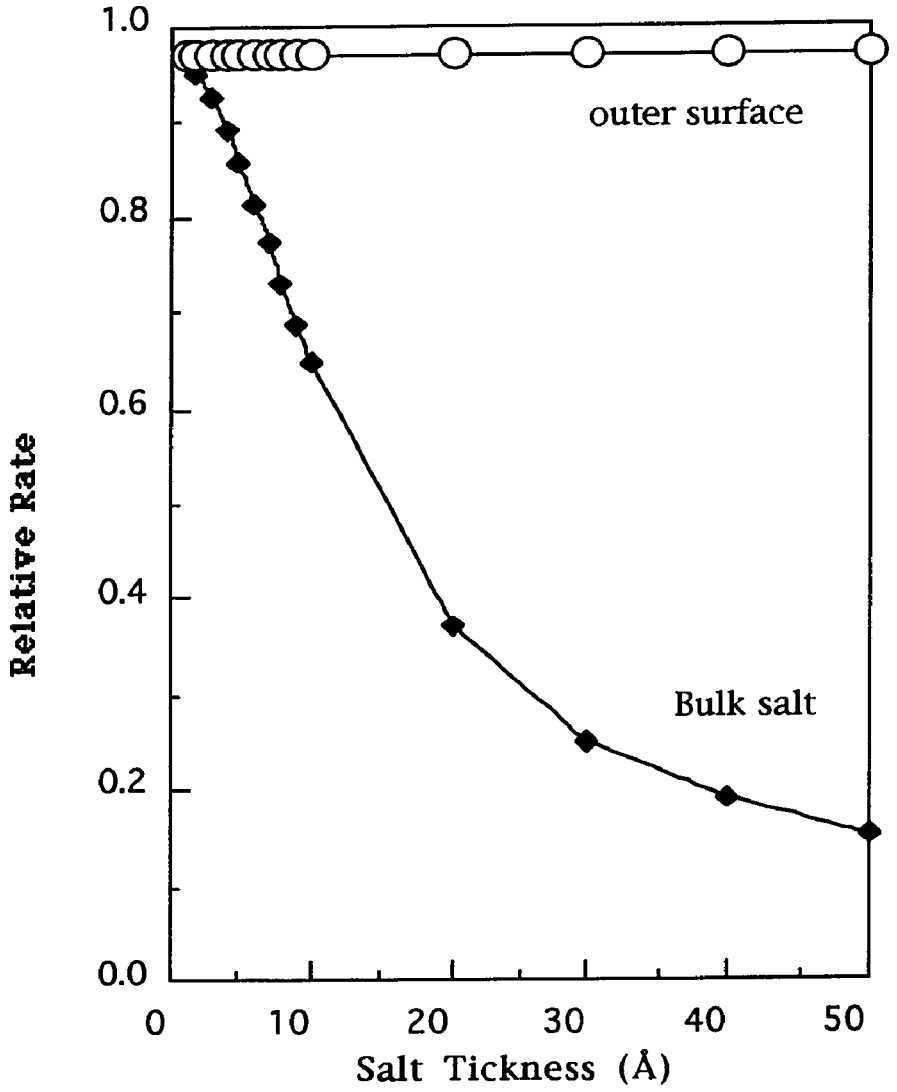

Figure 52. Calculated Relative Reaction Rate as a Function of the Salt Thickness

The experiments to determine differences in cyclohexene reaction rates as a function of the salt thickness were not completed. Although the effect of salt thickness on the reaction rate was not determined, differences in the selectivity of the molten salt-platinum system compared with conventionally supported Pt^o catalysts indicate that the platinum was not located on the outer surface of the melt. If this were the case, comparable reactivity to a conventionally supported platinum reforming catalyst would have been observed for the molten salt-platinum system.

The molten salt-platinum system did not exhibit the selectivity of a typical platinum reforming catalyst. The data in Table 33 (p. 140) show that the system was active for cyclohexene, a cyclic olefin and inactive for cyclohexane, a saturated hydrocarbon. There are two possible explanations for the observed selectivity: 1) selective diffusion through the melt to reach the Pt^o, or 2) modification of the Pt^o by a medium effect of the melt. Because of the weakly acidic nature of the salt, olefins would be drawn into the salt by complexation of the π system, whereas hydrocarbons would not reach the catalyst because they can not form complexes and would not be soluble. The lack of hydrocarbon dehydrogenation is consistent with this picture. Not consistent is the unreactively of 1-hexene, which may be explained by the lack of strongly acidic sites. The reforming of linear molecules, to their cyclic counterparts, requires strongly acidic sites for the formation of carbonium ion intermediates, which are not present in the molten salt system.[92] The observed selectivity is likely a result of these factors.

Of the substrates examined (Table 33, p.140), only cyclohexene and tetralin showed any reactivity, suggesting that reactivity is limited to cyclic olefins, which already have the ring formed on the pathway to an aromatic

product. Isomerization reactions that are attributed to the acid component of reforming catalysts were absent. 1-Hexene and n-heptane, which, under conventional reforming conditions with acidic catalyst supports, are cyclized and dehydrogenated to benzene and toluene, respectively, do not react.[112] Conversions under conventional reforming conditions, to the aromatic products are generally greater than 50%, but are dependent on the particular catalyst used.[113] The observed reactivity in the molten salt system is consistent with metals on a non-acidic support, such as silica. A combination of Platinum and Rhenium supported on SiO_2 does not show any cycloehexane isomerization or cyclization.[113]

Possible Reaction Pathway

The plausibility of cyclohexene dehydrogenation proceeding stepwise through a diene intermediate was investigated. Both of the cyclohexadiene isomers were examined as possible intermediates of the cyclohexene dehydrogenation and/or the disproportionation reaction pathway using the single injection apparatus. As discussed in the introduction, the bimolecular surface mechanism on a supported metal produced 1,3-cyclohexadiene and cyclohexane.[100] Kinetic data from cyclohexene dehydrogenation in tetrahydrofuran solutions on black palladium showed that the reaction goes through a cyclohexadiene intermediate.[114] In the molten salt-platinum system cyclohexane and benzene were produced from the reaction of 1,3-cyclohexadiene, but rapidly deactivated the molten salt-platinum system (see Table 32, p.139). The loss of catalytic activity from the reaction of 1,3-cyclohexadiene eliminated this substrate as an intermediate of the cyclohexene dehydrogenation pathway on the molten salt-platinum catalyst.

1,4-Cyclohexadiene reacted completely on the molten salt-platinum catalyst to produce cyclohexane and benzene. This same reaction of 1,4-cyclohexadiene ocurred in the absence of platinum. Because no rate data are available, 1,4-cyclohexadiene can not be confirmed or eliminated as an intermediate in the dehydrogenation of cyclohexene. The loss of a hydrogen from either cyclohexadiene isomer would produce the same intermediate. This intermediate is also eliminated because the 1,3 isomer can not be on the reaction pathway.

Cyclohexene can undergo dehydrogenation by two different reactions. Dehydrogenation to benzene and two moles of hydrogen is the favored reaction on conventional reforming catalyst at temperatures above 300°C.[94] Cyclohexene can also undergo disproportionation to benzene and two equivalents of cyclohexane. As discussed in the introduction, the thermodynamically favored cyclohexene reaction at 425°C is dehydrogenation. Equilibrium constants calculated from the thermodynamic data from Stull & Westrum[97] are different from those reported by Epstein[115] et. al. The difference arises from the ΔH_f^o used by Epstein. Epstein used the value for the liquid state rather than for the gas phase value. His values are in error by the heat of vaporization.

The thermodynamically favored pathway at 425°C is dehydrogenation (Figure 26, p. 126). The calculated ratio of dehydrogenation to disproportionation at 425°C is 820:1. The reactions carried out show that disproportionation is the experimentally favored pathway, indicating that the reaction is under kinetic control, unlike a conventional Pt catalyst at 425°C.[87]

Reactivity of Cyclohexene

Cyclohexene was further investigated because it was the most reactive of the compounds examined. Complete cyclohexene reactivity was observed under the reaction conditions (425°C, 1.7 ml/min carrier gas {He, N_2, He(5% H_2)},1 ml cyclohexene/ hr) for a prolonged period. The turnover number is defined as the amount of cyclohexene introduced per mole of platinum. This normalizes the data to the amount of platinum used. Complete cyclohexene reactivity (see Figures 31,32,33 and 35: p. 141, 143, 145, 147) was observed, in most cases, for a catalyst containing platinum until a turnover of 500 was reached. This is much slower deactivation than supported $PtCl_2$ (Figures 29,30: p. 138, 138) or a conventionally supported platinum catalyst which deactivates quickly at temperatures above 150°C due to coking.[95]

The selectivity (dehydrogenation : disproportionation) for the reaction of cyclohexene varies with the amount of cyclohexene that has been introduced. In most cases (Figures 31,32,33 and 35) dehydrogenation is favored in the early stage of a run. As more cyclohexene is introduced, disproportionation always becomes the favored reaction pathway. Variation in selectivity decrease with a reduction in reactivity. The kinetically favored reaction dominates in the molten salt-platinum system.

Differences in activity were examined for several salt loadings. Figure 41(p. 154) shows the effect of increasing the amount of salt while maintaining a constant concentration of platinum in the salt. The higher the loading of the salt, the slower the rate of deactivation. Differences in selectivity (Figures 42, p. 156) are also observed. The preferred reaction in the 10% salt loading initially favors disproportionation. As more cyclohexene is introduced, dehydrogenation becomes favored for a short period of time before

disproportionation is again favored. The run using 7.4% salts shows a consistent preference for disproportionation. The lowest loading of salt initially prefers disproportionation; when reactivity has decreased, dehydrogenation predominates.

The reaction selectivity also varies with salt loading. As shown in Figure 42 disproportionation is the preferred reaction at higher salt loadings. Dehydrogenation becomes the favored reaction for a catalyst that contained 2.5% salts. The difference in selectivity indicates that the platinum is affected by the presence of the salts. The selectivity differences may be due to diffusion through the salt to reach the catalyst.

The effect of the carrier gas on the reaction of cyclohexene was examined in the molten salt-platinum system. Cyclohexene reactivity is not affected by changing the carrier gas from nitrogen (Figure 31, p. 141) to helium (Figure 32, p. 143) or helium containing 5% hydrogen (Figure 33, p. 145) under the standard conditions used. All three gases show complete reactivity to a turnover of at least 400. The initial selectivity (Figure 34, p. 146) is dependent on the carrier gas used. Initially, dehydrogenation is favored for helium and helium (5% H_2), whereas disproportionation is favored with nitrogen. As more cyclohexene is introduced, disproportionation gradually becomes the preferred reaction. In the case of nitrogen, dehydrogenation is preferred for an intermediate period before reverting back to disproportionation. For those carrier gases examined, disproportionation, the kinetically controlled reaction, occurs more readily than thermodynamically predicted reaction.

After the catalyst had been deactivated (Figure 35, p. 147) activity could be regained by oxidizing the catalyst. The catalyst was exposed to an atmosphere of oxygen (1.7 ml/min (25°C)) at the reaction temperature for a

prolonged period of time. Three time periods were investigated: 5.5 hr. (Figure 36p, 148), 7 days (Figure 37, p. 150), and 2.7 days (Figure 38, p. 151). In all cases, complete cyclohexene reactivity was regained. The rate at which the regenerated catalyst was deactivated was dependant on the length of oxygen exposure. Reactivity comparable to the original catalyst, was regained for the 7 day exposure, but in the other two time exposures, deactivation occurred more quickly than the original catalyst. The selectivity of the reaction was altered by oxygen exposure. Disproportionation is the initially favored reaction in the regenerated catalysts. The extent of dehydrogenation increases with increasing use. The nature of the catalyst changes with oxidation, which is observed by changes in reaction selectivity. The ability to regenerate the catalyst suggests that the deactivation may be due to coke formation, which can be burned off by reaction with oxygen.

Other Systems Investigated

The other systems investigated demonstrate that the activity of Pt^{o} (see Table 36, p. 191) in a molten salt is not limited to one particular melt and that the nature of the melt can affect the type of reactions that occur. The K-Li-Na | |Br system showed the same behavior as the chloride system: high reactivity of cyclohexene and no reactivity of heptane. The photograph (Figure 46, p. 160) of a K-Mg | |Cl-Pt catalyst suggests that the salts are hydrated. This is not surprising because the material was exposed to air and magnesium bromide is very hygroscopic. Cyclohexene did not deactivate the system rapidly (Figure 47, 100% cyclohexene reactivity: p. 162). This data suggests that there is not a large difference in changing the counter ion from chloride to bromide for the reaction of cyclohexene and heptane.

The reactivity of cyclohexene was examined in a K-Mg | |Br melt containing platinum. The melt containing a divalent cation exhibited reactivity different from the K-Li-Na | |Cl platinum containing system (Table 36). The catalyst became inactive to cyclohexene more rapidly than in the chloride system and also produced different products (Figure 48, p. 164). The same result was obtained when a reactor was maintained at 380°C (Figure 49, p. 165). The production of a small amount of methylcyclopentane indicating that this melt is acidic, inducing rearrangement of the starting material. This shows that there is a difference in the reactions that occur when there is a divalent cation present and that the nature of the melt can be varied by changing the components of the melt.

Table 36. Reactivity of Substrates in Melts Containing Platinum at 425°C.

Melt	Reactant	Product (%)	
K-Li-Na	|Cl	Cyclohexene	Cyclohexane	(~55%)
		Benzene	(~45%)
	Heptane	no reaction	
K-Li-Na	|Br	Cyclohexene	Benzene	(~45%)
		Cyclohexane	(~55%)
	Heptane	no reaction	
Mg-K	|Br	Cyclohexene	Benzene	(~49%)
		Cyclohexane	(~49%)
		Methylcyclopetane	(~1%)

The nickel system (Ni-Li-K | | Cl) did not show any cyclohexene reactivity (Table 35). This was a melt that included nickel as part of the melt rather than an added species. The nickel may not have reached a metallic state because reduction (-0.795 V, vs Pt(II)-Pt(0) K-Li | | Cl at 450°C[116]) is not favorable. Conventional reforming catalysts require the nickel to be in the metallic state. Therefore, to examine nickel as a catalyst, insuring that nickel is in the metallic state, is necessary.

System Reactivity

A loss in catalytic activity for the systems was experienced. There was no cyclohexene reactivity observed in a reactor that had been stored under nitrogen for three months. The reactor had been decommissioned when 35% cyclohexene reactivity was observed (Figure 31, p. 141). This same reactor, setup under identical conditions, did not show any cyclohexene reactivity. The inactivity of the K-Li-Na | | Br platinum containing system is shown in Figure 50 (p. 166). Figure 47 (p. 162) shows the reactivity of a sample of the same batch of catalyst several months earlier.

The reason for the loss in catalytic activity in the system is not known. The system was rebuilt, a catalyst was carefully prepared under nitrogen, but the reactivity of the system was never regained. This indicates that if a poison is present, it need only be present in a very small amount.

Summary

The results discussed show that a platinum catalyst can be supported within a molten salt. Although the platinum is in the same valence state (Pt^o) as a traditionally supported platinum reforming catalyst, the selectivity

of the molten salt system has been altered. Cyclohexene was shown to be very reactive in this system, forming the kinetically favored products. Cyclohexene reactivity is not limited to one melt, but the highest amount of cyclohexene reactivity with the slowest deactivation was observed in the melts containing Group I halides with platinum added.

Experimental

Materials

The reactivity of a platinum catalyst supported in a molten salt has been examined. The phase diagram for the principal melt used, a K-Li-Na | |Cl eutectic, is shown in Figure 52. The eutectic at 346°C is composed of 8.6 mole% NaCl, 55.7% LiCl, and 35.6% KCl. Sodium chloride (Fisher), lithium chloride (Fisher), and potassium chloride (Fisher) were dried under vacuum at 110°C prior to melt preparation. The solid support, Chromosorb P-AW (Manville, 80-100 mesh), was also dried under vacuum at 110°C. Chromosorb P-AW is calcined diatomite (91.6% SiO_2, 4.1% Al_2O_3, 1.4% Fe_2O_3, 0.2% TiO_2, 0.5% MgO, and 0.9% $Na_2O + K_2O$) that has been washed with acid. Platinum (II) chloride was used as received from Aldrich.

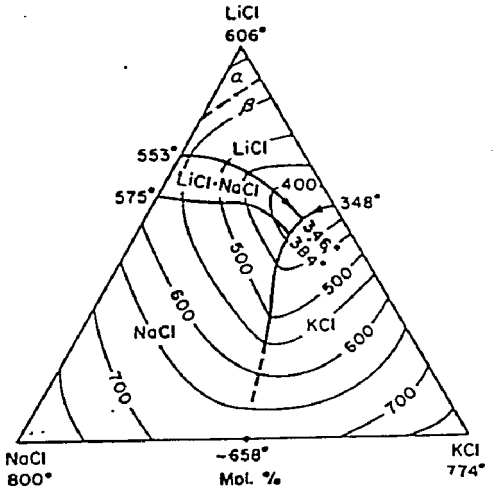

Figure 53. Na-Li-K | | Cl Phase Diagram.[117]

A typical catalyst contained approximately 10 wt% salts, 1% $PtCl_2$ and 89% solid support. The catalyst was prepared by adding platinuous chloride (0.82 g) dissolved in 400 ml of concentrated hydrochloric acid (Fisher) to an aqueous solution (100 ml) of the eutectic combination of the salts (9 g) in a 1 L round bottom flask. Chromosorb P-AW (74 g) was added to the acidic solution and stirred at room temperature for one hour. The liquid was removed by rotary evaporation, leaving a mixture deposited on the solid support. This was then dried in vacuo at 110°C to constant weight.

Systems involving other melts and platinum catalyst were prepared in a similar manner. A eutectic (333°C) containing 35.6 mole% potassium bromide (Aldrich) and 64.4% magnesium bromide (Alfa) (Figure 54) was prepared using hydrobromic acid rather than hydrochloric acid. The phase diagram for a sodium bromide (Aldrich), lithium bromide (Aldrich), and potassium bromide melt is shown in Figure 55. The eutectic used (324°C Li (57.5 mol%)-Na (7.5)-K (35.0) | | Br) was also prepared from a hydrobromic acid solution.

A nickel (II) chloride (Aldrich), lithium chloride, potassium chloride system was investigated. The phase diagram for this system has not been published, but a eutectic composition (Ni (14 mol%)-Li (50%)-K (36%) | | Cl, 360°C) has been reported.[118] This catalyst was prepared from an aqueous solution of the salts deposited on the solid support, as previously described.

The chief organic substrate examined was cyclohexene, which was used as received from Aldrich. Other substrates studied include: benzene (Aldrich), n-butyl benzene (Aldrich), 1,3-cyclohexadiene (Aldrich), 1,4-cyclohexadiene (Aldrich), cyclohexane (Fisher), heptane (Aldrich),

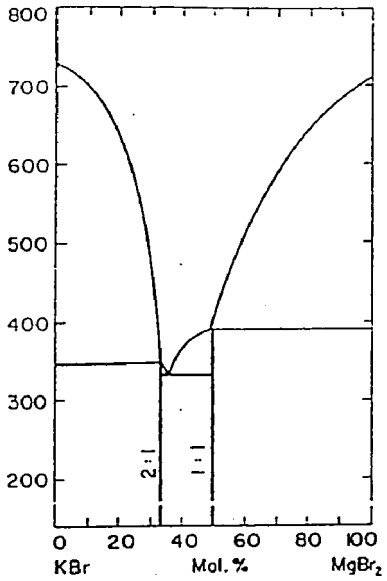

Figure 54. KBr-$MgBr_2$ Phase Diagram.[119]

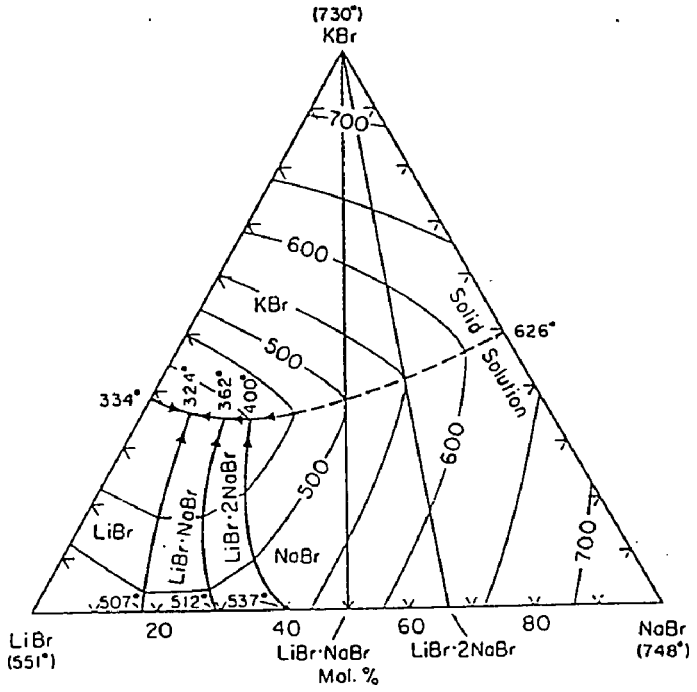

Figure 55. Na-Li-K | | Br Phase Diagram.[120]

1-hexene (Aldrich), naphthalene (Aldrich), tetralin (Aldrich) and toluene (Aldrich), all of which were used as received.

Nitrogen, helium, and helium with 5% hydrogen and oxyen were obtained from Linde and used without further purification.

Single Injection Apparatus

Either a single injection apparatus or a continuous flow apparatus were used to study a catalyst system. The single injection apparatus, shown in Figure 56, consisted of an injector assembly, reactor, and an analytical section. The injector was (Figure 57) constructed from a 2" X 2.5" aluminum block. Wells were created to hold the heater and thermocouple. The injector was maintained at an elevated temperature with a cartridge heater and the temperature was monitored with a thermocouple. A tee was created in the aluminum block by the main bore (0.25"), which ran the the length of the block, and a second bore that intersected the main bore perpendicularly. All three of the openings had 1/8" NPT female threads. Stainless steel Swagelok® fittings were used to attach the outlet and carrier gas inlet to stainless steel tubing. A septum (Septa 77, J&W) sealed a fitting having two female 1/8" NPT threads. The septum was compressed against the fitting with a cap that had a hole in it to allow passage of a needle.

The substrate was introduced into the injector through the septum with a Hamilton 100μl syringe (710 N 100μl). A continuous flow of an inert gas carried the substrate, usually 100μl, through the system. Carrier gas (Nitrogen or Helium) flow was controlled and monitored with a Tylan Mass Flow Controller (FC-260) operating at room temperature. Prior to mixing

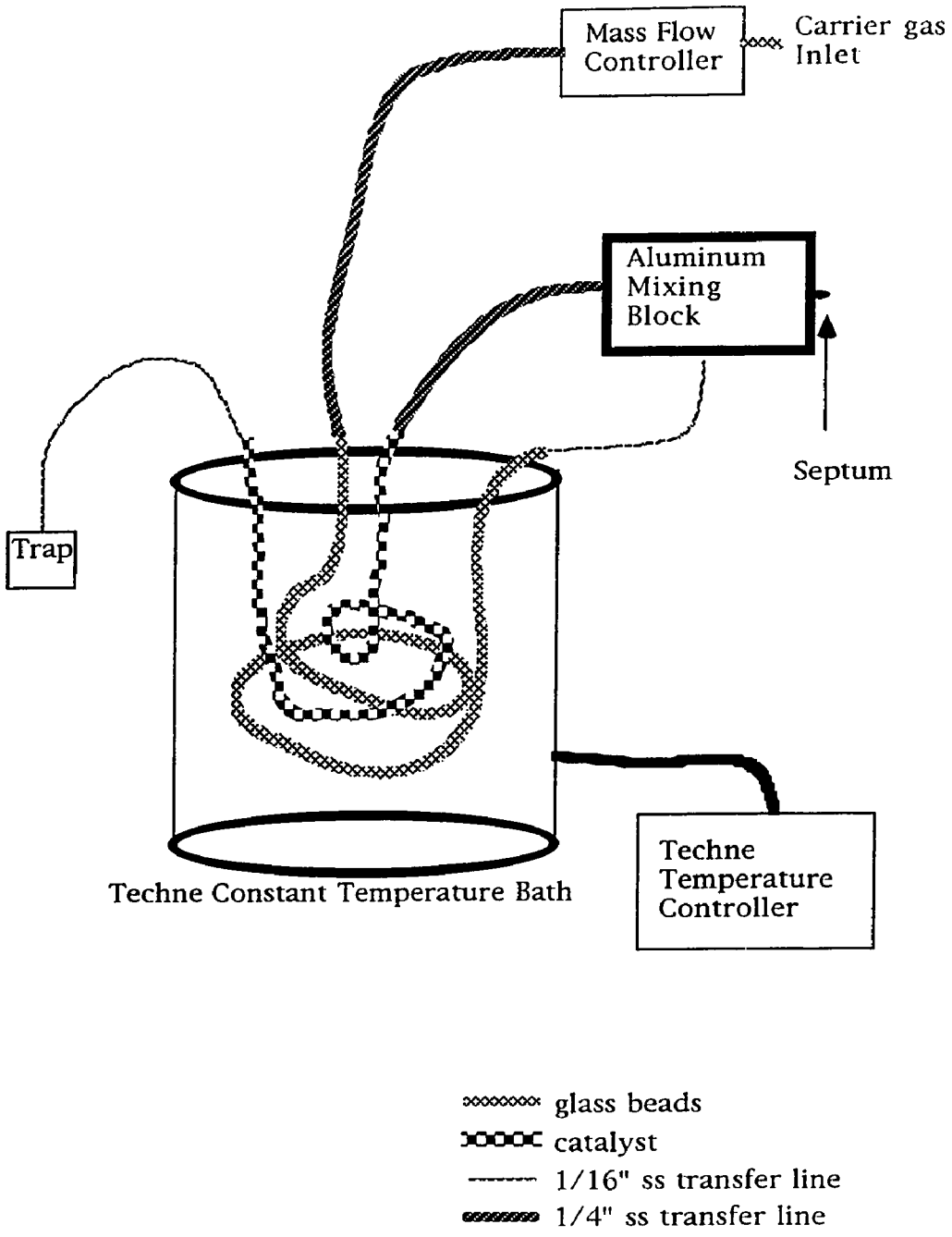

Figure 56. Single Injection Apparatus

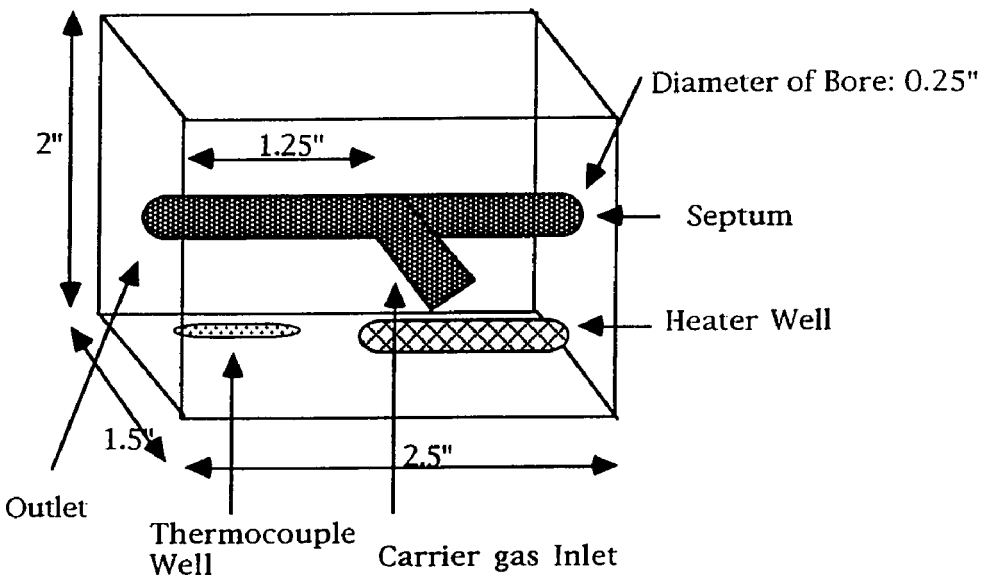

Figure 57. Single Injection Injection Assembly

with the organic substrate, the carrier gas was preheated by passage through a column of glass beads maintained at the reaction temperature.

The reactor was constructed of 1/4" o.d. 304 stainless steel tubing (Supelco) having a wall thickness of 0.021 in. Stainless steel Swagelok® connectors were used to connect the reactor to the injection block. Catalyst filled the reactor tubing, except at the ends which were not immersed in the sand bath. Heating tapes (Thermolyne Fibrox®) were used to maintain the transfer lines at elevated temperatures. The section of the reactor filled with catalyst was immersed in a Techne SBL-2 constant temperature bath. Compressed air (30 scfm) fluidized the constant temperature sand bath, which was controlled with a Techne TC 4A Temperature Controller. The temperature of the reactor was monitored by several thermocouples attached directly to the reactor tubing. A 1/16" s.s. o.d. (0.030" i.d.) transfer line connected the outlet of the reactor to a trap used to collect the reaction products.

The analytical section consisted of trapping and analyzing the reaction product. The apparatus shown in Figure 58 was used to collect the reaction products. The apparatus was connected to the transfer line from the outlet of the reactor using a 60% polyimide-40% graphite ferrule (American Scientific Products) in a Swagelok® fitting. Carrier gas and substrate were cooled by dry ice held in the plastic cup as they were carried through a 1/8" o.d. glass tube. Reaction products were trapped in a 1 ml conical vial (Supelco) maintained at -78°C. A sample of the collected material was analyzed by gas chromatography using a Hewlett Packard 5880 GC. A sample of approximately 0.2μl was injected into the gc with a Hamilton syringe (701N 10μl). Baseline separation of the components was obtained with a

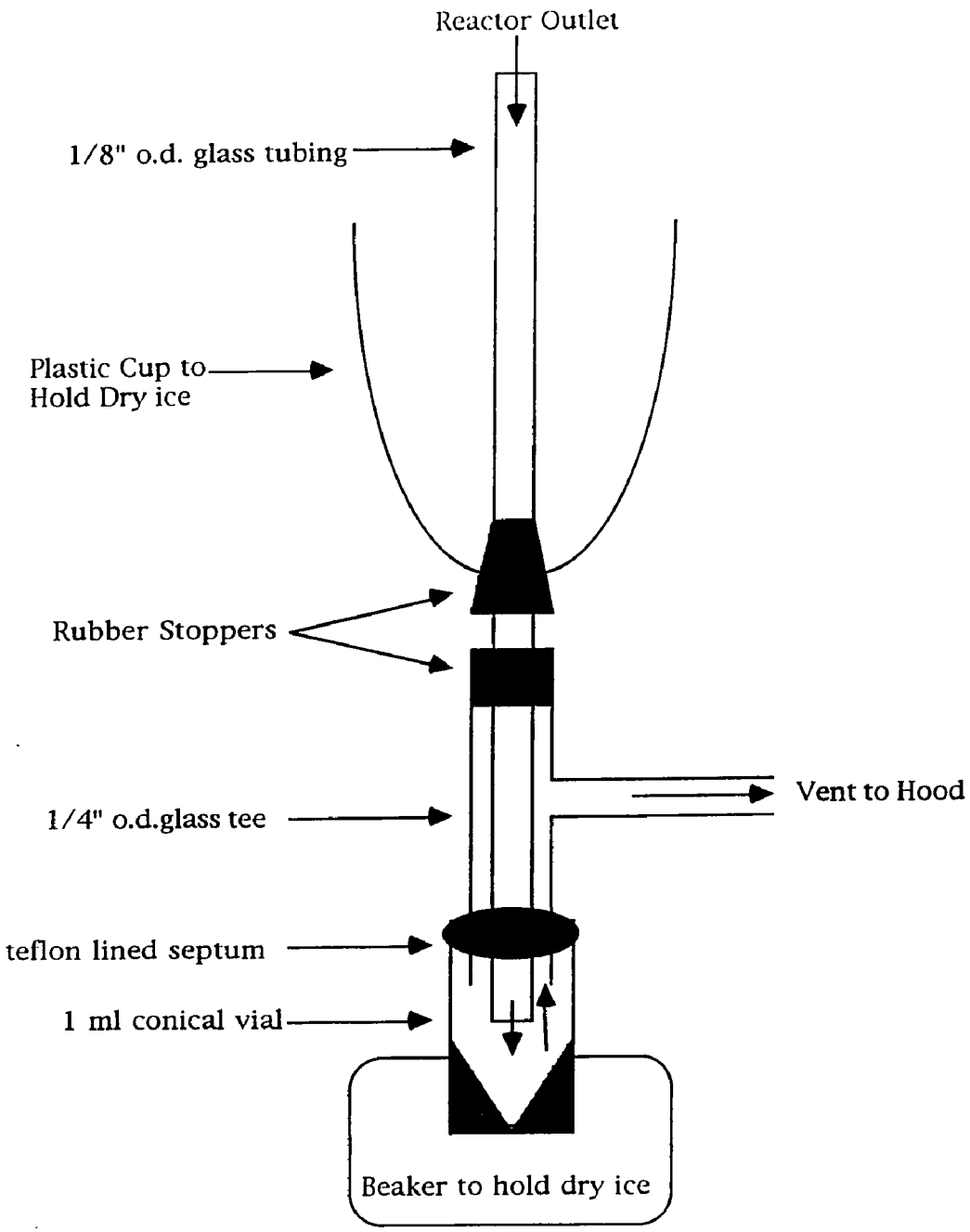

Figure 58. Trap to Isolate Products

6' x 1/8" o.d. column packed with 10% OV-351 supported on Chromosorb W-AP (Analabs). The run started with an oven temperature of 70°C, held for one minute before the temperature was ramped to 150°C at 10° per minute, held for 5 minutes. The injector was maintained at 200°C and the thermal conductivity detector was kept at 250°C. The carrier gas (helium or nitrogen) used for the chromatography had a flow rate of approximately 20 ml/min.

Continuous Flow Apparatus

The continuous flow apparatus is diagramed in Figure 59. It consists of an injection assembly, reactor and analytical section. The aluminum injector was modified slightly from the single injector assembly. The substrate was introduced into the injector through a 1/16" o.d., 0.020"i.d. s.s. tube (Figure 60), rather than a septum. The bore of s.s. fitting was enlarged to allow the tubing to pass through the fitting and extend 2" into the injection block. A continuous stream of starting material was achieved with either a Beckman 100-A HPLC pump or a 25 ml aluminum syringe used in combination with an Orion 341-A Syringe Pump.

The syringe was composed of a Teflon coated plunger from a Hamilton 25 ml glass syringe (1025) and an aluminum barrel. The barrel is shown in Figure 61. The aluminum syringe was designed for safety considerations, whereas a glass syringe could have broken, leaving an organic liquid near the large heat source of the sand bath. The syringe was connected to the injection block with 1/16" o.d. 0.020" i.d. s.s. tubing with Swagelok® fittings.

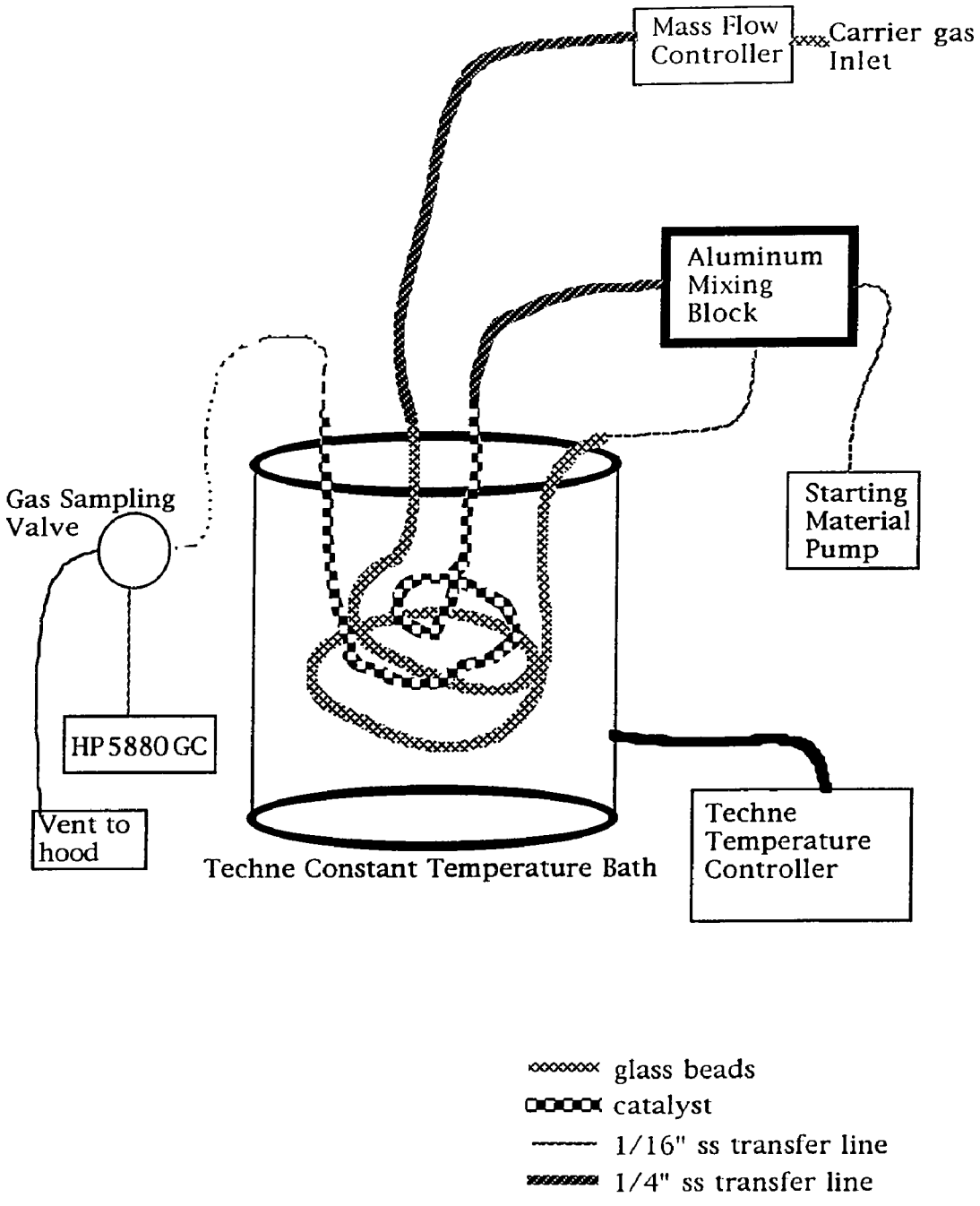

Figure 59. Continuous Flow Apparatus.

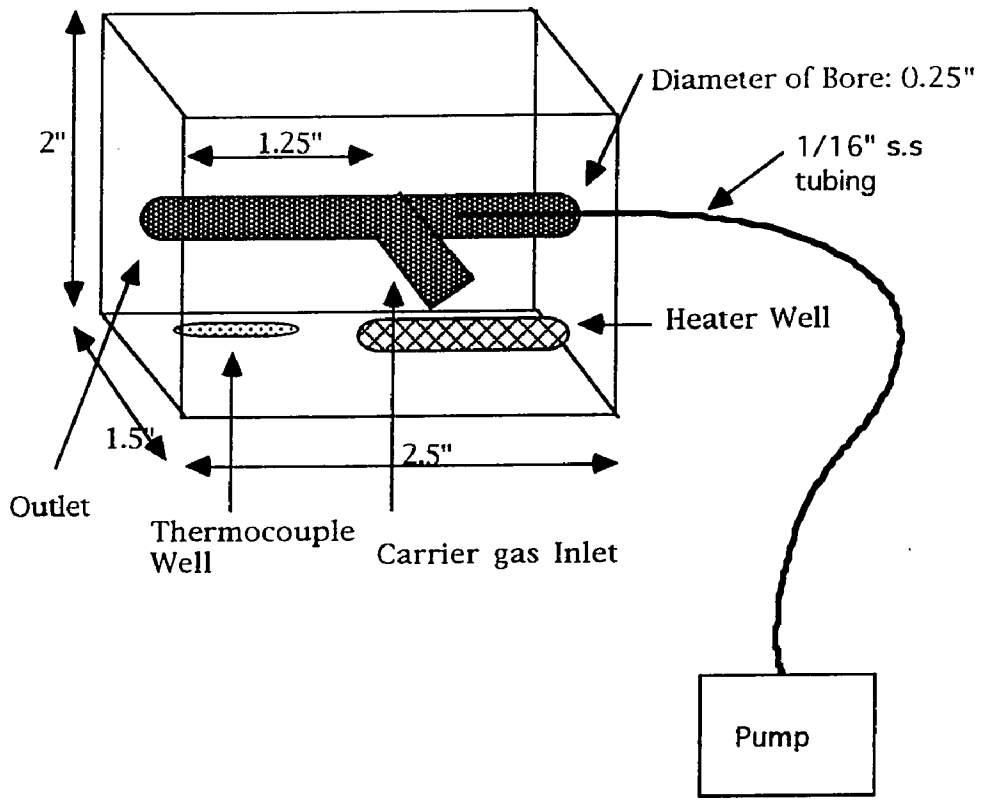

Figure 60. Continuous Flow Injection Assembly.

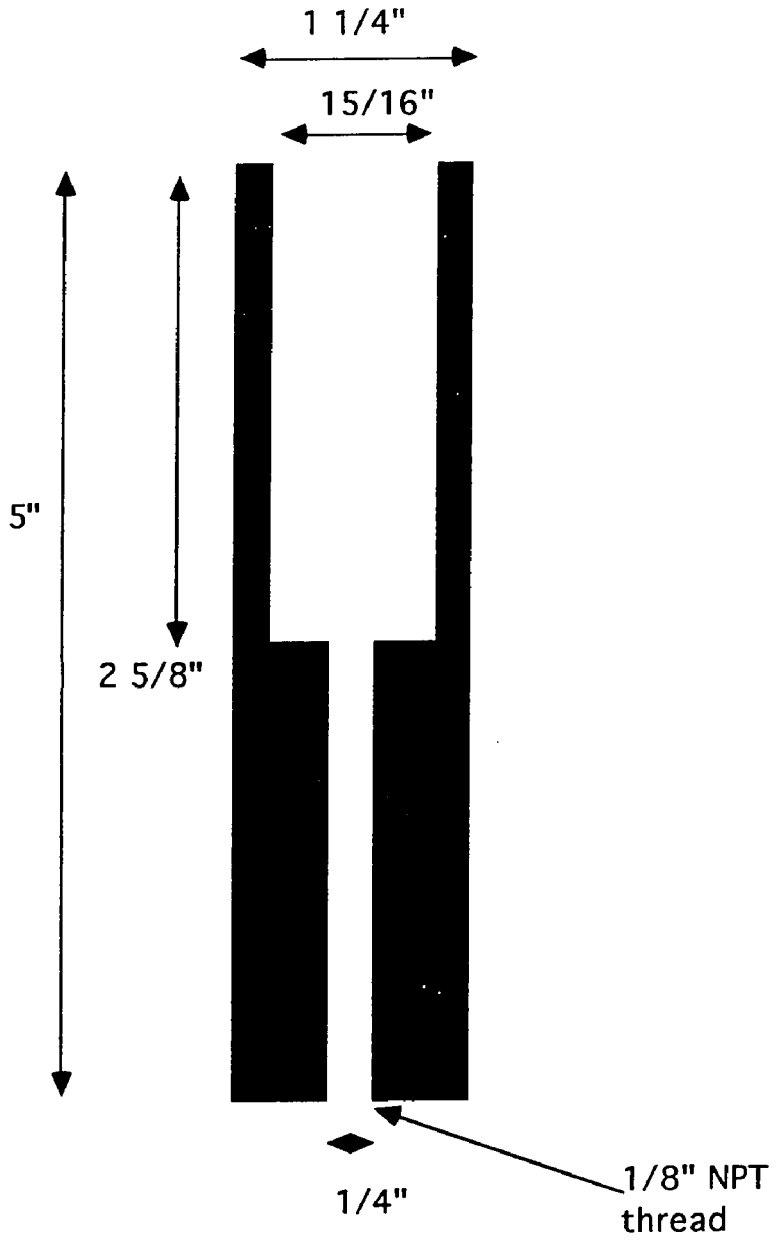

Figure 61. Aluminum Syringe.

A continuous flow of an inert gas carried the substrate through the system. Carrier gas (Nitrogen or Helium, Linde) flow was controlled and monitored with a Tylan Mass Flow Controller (FC-260) operating at room temperature. The carrier gas was preheated prior to mixing with the organic substrate by passage through a column of glass beads maintained at the reaction temperature.

The reactor was constructed and used in the same manner as the single injection reactor.

The analytical section was modified by inclusion of a heated sampling valve and elimination of the trap. The outlet of the reactor was connected to a Valco 6 port valve (6C6UWT) fitted with a 50 μl sample loop (Figure 62). A continuous stream of gas from the reaction passed through the sample loop while in the 'load' position. When the valve was turned by an electric actuator (Valco, EQ60) to the 'empty' position, 50μl of gas was injected into the gc. Any effluent not sampled was vented to a hood. The same gc conditions and column previously described were used.

ESCA

The ESCA spectra were obtained using a Scienta ESCA 300 Spectrometer.

Single Injection Procedures

Single injection reactions had a measured amount of starting material, usually 100μl, rapidly injected through a septum into the mixing block, which was maintained at 200^{o}C. The sample was carried through the system with a flow of either helium or nitrogen at approximately 1.5 ml/min at 25^{o}C.

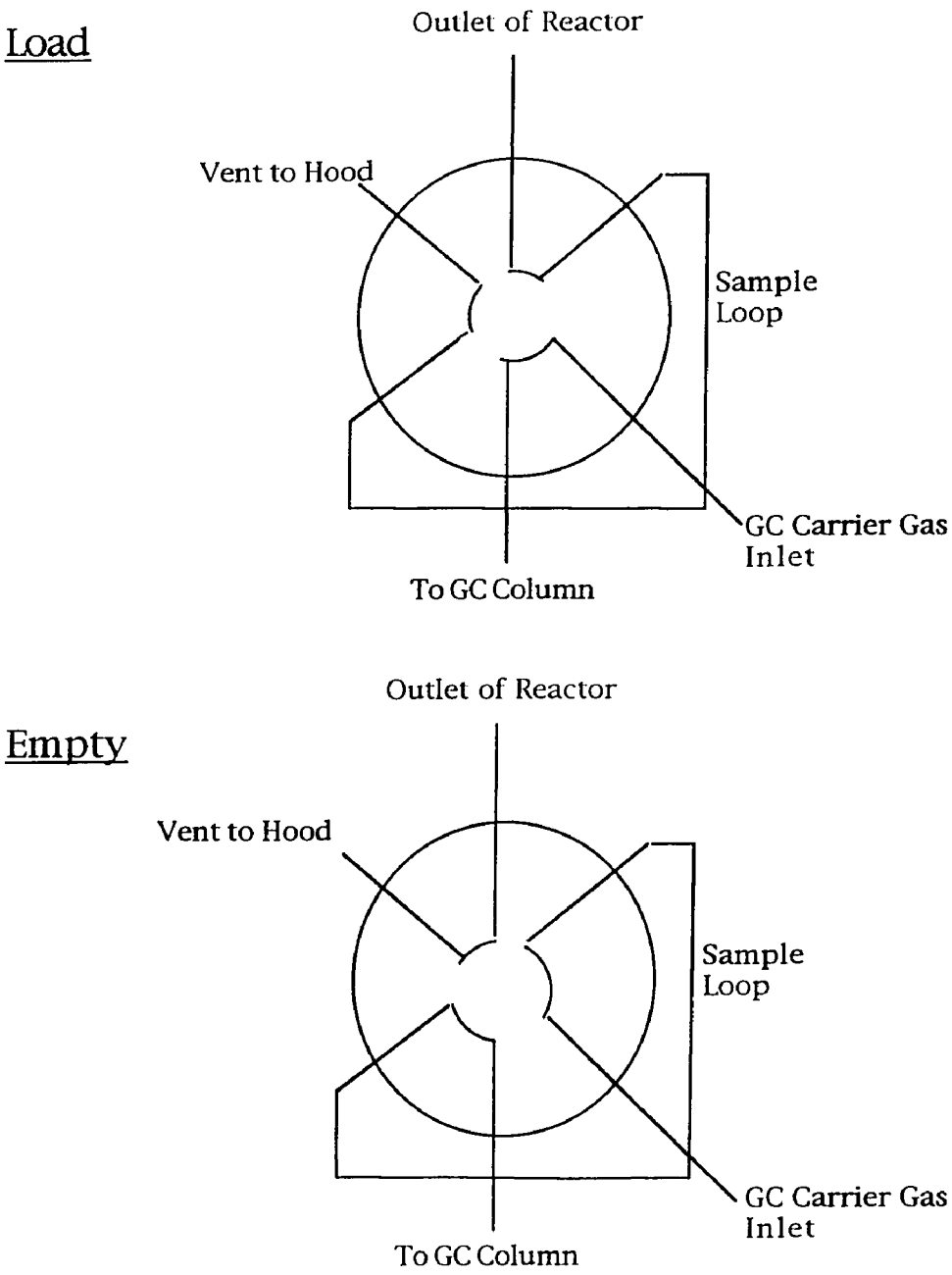

Figure 62. Valve Diagram

The same type of gas was used for the chromatography. The temperature of the heated transfer lines into and out of the reactor was monitored with Omega Type J thermocouples (TJ 36-IC-SS-116U-12-BX) and maintained at 300°C.

The reactor, filled with catalyst, was maintained at the desired constant temperature in the sand bath. One hour was allowed before a run was initiated to allow the system to reach the desired temperature and equilibrate. Reactor columns were constructed of 1/4" o.d. 304 SS with a inner diameter of 0.209" and filled with the desired catalyst. The tubing was cleaned first with acetone then with deionized water to remove oils deposited during manufacturing. Vacuum was applied for one hour at room temperature to remove any residual water from the tubing. The tubing was plugged at one end with glass wool to keep the catalyst in the column. As the catalyst was added to the tubing it was packed down by vibrating the tubing with an electric engraver. When the desired amount of catalyst had been added another piece of glass wool was used to plug the open end of the column. The tubing was coiled in such a manner that most of the catalyst was in the same horizontal plane of the sand bath. The ends were bent perpendicular to the coil. A transfer line was attached to the reactor outlet. The end leading to the injector had an additional 90° bend to allow attachment to the injector. Typical reactor columns were six feet long and contained approximately 15 g of catalyst.

The reaction product was collected as previously described over approximately one hour and then analyzed by gas chromatography. Product was typically isolated in yields greater than 95%. The retention times of the reaction products were compared with authentic samples to determine their

identity. The identity of the products from several runs was confirmed by GC/MS using a Finnigan 4023 quadrapole gc/ms operated in the electron ionization mode.

Quantitative results were obtained by determining the response factors for the products obtained. By analysis of several known mixtures it was determined that the response factors were the same, within experimental error, for cyclohexene (1.01), cyclohexane (1.00), and benzene (1.01). The ratio of cyclohexene disproportionation reaction was compared with cyclohexene dehydrogenation. The amount of cyclohexene disproportionation was found directly from the amount of cyclohexane produced; the extent of dehydrogenation was calculated from the amount of benzene and cyclohexane produced, as described in the results section. The ratio of the two reactions was followed as a function of the amount of cyclohexene introduced into the system per mole of Pt.

Injections of starting material were repeated at approximately one hour intervals. Approximately ten reactions were conducted per day until the catalyst showed less than 5% reactivity.

The cyclohexene reactivity of a system was determined prior to screening another substrate. Cyclohexene reactivity was examined to insure that the system was operating with complete cyclohexene conversion. The substrate of interest was examined and then cyclohexene reactivity was reexamined. This was done so that catalyst deactivation could be observed.

Continuous Flow Procedures

The starting material was introduced into the system at a constant rate of approximately 1 ml/hr. The sample entered into the mixing block, which

was maintained at 200°C. The substrate was carried through the system with a flow of either helium or nitrogen (approximately 1.5 ml/min at 25°C). The same type of gas was used for the chromatography. The temperature of the heated transfer lines into and out of the reactor were monitored with Omega Type J thermocouples (TJ 36-IC-SS-116U-12-BX) and maintained at 300°C.

The reactor was prepared and used in the exact manner described under single injection procedures. The sample was analyzed under the same chromatography conditions as previously described, except that the sample was injected via a valve maintained at 250°C in the valve box of the gc. The effluent stream was sampled at approximately 25 minute intervals. Quantitative results were obtained as described in the single injection procedure. Runs were conducted until the catalyst showed less than 5% reactivity, which usually took 5 days.

References

1. Entwistle, I.D.; Jackson, A.E.; Johnstone, R.A.W. ; Telforford, R.P. J.C.S. Perkin I, **1977**, 443-4.
2. House, H.O. Modern Synthetic Reactions; Benjamin/Cummings, Reading Mass., 1972.
3. Porter, H.K. Organic Reactions, Vol. 20: John Wiley & Sons, Inc.: New York, 1973.
4. Johnstone, A.W.; Wilby, A.H.; Entwistle, I.D. Chem. Rev. **1985**, *85*, 129-170.
5. Ono, A.; Sasaki, H.; Yaginuma, F. Chem. Ind. **1983**, 480.
6. Cowan, J.A. Tetrahedron Lett. **1986**, *27*, 1205-8.
7. Kano, S.; Tanaka, Y.; Sugino, E.; Hibino, S. Synthesis, **1980**, 695-697.
8. Lalancette, J.M.; Brindle, J.R. Can. J. Chem. **1971**, *49*, 2290-5.
9. Petrini, M.; Ballini, R.; Rosini, G. Synthesis, **1987**, 713-4.
10. Campaigne,. Org. Syn. Coll. Vol. 4, **1963**, 31.
11. Furst, A.; Berlo, R.C.; Hooton, S. Chem. Rev. **1965**, *65*, 51-68.
12. Schiessl, H.W. Aldrichimica Acta, **1980**, *13*, 33-40.
13. Rothenburg, R.V. Chem. Ber. **1893**, *26*, 2060-1.
14. Huang-Milon J. Am. Chem. Soc. **1948**, *70*, 2802-2805.
15. Calculated from data in: Stull, D.R.; Westrum, E.F.; Sinke, G.C. The Chemical Thermodynamics of Organic Compounds **1969**, and Landout Bornstein, Band II, Theil, p 188.
16. Balcom, D.; Furst, A. J.Am. Chem. Soc. **1953**, *75*, 4334.
17. Leggetter, B.E.; Brown, R.K. Can. J. Chem. **1960**, *38*, 2363-66.

18. Ayyangar, N.R.; Lugade, A.G.; Nikrad, P.V.; Sharma, V.K. Synthesis, **1981**, 640-643.

19. Han, B.H.; Sin, D.H.; Lee, H.R.; Ro, B.H. Bull. Korean Chem. Soc. **1989**, *10*, 315-6.

20. Petrier, C.; Luche, J.L.; Lavaitte, S.; Morat, C. **1989**, *54*, 5313-7.

21. Han, B.H.; Jang, D.G. Tetrahedron Lett. **1990**, *31*, 1181-2.

22. Park, M.K.; Jang, D.G.; Han, B.H. Bull. Korean Chem. Soc. **1991**, *12*, 709: CA **1992**, *116*, 128258w.

23. Stepanova, T.F.; Ginzburg, O.F. Zh. Prikl. Khim. (Leningrad) **1973**, *46*, 1159-60. CA **1973**, *79*, 42068q.

24. Han, B.H.; Shin, D.H.; Cho, S.Y. Tetrahedron Lett. **1985**, *26*, 6233-6234.

25. Hirashima, T.; Manabe, O. Chem. Lett. **1975**, 259-60.

26. Miyata, T.; Ishino, Y.; Hirashima, T. Synthesis, **1978**, 834-5.

27. Haber Z. Elektrochem, **1898**, *4*, 506-513.

28. Holleck, V.L.; Schindler, R. Zeitschrift fur Electrochemie **1956**, *60*, 1138-1141.

29. Shikata, M. Trans. Faraday Soc. **1925**, *21*, 42.

30. Baizer, M.M.; Lund, H. ed. Organic Electrochemistry **1983** Mercel Dekker New York pg 296.

31. Audrieth, L.F.; Ogg, B.A. The Chemistry of Hydrazine; John Wiley & Sons, Inc.: New York, 1951.

32. Mills, C. J. Chem. Soc. **1895**, *67*, 925-932.

33. Smith, P.A.S. Open-Chain Nitrogen Compounds, Vol. II. W.A. Benjamin, Inc., New York 1966. Page 321.

34. Bigelow, H.E. Chem. Rev. **1931**, *9*, 117-167.

35. Bamberger, E. Chem. Ber. **1894**, *27*, 1548-1557.

36. Sidgwick, N.V.; Millar, I.T.; Springall, H.D. The Organic Chemistry of Nitrogen, **1966**, Clarendon Press, Oxford.

37. Ogata, V.; Tsuchida, M.; Takagi, V. J. Am. Chem. Soc. **1957**, *79*, 3397-3401.

38. Bavin, P.M.G. Can. J. Chem. **1958**, *36*, 238-241.

39. Maurel, R.; Menezo, J.C. J. Catalysis **1978**, *51*, 293-295.

40. Schmidt, E.W. "Hydrazine and its Derivatives" Wiley, New York, **1984**.

41. Republic of France, British Patent 1,183,079, **1970**.

42. Blodk, J.; Schulz-Ekloff, G. J. Catalysis **1973**, *30*, 327-329.

43. Ertl, G.; Tornau, J. Z. Physik. Chem. NF 93 (1974) 109-118

44. Spiro, M. Catalysis Today **1990**, *7*, 167-178.

45. Hutchins, L.G.; Pincock, R.E. J. Org. Chem. **1980**, *45*, 2414-2418.

46. Austin, J.M.; Groenewald, T.; Spiro, M. J.Chem. Soc. Dalton Trans., **1980**, 854-859.

47. Terpko Heck J. Org. Chem. **1980**, *45*, 4992-3.

48. Rajagopalan, P.; Advani, B.G.; Talaty, C.N. Org. Syn. **1973**, Coll. Vol. 5 page 504.

49. Lindsay, R.O.; Allen, C.F.H. Org. Syn Coll. Vol. 3. John Wiley & Sons Inc., New York, **19**, page 710

50. Beilsteins Handbuch Der Organischen Chemie, **1922**, *5*, 276.

51. Kamm, O. Org. Syn. Coll. Vol. 1. John Wiley & Sons Inc., New York, **1946**, pg 445.

52. The Merck Index, Tenth Ed. , Merck & Co., Inc. Rahway, **1983**, pg. 7176.

53. Wheeler, O.H.; Gore, P. J. Am. Chem. Soc. **1956**, 78, 3363-3366.

54. Penneman, R.A.; Audrieth, L.F. Anal. Chem. **1948**, *20*, 1058-1061.

55. Bordun, M.; O'Connor, J.M.; Padmanabhan, G.R.; Mollica, J.A. Anal. Chem.**1977**, *49*, 161-162.

56. Giles, C.; Smith, D. J. Colloid and Interface Science **1974**, *47*, 755-765.

57. Duffey, G. Physical Chemistry; McGraw Hill, NY 1962.

58. The Lewis Acid-Base Concepts Jensene, W.B. John Wiley & Sons NY 1980.

59. Isaacs, N.S. Physical Organic Chemistry , John Wiley & Sons NY, 1987.

60. Lowski, W. Nitrenes, Interscience, N.Y. 1970.

61. Ege, S.; Sharp, R. J. Chem. Soc. **1971**, 2014-2015.

62. Brinkman, V.G. Kolloid Z. **1951**, *123*, 116-129.

63. Keier, N.P.; Astaf'ev, I.V. Kinetics and Catalysis **1962**, *3*, 320-321.

64. Yamabe, H.; Kato, H.; Yonezawa, T. Bul. Chem. Soc. Japan **1971**, *44*, 22-27.

65. Pasto, D. J. Am. Chem. Soc. **1979**, *101*, 6852-6857.

66. Nelsen, S.F.; Rumack, D.T.; Moet-Ner, M. J. Am. Chem. Soc. **1988**, *110*, 7945-7961.

67. Bodor, N.; Dewar, J.; Jennings, W.; Worley, S. Tetrahedron **1970**, *26*, 4109-4113.

68. Nelsen, S.F.; Blackstock, S.C.; Yumibe, N.P.; Frigo, T.B.; Carpenter, J.E.; Weinhold, F. J. Am. Chem. Soc. **1985**, *107*, 143-149.

69. Nelson, S.F.; Peacock, V.; Weisman, G.R. J. Am. Chem. Soc. **1976**, *98*, 5269-5277.

70. Urry, W.H.; Szecsi, P.; Ikoku, C.; Moore, D.W. J. Am. Chem. Soc. **1964**, *86*, 2224-2229.

71. Bansa, R.C.; Donnet, J.; Stoeckli, F. Active carbon 1988 Marcel Dekker, Inc. NY pg 422.

72. Handbook of Chemistry and Physics 63rd Edition **1982** CRC Press, Inc. Boca Raton.

73. Bansa, R.C.; Donnet, J.; Stoeckli, F. Active carbon 1988 Marcel Dekker, Inc. NY pg 422.

74. The chemistry of Peroxides S. Patai, 1983 wiley pg 43.

75 Kwang Kim, personal communication.

76. Cabot Techincal Report S-136, Cabot Corporation.

77. Mantell, C.L. Industrial Carbon D.Van Nostrand Company, Inc. 1946 new york

78. Reynolds, W.N. Physical Properties of Graphite, Elsevier, N.Y. 1968.

79. Padwa, A. 1,3-Dipolar Cycloaddition Chemistry, Volume 2, Wiley, New York, 1984.

80. Noller, C.R. Chemistry of Organic Compounds 3rd ed. Saunders, Philadelphia, 1966, p 690.

81. Bowyer, W.J.; Evans, D.H. J. Org. Chem. **1988**, *53*, 5234-5239.

82. Mann, C.K.; Barnes, K.K. Electrochemical Reactions in Non-Aqueous Systems, Mercel Dekker Inc., Nwy York, 1970.

83. Furst, A.; Moore, R.E. J. Am. Chem. Soc. **1957**, *79*, 5492-5493.

84. Ross, S.D.; Kahan, G.J.; Leach, W.A. J. Am. Chem. Soc. **1952**, *74*, 4122-4126.

85. Buchi, G.; Ayer, D.E. J. Am. Chem. Soc. **1956**, 78, 689-690.

86. Hwu, J.R.; Wong, F.F.; Shiao, M. J. Org. Chem. **1992**, *57*, 5254-5355.

87. Smith, P.A.S.; Hall, J.H. J. Am. Chem. Soc. **1962**, *84*, 480-485.

88. Urry, W.H. J. Am. Chem. Soc., **1957**, *79*, 6568-6569.

89. King, D.; Bard, A. J. Am. Chem. Soc. **1965**, *87*, 419-423.

90. Coffield, J.E.; Mamantov, G.; Zingg, S.P.; Smith, G.P. J. Electrochem. Soc. **1991**, *138*, 2543-2549.

91. Pagni, R.M. *In Advances in Molten Salt Chemistry 6*; Mamantov, G; Mamantov, C.B.; Braunstein, J. Ed.; Elsevier: New York, 1987; Chapter 4.

92. Bond, G.C. *Catalysis by Metals*: Academic Press: New York, 1962: Chapter 19.

93. Posner, G.H. Angew Chem Int Ed Engl, **1978**, *17*, 487-496.

94. Bond, G.C. *Heterogenous Catalysis: Principles and Applications*, Oxford University Press: New York, 1987: page 111.

95. Lossens, L.W.; Petersen, E.E. J. Catalysis **1982**, *76*, 265-273.

96. Rebhan, D.M.; Haensel, V. J. Catalysis **1988**, *111*, 397-408.

97. Equilibrium constants calculated from the data of Stull, D.R.; Westrum, E.F.Jr.; Sinke, G. *The Chemical Thermodynamics of Organic Compounds*; Wiley & Sons, New York, 1969 p344, 347, 367.

98. Land, D.P.; Pettiette-Hall, C.L.; McIver, R.T.; Hemminger, J.C. J. Am. Chem. Soc. **1989**, *111*, 5970-5972.

99. Pettiett-Hall, C.L.; Land, D.P.; McIver, R.T.Jr.; Hemminger, J.C. J. Am. Chem. Soc.,**1991**, *113*,2755-2756.

100. Carra, S.; Ragaini, V.; Guella, F. J. Catalysis, **1967**, *8*, 261-271.

101. Volkov, S.V. Chem. Soc. Rev. **1990**, *19*, 21-28.

102. Parshall, G.W. J. Am. Chem. Soc. **1972**, *94*, 8716-8719

103. Kennedy, J.H.; Buse, C. J. Org. Chem. **1971**, *36*, 3135-3138.

104. Rony, P.R. Chemical Engineering Science,**1968**, *23*, 1021-1034.

105. Salarzadeh, I.; Tariq, S.A. Aust. J. Chem, **1986**, *39*, 1119-1127.

106. Buchanan. A.C.III; Chapman, D.M.; Smith, G.P. J. Org. Chem. **1985**, *50*, 1702-1711.

107. Parshall, G.W. US 3,657,368 (1972).

108. Parshall, G.W. US 3,565,823 (1971).

109. Parshall, G.W. US 3,919,271 (1975).

110. Parshall, G.W. US 3,832,391 (1974).

111. Wagner, C.D.; Riggs, W.M.; Davis, L.E.; Mouldne, J.F.; Muilenberg, G.E.(ed) *Handbook of X-Ray Photoelectron Spectroscopy*: Perkin-Elmer Corporation, 1979, 152-153.

112. Shum, V.; Butt, J.; Sachtler, M. J. Catalysis, **1985**, *96*, 371-380.

113. Davis, B.; Venuto, P. J. Org. Chem. **1971**, *36*, 337-339.

114. Carra, S.; Beltrame, P.; Ragini, V. J. Catalysis **1964**, *3*, 353.

115. Epstein, M.B.; Pitzer, K.S.; Sossini, F.D. J. Catalysis **1949**, *42*, 379-382.

116. Laitnen, H.A.; Liu, C.H. J. Am. Chem. Soc. **1958**, *80*, 1015-1020.

117. Levin, E.M.; Robbins, C.R.; McMurdie, H.F. *Phase Diagrams for Ceramists*: The American Ceramic Society, Columbus, OH;1964, fig.1407.

118. Song, C.;Nomura, M.; Miyake, M. Fuel, **1986**, *65*, 922-926.

119. Levin, E.M.; Robbins, C.R.; McMurdie, H.F. *Phase Diagrams for Ceramists*: The American Ceramic Society, Columbus, OH;1964, fig.1187.

120. Levin, E.M.; Robbins, C.R.; McMurdie, H.F. *Phase Diagrams for Ceramists*: The American Ceramic Society, Columbus, OH;1969, fig.3542.

121. Gmeling Handbuch der anorgainscher chemie 21, 6, 375: 20, 1, 329: 22, 1, 13.

122. Vayenas, C.G.; Verkios, X.E. in Catalyst Technology, Mukhlyonov, I.P. editor, Chapter 4.

123. Coulson & Richardson Chemical Engineering, Volume 2. Pergamon Press, N.Y. 1965, page 304.

Appendix 1. Decomposition of Hydrazine on Several Carbons in Refluxing IPA (Table 8)

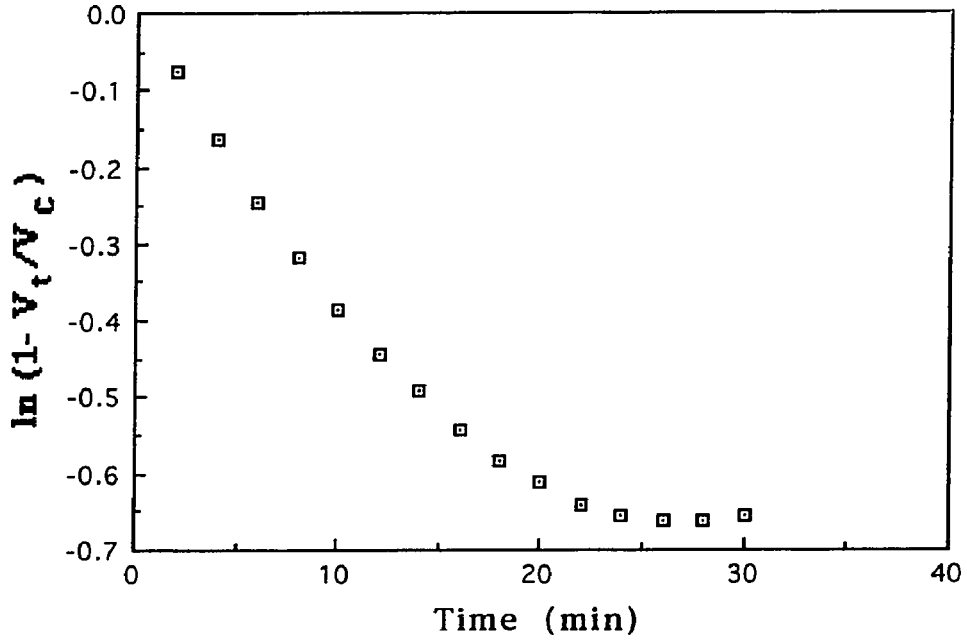

Figure A1-1. Decomposition of Hydrazine Monohydrate on Aqua A -$FeCl_3$

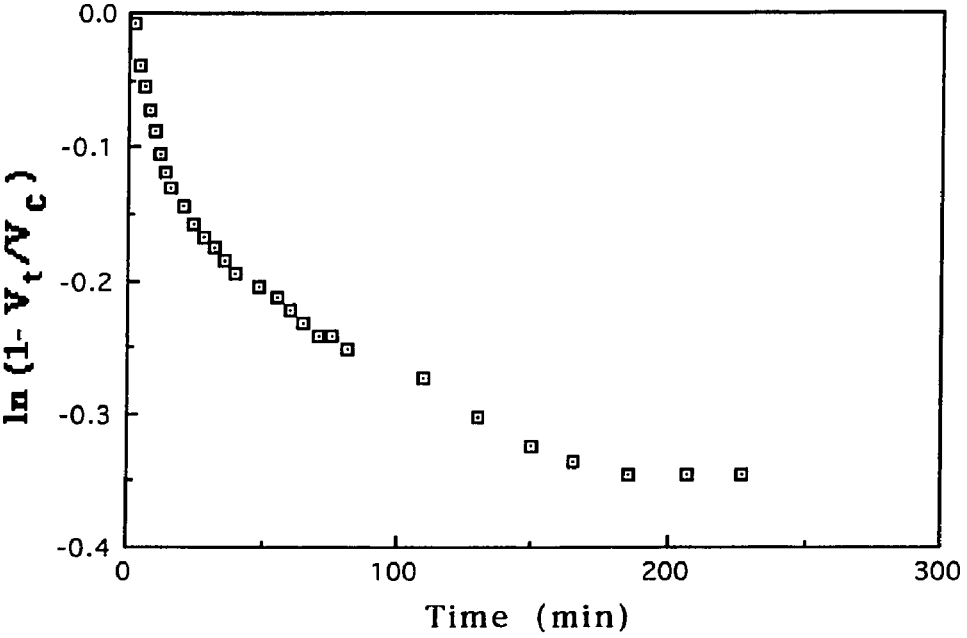

Figure A1-2. Decomposition of Hydrazine Hydrate on Mogul L

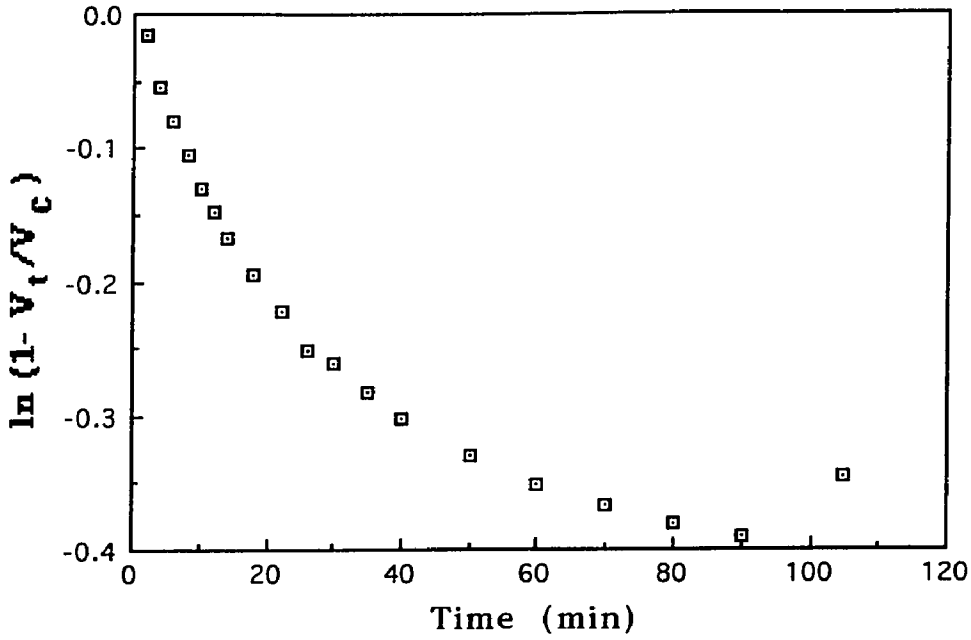

Figure A1-3. Decomposition of Hydrazine Hydrate on Mogul L-$FeCl_3$

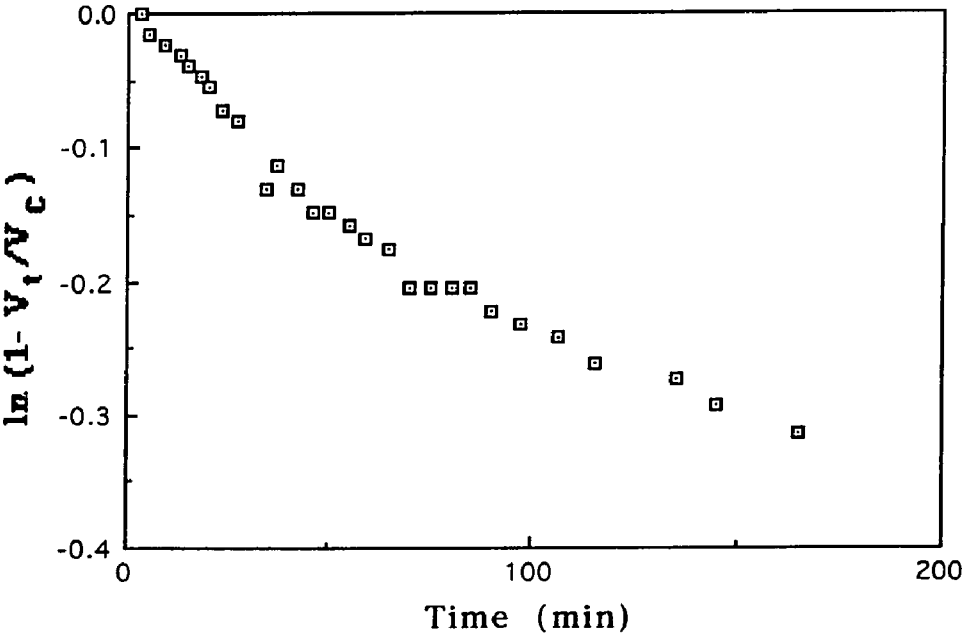

Figure A1-4. Decomposition of Hydrazine Hydrate on Black Pearls L

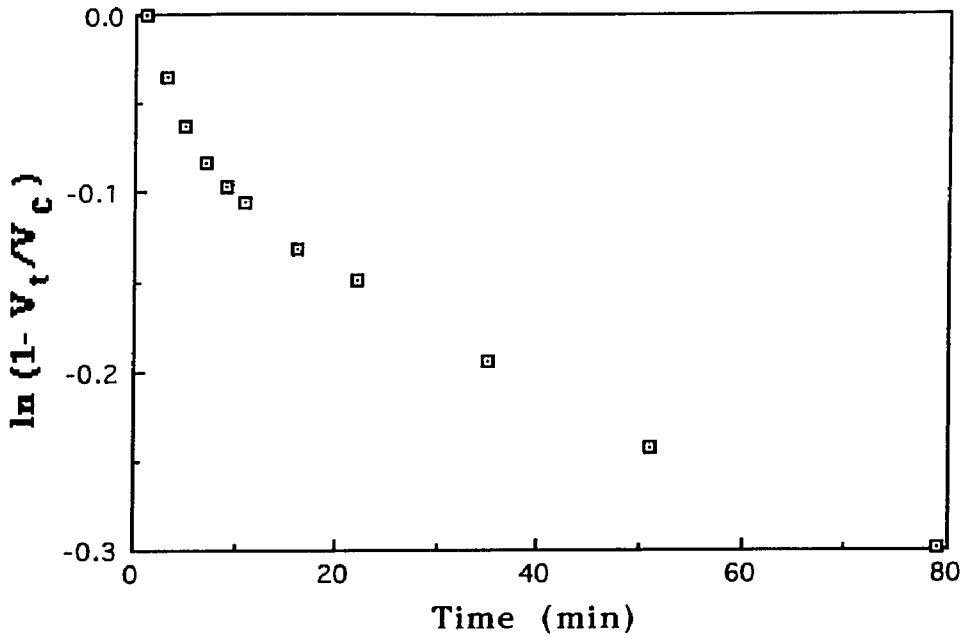

Figure A1-5. Decomposition of Hydrazine Hydrate on Black Pearls L-$FeCl_3$

Appendix 2. Langmuir Adsorption Plots

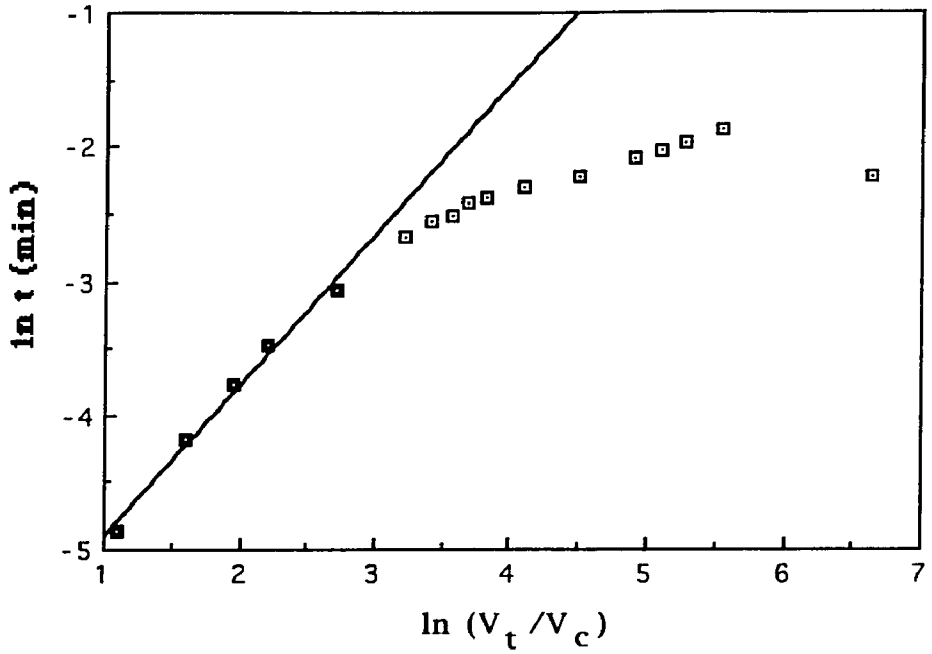

Figure A2-1. Langmuir Adsorption on Graphite

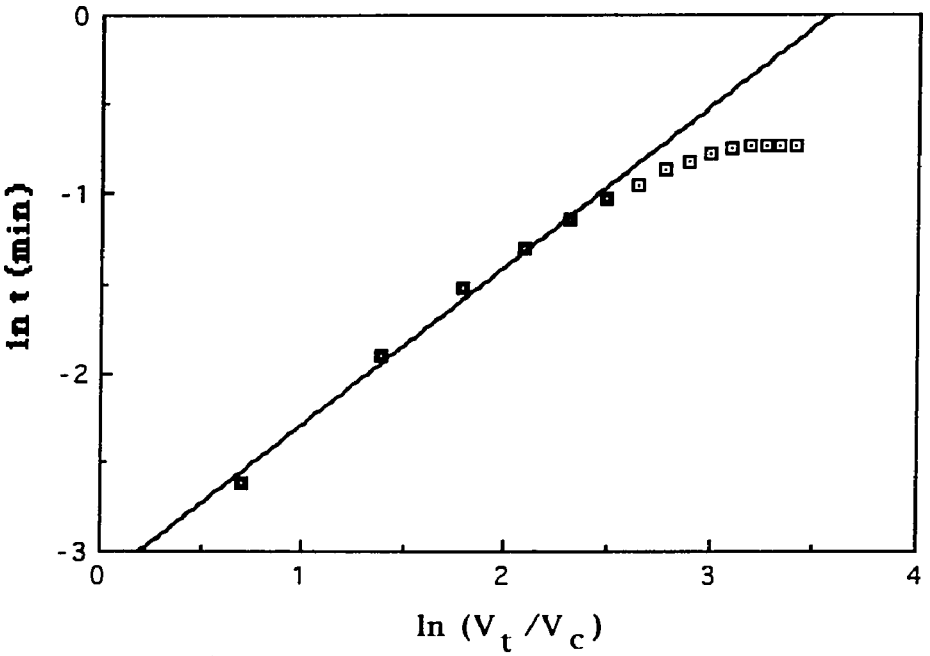

Figure A2-2. Langmuir Adsorption on Aqua A-$FeCl_3$

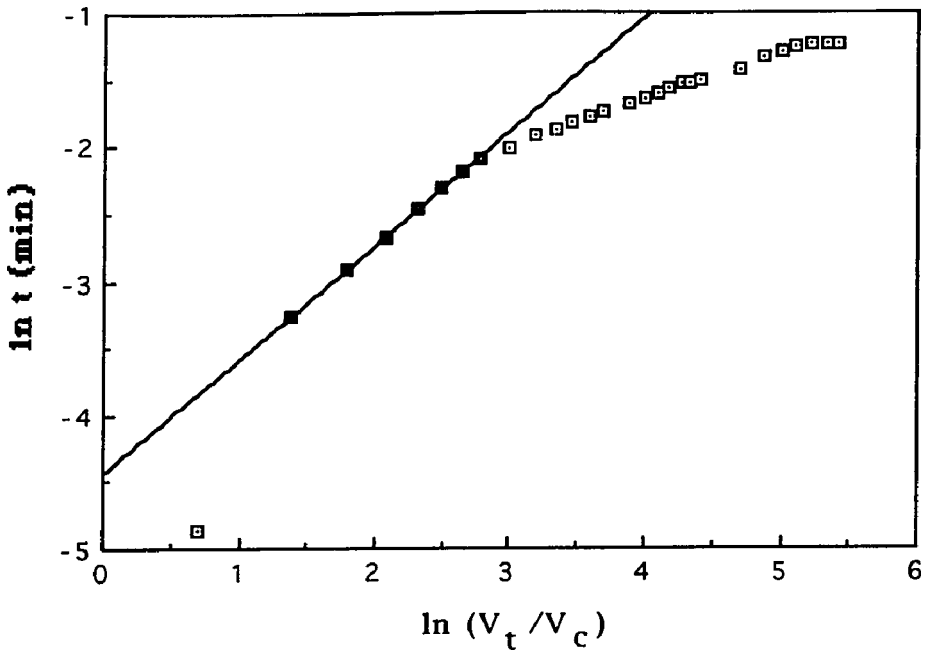

Figure A2-3. Langmuir Adsorption on Mogul L

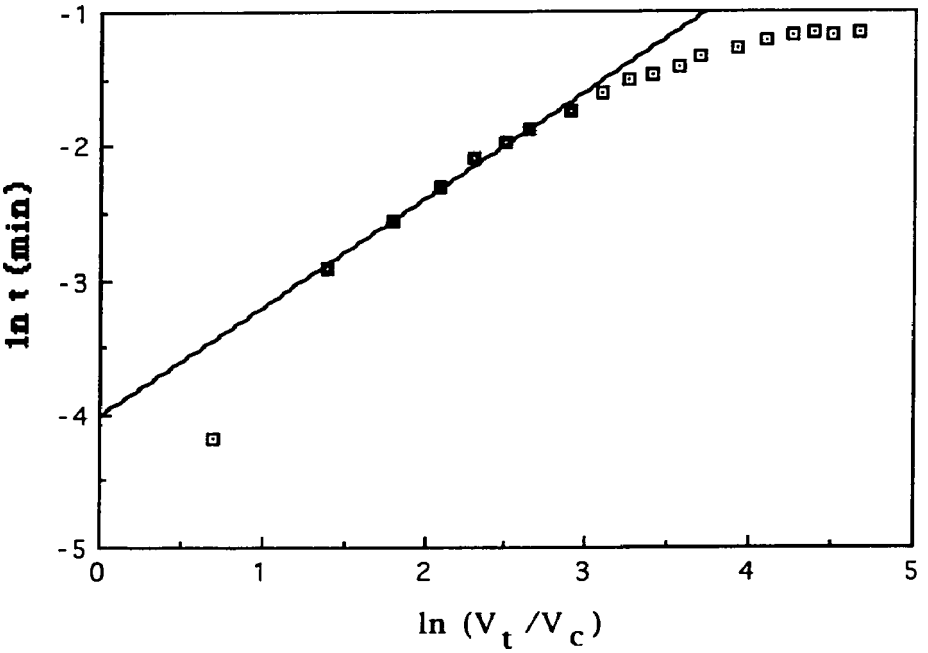

Figure A2-4. Langmuir Adsorption on Mogul L-$FeCl_3$

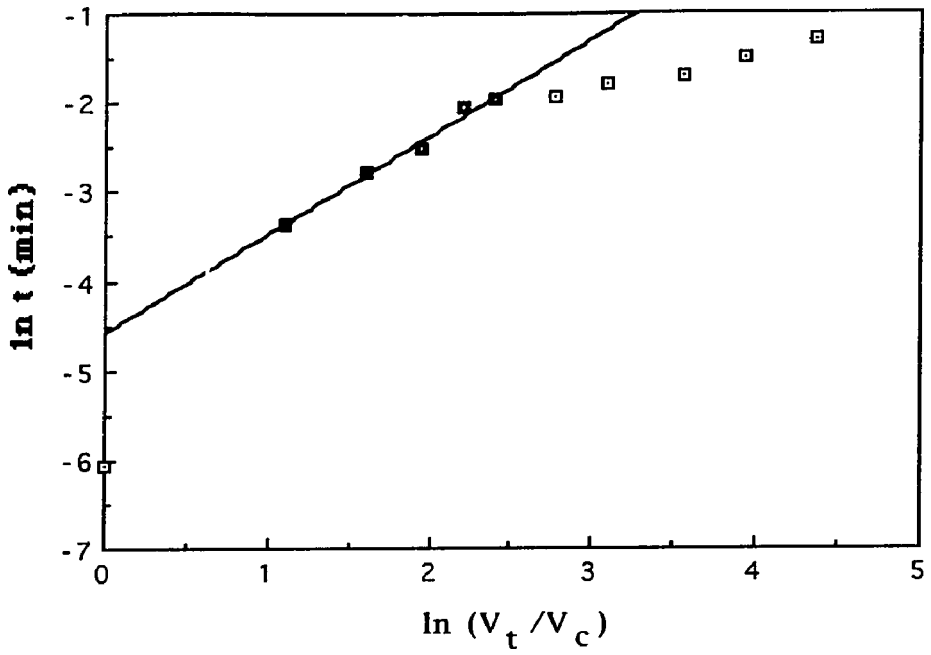

Figure A2-5. Langmuir Adsorption on Black Pearls L

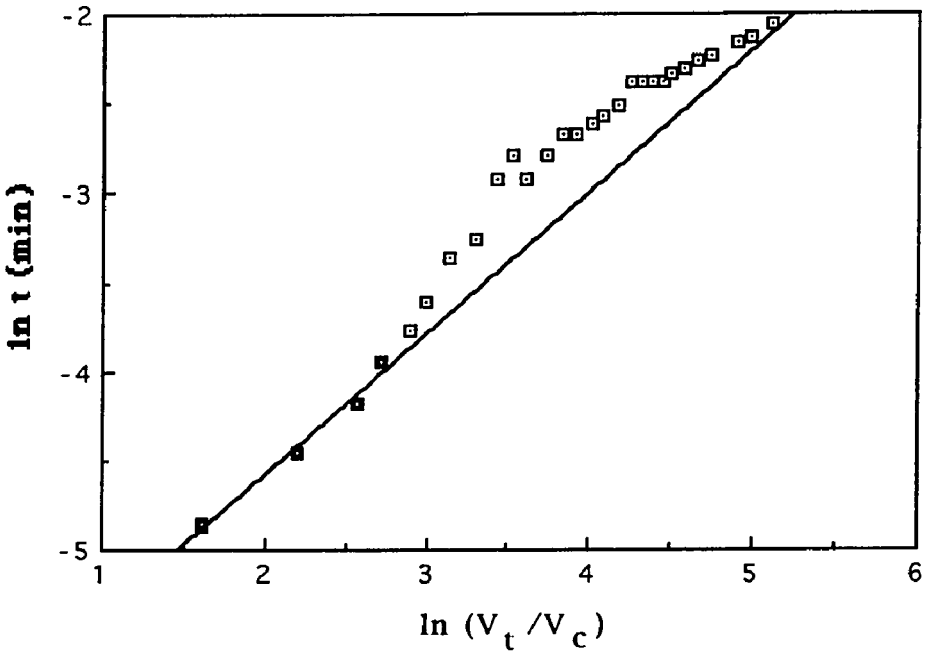

Figure A2-6. Langmuir Adsorption on Black Pearls L-$FeCl_3$

Appendix 3. Various Stirring Rates

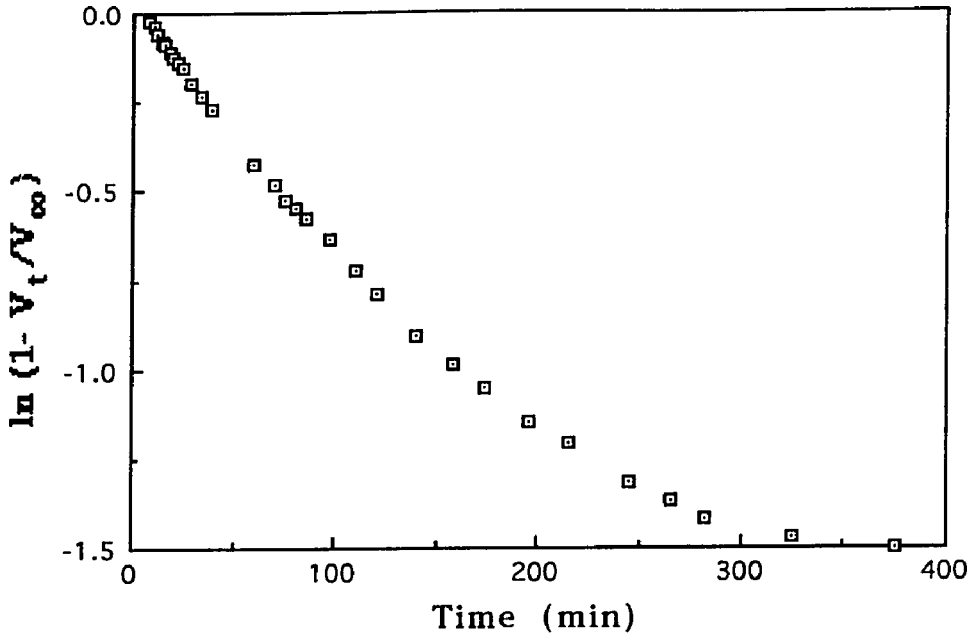

Figure A3-1. Reduction of Nitro Meta Base With Stirring Speed at 1.

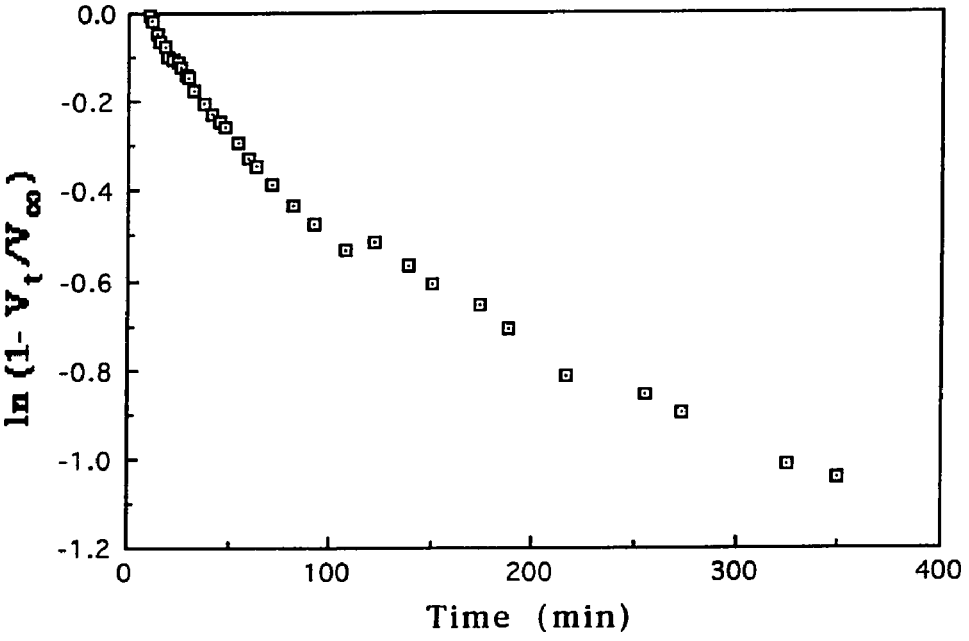

Figure A3-2. Reduction of Nitro Meta Base With Stirring Speed at 2.

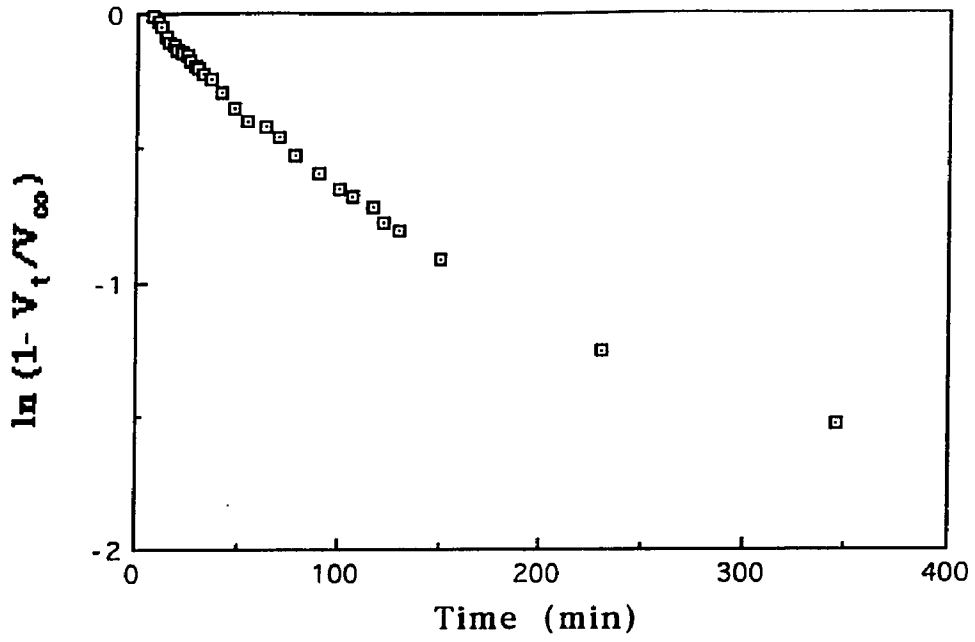

Figure A3-3. Reduction of Nitro Meta Base With Stirring Speed at 4.

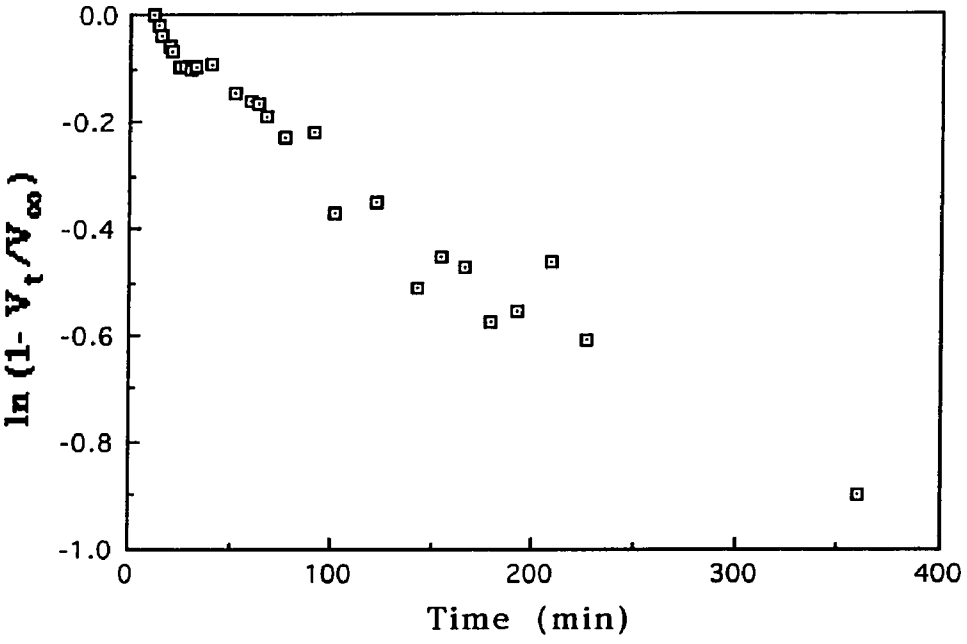

Figure A3-4. Reduction of Nitro Meta Base With Stirring Speed at 5.

Appendix 4. Hydrazine Monohydrate Reduction of Nitro Meta Base at Various Concentrations (Table 11)

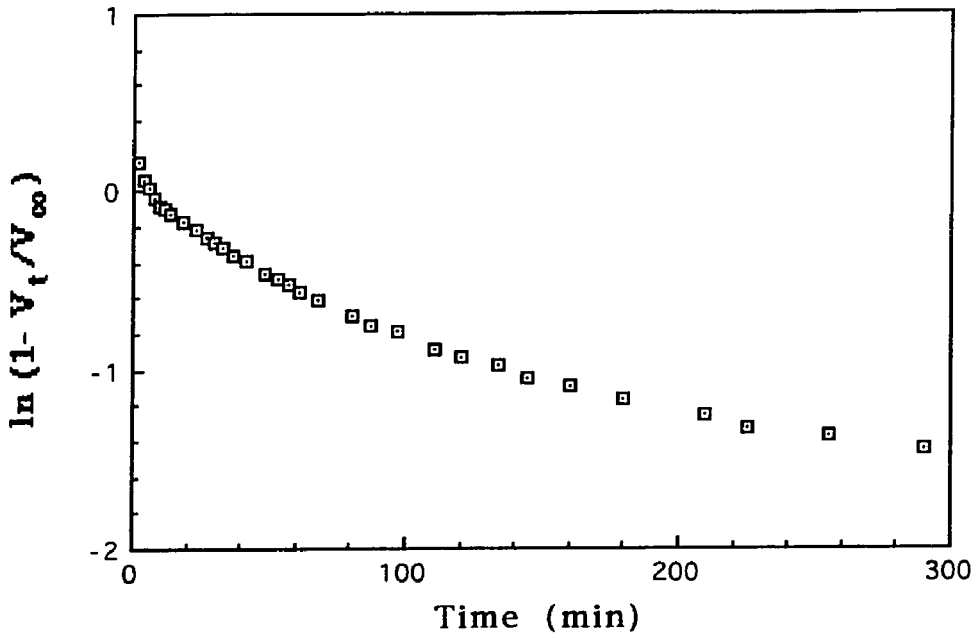

Figure A4-1. Nitro Meta Base at 0.121 M

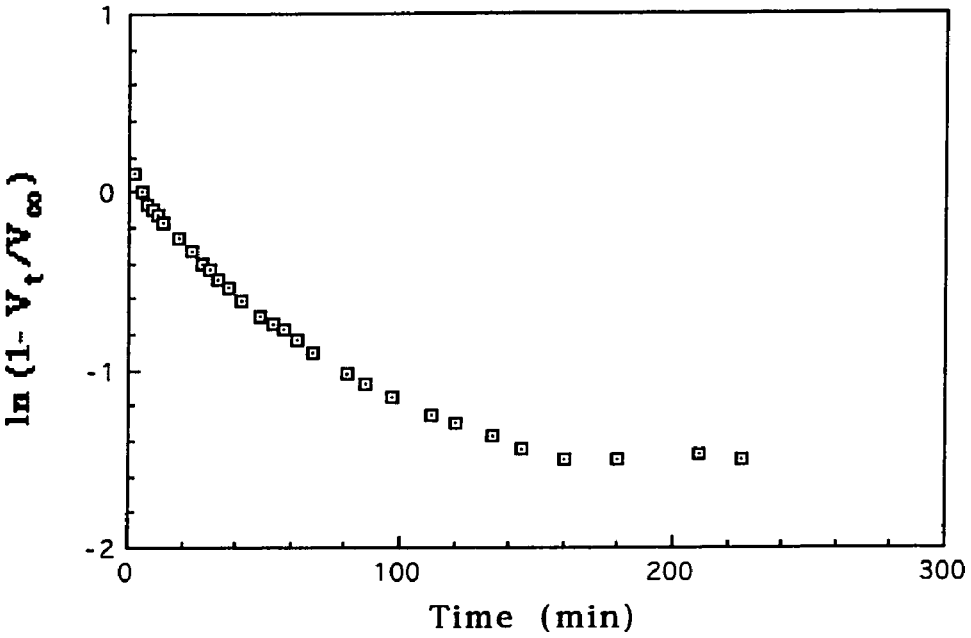

Figure A4-2. Nitro Meta Base at 0.182 M

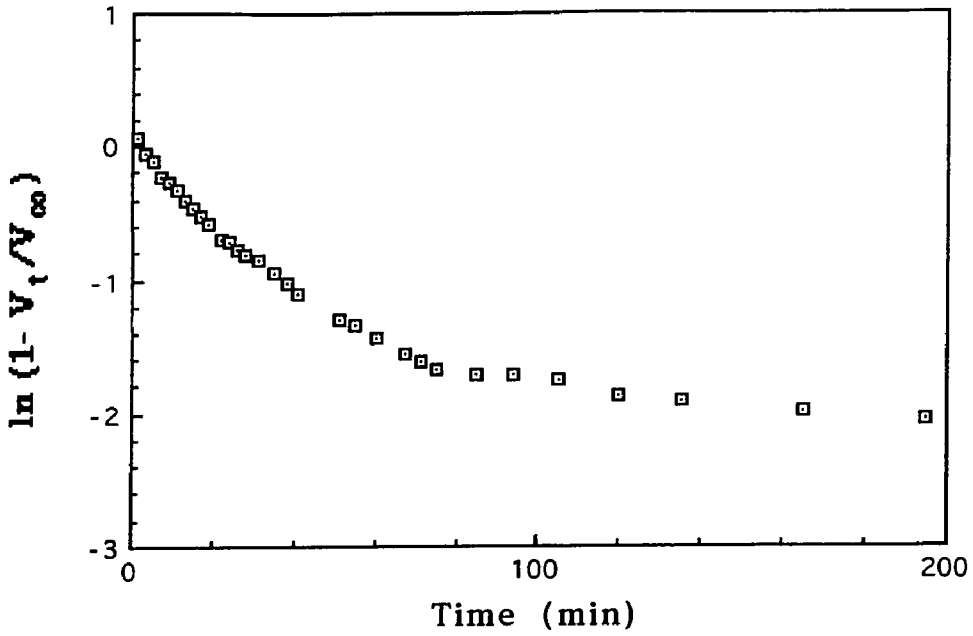

Figure A4-3. Nitro Meta Base at 0.364 M

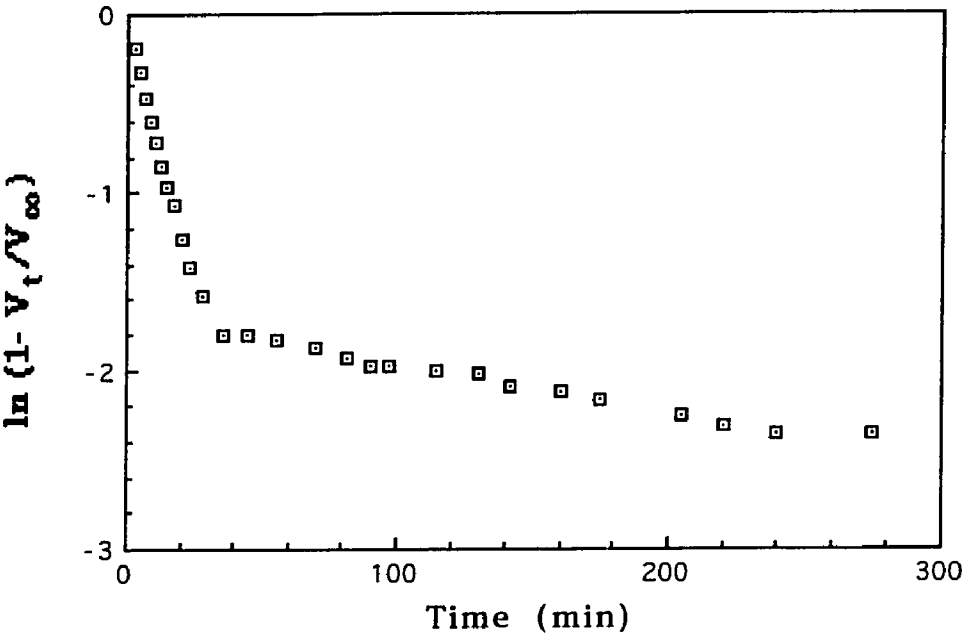

Figure A4-4. Nitro Meta Base at 0.762 M

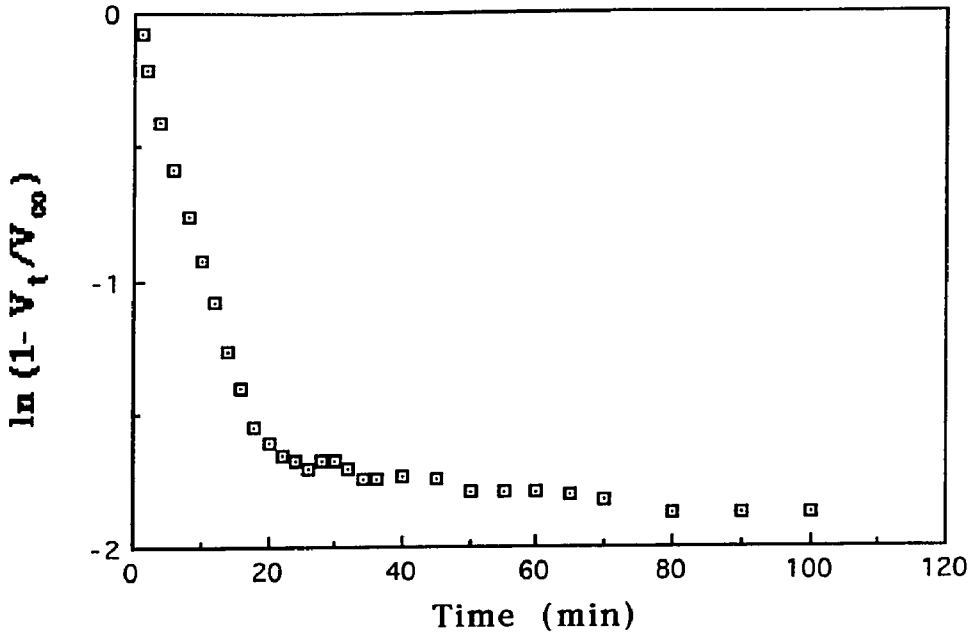

Figure A4-5. Nitro Meta Base at 1.08M

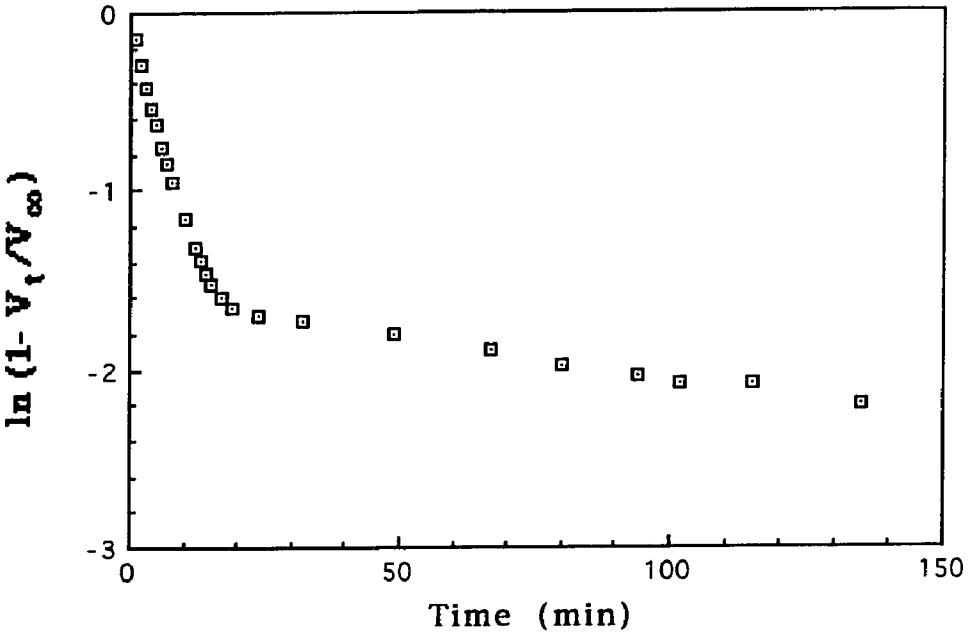

Figure A4-6. Nitro Meta Base at 1.48 M

Appendix 5. Various Ratios of Graphite to Nitro Meta Base (Table 15)

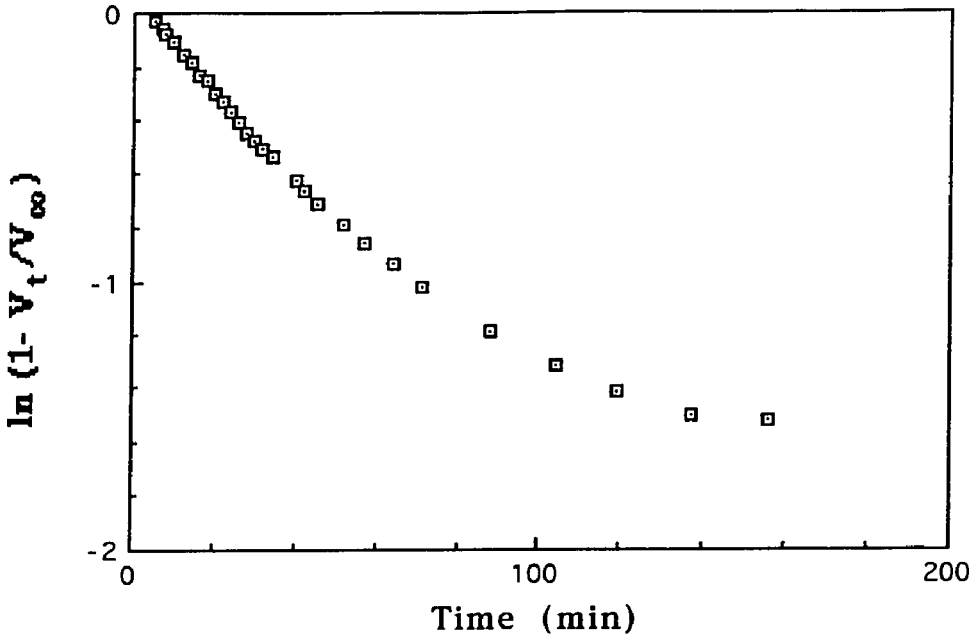

Figure A5-1. Ratio of Graphite to Nitro Meta Base: 1.26

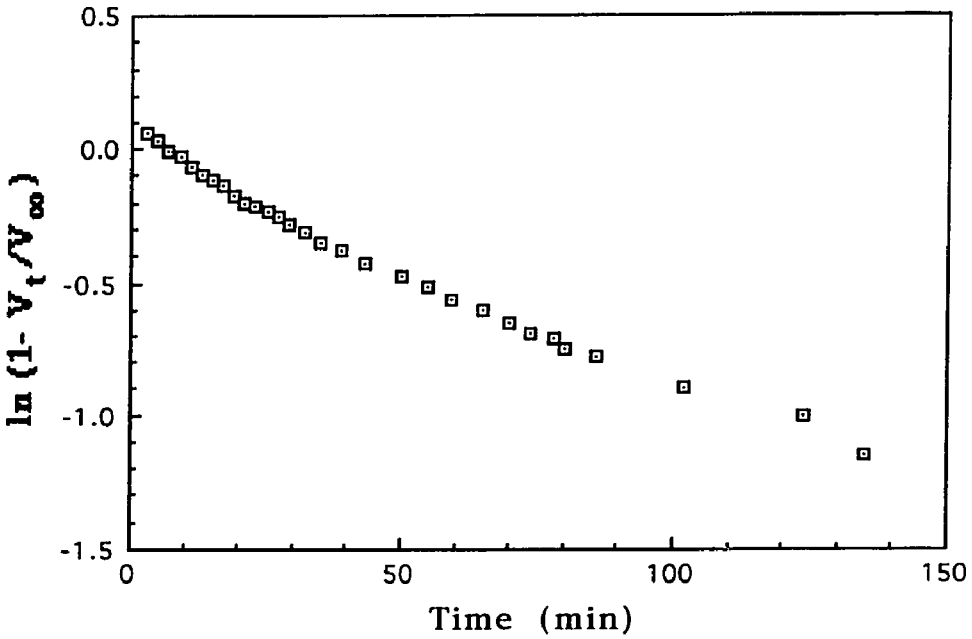

Figure A5-2. Ratio of Graphite to Nitro Meta Base: 1.02

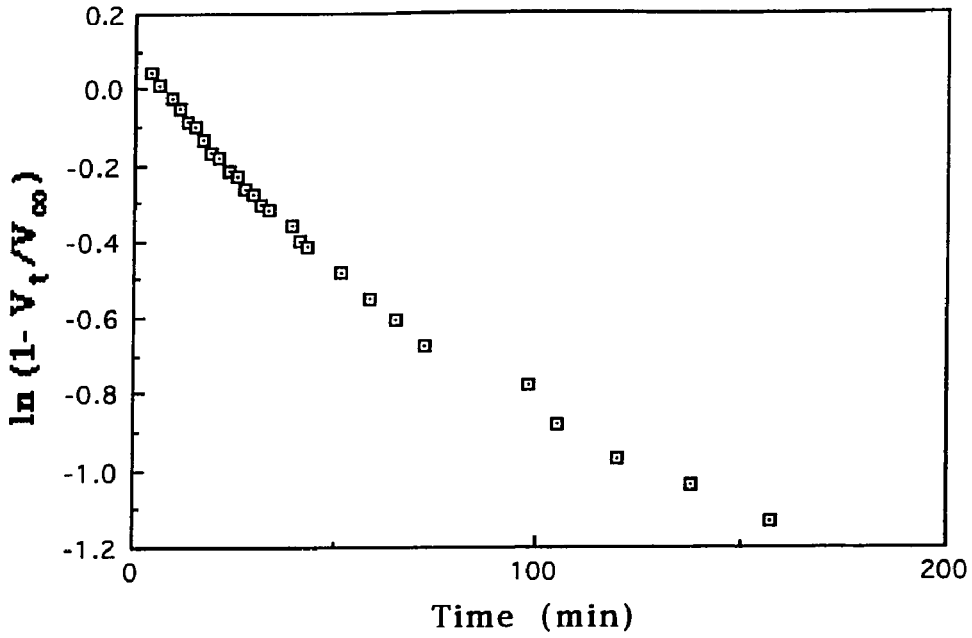

Figure A5-3. Ratio of Graphite to Nitro Meta Base: 0.57

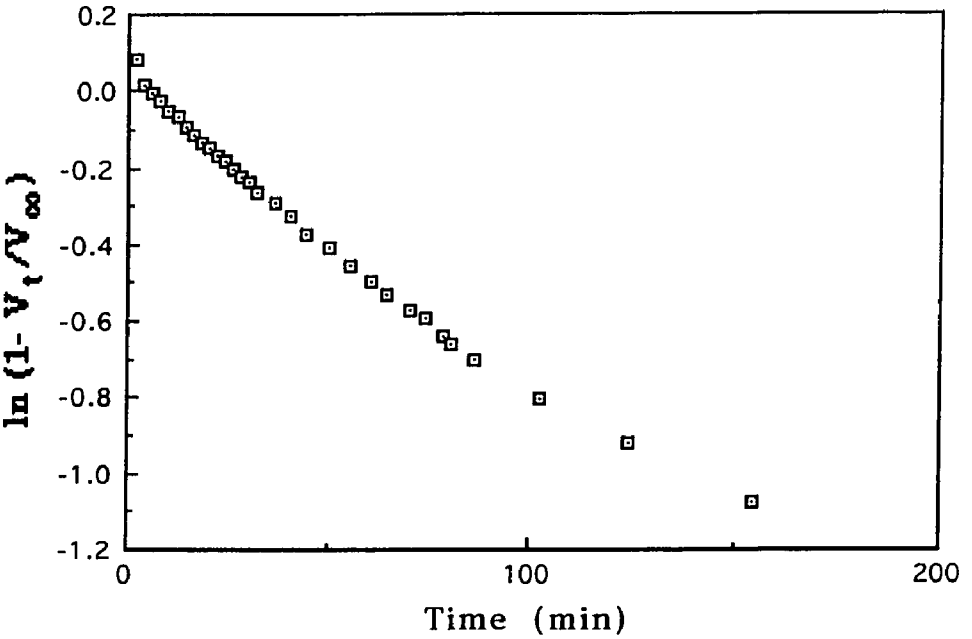

Figure A5-4. Ratio of Graphite to Nitro Meta Base: 0.53

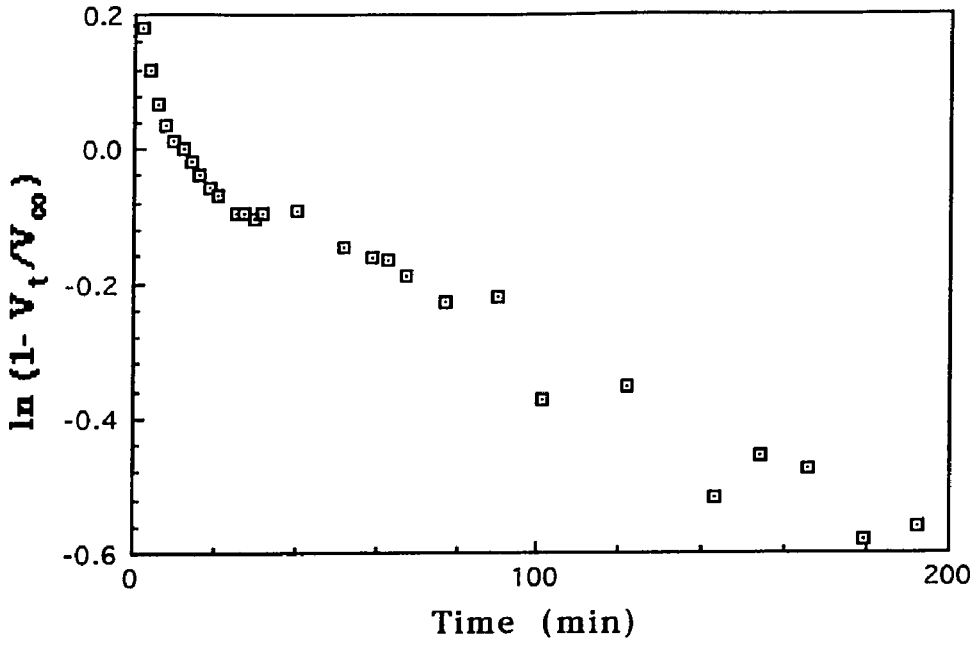

Figure A5-5. Ratio of Graphite to Nitro Meta Base: 0.12a

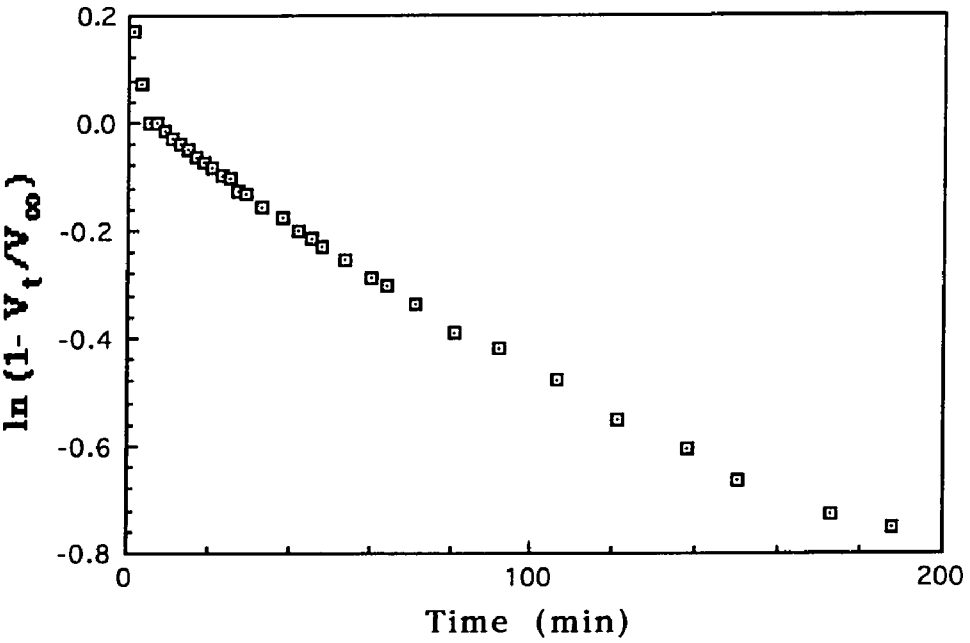

Figure A5-6. Ratio of Graphite to Nitro Meta Base: 0.12b

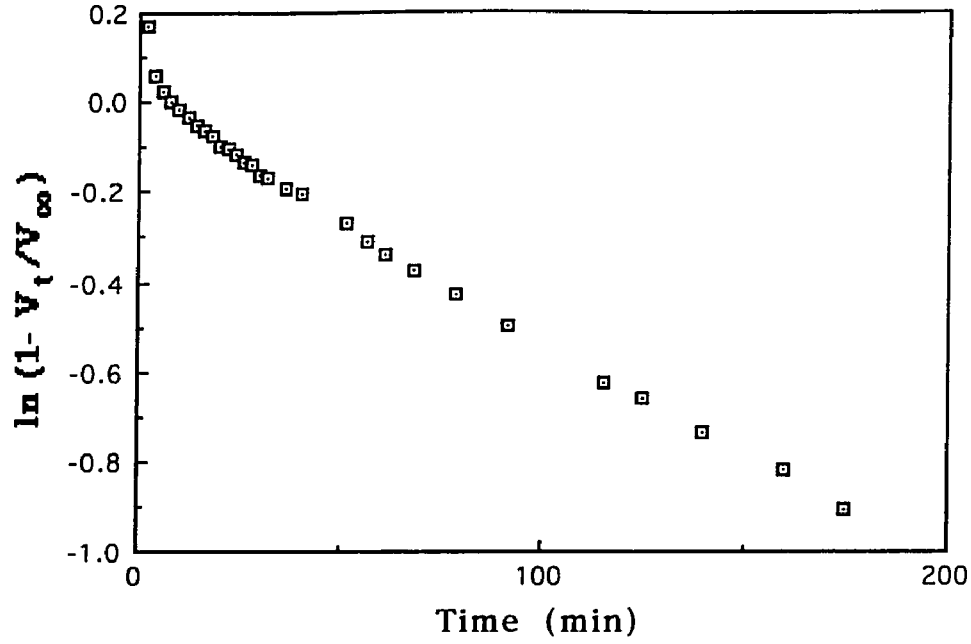

Figure A5-7. Ratio of Graphite to Nitro Meta Base: 0.06

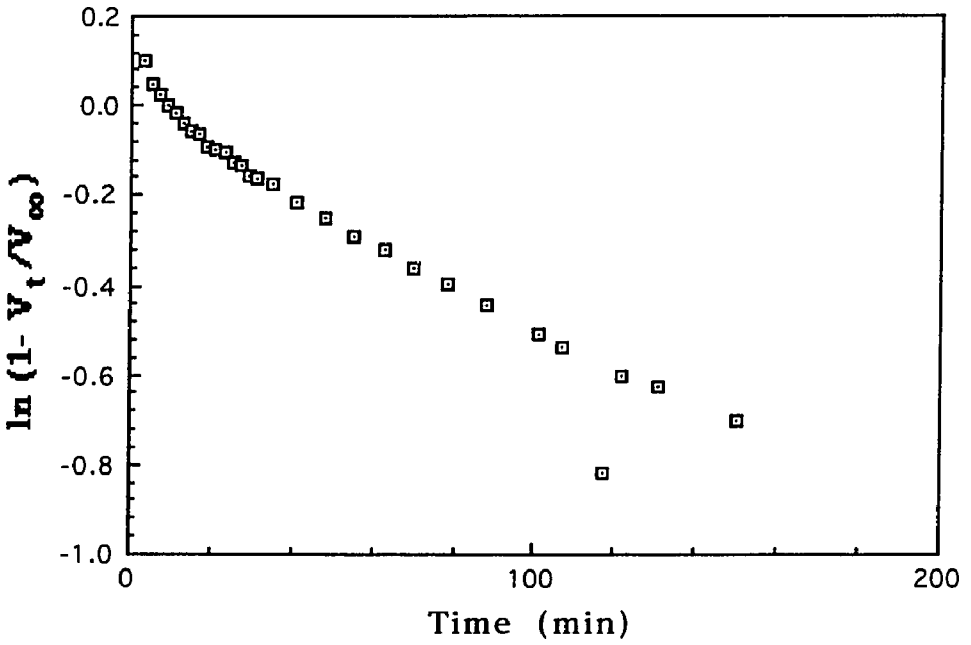

Figure A5-8. Ratio of Graphite to Nitro Meta Base: 0.056

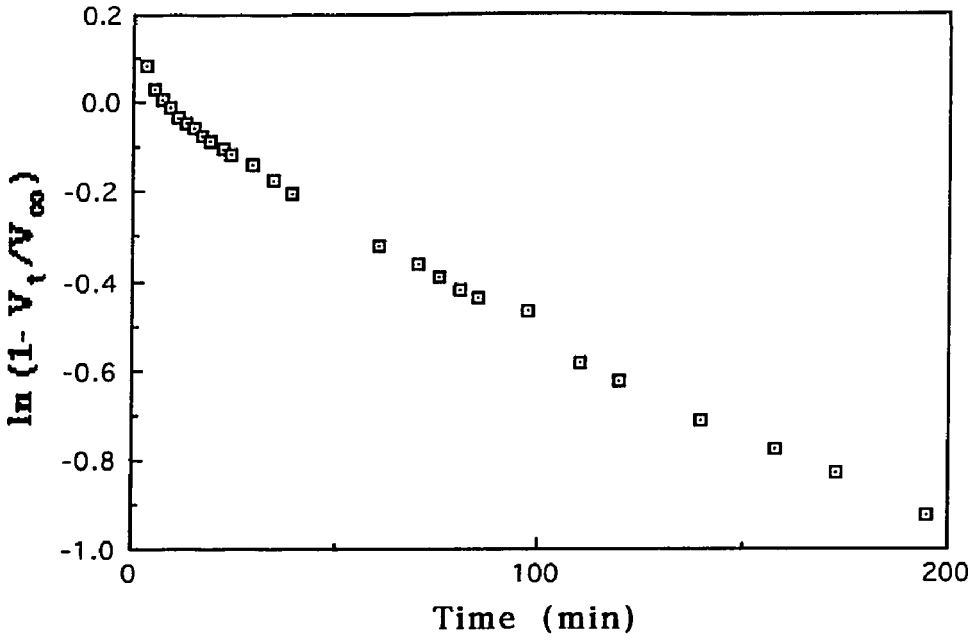

Figure A5-9. Ratio of Graphite to Nitro Meta Base: 0.031 a

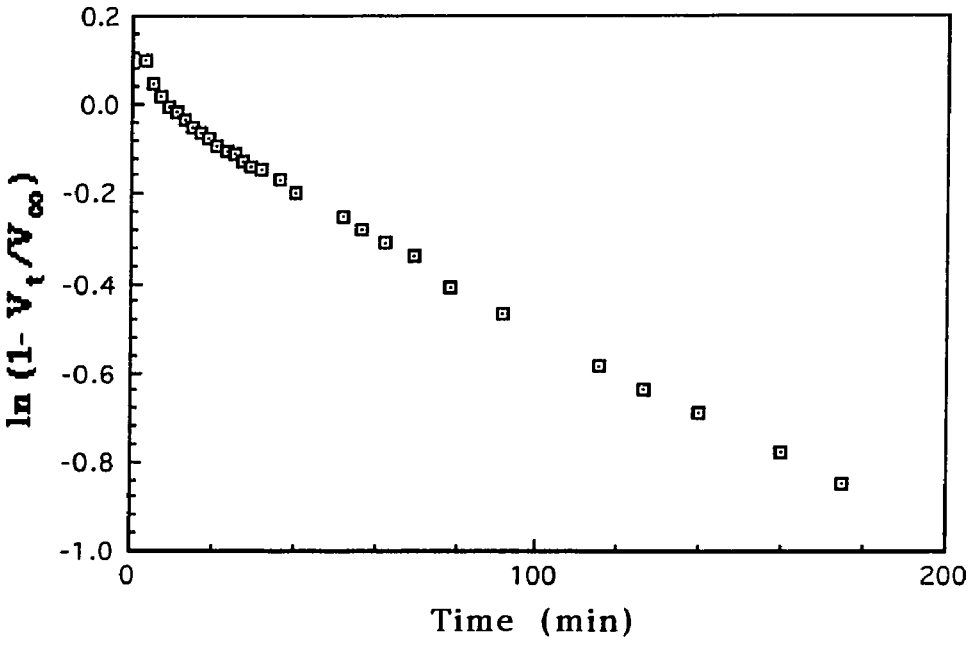

Figure A5-10. ratio 0.031 b

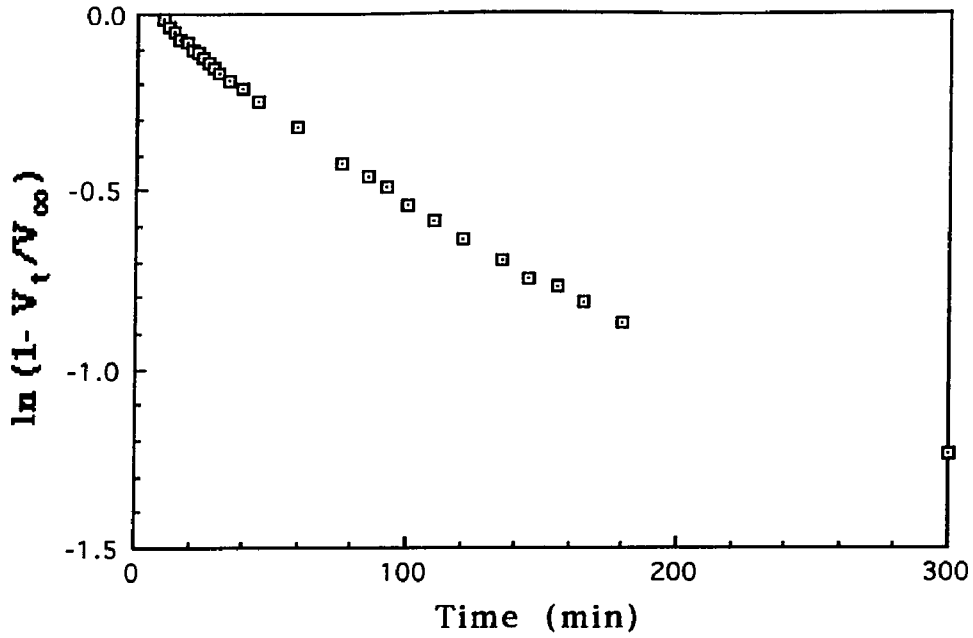

Figure A5-11. no graphite present

Appendix 6. Hydrazine Reduction of Nitro HPS and POP(1) with Various Ratios of Graphite to Nitro Compound (Table 13)

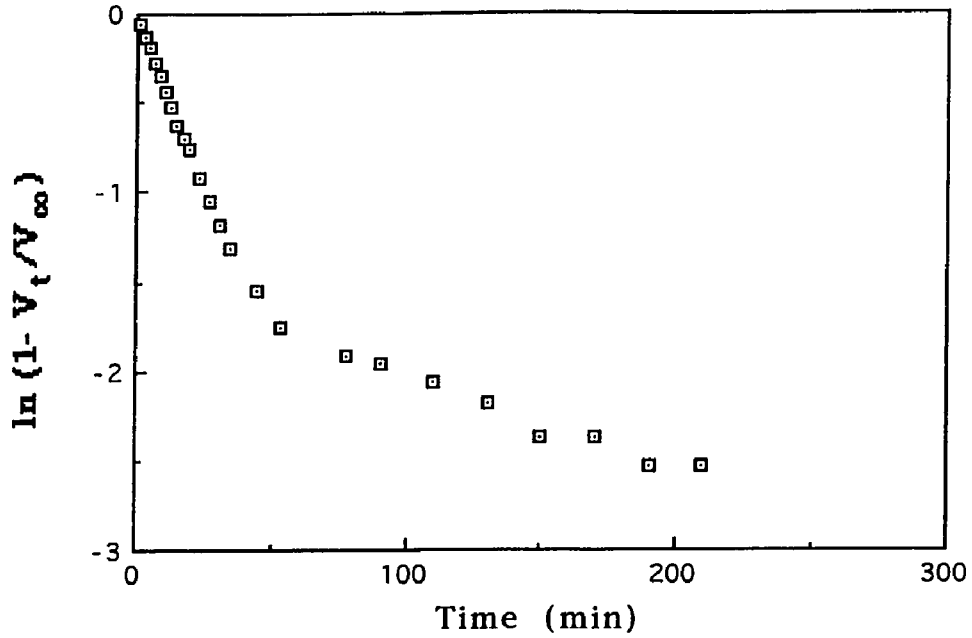

Figure A6-1. Ratio of Graphite to HPS: 1.0

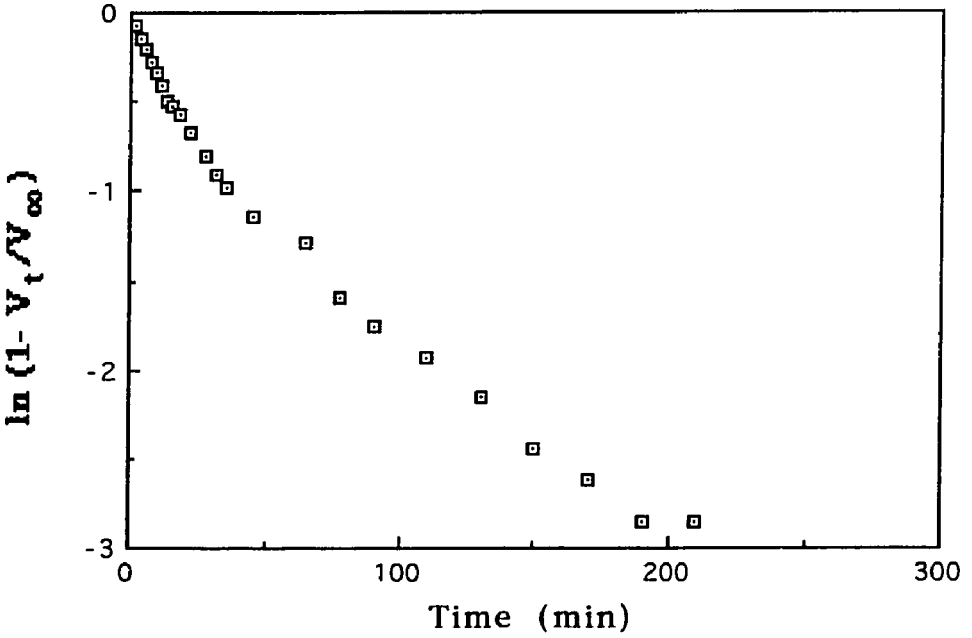

Figure A6-2. Ratio of Graphite to HPS: 0.30

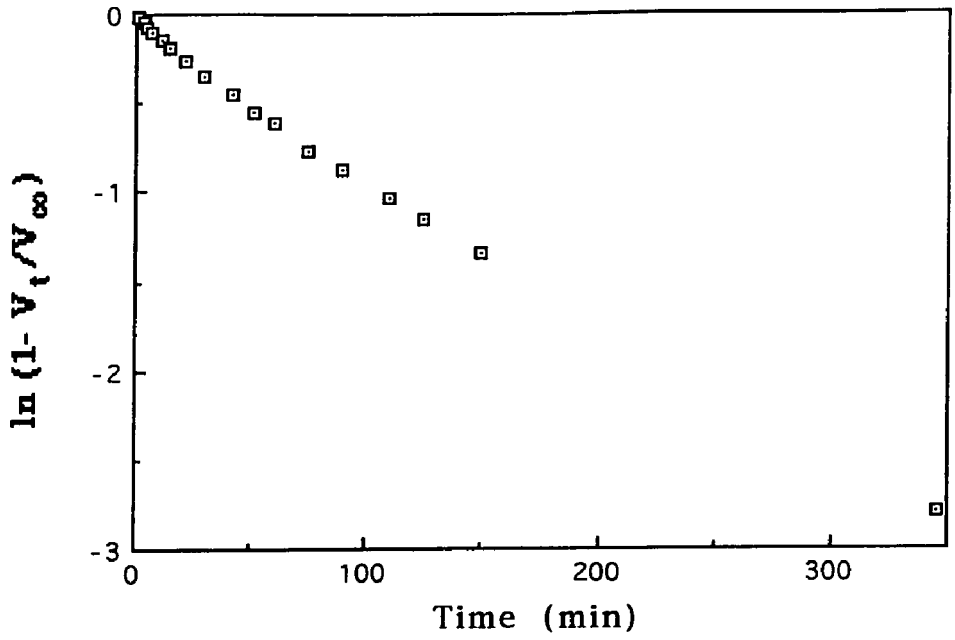

Figure A6-3. Ratio of Graphite to HPS: 0.10

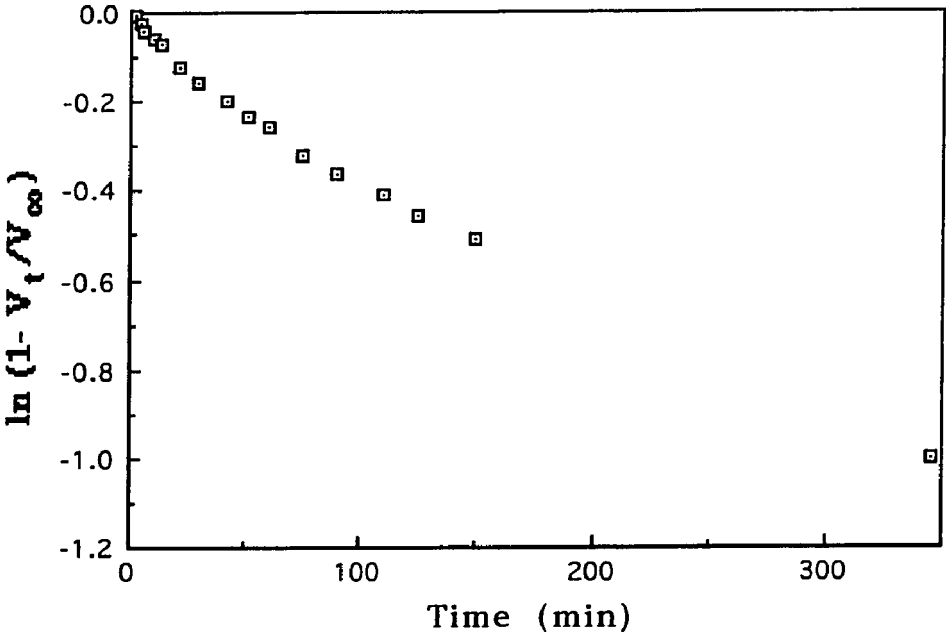

Figure A6-4. Ratio of Graphite to HPS: 0.05

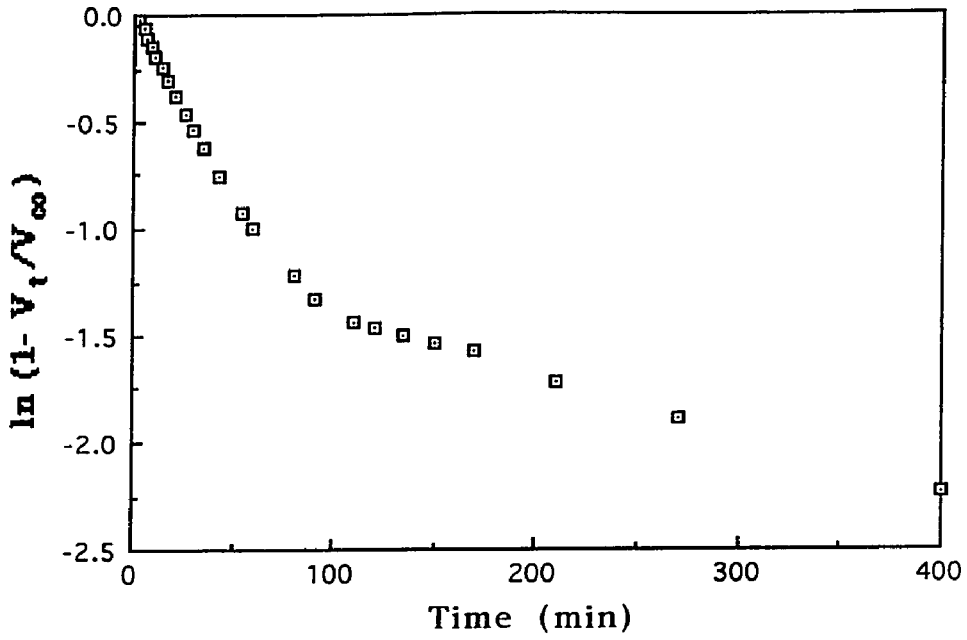

Figure A6-5. Ratio of Graphite to POP(1): 1.0

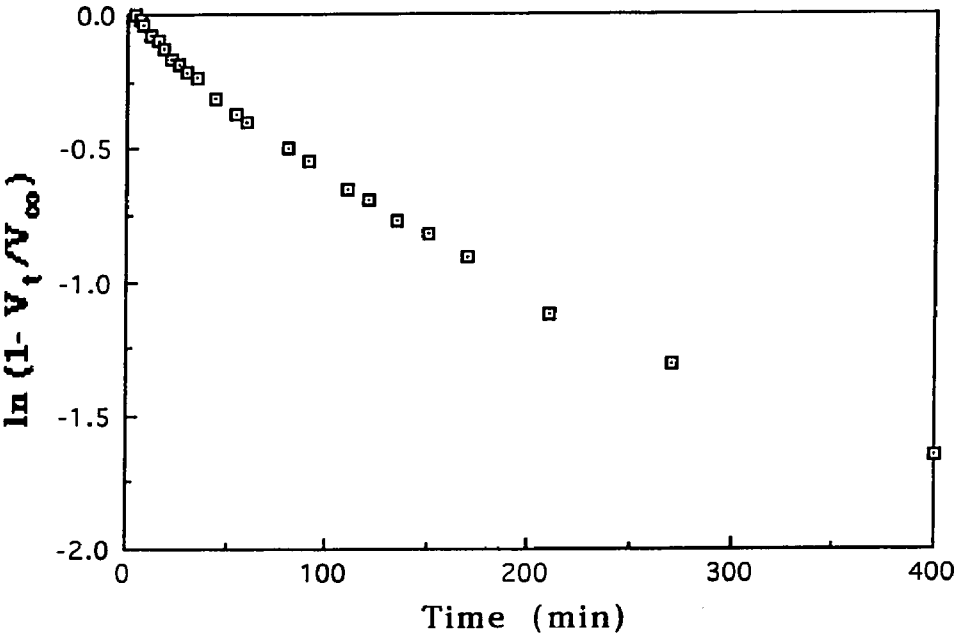

Figure A6-6. Ratio of Graphite to POP(1): 0.289

Appendix 7. Reduction of Nitro HMI with Various Carbons (Table 14)

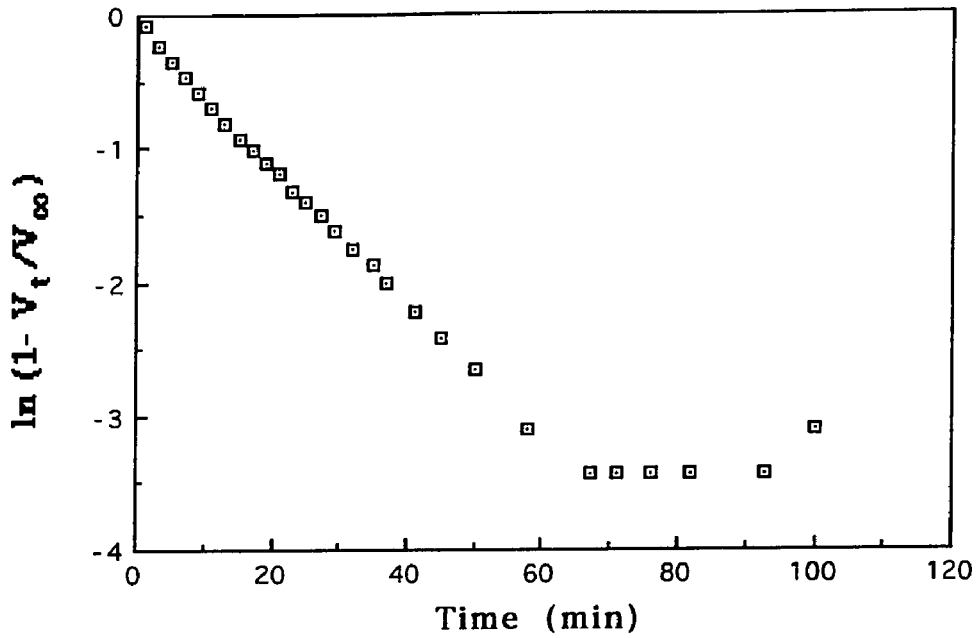

Figure A7-1. Hydrazine Monohydrate Reduction of Nitro HMI with Aqua A

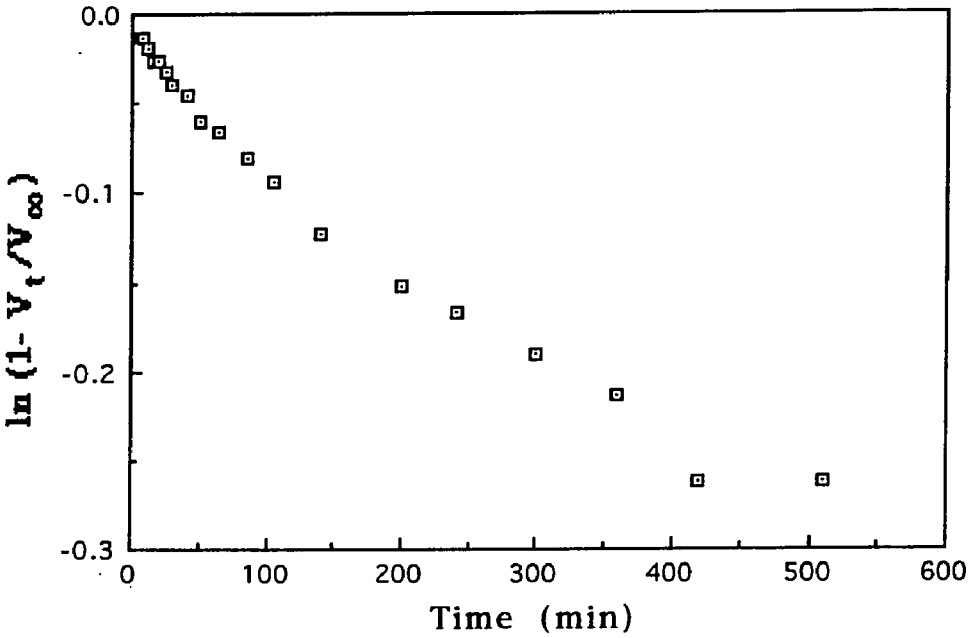

Figure A7-2. Hydrazine Monohydrate Reduction of Nitro HMI with Beulah Zap

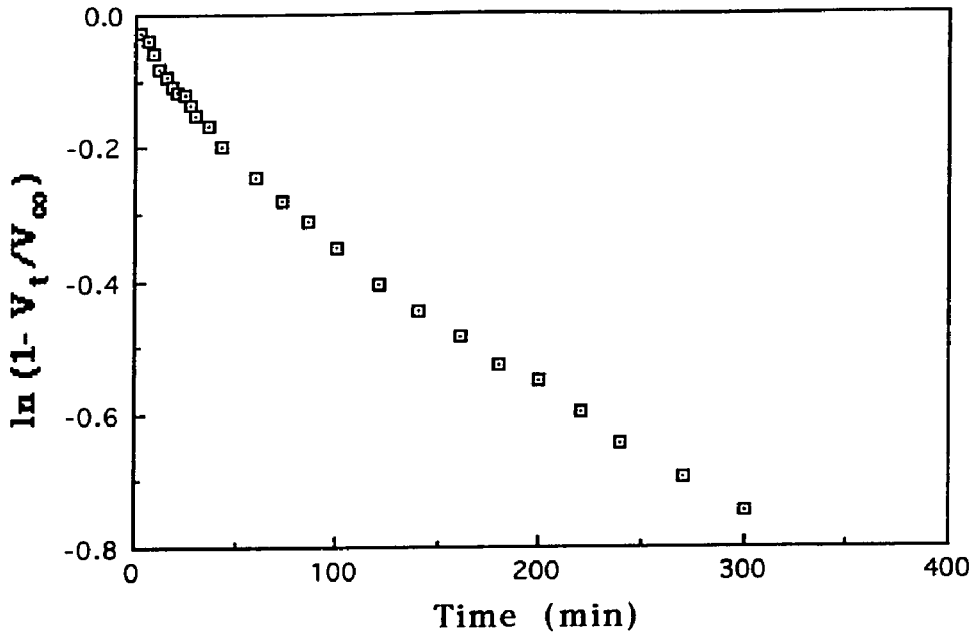

Figure A7-3. Hydrazine Monohydrate Reduction of Nitro HMI with Black Pearls 2000

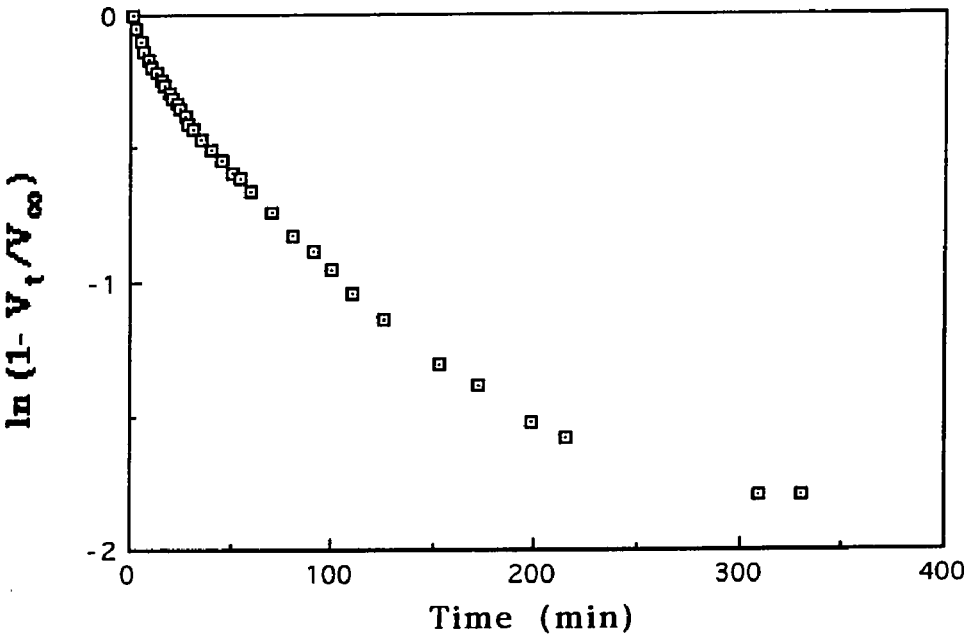

Figure A7-4. Hydrazine Monohydrate Reduction of Nitro HMI with Coconut Charcoal

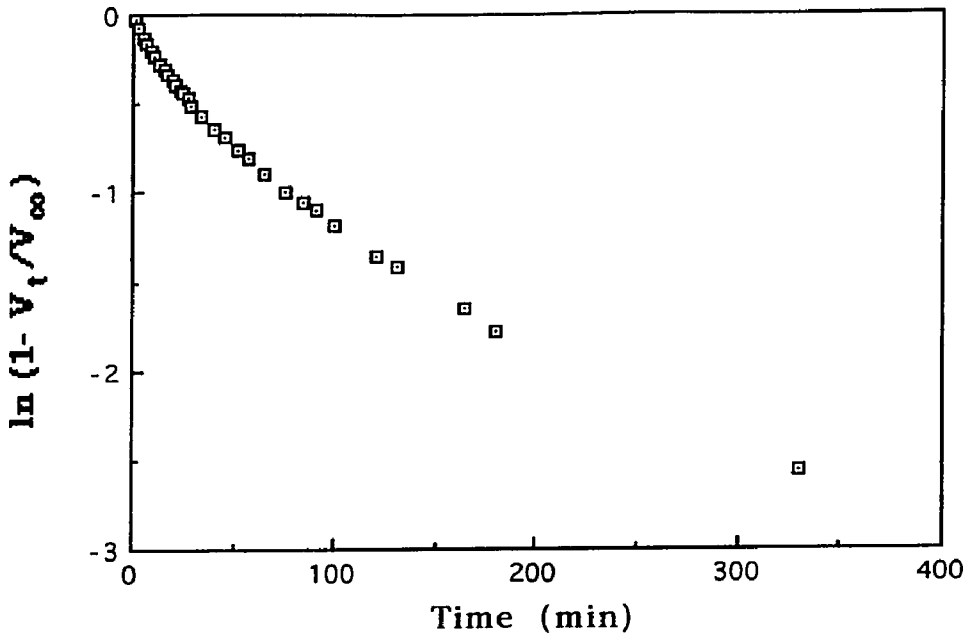

Figure A7-5. Hydrazine Monohydrate Reduction of Nitro HMI with Darco

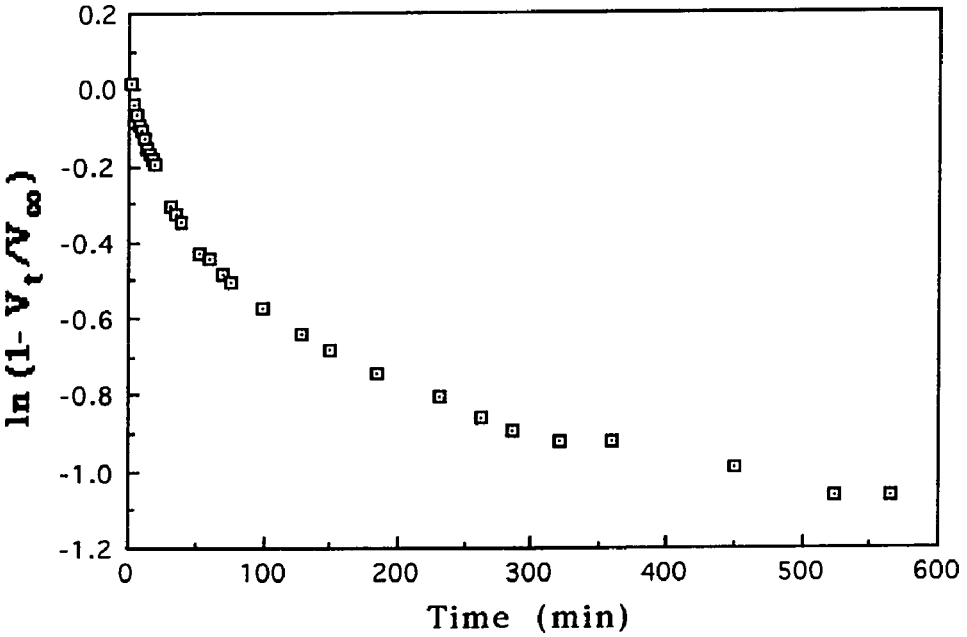

Figure A7-6. Hydrazine Monohydrate Reduction of Nitro HMI with Graphite

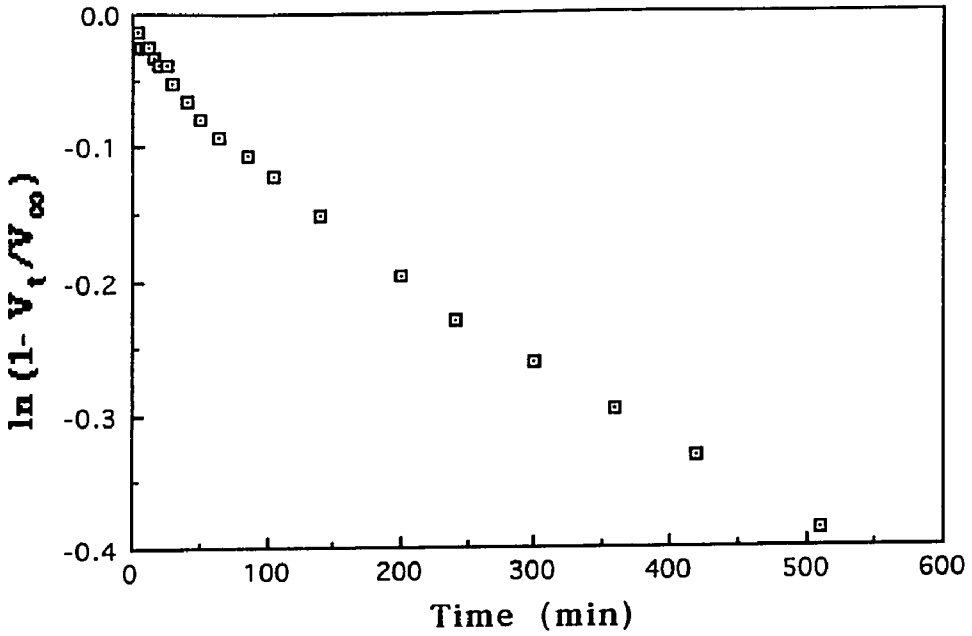

Figure A7-7. Hydrazine Monohydrate Reduction of Nitro HMI with Illinois #6

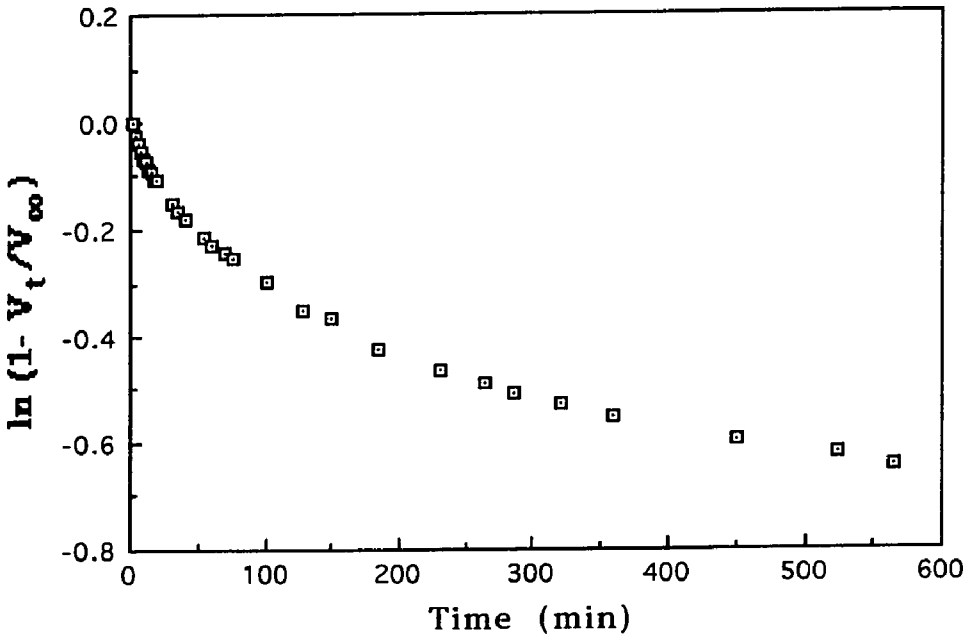

Figure A7-8. Hydrazine Monohydrate Reduction of Nitro HMI with Kingsford HMI

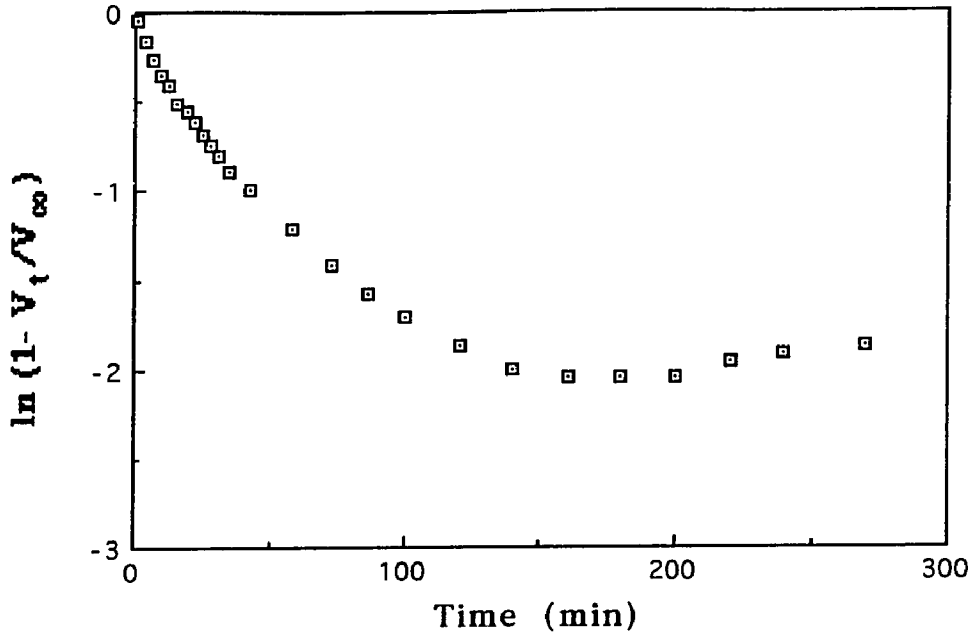

Figure A7-9. Hydrazine Monohydrate Reduction of Nitro HMI with Monarch 1300

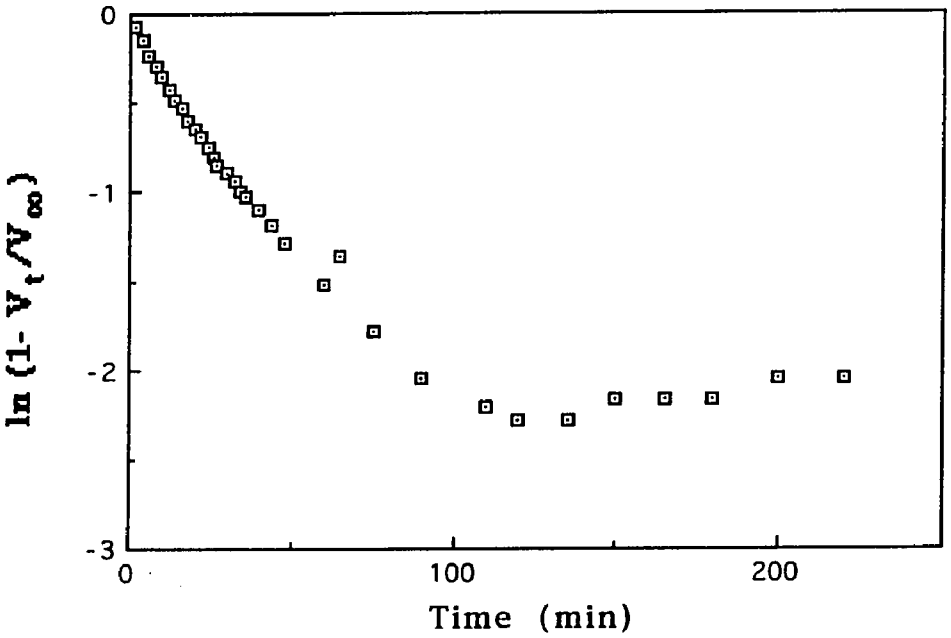

Figure A7-10. Hydrazine Monohydrate Reduction of Nitro HMI with Monarch 1000

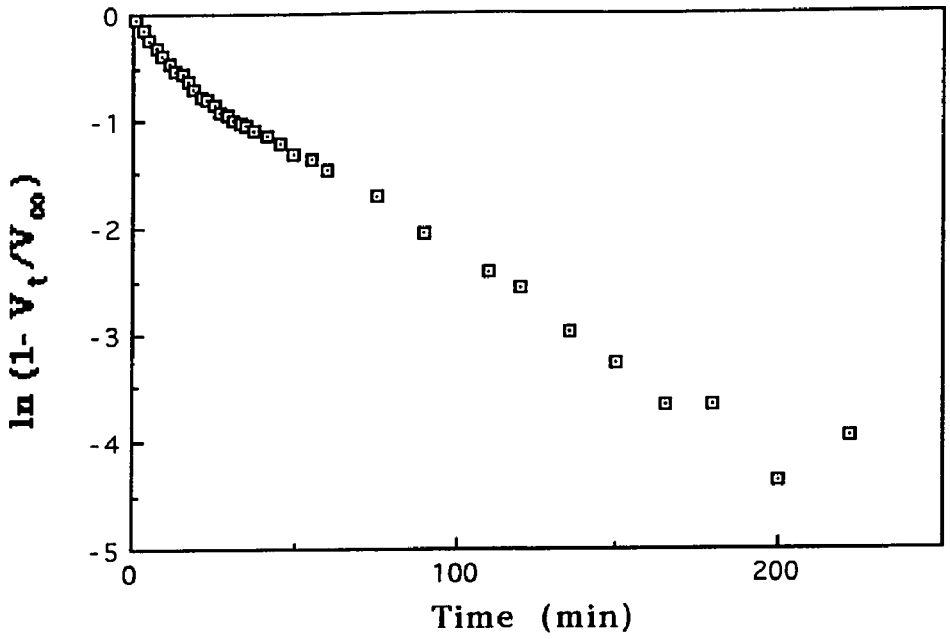

Figure A7-11. Hydrazine Monohydrate Reduction of Nitro HMI with Mogul L

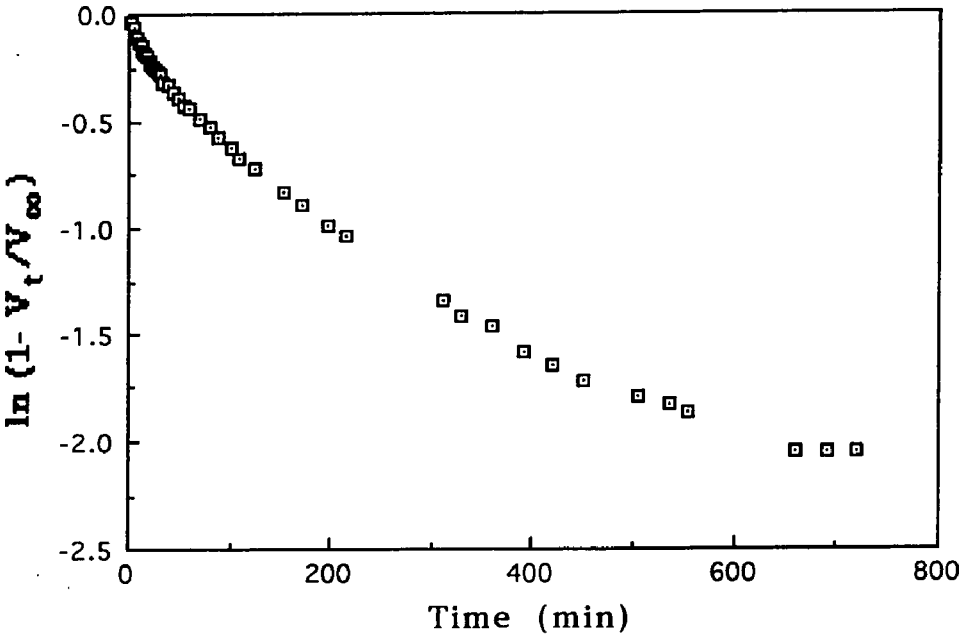

Figure A7-12. Hydrazine Monohydrate Reduction of Nitro HMI with Norit

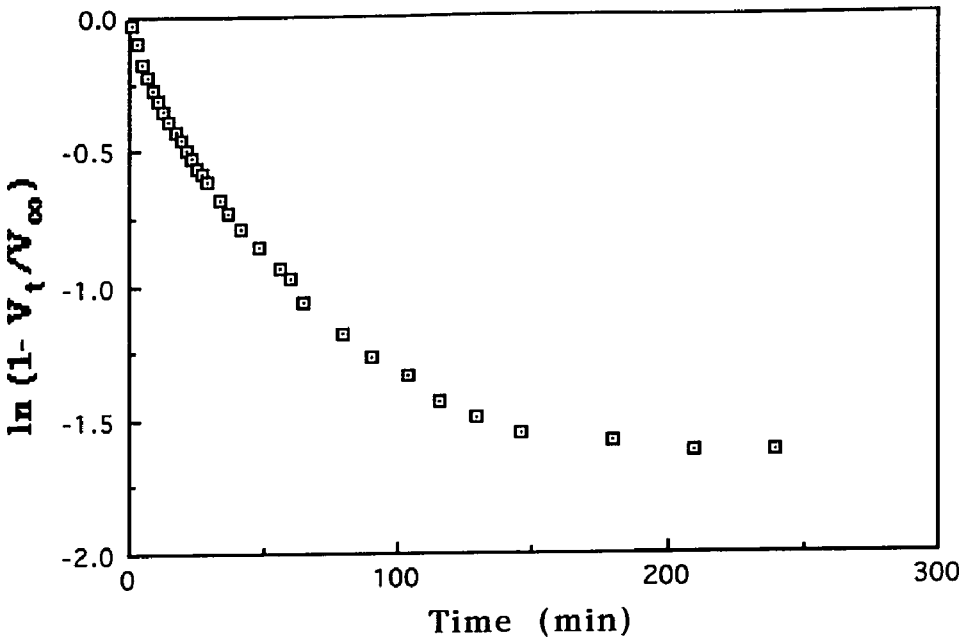

Figure A7-13. Hydrazine Monohydrate Reduction of Nitro HMI with Nuchar SA

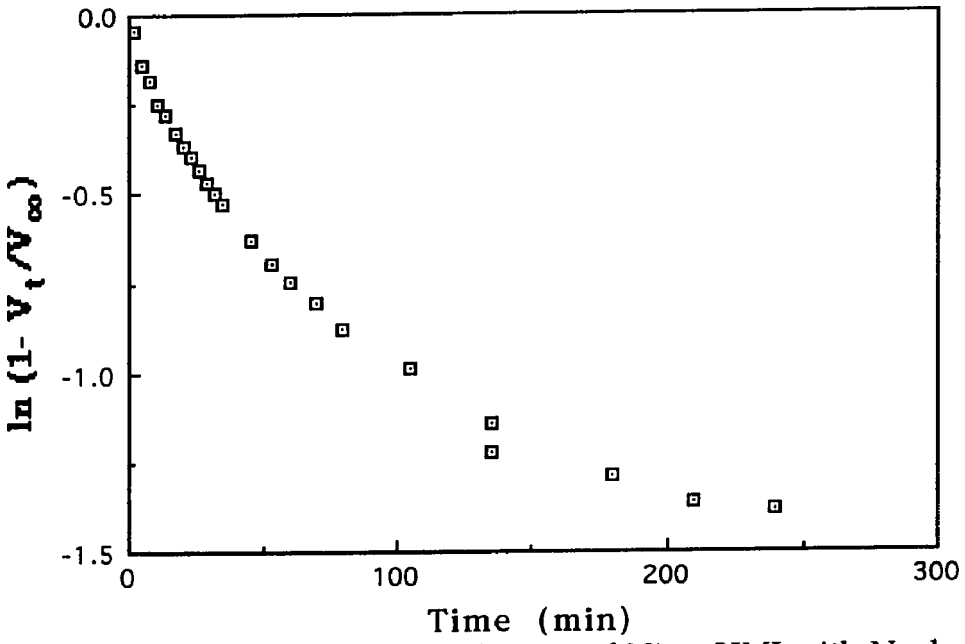

Figure A7-14. Hydrazine Monohydrate Reduction of Nitro HMI with Nuchar SA-20

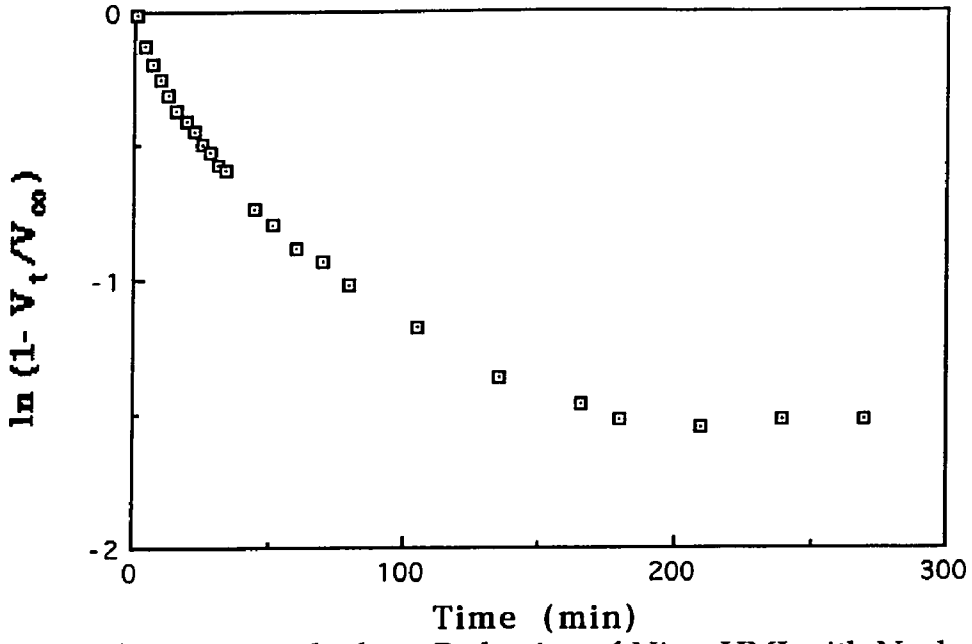

Figure A7-15. Hydrazine Monohydrate Reduction of Nitro HMI with Nuchar SN-20

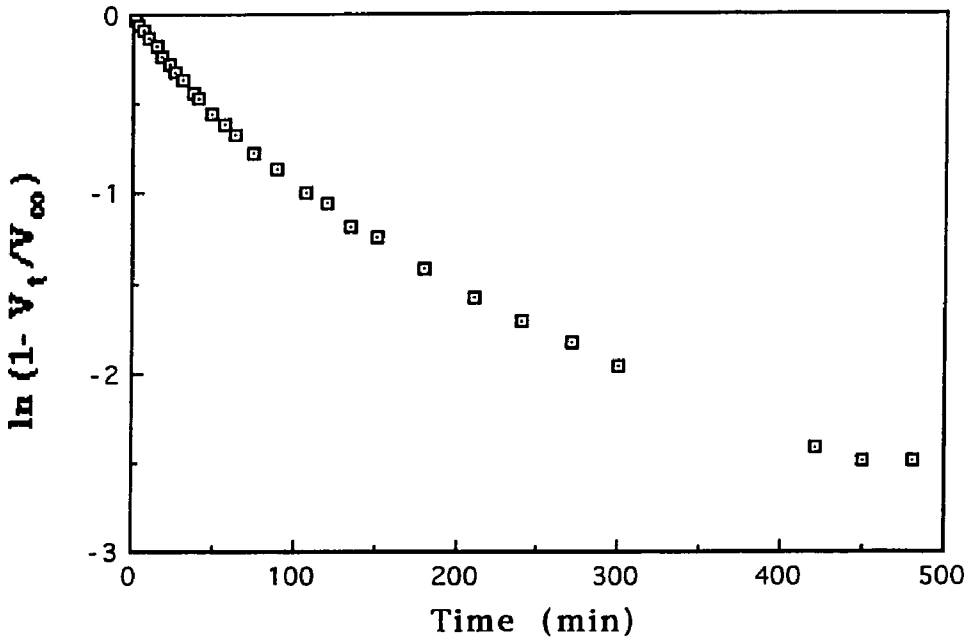

Figure A7-16. Hydrazine Monohydrate Reduction of Nitro HMI with Regal 400R

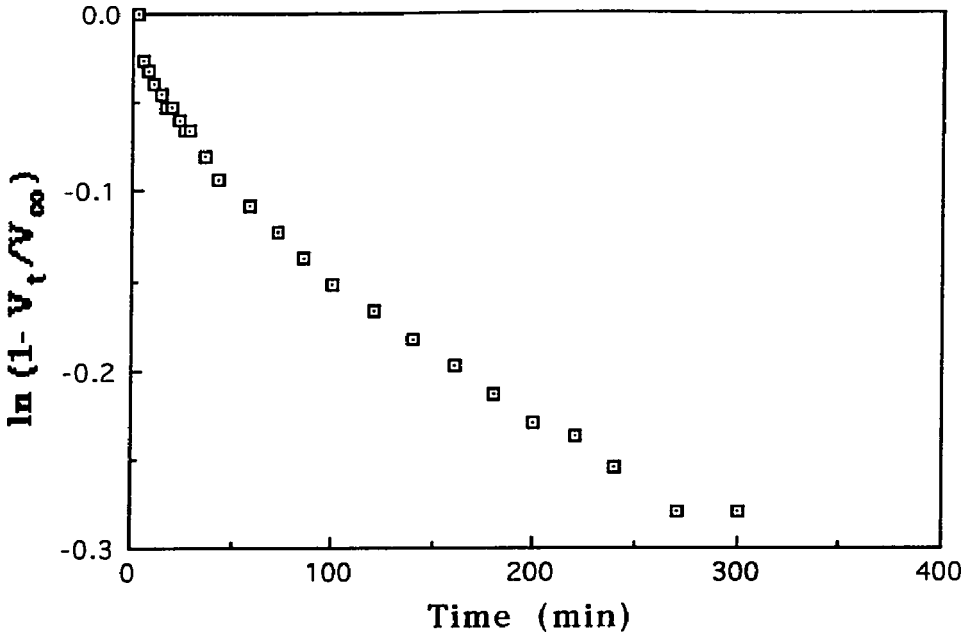

Figure A7-17. Hydrazine Monohydrate Reduction of Nitro HMI with Vulcan XC-72R

Appendix 8. Hydrazine Monohydrate Reduction of Nitro HMI with Oxidized Carbons (Table 16)

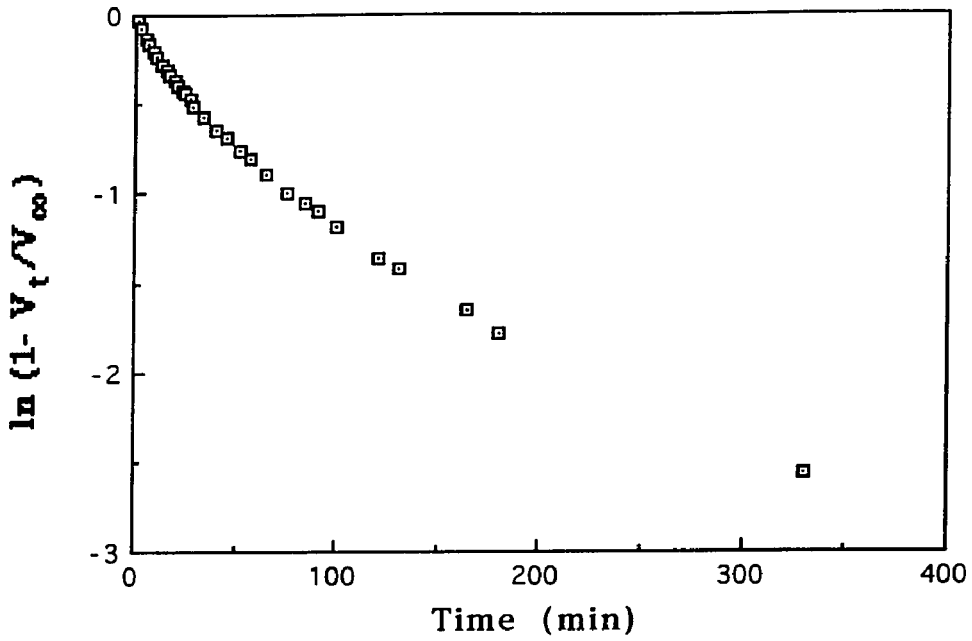

Figure A8-1. Untreated Nuchar SA

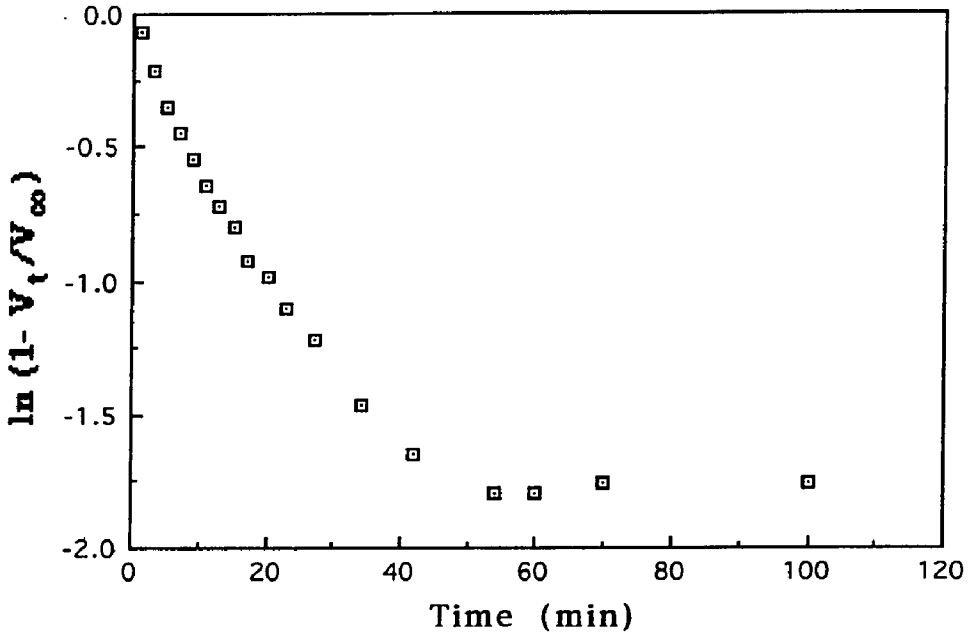

Figure A8-2. Nuchar SA Contact Oxidation

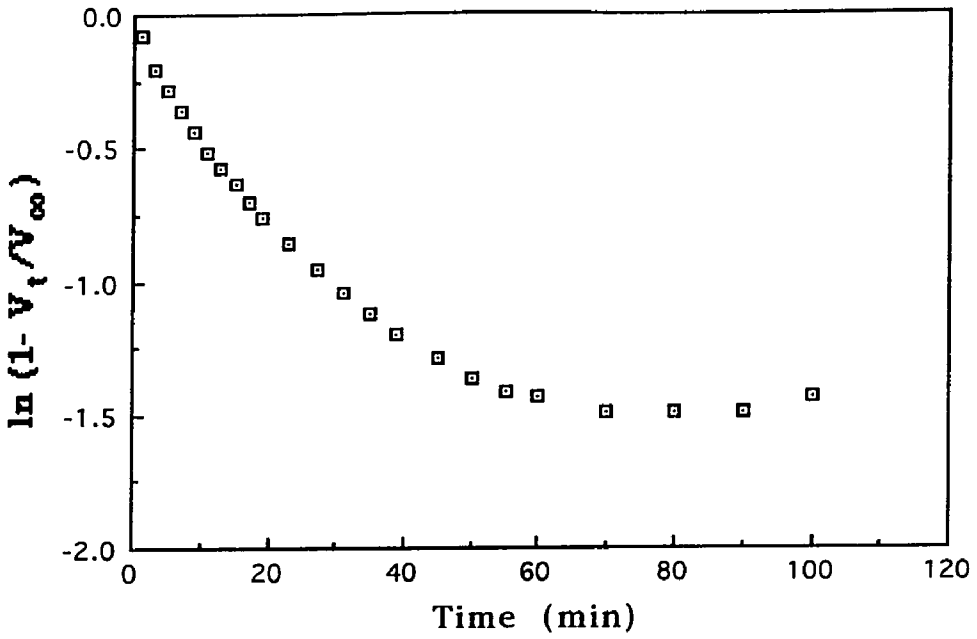

Figure A8-3. Nuchar SA oxidized 1 hr

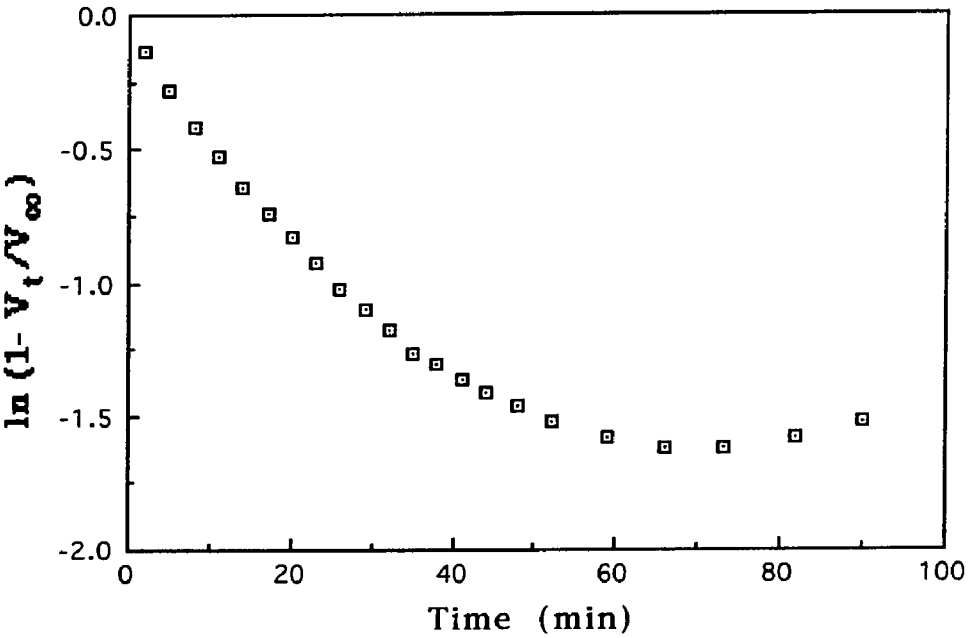

Figure A8-4. Nuchar SA oxidized 16 hr

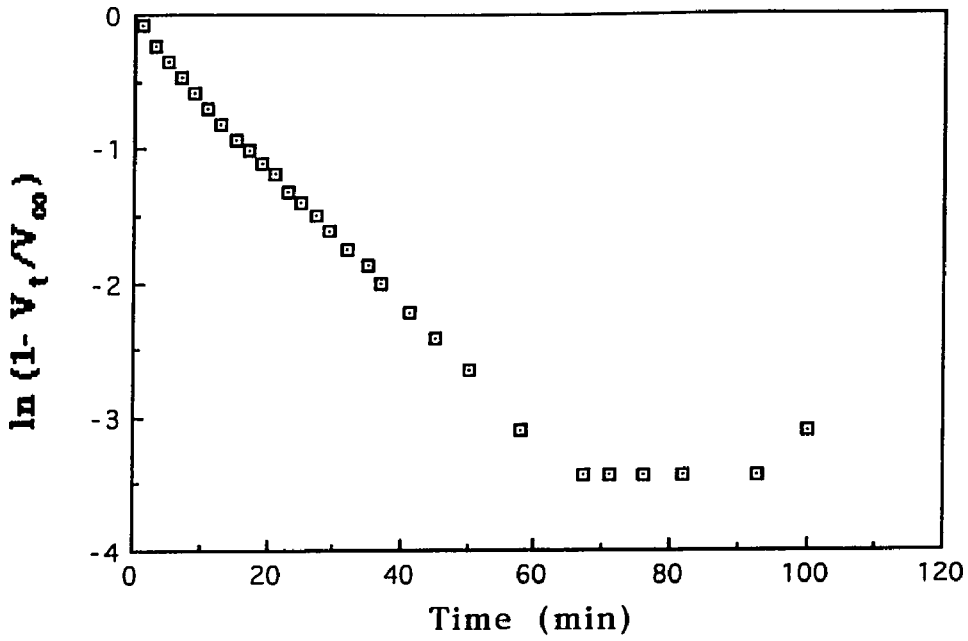

Figure A8-5. Untreated Aqua A

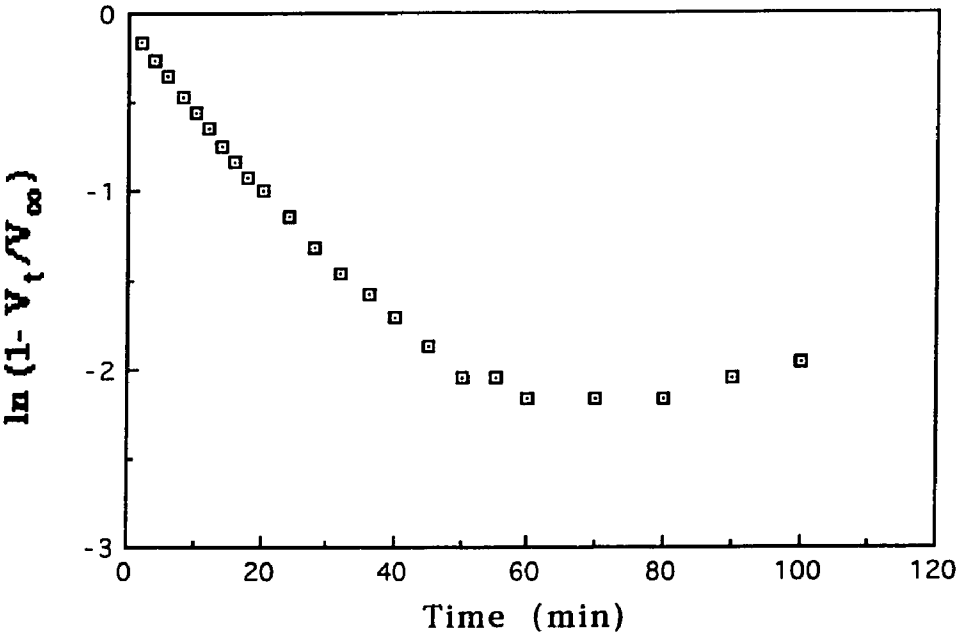

Figure A8-6. Aqua A Oxidized 1 hr

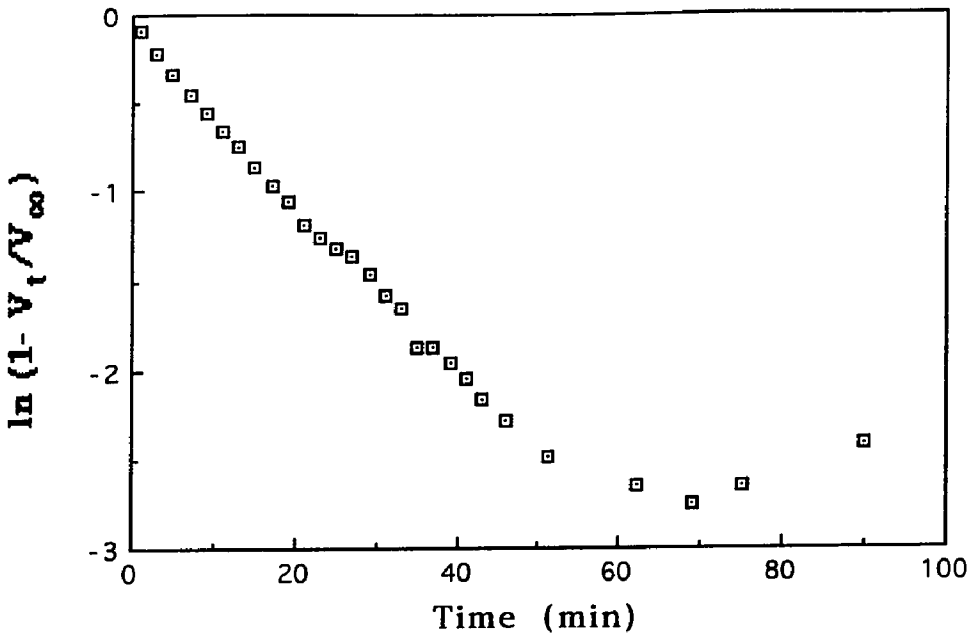

Figure A8-7. Aqua A 24 hr Oxidation

Appendix 9. Reduction of POP(1) with Various Carbons (Table 17)

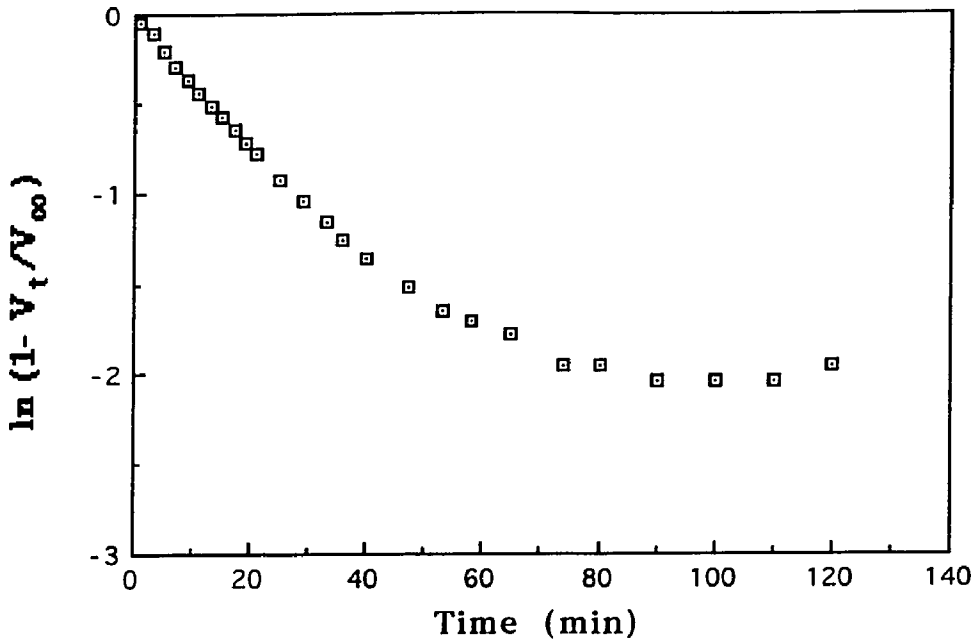

Figure A9-1. Hydrazine Monohydrate Reduction of POP(1) with Aqua A

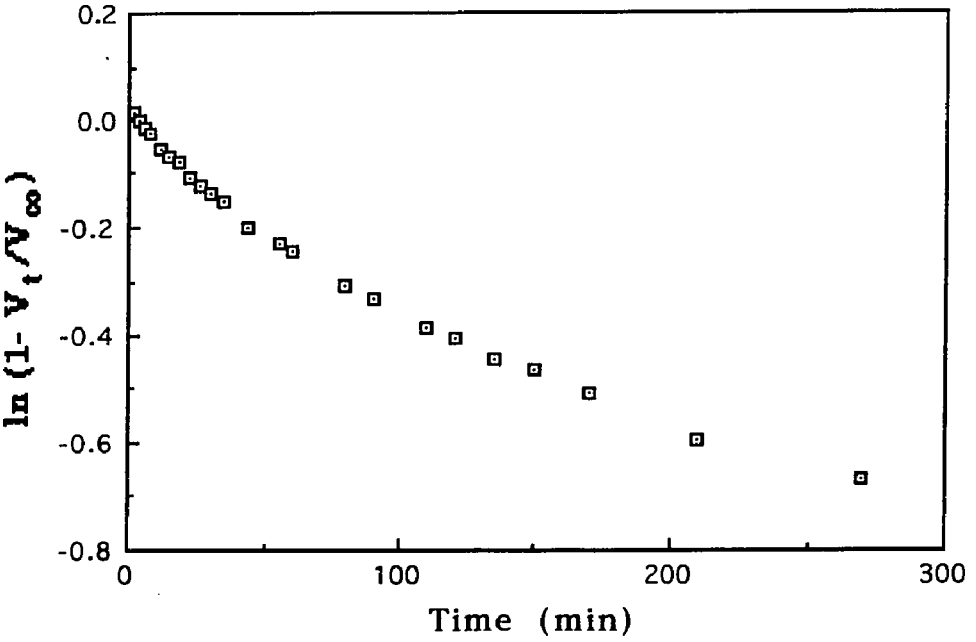

Figure A9-2. Hydrazine Monohydrate Reduction of POP(1) with Graphite

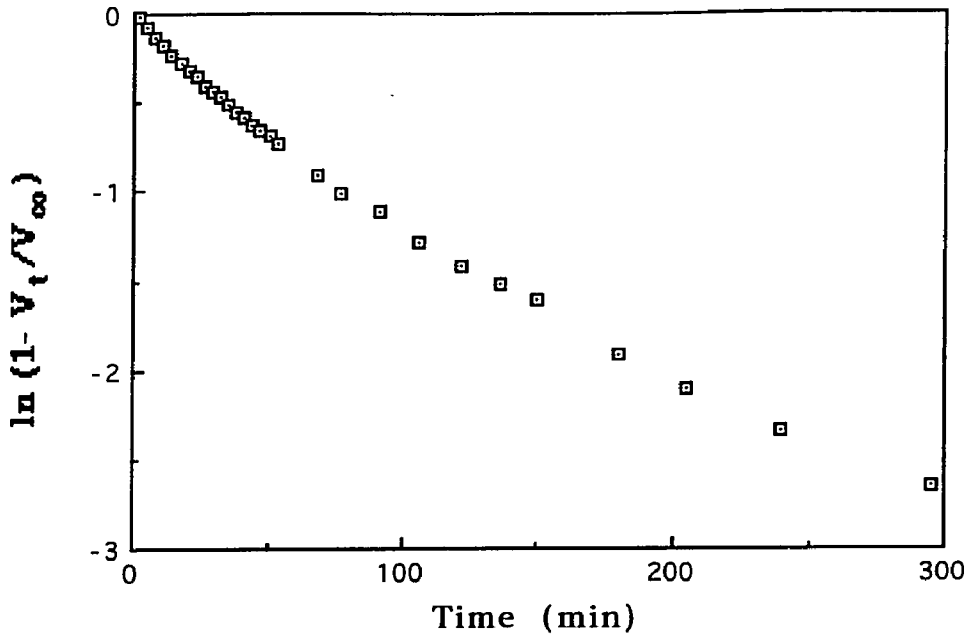

Figure A9-3. Hydrazine Monohydrate Reduction of POP(1) with Darco

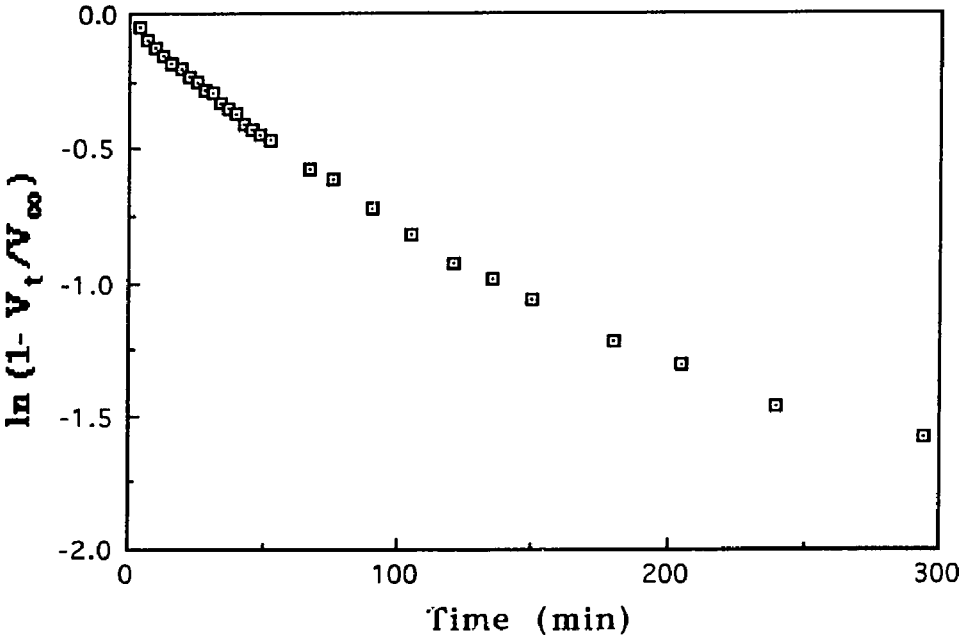

Figure A9-4. Hydrazine Monohydrate Reduction of POP(1) with Coconut Charcoal

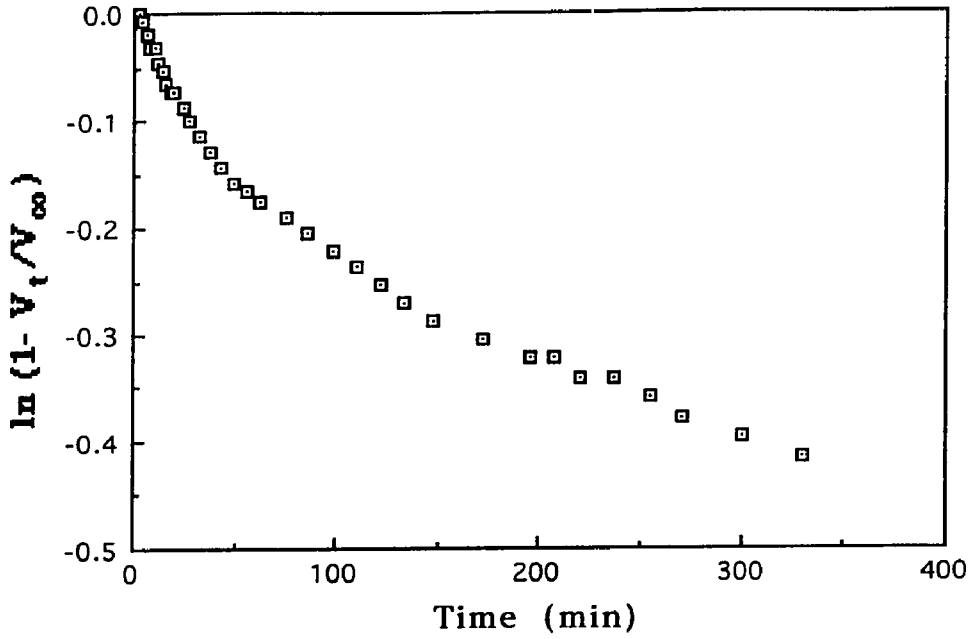

Figure A9-5. Hydrazine Monohydrate Reduction of POP(1) with Kingsford Charcoal

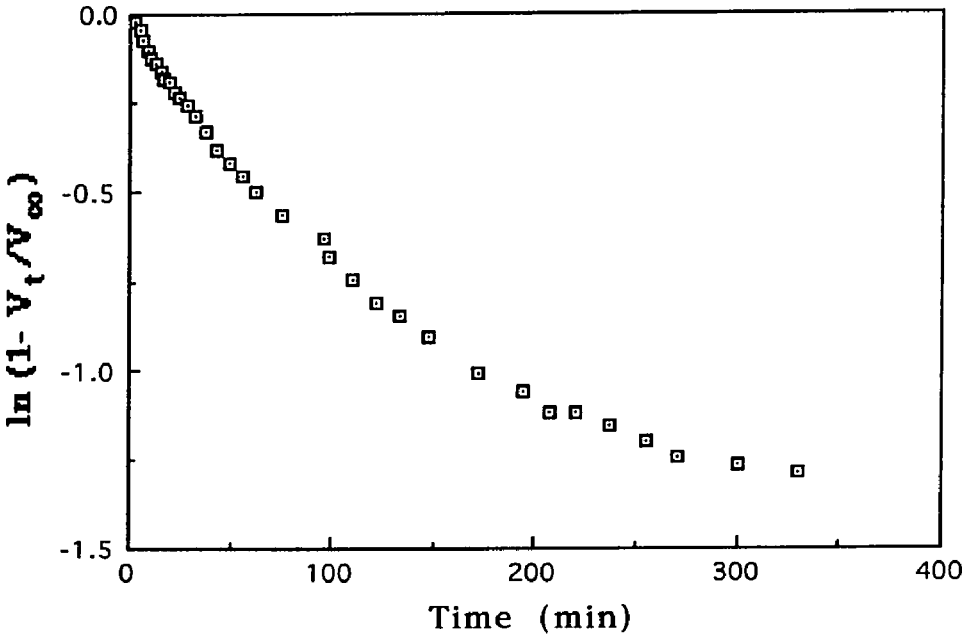

Figure A9-6. Hydrazine Monohydrate Reduction of POP(1) with Norit

Appendix 10. Hydrazine Monohydrate Reduction of Nitro HMI with Darco and Various Metal (Table 18)

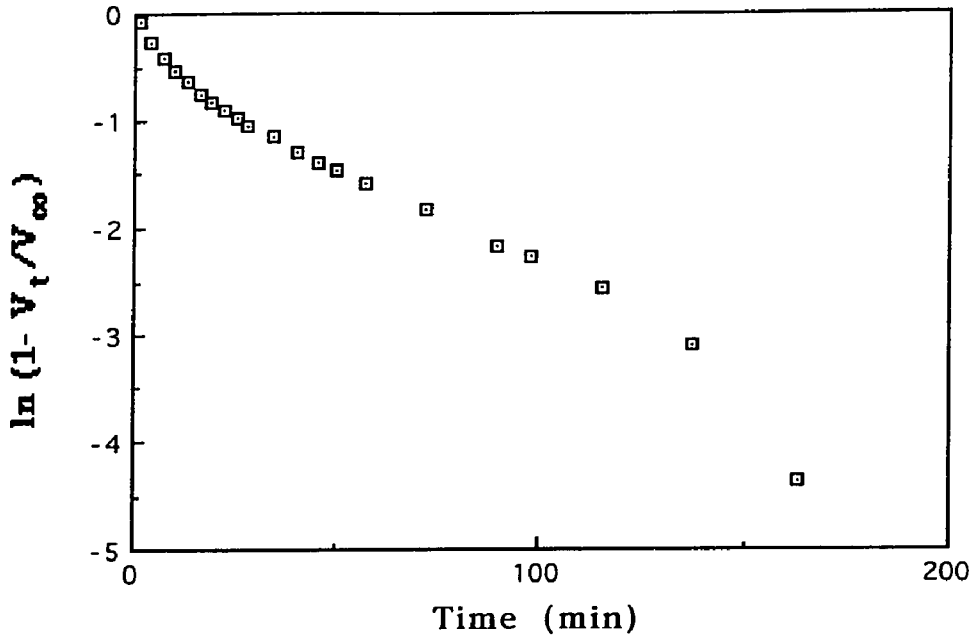

Figure A10-1. Hydrazine Monohydrate of Nitro HMI with Darco and $FeCl_3$

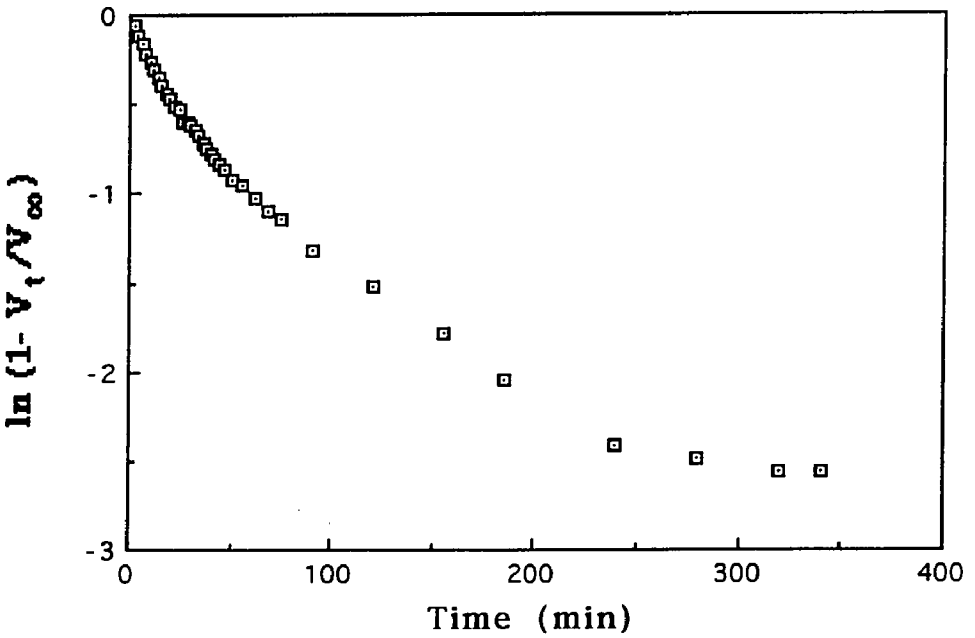

Figure A10-2. Hydrazine Monohydrate of Nitro HMI with Darco and $CrCl_3$

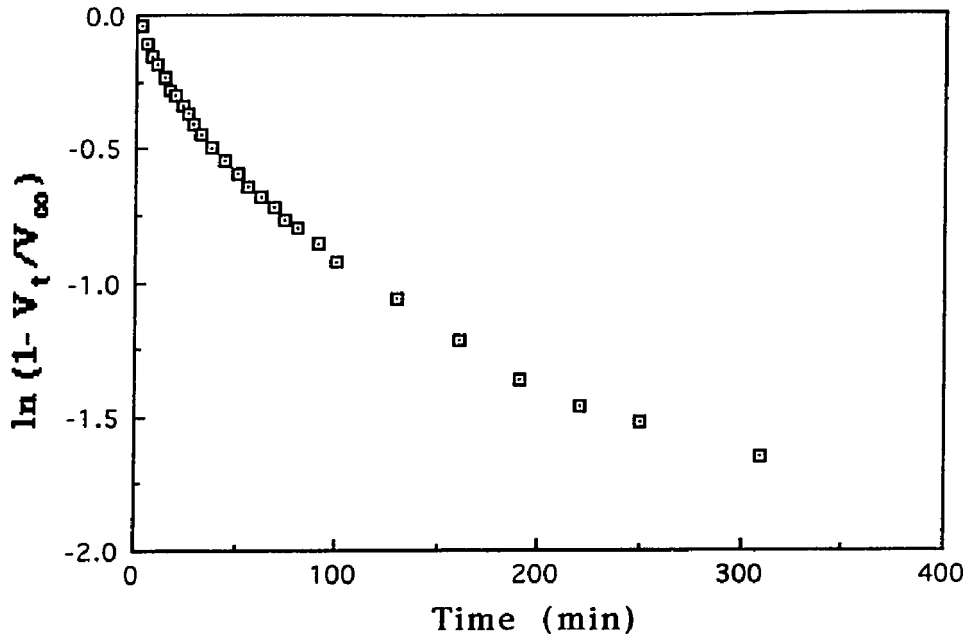

Figure A10-3. Hydrazine Monohydrate of Nitro HMI with Darco and $MnCl_2$

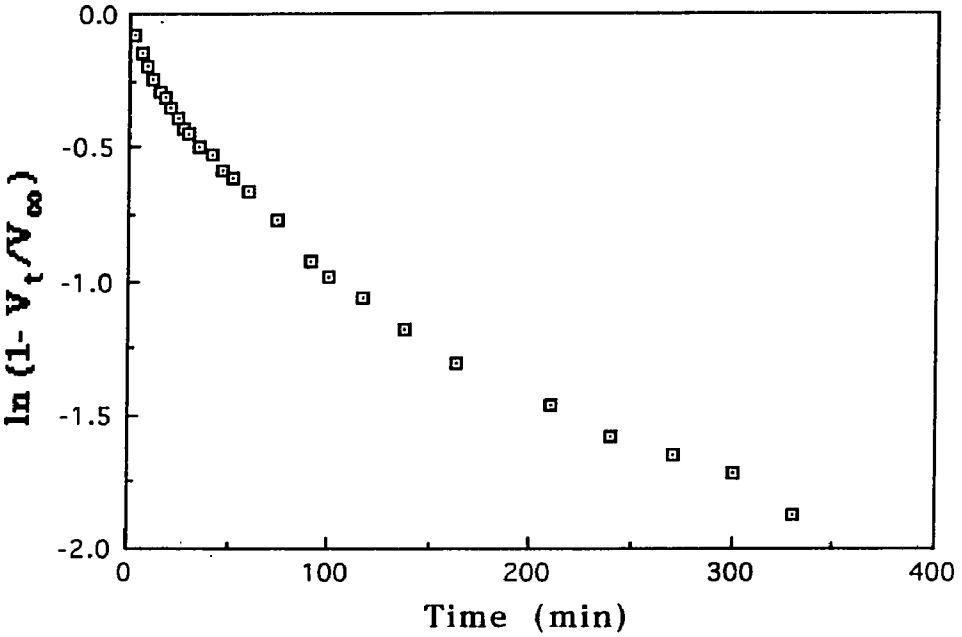

Figure A10-4. Hydrazine Monohydrate of Nitro HMI with Darco and $SnCl_4$

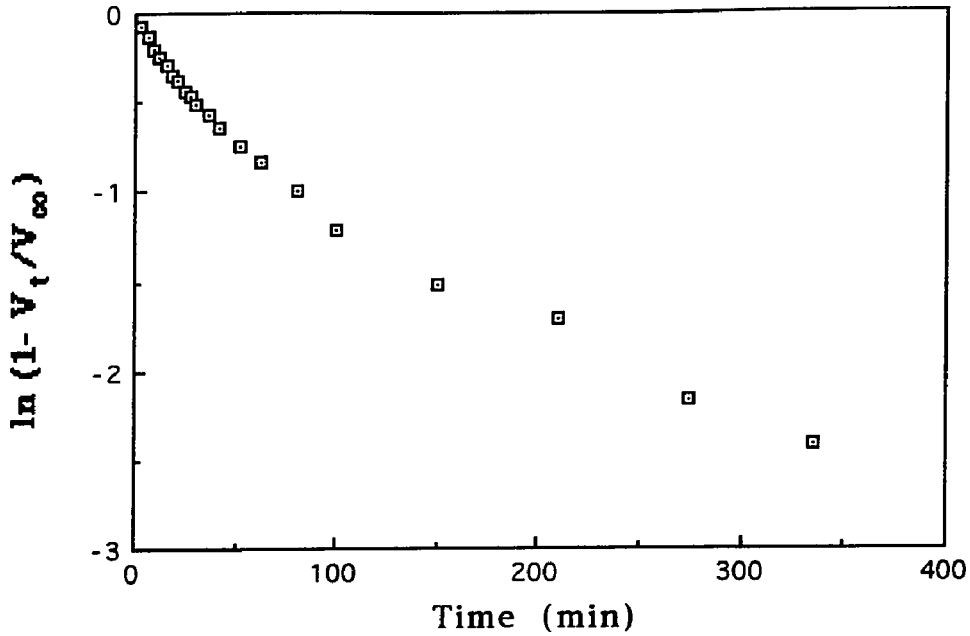

Figure A10-5. Hydrazine Monohydrate of Nitro HMI with Darco and $TiCl_4$

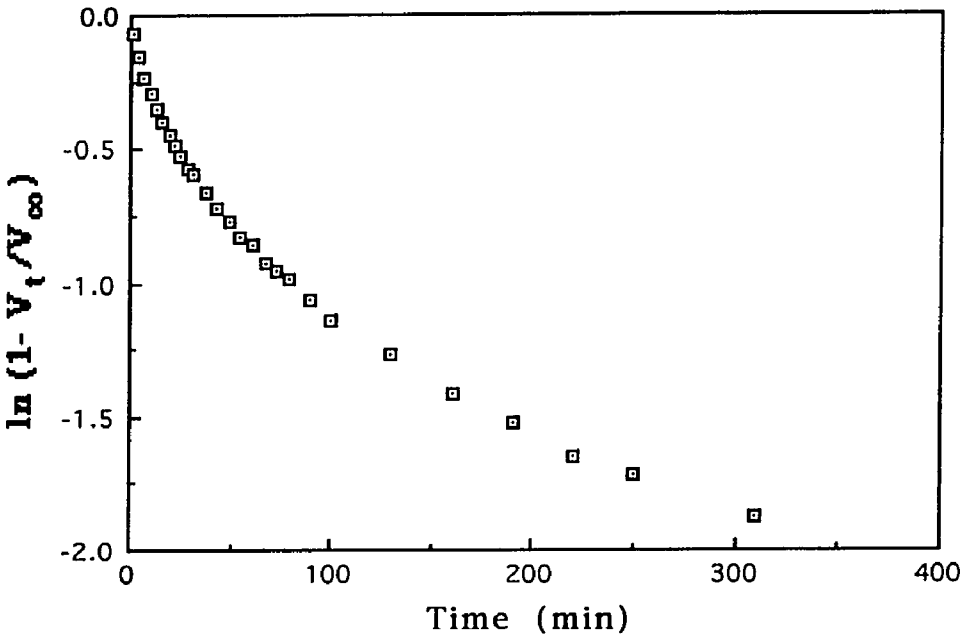

Figure A10-6. Hydrazine Monohydrate of Nitro HMI with Darco and $CoCl_2$

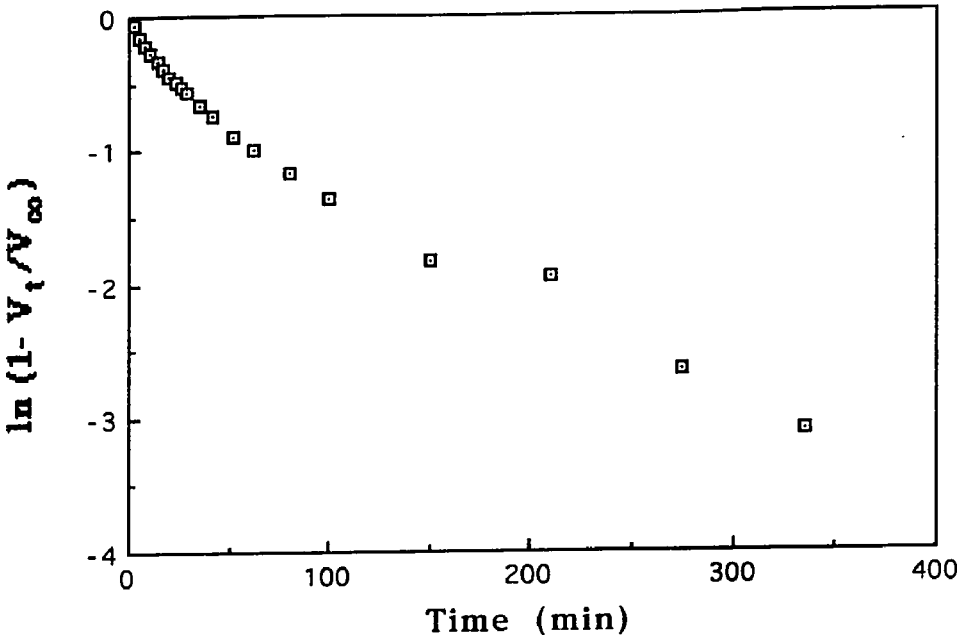

Figure A10-7. Hydrazine Monohydrate of Nitro HMI with Darco and $CuCl_2$

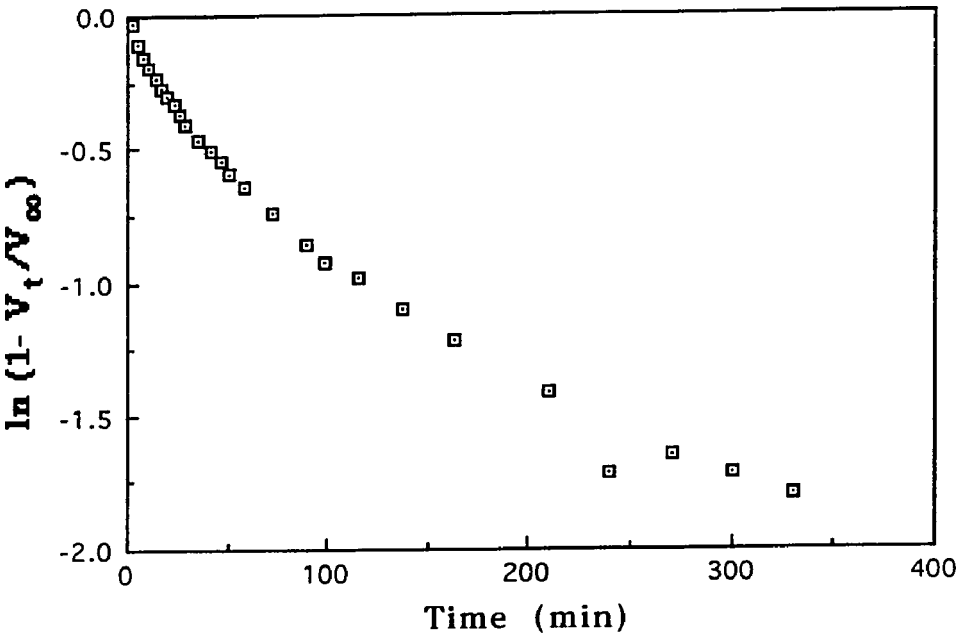

Figure A10-8. Hydrazine Monohydrate of Nitro HMI with Darco and $ZnCl_2$

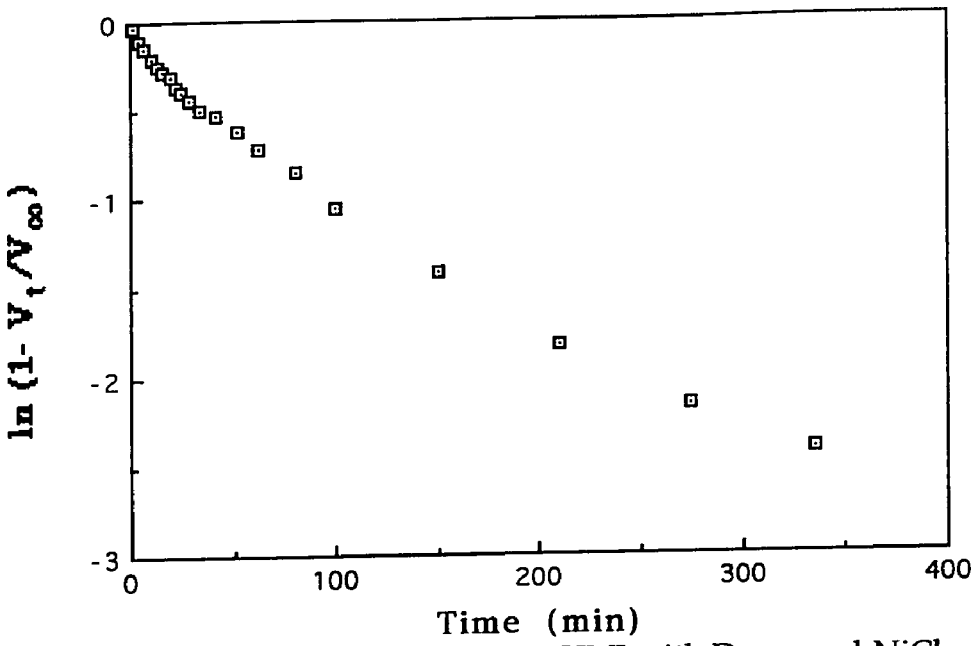

Figure A10-9. Hydrazine Monohydrate of Nitro HMI with Darco and $NiCl_2$

Appendix 11. Hydrazine Monohydrate Reduction of Nitro HMI With Various Amounts of Aqua A and $FeCl_3$ (Table 19)

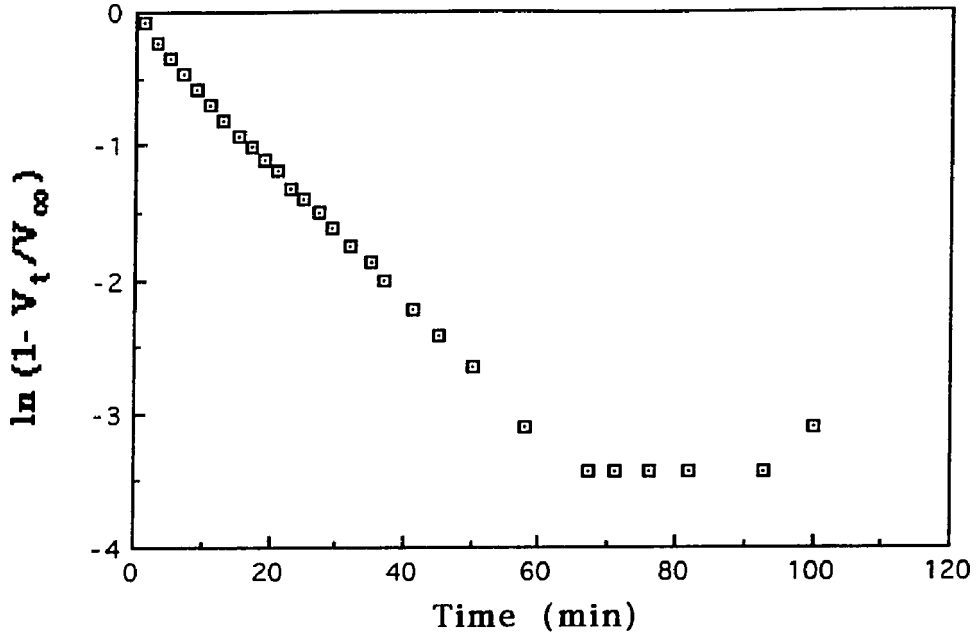

Figure A11-1. Hydrazine Monohydrate Reduction of Nitro HMI with Aqua A (0.739g)

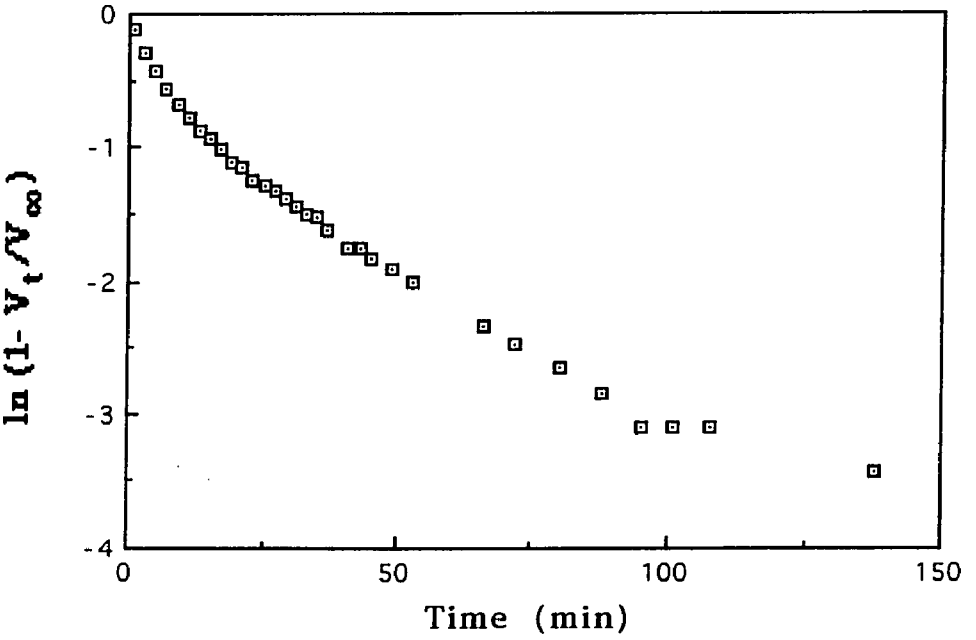

Figure A11-2. Hydrazine Monohydrate Reduction of Nitro HMI with Aqua A (0.351g) and $FeCl_3$ (0.019 g)

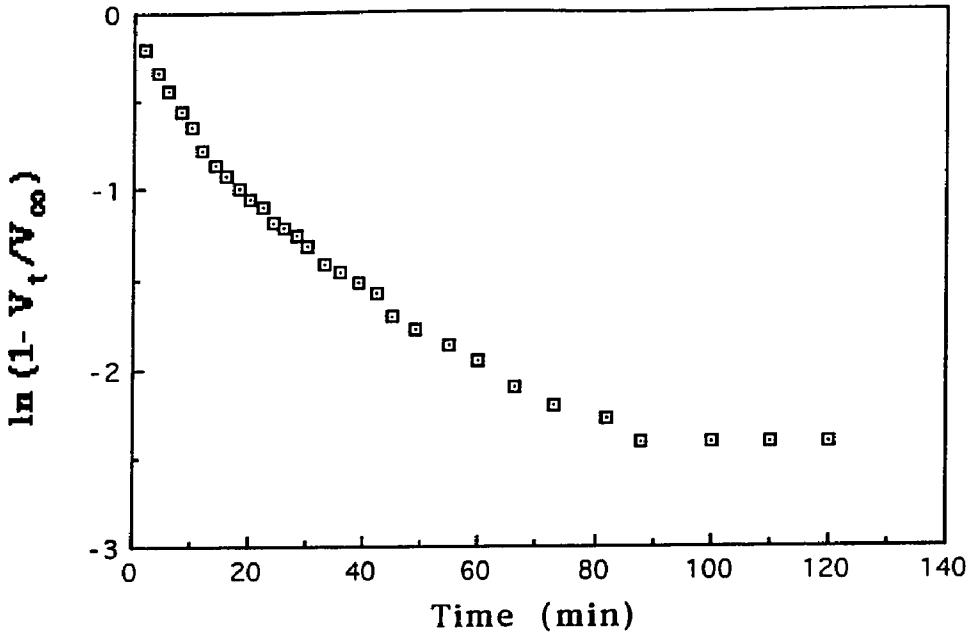

Figure A11-3. Hydrazine Monohydrate Reduction of Nitro HMI with Aqua A (0.380g) and $FeCl_3$ (0.109g)

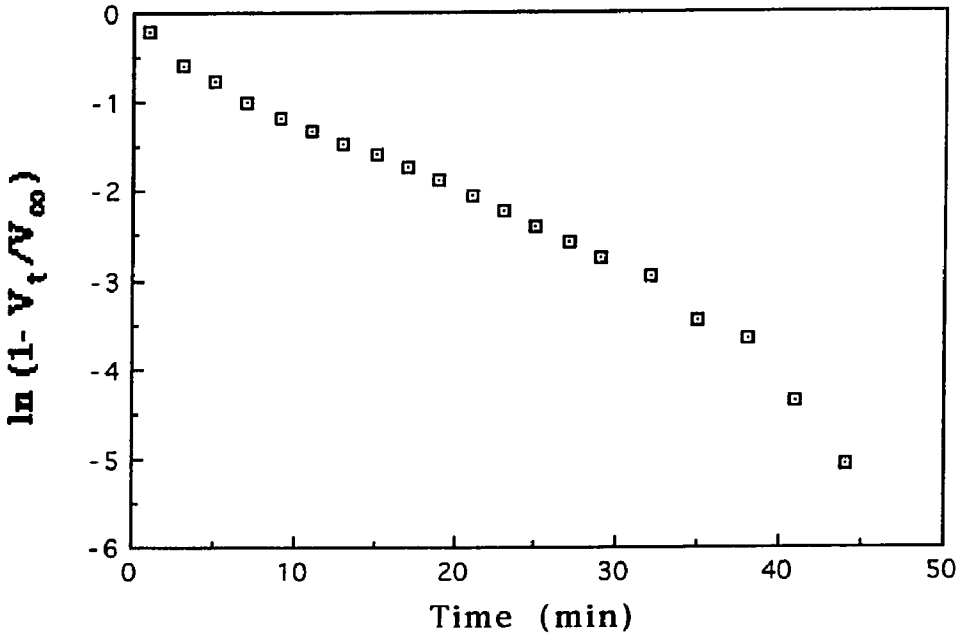

Figure A11-4. Hydrazine Monohydrate Reduction of Nitro HMI with Aqua A (0.721g) and $FeCl_3$ (0.018 g)

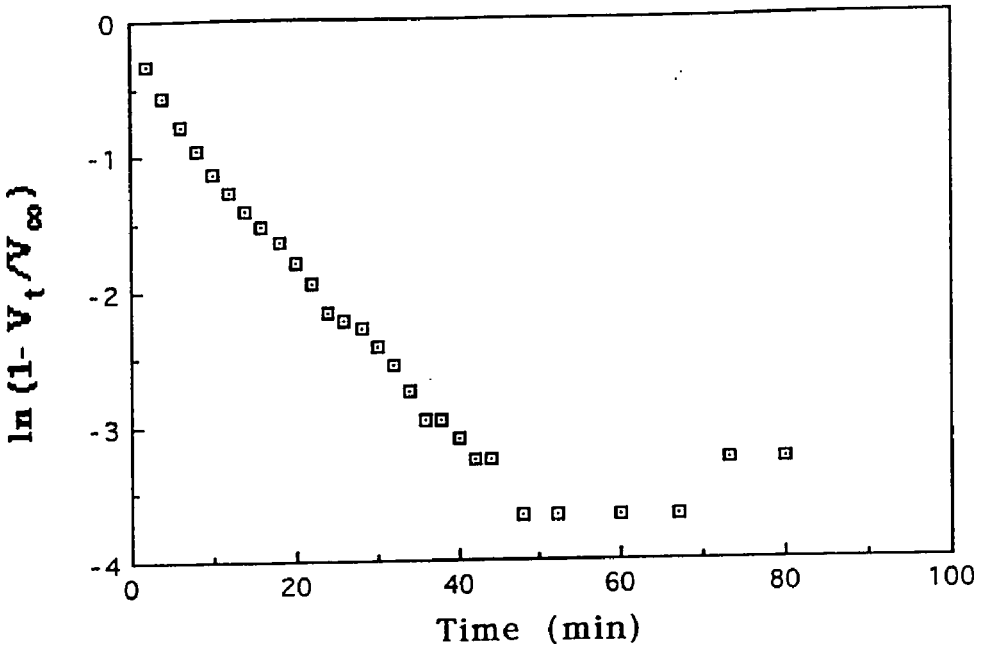

Figure A11-5. Hydrazine Monohydrate Reduction of Nitro HMI with Aqua A (0.69g) and $FeCl_3$ (0.053g)

Appendix 12. Reusability of Mogul L-$FeCl_3$ from the Hydrazine Hydrate Reduction of Nitro HMI (Table 20)

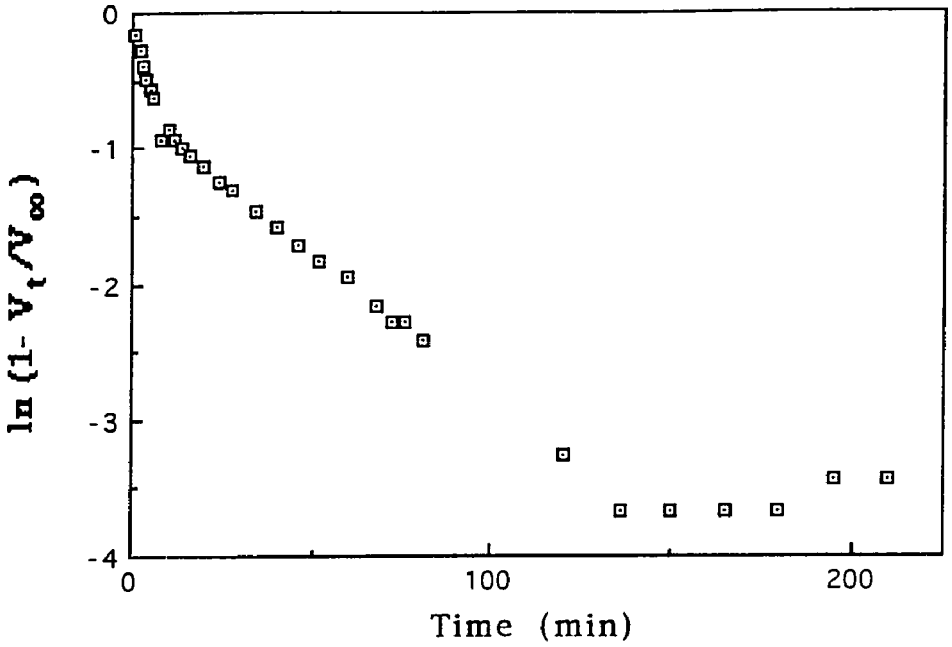

Figure A12-1. RUN #1

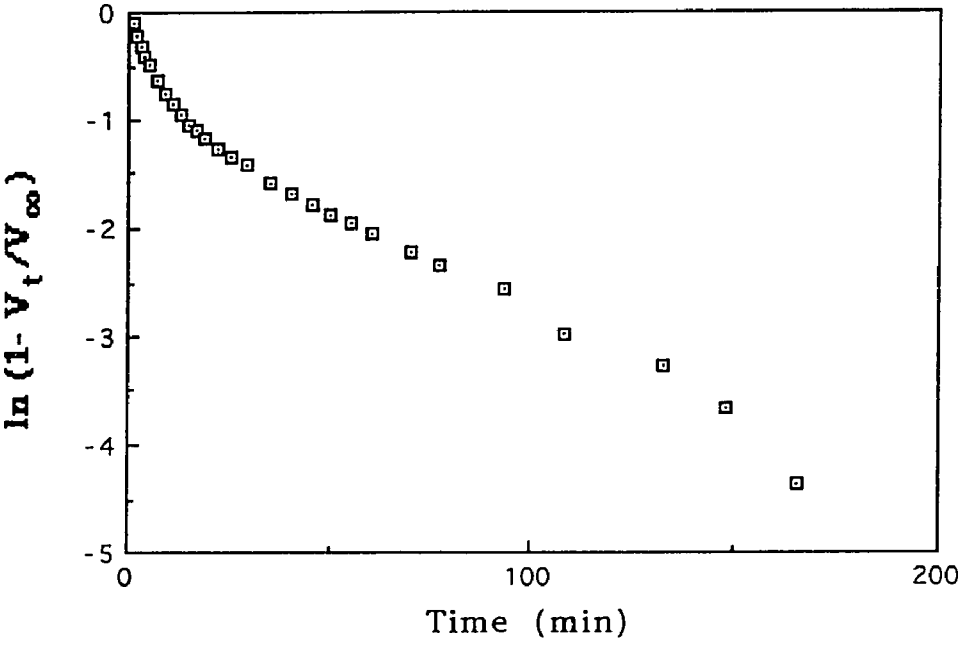

Figure A12-2. RUN #2

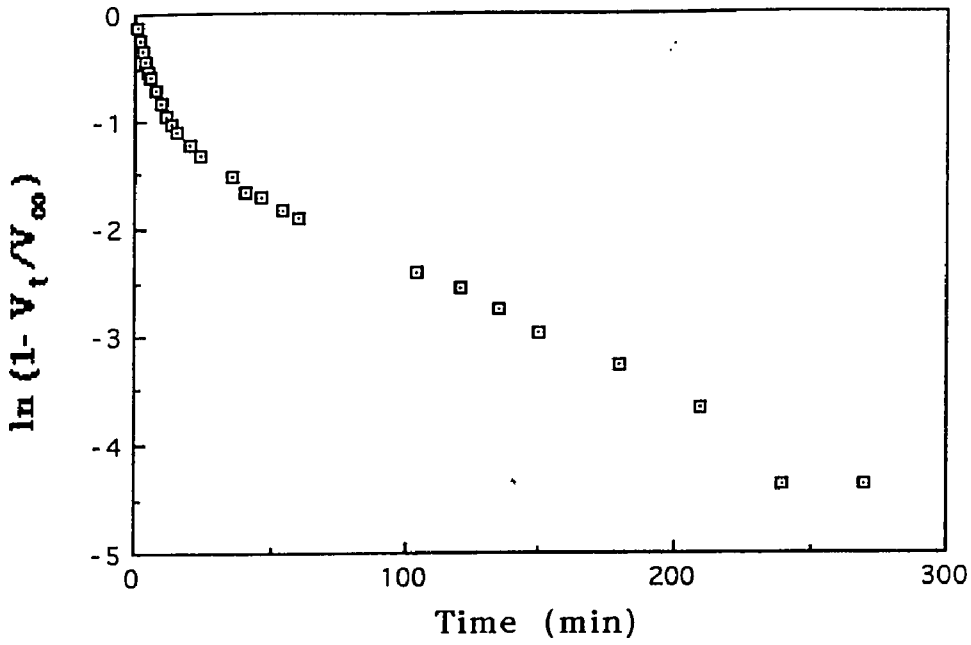

Figure A12-3. RUN #3

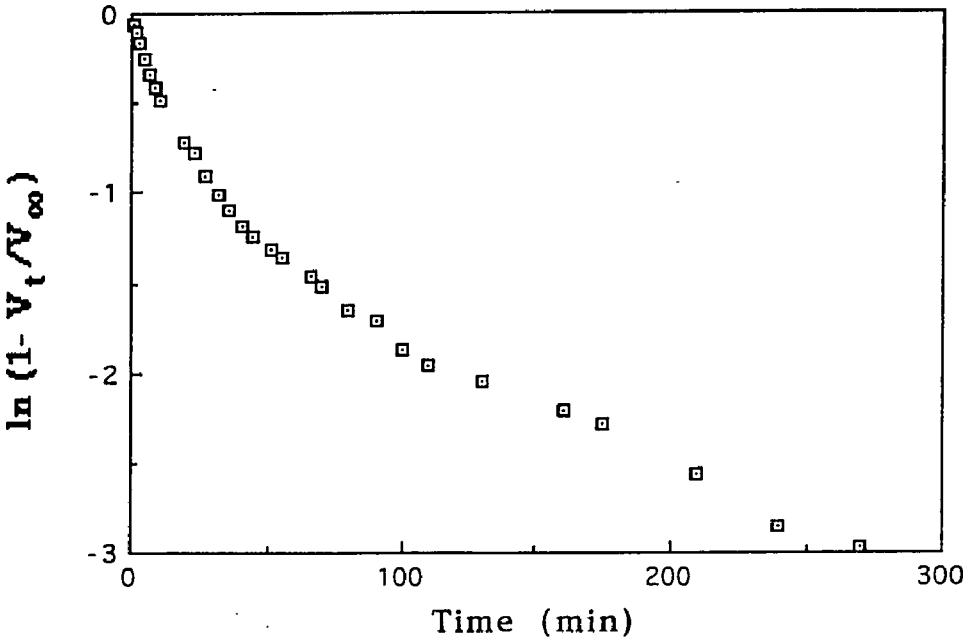

Figure A12-4. RUN #4

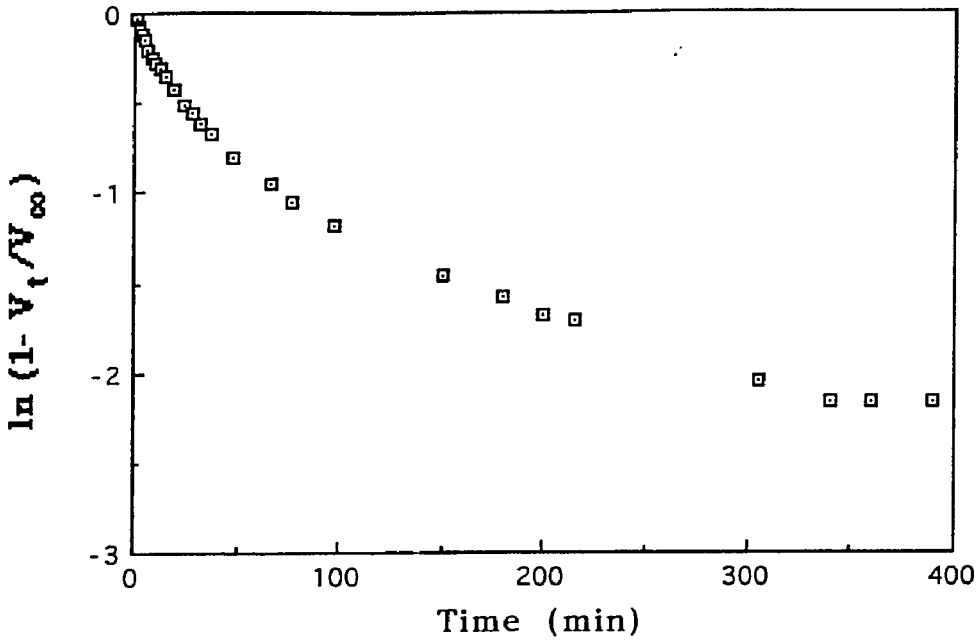

Figure A12-5. RUN #5

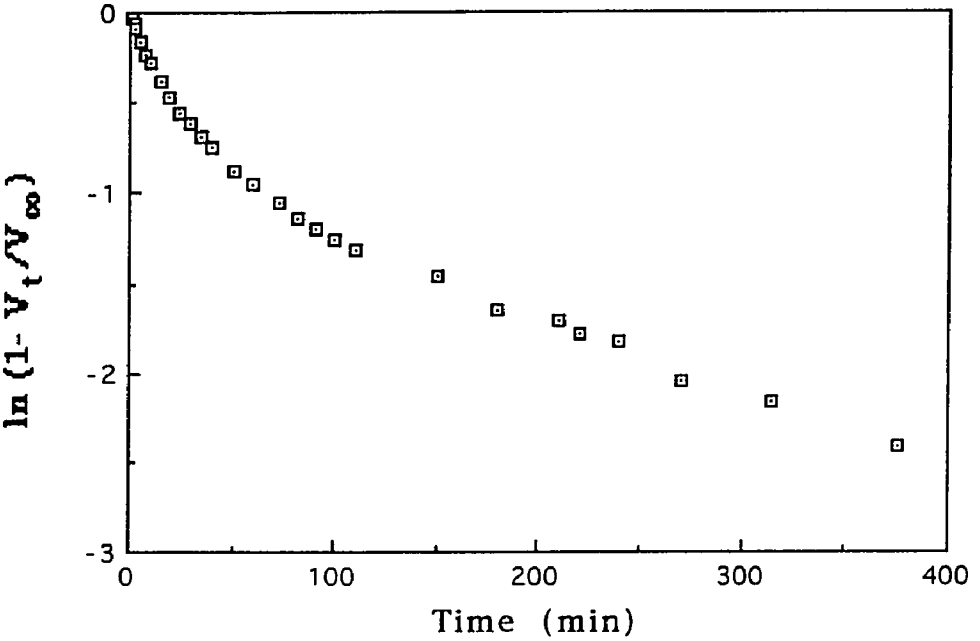

Figure A12-6. RUN #6

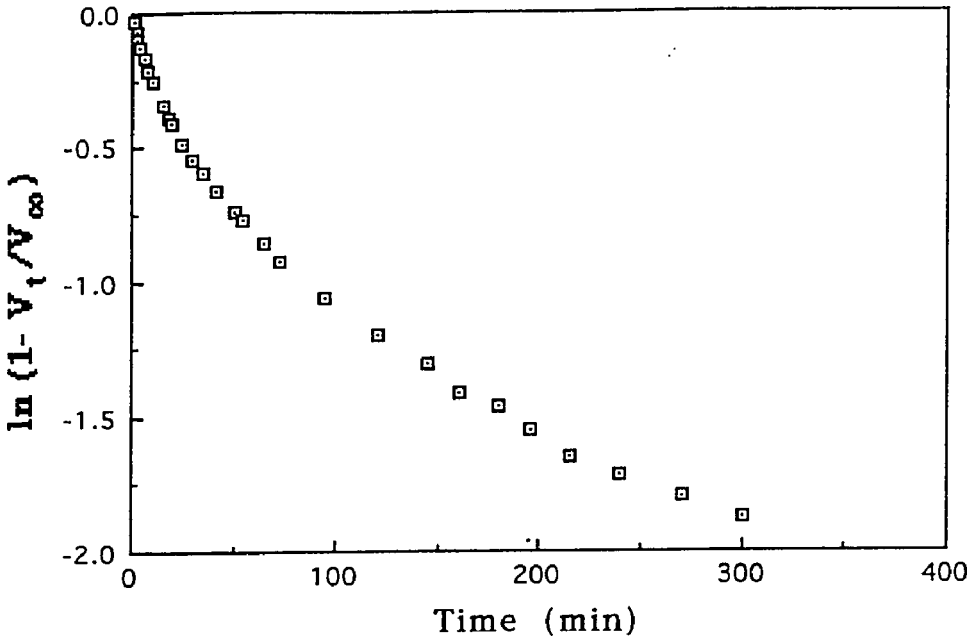

Figure A12-7. RUN #7

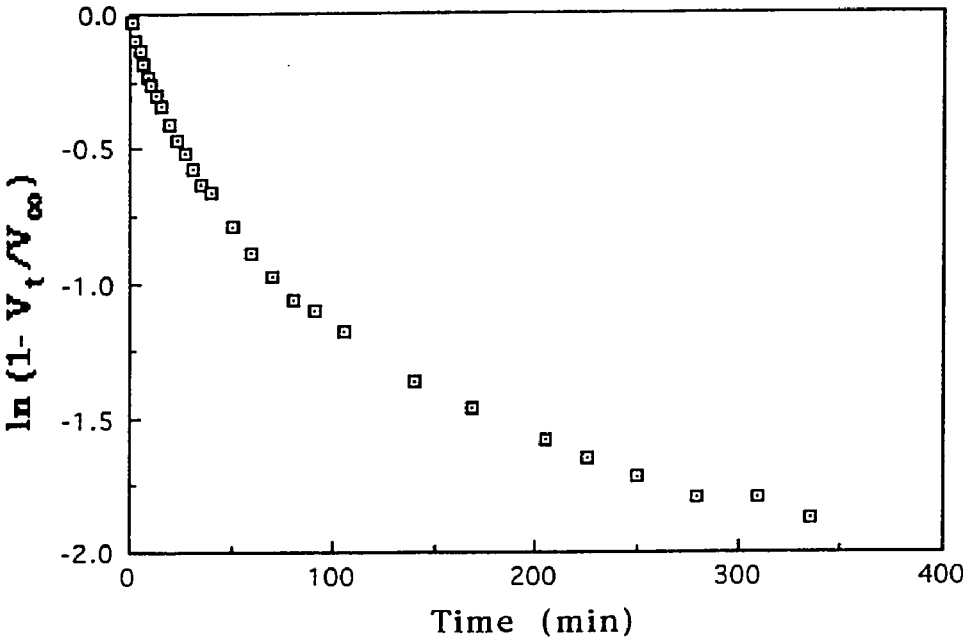

Figure A12-8. RUN #8

Appendix 13. Reusability of Black Pearls L-$FeCl_3$ from the Hydrazine Hydrate Reduction of Nitro HMI (Table 21)

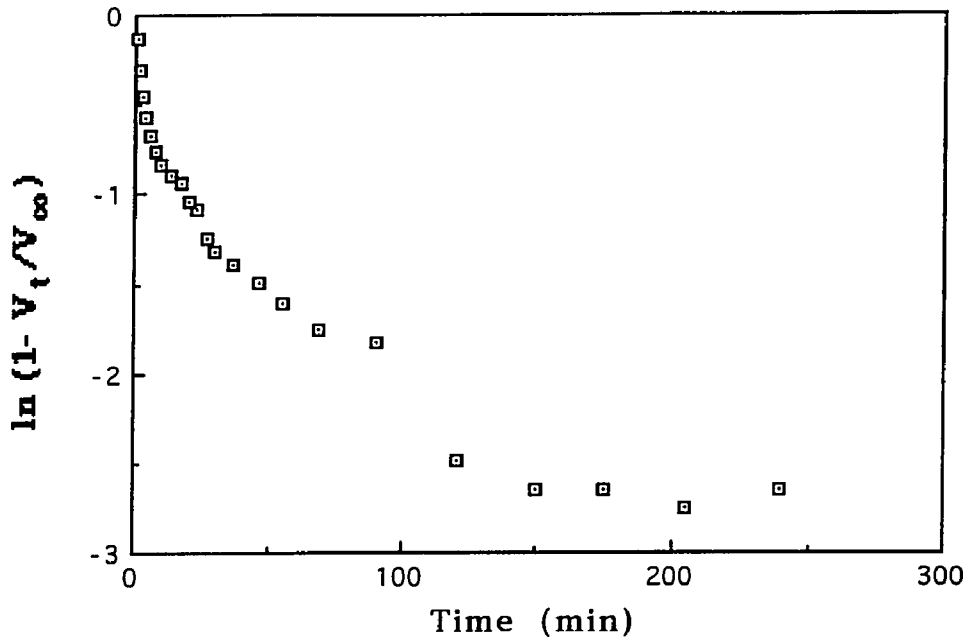

Figure A13-1. RUN #1

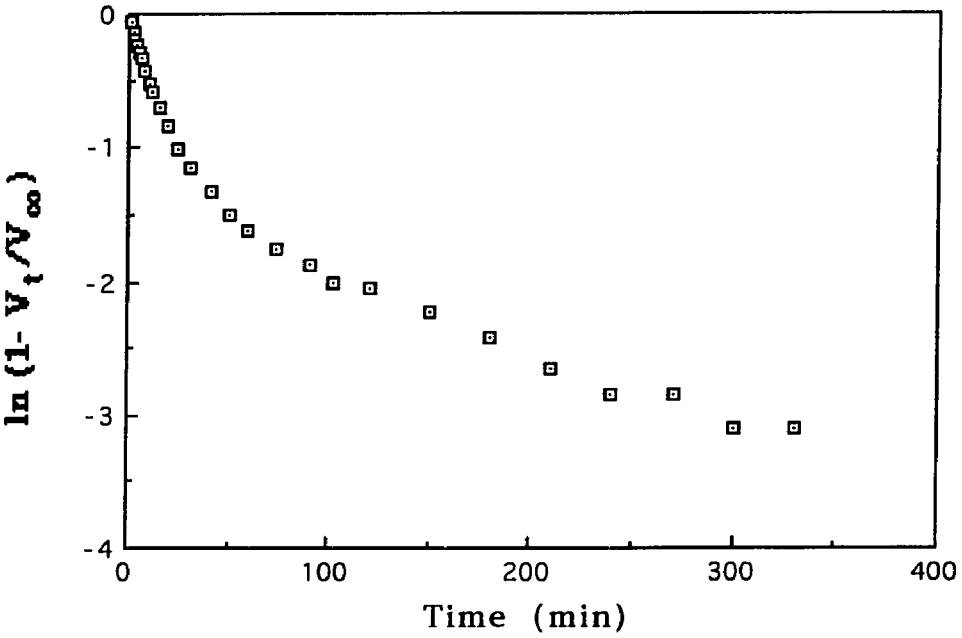

Figure A13-2. RUN #2

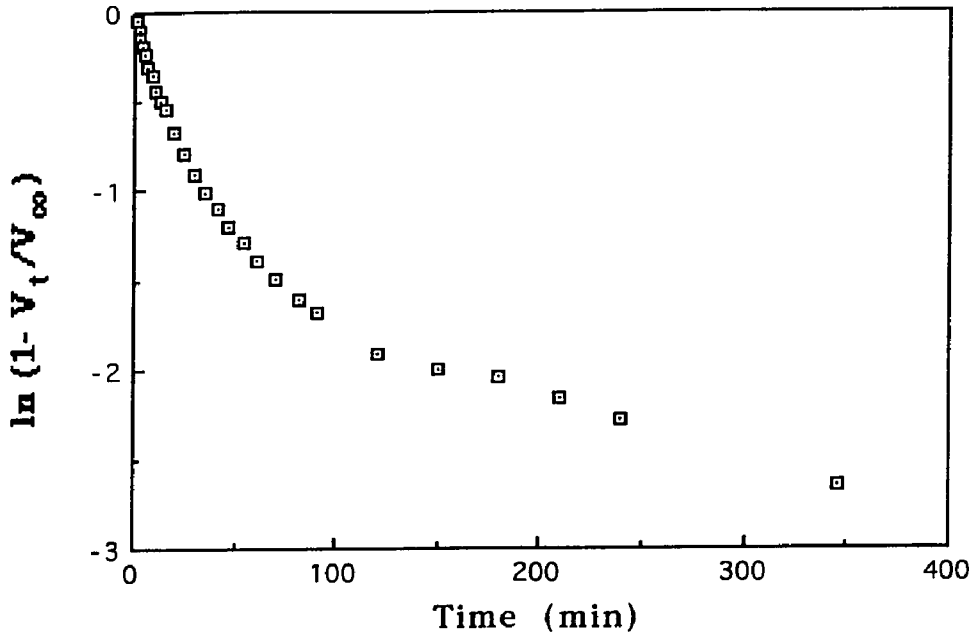

Figure A13-3. RUN #3

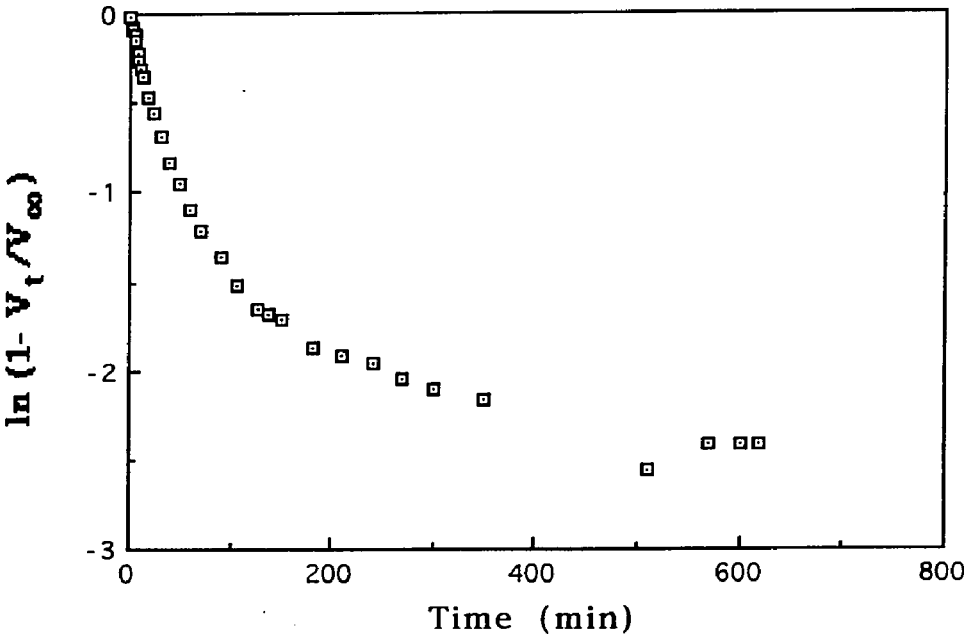

Figure A13-4. RUN #4

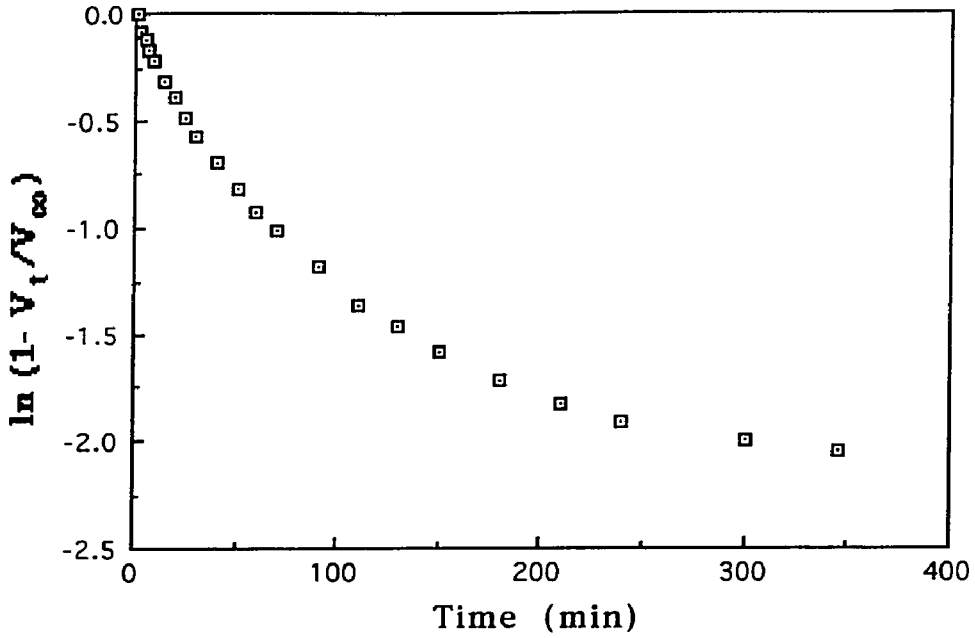

Figure A13-5. RUN #5

Appendix 14. Reusability of Black Pearls L-$FeCl_3$ from the Hydrazine Hydrate Reduction of HPS (Table 24)

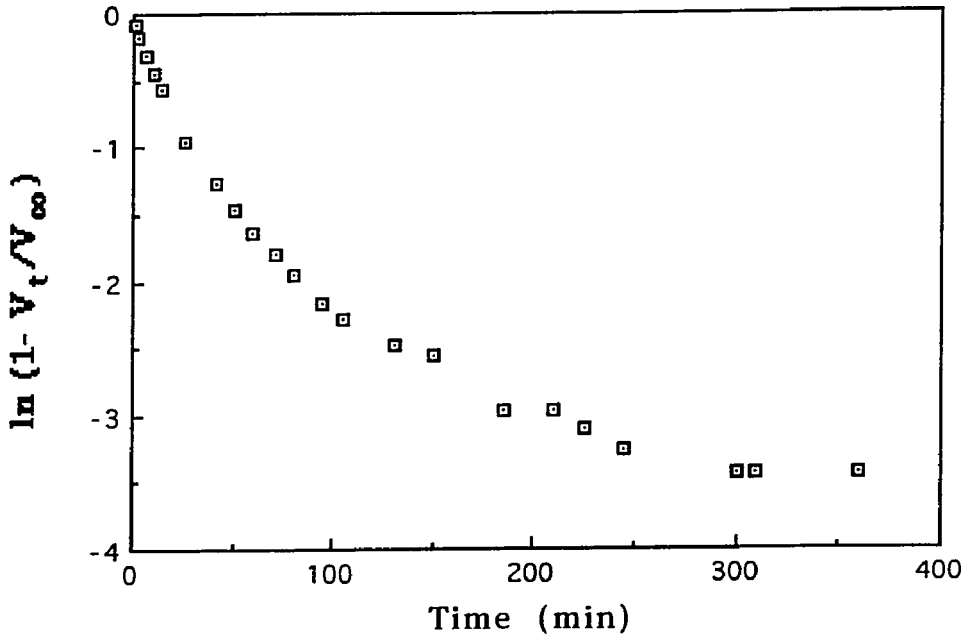

Figure A14-1. RUN #1

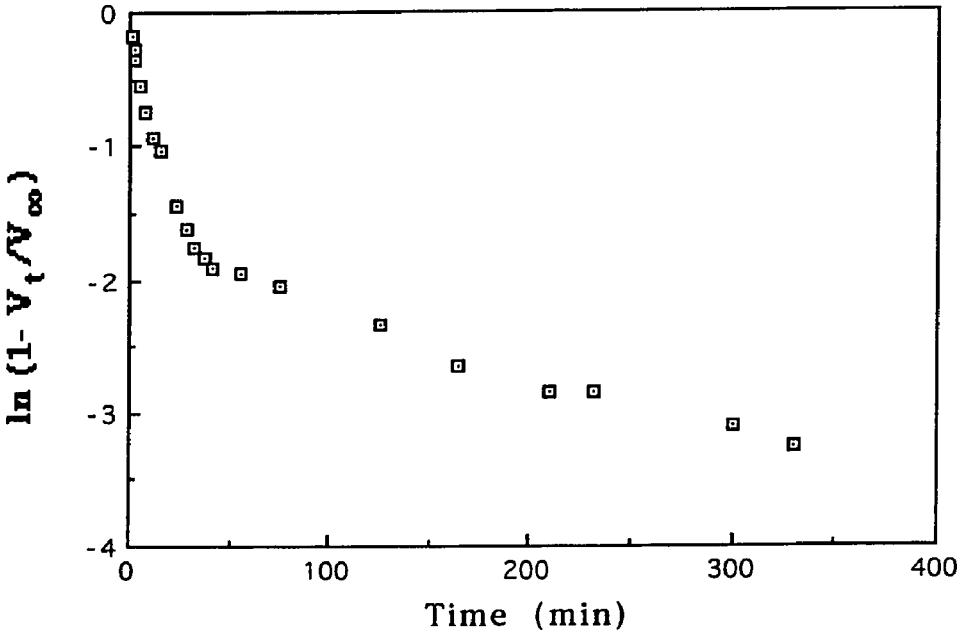

Figure A14-2. RUN #2

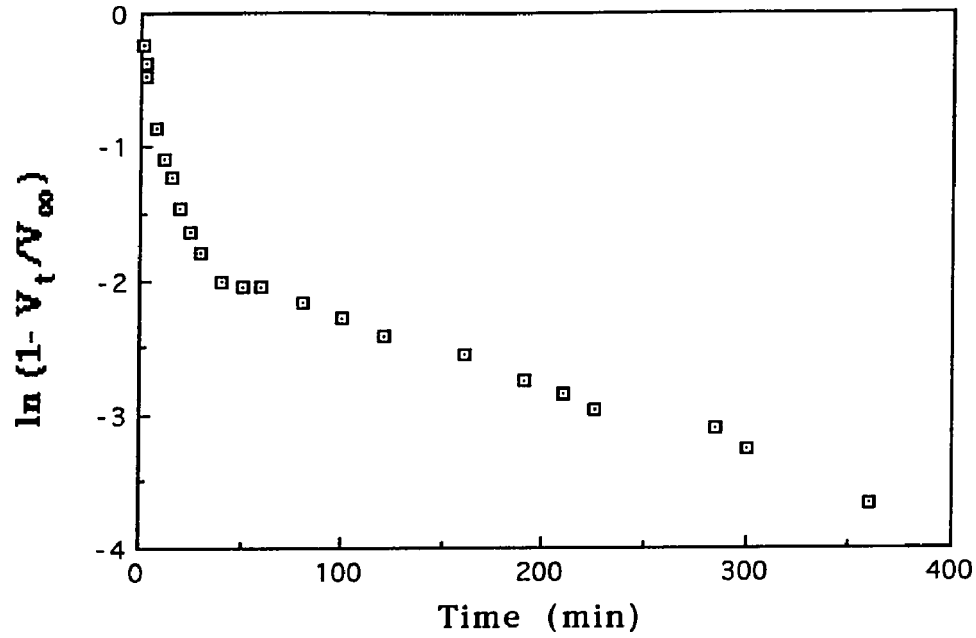

Figure A14-3. RUN #3

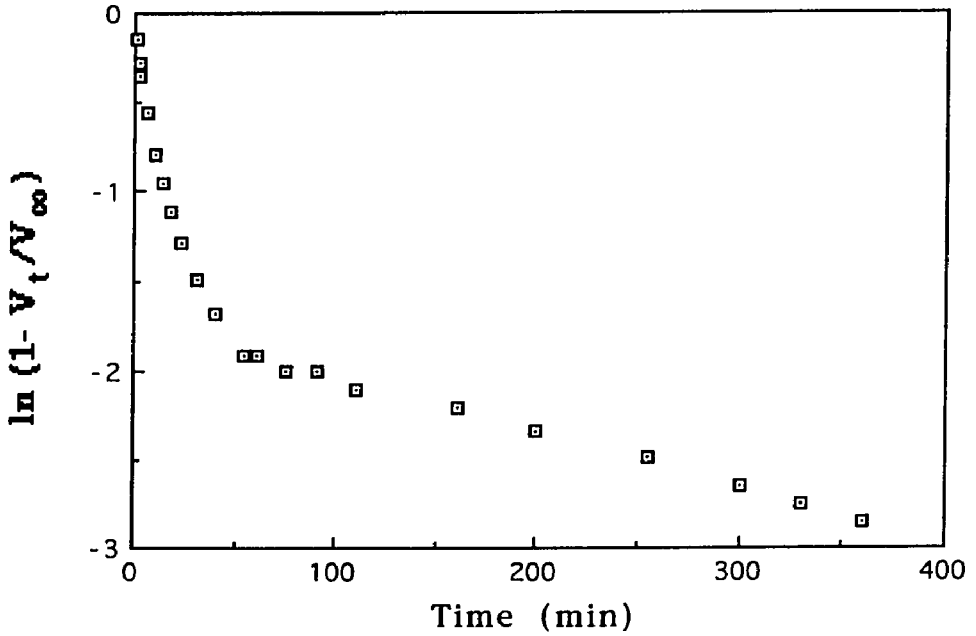

Figure A14-4. RUN #4

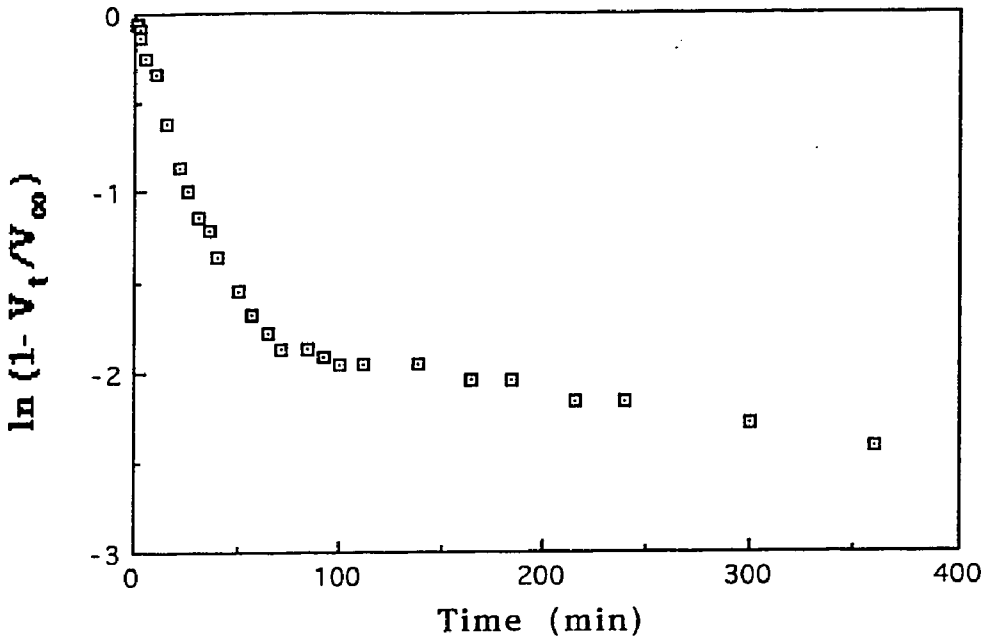

Figure A14-5. RUN #5

Appendix 15. Comparison of Hydrazine Hydrate and Hydrazine Monohydrate (Table 23)

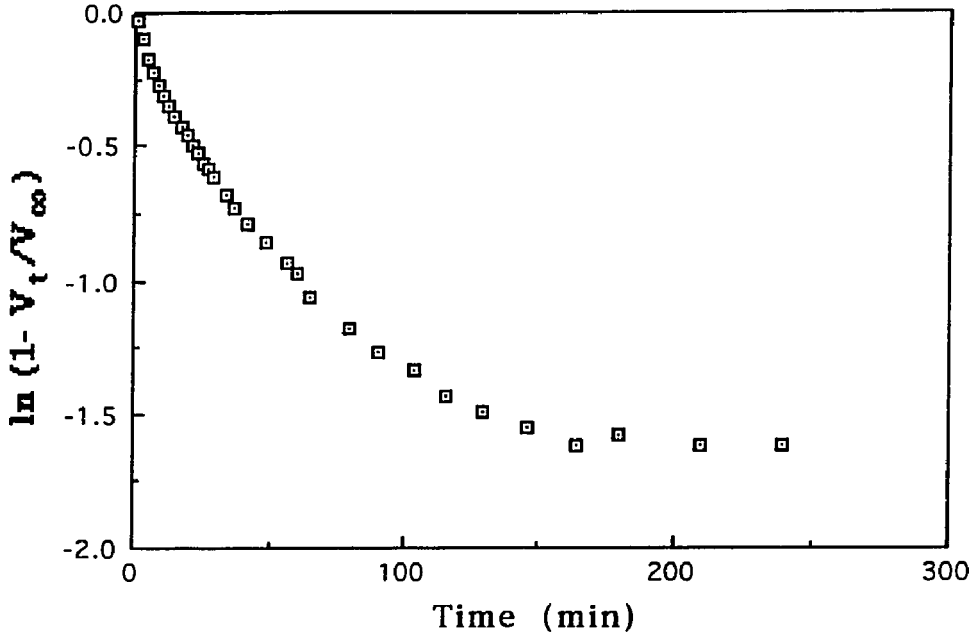

Figure A15-1. Hydrazine Monohydrate Reduction of Nitro HMI with Nuchar SA

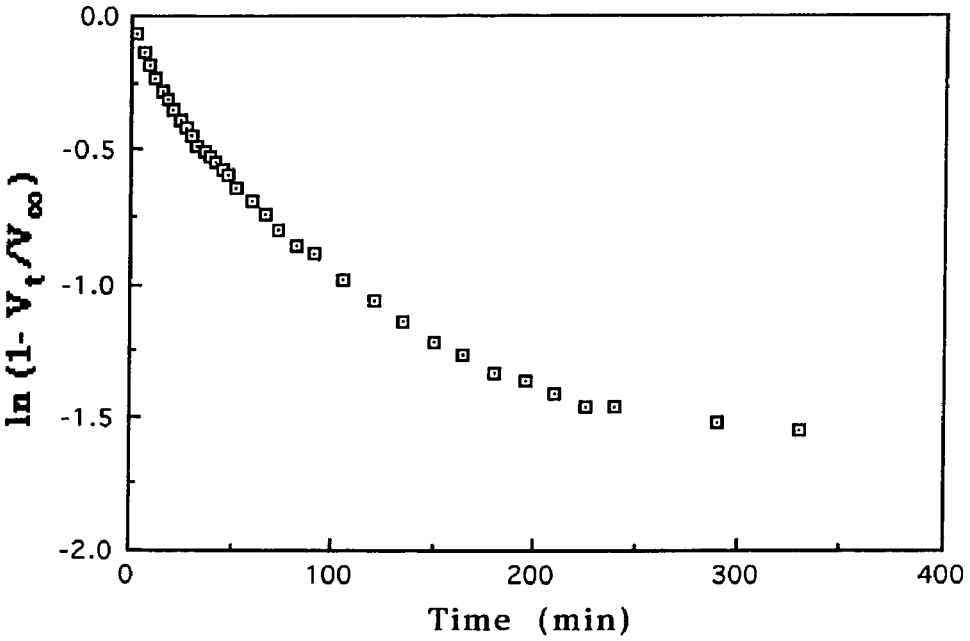

Figure A15-2. Hydrazine Hydrate Reduction of Nitro HMI with Nuchar SA

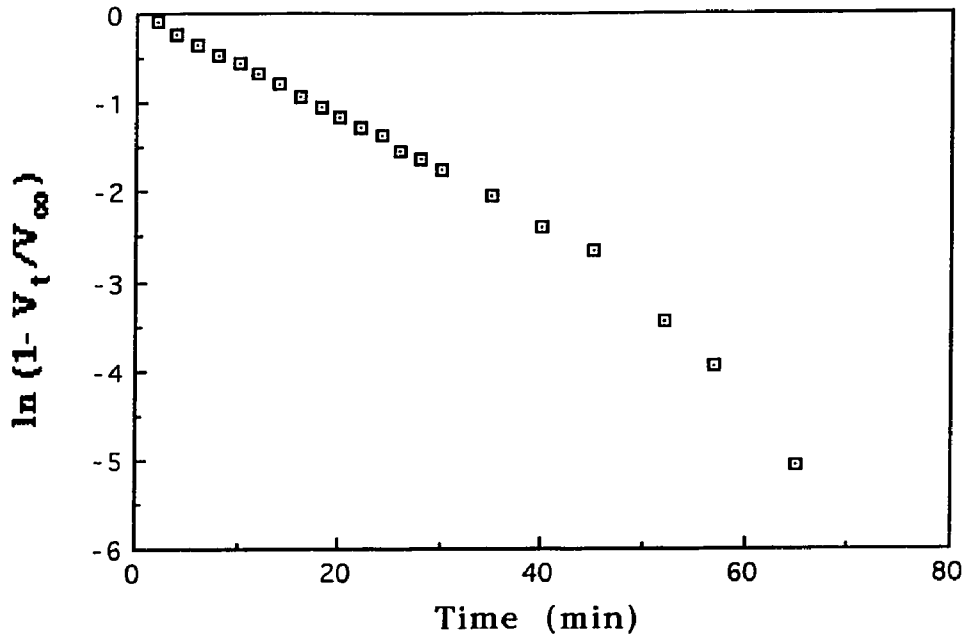

Figure A15-3. Hydrazine Monohydrate Reduction of HPS with Aqua A

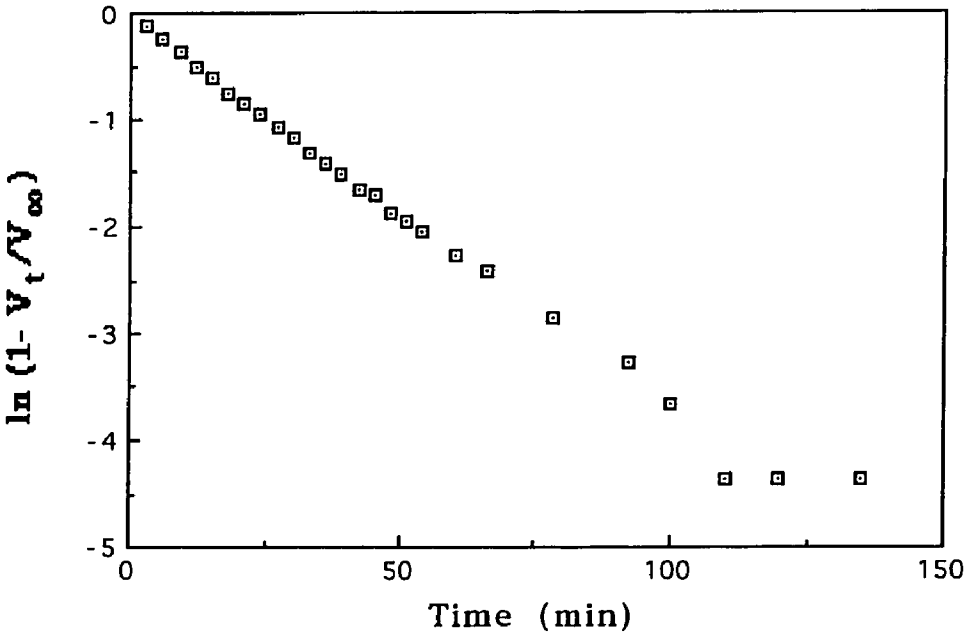

Figure A15-4. Hydrazine Hydrate Reduction of HPS with Aqua A

Appendix 16. Hydrazine Hydrate Reduction of Substituted Nitrobenzene with BPL (Table 24)

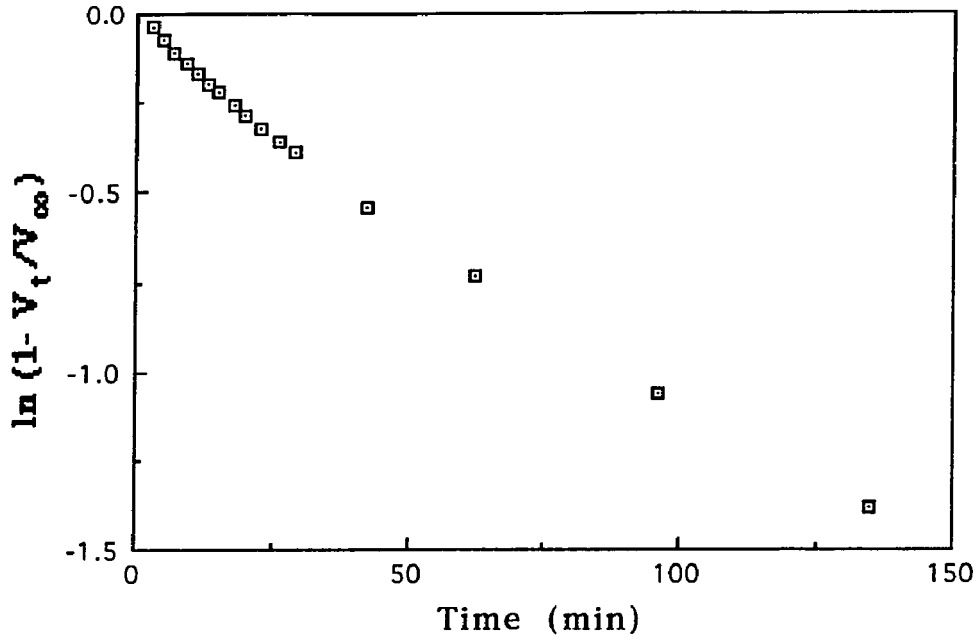

Figure A16-1. Reduction of 3-Nitro-α-α-αtrifluorotoluene

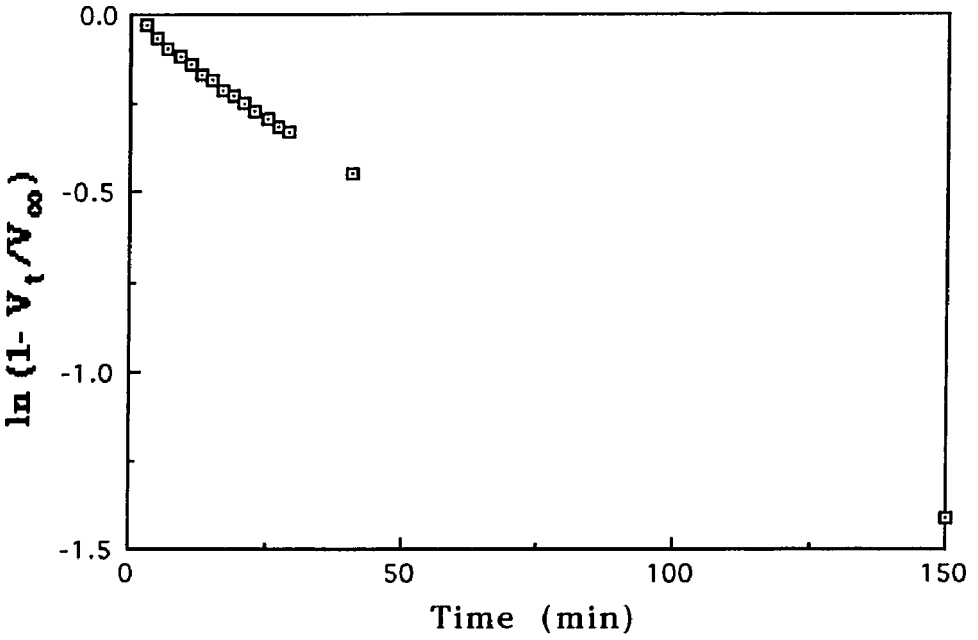

Figure A16-2. Reduction of 1-Iodo-3-nitrobenzene

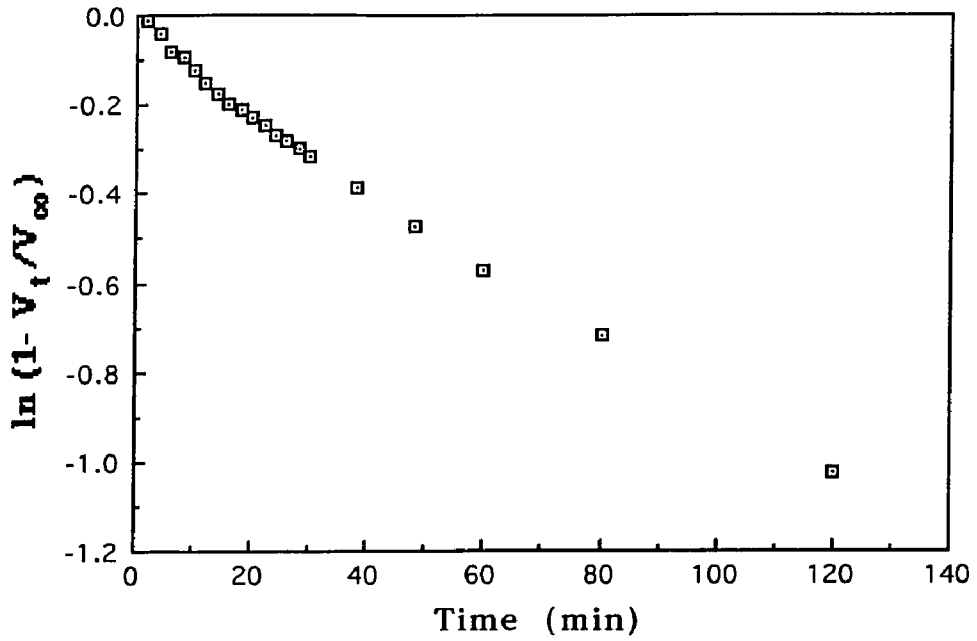

Figure A16-3. Reduction of 1-Bromo-4-nitrobenzene

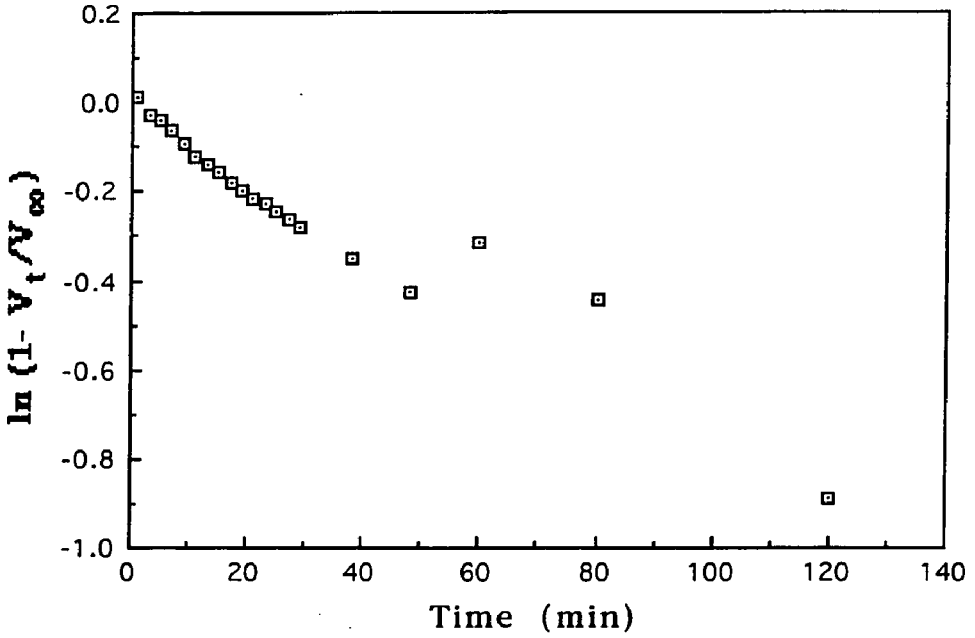

Figure A16-4. Reduction of 1-Chloro-4-nitrobenzene

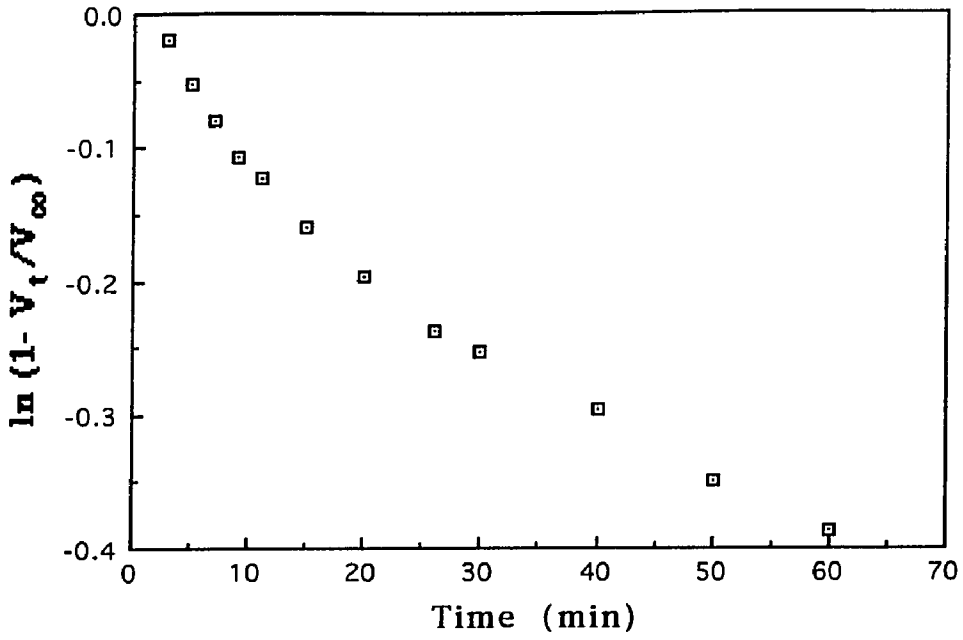

Figure A16-5. Reduction of Nitrobenzene

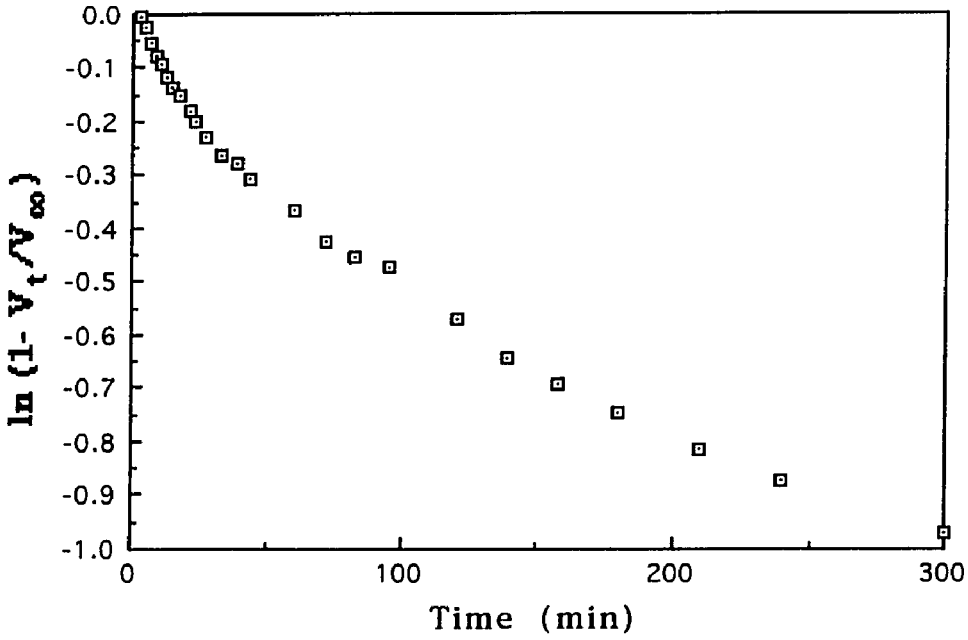

Figure A16-6. Reduction of 4-Nitrotoluene

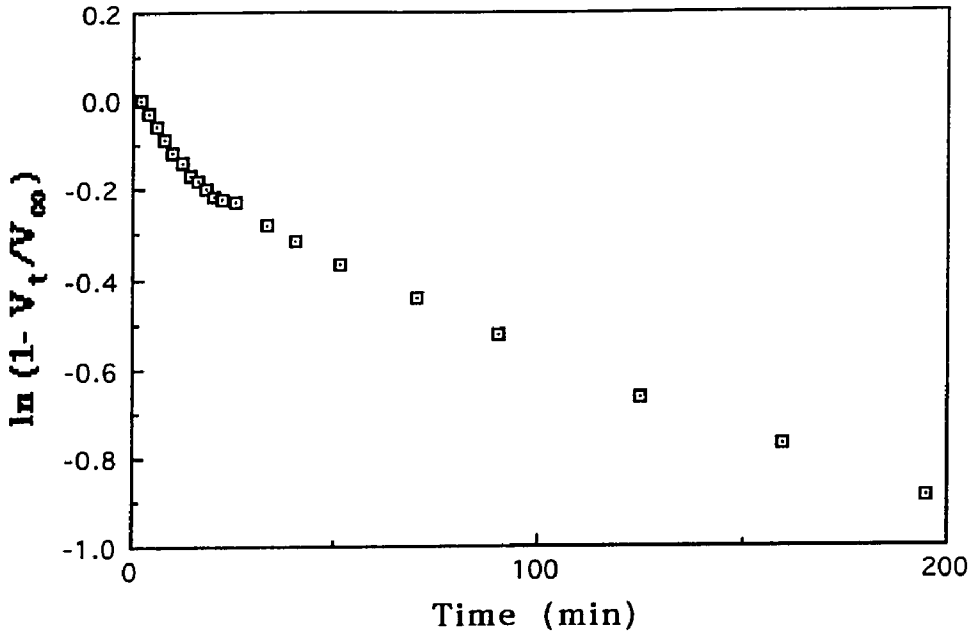

Figure A16-7. Reduction of 4-Nitroanisole

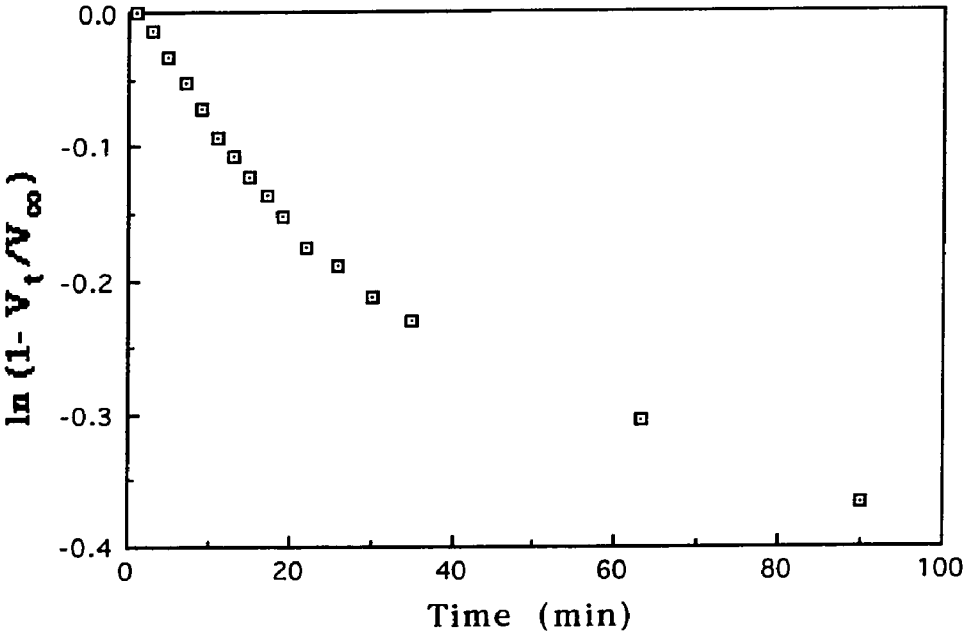

Figure A16-8. Reduction of 4-Nitrophenol

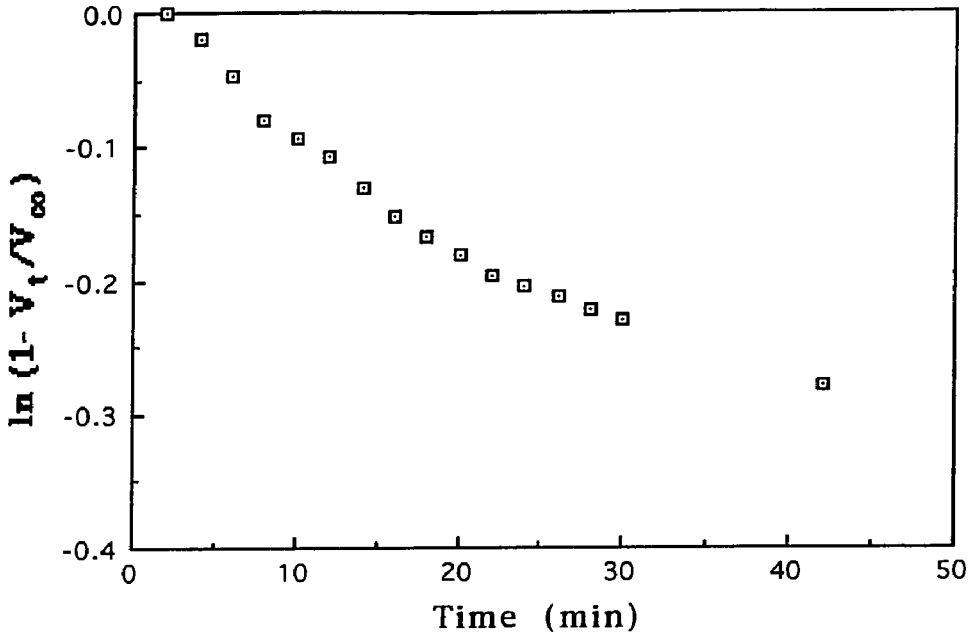

Figure A16-9. Reduction of 4-Nitroaniline

Appendix 17. Recommended Synthetic Procedure

The following is a recommended synthetic procedure for the hydrazine hydrate reduction of nitroaroamatic compounds with a carbonaceous catalyst. Dissolve the nitro compound in an alcoholic solvent (methanol, ethanol, or isopropanol) in a multi-neck round bottom flask. The concentration of the nitro compound can be as high as desired. Add approximately 15%, by weight, of an activated carbon and 1%, by weight, of $FeCl_3$. The iron can be omitted if complexation can occur with the compound being reduced. Place 1.6 molar equivalents (relative to the nitro compound) of hydrazine hydrate in a pressure equalizing addition funnel. Attach the funnel to the round bottom flask that has also been fitted with a reflux condensor. After the system has been purged for 5 minutes with an inert gas (Nitrogen, Argon), maintain positive pressure over the system (through the outlet of the condensor). With magnetic stirring, heat the mixture to reflux. Add the hydrazine hydrate dropwise, over a period of one hour, to the refluxing mixture. Monitor the reaction by TLC. When complete conversion to the aniline has been achieved cool the mixture and filter. A filtration aid, such as Celite, will expedite suction filtration. The aniline can be isolated by removal of the solvent by rotary evaporation. Conversion should be quantitative with high aniline recovery(> 95%).

Appendix 18. Calculation of the salt thickness on the solid support

Assume 1 g total: 0.9 g support, 0.1 g salt (10%)

Average diameter of a particle for 60-80 mesh material =

216 μm= 0.0216 cm = 2.16×10^{-4}m

r = 1.08×10^{-4}m

Surface Area of a particle = $4 \pi r^2 = 1.4657 \times 10^{-7}$ m^2

(neglecting pores)

Volume of a particle = $4/3 \pi r^3 = 5.27667 \times 10^{-12}$ m^3

Surface Area of the support = 4 m^2/g (data from Manufacturer)

Particles per g support = (4 m^2/g)(1 particle/ 1.4657×10^{-7} m^2)

= 2.7×10^7 particles per gram of support

have 0.9g which corresponds to 2.4×10^7 particles

Volume of Salt:

	g salt	Density(l)[121]	Volume of Salt for 0.1g
NaCl	0.00902 g	1.5504 g/ml	0.005818 ml
LiCl	0.04288 g	2.073 g/ml	0.02068 ml
KCl	0.04810 g	1.518 g/ml	0.03169 ml
Total	0.1000 g		0.05819 ml

Volume of salt for one particle = 0.05819 ml salts/ $2.4 \times 10^7 = 2.369 \times 10^{-9}$ ml salt per one particle support

$V_{total} = V_{salt} + V_{particle} = 2.369 \times 10^{-9} + 5.27667 \times 10^{-6}$ cm^3

= 5.27904×10^{-6} cm^3

$V_{total} = 5.344 \times 10^{-6} = 4/3 \pi r^3$

$r_{total} = 0.01084$ cm = $r_{salt} + r_{particle}$

$r_{salt} = 0.0108016$ cm- 0.01080 cm = 0.0000016 cm = 160 Å

Appendix 19. Relative rate determination for the Two Possible Locations of the Platinum in the Salt

Case 1. Platinum on the outer surface of the salt.

$$r_{\bigcirc} = k \frac{C^{o}_{\bigcirc}}{m}$$

Where: r = the relative rate of cyclohexene reaction
k = the rate constant
m = Henry's Law constant
C^{o} = the outer surface concentration of cyclohexene

Case 2. Platinum distributed throughout the salt

Using a modified Thiele Modulus[122] (Φ), which is defined as:

$$\Phi_L = L \left\{ \frac{k\, c_s^{\,m-1}}{D} \right\}^{1/2}$$

Where: L = thickness of the salt
D = diffusion rate through the salt (estimated later)
c_s = surface concentration of cyclohexene

Letting m=1

$$\Phi_L = L \left\{ \frac{k}{D} \right\}^{1/2}$$

And defining an effectiveness factor (η) as:

$$\eta = \frac{\tanh \Phi_L}{\Phi_L} = \frac{r_{\bigcirc}}{r^{o}_{\bigcirc}}$$

Where r^{o} = relative rate of reaction on the outer surface (case 1.)

Rearranging for the relative rate of cyclohexene reaction and substituting the effectiveness factor,

$$r_{\hexagon} = \frac{\eta\, k\, r^{o}_{\hexagon}}{m} = \frac{\tanh \Phi_L \; k\, C^{o}_{\hexagon}}{\Phi_L \qquad m}$$

Substituting the Thiele Modulus into the above equation

$$r_{\hexagon} = \frac{\tanh\left[L\left\{\frac{k}{D}\right\}^{1/2}\right] \quad k\, C^{o}_{\hexagon}}{L\left\{\frac{k}{D}\right\}^{1/2} \qquad m}$$

The figure was generated using the following data:

$k = 10^{7}\ sec^{-1}$

$m = 1$

$C^{o} = 0.97$ moles cyclohexene / l gas

$D = 6.08 \times 10^{-8}\ cm^2/sec$

$C^{o}_{cyclohexene}$ was calculated assuming that the volume of cyclohexene is negligible.

D was estimated using the Stokes-Einstein equation[123] for liquid phase diffusivities in dilute solutions as follows:

$D = (1.05 \times 10^{-9})\, T / \mu\, V_b^{1/3}$

$= (1.05 \times 10^{-9})(700) / (2.519\ cP)(110.8)^{1/3}$

$= 6.08 \times 10^{-8}\ cm^2/sec$

with V_b (molar volume of the diffusing solute) calculated from Kopp's Law: 6 carbons, 10 hydrogens and -15 for a ring system

$= 6 \times 14.8 + 10 \times 3.7 - 15 = 110.8\ cm^3/mol$

μ is the viscosity of the cyclohexene in the gas which is estimated to be 2.519 cP.

Vita

The author was born in Los Angeles, CA on March 3, 1963. He received a B.S. degree in Chemistry from Moravian College in 1987. He is currently employed by Cambridge Isotope Labs in Woburn MA.